

THE SIGNIFICANCE
OF
POISSON'S RATIO IN THE DETERMINATION
OF
STRESS AND SETTLEMENT IN SOILS

H. P. RAUCH

THE SIGNIFICANCE
OF
POISSON'S RATIO IN THE DETERMINATION
OF
STRESS AND SETTLEMENT IN SOILS

H.P. RAUCH
B.Sc.(Eng.) (Read), A.M.(S.A.) P.C.E.

A thesis presented to the University of the
Witwatersrand, for the degree Master of Science
in Civil Engineering.



THIS IS TO CERTIFY THAT THIS THESIS IS A
REPORT OF THE RESULTS OF MY OWN INVESTIGA-
TIONS AND WORK CARRIED OUT WHILE ENGAGED
INITIALLY IN FULL-TIME POST-GRADUATE STUDY
ON A ONE-YEAR S.A.R. & H. RAILWAY ENGINEER-
ING SCHOLARSHIP, AND SUBSEQUENTLY IN PART-
TIME STUDY ON MY OWN.

H.P. Rauch

H.P. RAUCH.

ACKNOWLEDGEMENTS

In presenting this thesis, the Author gratefully wishes to thank:

- (a) The South African Railways and Harbours Administration for having made it possible for him to execute this thesis;
- (b) Prof. J.F.B. Jennings, Head of the Department of Civil Engineering, Witwatersrand University, for his guidance as Supervisor of the work;
- (c) Mr. K. Knight, Lecturer in the Department of Civil Engineering, Witwatersrand University, for his assistance in connection with the practical work;
- (d) Mrs. E. Rauch, for having typed and prepared the manuscript for presentation.

C O N T E N T S

	Page
SYNOPSIS	1
CHAPTER 1 : INTRODUCTION	2
CHAPTER 2 : ELASTIC THEORY CONSIDERATIONS	4
CHAPTER 3 : POISSON'S RATIO IN RELATION TO ELASTIC MATERIALS	7
1. Historical	7
2. The possible Range of Values of Poisson's Ratio for Homogeneous, Isotropic, Elastic Materials	8
3. Values of Poisson's Ratio for Practical Materials	11
CHAPTER 4 : POISSON'S RATIO IN RELATION TO ELASTIC STATES OF STRESS AND STRAIN	14
1. Introduction	14
2. Plane Stress and Plane Strain	14
3. The Moduli of Elasticity in relation to States of Plane Stress and Plane Strain	15
4. Poisson's Ratio in relation to States of Stress and Strain in a Semi-infinite Elastic Solid	16
CHAPTER 5 : THE EFFECT OF VARIOUS VALUES OF POISSON'S RATIO ON THE STRESS DISTRIBUTION IN A SEMI-INFINITE ELASTIC SOLID DUE TO AN APPLIED VERTICAL POINT LOAD	20
1. Introduction	20
2. Stress Calculations and Curves	20
3. Discussion	43
CHAPTER 6 : CURRENT CONCEPTS OF ELASTICITY AND POISSON'S RATIO IN SOILS WORK	45
1. Applicability of the Elastic Theory to Soils	45
2. Settlement Analysis for Saturated Clays	45
3. The Laboratory Oedometer Test	46
4. The Westergaard Equations	47
CHAPTER 7 : LABORATORY TESTS	48
1. Theoretical Considerations	48
2. The Test Soil	49
3. Design of the Experimental Work	51
4. The Test Apparatus	54
5. The Test Series	60
6. Test Observations and Curves	63
7. Discussion	116
CHAPTER 8 : REDUCTION OF TEST RESULTS AND THE DETERMINATION OF POISSON'S RATIO	120
1. Introduction	120
2. Rate of Plug Movement due to Leakage only during Actual Test	120
3. Time Effects during Test	125
1. Initial Volume of Test Samples	127
2. Calculation of Poisson's Ratio	128
CHAPTER 9 : DISCUSSION OF TEST RESULTS	155
CHAPTER 10 : CONCLUSIONS	164

APPENDIX I	: The possible Algebraic Signs of the Moduli of Elasticity E , G and K	Page 168
APPENDIX II	: Steps in the Final Reduction of the Mathematical Expressions in Element's paper (Ref.12)	169
APPENDIX III	: 1. Comparison of Values of Maximum Shear Stress (S_{max}) as determined from Equations 5.3 and 5.5	173
	2. Determination of the Points of Intersection of Stress Contour Lines with the Surface $z=0$ of a Semi-infinite Solid in the case of Stress Contour Diagrams for σ_r , σ_t and S_{max}	176
APPENDIX IV	: 1. Moisture Content Determinations	179
	2. Determination of the Initial Void Ratio (e) and Degree of Saturation (S_r) of each Test Sample	180
APPENDIX V	: 1. Calibration of Capillary Tube used	181
	2. Calculation of Plug Movement due to Spindle Entry only	181
REFERENCES		183

SYNOPSIS

This report describes investigations carried out in order to obtain a better understanding of the concept of Poisson's Ratio as related to the determination of stress and settlement in soils.

Since Poisson's Ratio is primarily a concept associated with the elastic property of materials and therefore generally only enters into soils work in connection with applying the elastic theory to soils, the investigations commence with a brief review of the basic principles of the elastic theory and the elastic properties of materials. It is found that Poisson's Ratio for elastic materials can only fall within the range zero - 0.50.

Consideration is then given to certain 2-dimensional and 3-dimensional problems of stress and strain in the theory of elasticity. It is found that the moduli of elasticity do not affect the stress distribution and hence also the strains in 2-dimensional problems. For the basic 3-dimensional problem viz. that of a vertical point load applied to the horizontal surface of a semi-infinite solid, the effect of various values of Poisson's Ratio on the resulting stress distribution is then considered. The results are presented mainly in the form of stress contour diagrams. These show that in the case of the Maximum Shear Stress (S_{max}) which is a major concern, the stress distribution is insignificantly affected by variation in the value of Poisson's Ratio below a certain comparatively shallow depth. Furthermore, on the axis of loading where the maximum stress values occur, the variation in S_{max} corresponding to the extreme limits of the range of Poisson's Ratio values applicable to elastic materials as mentioned above, is only a constant 14%.

Attention is then turned more directly towards the elastic theory and Poisson's Ratio in relation to soils, and current concepts of elasticity and Poisson's Ratio in soils work are then briefly reviewed. As a result of subsequent discussions, it becomes clear that for all types of saturated soils (i.e. both cohesive and cohesionless), Poisson's Ratio can only have the value 0.50 for the purposes of elastic considerations.

An attempt to determine Poisson's Ratio for a soil from laboratory conducted triaxial shear tests, is then described in full. The results of 6 tests conducted show that the value of Poisson's Ratio for the silty sand test soil used (moisture content between 1-25) lies between 0.14 and 0.24. This order of the values obtained, is found to compare favourably with the order of values obtained by overseas investigators (using methods other than that mentioned above) for various soil types at moisture contents less than saturation value.

It is finally concluded that Poisson's Ratio is only of limited significance in both the determination of stress and settlement in soils. As regards the values of Poisson's Ratio applicable to various soil types for the purposes of elastic considerations, it is concluded that Poisson's Ratio is in the first instance dependent on the moisture content of a soil; secondly, that the value of Poisson's Ratio for all types of saturated soils is 0.50; and thirdly, that in the case of partially saturated soils, the values of Poisson's Ratio for sands are less than those for clays. A suggested graphical relation between Poisson's Ratio and Degree of Saturation is then given in conclusion.

CHAPTER 1

INTRODUCTION

The essential requirement of any foundation is that it must be able to support any form of superimposed loading in a safe and stable manner and without detriment to the latter. A soil as the most common type of foundation material encountered in practice, must comply with this requirement. A thorough understanding of the stresses and strains in soil foundations resulting from a superimposed loading is thus essential.

There are in general two approaches to foundation design in the more specific sense of bearing capacity of a soil foundation. Firstly, there is the method known as Limit Design, wherein the safe allowable bearing capacity of a soil is obtained from a determination of its ultimate bearing capacity to which a suitable factor of safety against such catastrophic shear failure is then applied, and secondly, the method of Stress Design, wherein a suitable factor of safety against possible overstress is used to obtain the allowable stress in the soil foundation.

In the case of the latter method of foundation design, some method of determining the stress induced in a soil by an applied loading is necessary. The only means by which this is possible is by the use of some theory relating force and the deformation it produces (as the fundamental alternatives for stress and strain), since it is a mechanical property of all matter that the application of load causes deformation. In some instances, however, deformation requires a certain amount of time to be effected, so that in the general case, load, deformation and time are involved. The simplest theory relating these variables is the theory of elasticity which holds for elastic materials, but this theory has the important limitation of applying only to cases wherein stress and strain are proportional and independent of time. Furthermore, as Taylor (1.1) mentions, "solutions based on the theory of elasticity are far from easy for all but the simplest of cases, and any general theory which covers even minor variations from simple, elastic conditions becomes unbelievably complex Thus the obtaining of a general stress-strain theory especially for cases where time effects enter, must be acknowledged as an impossible goal."

It has therefore become practice to use the theory of elasticity to evaluate stress and strain in soil masses, on the assumption that soils behave as perfectly elastic, homogeneous, isotropic materials. This assumption and its implications will be discussed in more detail later.

It is in the use of the elastic theory for the purposes of the design of soil foundations by the method of Stress Design that Poisson's Ratio as a property of an elastic material becomes involved, since mathematical expressions for stress and strain derived from the theory of elasticity frequently contain terms of Poisson's Ratio.

Experiments have shown (2.1) that in the case of a prismatic bar of elastic material in simple tension, the axial elongation is a constant for a bar of perfectly elastic material and is known as Poisson's Ratio, after the name of the French mathematician who was the first to determine a value for this ratio by using the molecular theory of structure of a material (see later Section 3.1). In this report, Poisson's Ratio will be denoted by the Greek letter μ .

Hence, /

Hence, in using expressions derived from the theory of elasticity to evaluate stress and strain in soil foundations, (the latter especially in the form of settlement), the soils engineer is faced with having to decide what value of Poisson's Ratio is applicable to the particular problem he is dealing with, and as yet there is a great deal of uncertainty in making such decisions.

The work described herein is an endeavour to obtain a better understanding of the concept of Poisson's Ratio as related to the determination of stress and settlement in soils by the use of the elastic theory.

In the first Chapters to follow, some aspects of the classical theory of elasticity and Poisson's Ratio in relation to this theory will be discussed, while later Chapters are directed towards the elastic theory and Poisson's Ratio in relation to soils. In particular, a determination of Poisson's Ratio for a soil from measurements made during a triaxial compression test, will be described and discussed.

CHAPTER 2

ELASTIC THEORY CONSIDERATIONS

Whenever dealing with problems relating to the theory of elasticity, it is important to bear in mind the assumptions on which the theory is based, as well as the limits of its applicability.

Most materials possess to some extent the property of elasticity⁽¹⁾, viz. that when deformed under the action of a system of applied forces of magnitude not exceeding a certain limit known as the elastic limit, the deformation disappears on removal of the forces and the body regains its original shape. On a broader basis, elasticity implies⁽²⁾ that there is a definite relation between force and deformation which is independent of any other variable such as time, so that on imposing a load a particular value of strain (or a measure of deformation) occurs, and if this load be removed and re-imposed, the same value of strain as previously will again occur. It should be noted therefore, that elasticity implies only a definite relation between force and deformation and not necessarily any particular relation, such as for instance a linear one.*

However, Robert Hooke⁽³⁾, (1634-1703) was the first to investigate the elastic property of materials more closely and he succeeded in establishing by experiment that in many instances the relation between the magnitude of the forces and the deformations that they produce was approximately linear up to the elastic limit. This approximately linear relation between force and the deformation it produces, is the basis of the so-called Hooke's Law which assumes the ideal material in which the relation between force and deformation is in fact perfectly linear. Hooke's Law subsequently became the basis on which the theory of elasticity was developed, so that the term 'elasticity' used in relation to the theory of elasticity actually implies linear elasticity in accordance with Hooke's Law. Throughout this report, therefore, the term 'elasticity' is intended to be understood in this sense.

For the purposes of mathematical treatment, the theory of elasticity assumes that all bodies are perfectly elastic, i.e. the theory assumes Hooke's Law as was mentioned above. Further, it assumes that the matter of such bodies is homogeneous i.e. that at every point of the body the elastic properties are identical in identical directions; and also that the bodies are isotropic i.e. that the elastic properties are the same in all directions.

The elastic theory can thus strictly be applied, in the first instance, only to materials which have properties in accordance with these assumptions on which the theory is based, and in addition, only to that range of loading during which such properties exist. However, although no material is known

which/

* It is well-known⁽⁴⁾ that a material such as rubber, for example, has a non-linear force:deformation relationship, due to the fact that as it is extended, it becomes more difficult to extend as the extension proceeds.

+ See also Ref. 1, p.208.

which satisfies all these assumptions completely, the theory has been applied to many materials with reasonable accuracy and to steel with great accuracy. In general, the accuracy with which the theory can be applied to any material will depend on how closely the above-mentioned assumptions are realized.

A very important aspect of the theory of elasticity which is often overlooked, is that it only considers two variables viz. force and deformation, or alternatively, stress and strain. All other possible variables such as time and mass are considered to be constant. The magnitude of stress is thus assumed to be independent of the rate of application of stress; also, an instantaneous application of stress is considered to produce an instantaneous strain, and in all cases, during strain the body suffers no change of mass. Hence the theory is not applicable to cases where time effects or change of mass effects occur during strain. In structural materials, both instantaneous strain and constant mass during strain are invariably realized, although in the case of strain certain materials (e.g., polymers) such as occur do also occur.

With regard to Poisson's Ratio: it has already been mentioned in Chapter 1 that it is a constant in the case of perfectly elastic materials. It should, however, be pointed out in view of the above discussions that this is actually only the case with the ideal material which behaves strictly according to Hooke's law. By implication, this also means that Poisson's Ratio for the ideal material is only constant within the elastic range of loading, i.e. while the relation between stress and strain is linear. In practice therefore, values of Poisson's Ratio are not rigidly constant within the elastic range and furthermore, when the elastic limit is exceeded Poisson's Ratio becomes a variable quantity with a value which is dependent upon stress. It is known that in the case of materials which contract under small load and expand when a state of failure is approached, Poisson's Ratio shows a considerable increase in value when the failure condition is approached.

However, it is of extreme importance to realize that when applying the theory of elasticity to any material, the value of Poisson's Ratio which is applicable, is strictly that constant value pertaining to the ideal elastic state assumed by Hooke's law. In general, Poisson's Ratio is always considered either in relation to the elastic state, especially as it will be shown in the next Chapter that the concept of Poisson's Ratio was originally derived from a consideration of the elastic state of materials. In this connection also, Taylor (1926) mentions that "The meaning of the elastic modulus given by Poisson's Ratio becomes obscure as soon as it is used in connection with non-elastic materials."

A second constant which is related to the elastic state of materials, is Young's modulus. The linear relation between stress and the deformation it produces, or alternatively, the linear relation between stress and strain, implies that the relation of stress-strain is a constant. This constant is known as Young's modulus denoted by the symbol E . The remarks made above for the case of Poisson's Ratio are also applicable in the case of Young's modulus. For the ideal elastic material Young's modulus therefore also has a constant value within the elastic range of loading.

These two constants are however not the only constants of elasticity. The Bulk Modulus (K) and the Modulus of Rigidity (G) are also such constants. It can be shown (see Section 3.2), that the constants of elasticity are inter-related. Yet, from the discussion to follow in the first Section of the next Chapter, it will be seen that for the complete definition of the elastic properties of a material, the elastic theory requires the use of only two such constants, the Modulus of Elasticity E (i.e. Young's Modulus) and Poisson's Ratio μ being the two most commonly selected (1.1).

CHAPTER 3

POISSON'S RATIO IN RELATION TO ELASTIC MATERIALS

3.1 Historical (5)

During the initial stages of the development of the theory of elasticity at the beginning of the 19th Century, the early investigators such as Navier, Cauchy, Poisson, Lamé, St. Venant, and others, all based their work on the so-called molecular theory viz. that the elastic property of a body can be explained in terms of some kind of attractive and repulsive forces between the ultimate particles of the body.

Navier in 1821, working from the molecular theory, was the first to establish a relation between the deformations and the molecular forces for an isotropic body. These relations were in the form of a set of three differential equations of equilibrium, which notably contained only one elastic constant. This idea, that the elastic properties of an isotropic body could be completely defined by one constant, say the modulus of tension (E), was accepted by the other early investigators already mentioned.

Poisson being very interested in the theory of elasticity based on the idea of molecular structure, obtained equations of equilibrium and boundary conditions similar to those obtained by Navier. Then applying his general equations to isotropic bodies, he found that for simple tension of a prismatic bar the axial elongation must be accompanied by a lateral contraction of magnitude μ , where $\mu = 0.25$. Thus, Poisson's value of $\mu = 0.25$ for the ideal isotropic material, was based on the uni-elastic-constant hypothesis of the molecular theory.

However, in the 1830's George Green offered a derivation of the equations of elasticity without using any hypothesis regarding the behaviour of the molecular structure of elastic bodies. His approach was a derivation of the stress-strain relations from a consideration of strain energy and showed that for an isotropic body two elastic constants were required, instead of one as demanded by the molecular theory. His paper started a serious controversy and gave rise to two schools of thought in the development of the theory of elasticity. As a result, several physicists became interested in the determination of elastic constants and tried to settle the argument by direct tests.

Experiments by R. W. Dumas and later by A. J. Rüchffert to determine values of Poisson's Ratio for various materials, in both cases showed values different to Poisson's theoretical value of $\mu = 0.25$. For steel a value of $\mu = 0.28$ was found. Although these and other experimental results were in conflict with the result from the uni-constant hypothesis, and could only be justified by adopting a two-elastic-constant hypothesis for isotropic bodies, the controversy could not be settled because it was always possible to argue that the materials used had not been perfectly isotropic.

George Green's result found further support when G. G. Stokes and Franz Neumann independently verified, by different theoretical approaches remote from the molecular theory, that two elastic constants were necessary to define the elastic properties of a material completely. It was only at the start of the 20th Century that W. Voigt, one of Neumann's pupils, finally settled the controversy by determining the elastic moduli of thin prisms cut out from single crystals of a material, and in

addition studying the compressibility of crystals under uniform hydrostatic pressure, and then showing that the results he obtained definitely disproved those relations between the elastic constants which follow from the uni-constant theory.

Thus the Navier-Poisson hypothesis regarding molecular forces was shown to be untenable and with it Poisson's value of $\mu = 0.25$ for the ideal isotropic material was shown to be inadmissible.

3.2 The possible Range of Values of Poisson's Ratio for Homogeneous, Isotropic, Elastic Materials

In discussing this problem it is useful to consider in the first instance the equations relating the various constants of elasticity (alternatively known as the moduli of elasticity). These equations are standard relationships in strength of materials and are dealt with fully in any text on the subject. Their derivations will therefore not be given again in full herein, but detailed reference will be given throughout.

These relationships are obtainable if considering a cube of perfectly elastic material of unit size subjected to the action of a three-dimensional system of principal stresses as shown in Fig. 3.1 below:

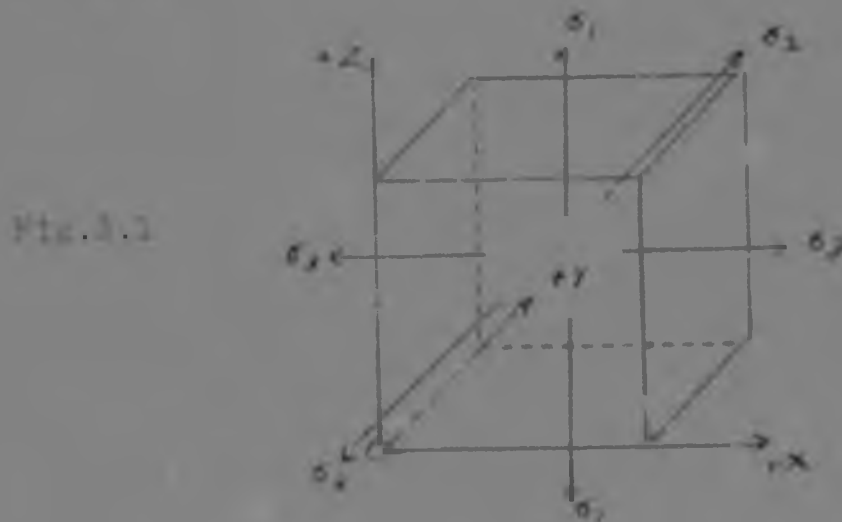


Fig. 3.1

It can be shown* that the sum of the strains along each of the principal axes of stress, is given by:

$$\epsilon_1 + \epsilon_2 + \epsilon_3 = \frac{1}{E} (\sigma_1 + \sigma_2 + \sigma_3)(1 - 2\mu) \dots\dots\dots 3.1$$

However, it can also be shown that the unit volume expansion or dilation (denoted by the Greek letter Δ) of the cube as a result of the action of the applied principal stresses is approximately (neglecting quantities higher than the first order) given by:

$$\Delta = \frac{\delta V}{V} = \epsilon_1 + \epsilon_2 + \epsilon_3 \dots\dots\dots 3.2$$

where V denotes the original volume of the cube and δV the subsequent change in volume.

Therefore, by combining 3.1 and 3.2:

$$\text{Dilation } (\Delta) = \frac{\delta V}{V} = \frac{1}{E} (\sigma_1 + \sigma_2 + \sigma_3)(1 - 2\mu) \dots\dots\dots 3.3$$

Beard

* Ref.2, p.52 and p.61-63.

Based on equation 3.3, it may be shown* that for fluid pressure conditions when $\sigma_1 = \sigma_2 = \sigma_3 = \sigma$ say, and $\epsilon_1 = \epsilon_2 = \epsilon_3 = \epsilon$ say,

$$\frac{\sigma}{\Delta} = \frac{E}{3(1-2\mu)} = K \quad \dots\dots\dots 3.4$$

where K is known as the 'modulus of elasticity of volume', or simply, the 'Bulk Modulus'. Furthermore, the condition that $\sigma_1 = -\sigma_2 = \tau$ say, and $\sigma_3 = 0$; and $\epsilon_1 = -\epsilon_2 = \epsilon$ say, and $\epsilon_3 = 0$; may be shown† to result in a pure shear state of stress, and hence a further relationship may be obtained‡:

$$\frac{\tau}{\delta} = \frac{E}{3(1+\mu)} = G \quad \dots\dots\dots 3.5$$

wherein τ is the pure shear stress, δ is the pure shear strain, and G is known as the 'modulus of elasticity in shear' or simply, the 'Modulus of Rigidity'.

Finally, by combining equations 3.4 and 3.5, it can readily be shown that:

$$3K(1 - 2\mu) = 2G(1 + \mu) \quad \dots\dots\dots 3.6$$

With regard to the algebraic signs of the three moduli of elasticity E , G and K , it can be shown (see Appendix I) that whatever the algebraic signs of the principal stresses and strains and the pure shear stresses and strains (i.e. whether they be positive or negative), these moduli of elasticity always have a positive value.

Stress(1) referring to question 2.1 above, points out that "if μ were greater than 1, or if μ were less than -1, either E or G would be negative, and hence for an isotropic solid Poisson's Ratio cannot exceed $\frac{1}{2}$ and cannot be less than -1", i.e. $-1 < \mu < 0.5$. Terzaghi (6) makes no direct statement on the possible range of values of μ , but when discussing μ in relation to elastic behaviour, he never seems to consider any values outside the zero-0.5 range*. For instance, in dealing with†(10.2) Steinbrenner's approximate solution for the computation of the settlement of loads covering a finite part of the surface of elastic layers on a rigid base, he shows as extreme limits the effects of $\mu = 0$ and $\mu = 0.5$ on the settlement influence value I_p , and the relevant curves for I_p are then only for μ values in the range zero-0.5. Taylor(1) again, makes no clear statement regarding the possible range of values of Poisson's Ratio. He states(2.3) that: "Poisson's Ratio has values in elastic materials that are always between zero and 0.5."

There thus appears to be agreement as far as the upper limit of μ is concerned, viz. that μ cannot be greater than 0.5 in elastic materials. The classical significance of a $\mu = 0.5$ condition in elastic materials is apparent from equation 3.3. Substituting $\mu = 0.5$, gives the Dilation (4) equal to zero, i.e. $\Delta V/V = 0$, i.e. $\Delta V = 0$, which means that no volume change occurs

under r/

*Ref.2, p.52 and p.1-63

†Ref.2, p.54-57.

‡One instance was found(5.1) where Terzaghi mentions $\mu > 0.5$, but this was in connection with conditions existing when the material approached a state of failure, i.e. conditions outside the elastic range.

under the action of applied stresses. For the case where ϵ_1, ϵ_2 and ϵ_3 are negative (i.e. applied compressive stresses) and $\mu = 0.5$, the material is said to be incompressible. Practical materials of this type are not uncommon, rubber being probably the best example (see Section 3.5).

Regarding the physical implications of a condition $\mu > 0.5$: It can be seen from Equation 3.3 that if $\mu > 0.5$, then $\delta V/V$ is negative, i.e. δV is negative, which implies that the material has suffered a volume decrease under the action of positive tensile stresses, or alternatively, the material has suffered a volume increase under the action of applied compressive stresses. It is inconceivable that either of these conditions can occur in practice under elastic conditions. All known materials show a volume decrease under compressive loading, and it will be shown (see discussion in Chapter 10) that soil over the linear range of the stress-strain curve is no exception. Further, as pointed out by Searle, $\mu > 0.5$ would render either the Bulk Modulus (K) or the Modulus of Rigidity (G) negative, and as already discussed, both K and G can only be positive for elastic materials.

Other examples such as a consideration of an isotropic elastic prism resting on a perfectly frictionless base as discussed by Terzaghi (8.3), also lead to impossible situations in the case of elastic materials. In the case mentioned, Terzaghi considers the 4 vertical sides of the isotropic, elastic prism to be confined between perfectly smooth vertical walls such that no lateral strain can occur due to the self weight of the material. From this condition he subsequently derives the relation

$$\frac{\delta h}{\delta z} = \frac{\mu}{1-\mu} = K_0 \dots\dots\dots 3.7$$

where K_0 in the theory of earth pressure is known as the "coefficient of earth pressure at rest", and is such that no lateral strains develop. If, in the above equation 3.7, $\mu > 0.5$, then $K_0 > 1$, which means that the lateral pressure δh induced by the vertical self weight of the material is greater than the vertical pressure itself due to the self weight. Such a condition is unknown in the case of elastic materials. In fact, $\mu = +1$ gives $K_0 = \infty$, which is clearly an impossible condition.

It therefore seems reasonable to conclude that there is an upper limit for elastic, isotropic materials, Poisson's Ratio cannot exceed 0.5.

In considering now the possible lower limit of Poisson's Ratio, the significance of a $\mu < 0$ condition will briefly be investigated. Firstly, as Searle pointed out, if μ is negative, it must have a lower limit of -1, since μ less than -1 would again render either the Bulk Modulus (K) or the Modulus of Rigidity (G) negative which is an impossible condition. Further, the physical implications of a negative Poisson's Ratio are apparent from a consideration of Poisson's Ratio itself in the first instance. From its definition, Poisson's Ratio is the ratio of the lateral contraction:longitudinal extension which is observed in the case of a bar of elastic material subjected to axial tensile loading, or the reversed conditions in the case of axial compressive loading. In both cases the lateral and longitudinal strains are considered to have the same algebraic signs, so that μ is always positive. A negative Poisson's Ratio would thus mean that either the sign of the lateral contraction is negative, which implies a lateral expansion accompanying a longitudinal extension; or, the sign of the longitudinal extension is negative, which implies a longitudinal contraction accompanying a lateral contraction. Both these concepts are inconceivable for any practical elastic material.

Also/

Also in the case of Terzaghi's isotropic elastic prism confined between perfectly smooth vertical walls, an impossible condition arises if μ is negative. From equation 3.7 again, if μ were negative, E would be negative, i.e., E is negative, since the vertical pressure due to the self weight of the material always acts down and is therefore always positive according to the sign convention used. A negative E implies that instead of the sides of the prism being acted upon by a lateral pressure due to the confining vertical walls which prevent lateral strain from occurring, the sides of the prism are acted upon by a lateral tension which prevents lateral expansion. This again is clearly an impossible condition.

Hence, it seems reasonable to conclude that Poisson's Ratio in practice cannot be negative for elastic, isotropic materials.

However, as previously mentioned, both Terzaghi and Taylor consider $\mu = 0$ to be the lower limit of Poisson's Ratio for elastic, isotropic materials. Poisson's Ratio equal to zero means that either, a longitudinal extension is accompanied by no lateral contraction; or, a longitudinal contraction is accompanied by no lateral expansion. Both conditions are not uncommon in practice. They usually occur where lateral expansion under compressive stress is completely prevented in one or other way. The laboratory oedometer test is a good example of this condition (see Section 6.3). In addition, literature will mention that Poisson's Ratio for cork can be taken as equal to zero, while the value for concrete is also close to zero, viz. in the range 0.001-0.125.

Hence, it seems reasonable to accept a value of zero as the lower limit of Poisson's Ratio, and it can therefore be concluded that for anisotropic, isotropic, elastic materials, Poisson's Ratio falls within the range zero-0.5.

3.3 Values of Poisson's Ratio for Practical Materials

It is of interest to note the following table of values of Poisson's Ratio, μ , Modulus of Elasticity E , & value of Rigidity G , and Bulk Modulus K , given by Faye and Leby (10) for various materials, which are however mainly metals. Both calculated and observed values are given for μ and G ; in the case of G , calculated values were obtained by using observed values of E and μ in equation 3.5 of present work. This equation can be rewritten:

$$\mu = \frac{E}{2G} - 1 \quad \dots\dots\dots 3.5(a)$$

and hence, using observed values of E and G , calculated values of μ were obtained. The Bulk Modulus K was obtained by calculation only, by using equation 3.1 of previously. The Authors mention also that the extent of the agreement between the calculated and observed values of μ and G , gives an indication of the degree of isotropy of the material.

Table I/

TABLE 3

MATERIAL	POISSON'S RATIO μ		YOUNG'S MODULUS E (10 ¹⁰ dynes/cm ²)	MODULUS OF RIGIDITY G (10 ¹⁰ dynes/cm ²)		BULK MODULUS K (10 ¹⁰ dynes/cm ²)
	OBSERVED	CALCULATED		OBSERVED	CALCULATED	
Aluminum (Worked)	0.33	0.310	7.06	2.61	2.63	7.46
Copper (Worked) pure	0.337	0.336	12.3	4.55	4.55	13.1
Gold (Worked) pure	0.412	0.415	8.0	2.77	2.80	16.6
Steel (Worked) 1 C	0.287	0.287	30.2	8.12	8.12	16.4
Lead (Cast) pure	0.446	-	1.0	-	0.562	5.00
Palladium (Cast) pure	0.393	0.310	11.3	5.11	4.04	17.2
Platinum (Cast) pure	0.387	0.360	10.8	6.10	3.04	24.7
Silver (Worked) pure	0.372	0.36	7.10	2.87	2.84	10.4
Tin (Cast) pure	0.35	-	5.4	-	2.04	11.39
Brass (Cast) 1	0.358	0.37	9.0	3.44	2.97	9.22
Constantin (Worked) *	0.325	0.320	16.6	6.18	6.11	13.8
Wrought iron (Worked) +	0.299	0.308	12.4	4.65	4.65	12.1
Zinc 1% P	0.21	-	8.7	3.8	-	-
Rubber (soft, vulcanized)	0.46-0.49	-	0.10-0.70	0.00016	-	-
Jena Glasses (crystal)	0.20-0.27	-	5.5-7.9	2.6-3.2	-	4.0-5.9
Jena Glasses (flint)	0.22-0.25	-	5.0-4.0	2.0-2.5	-	3.6-3.8

* 85 Cu, 7.2 Zn, 6.4 Sn; 60 Cu, 40 Ni
 + 84 Cu, 12% Ni, 4 Ni; 60 Cu, 40 Ni

15

In addition to the values of Poisson's Ratio given in the above Table (which are mainly for metals), the following values are available for materials other than metals: As mentioned at the end of the previous Section, Timoshenko(2.1) states that Poisson's Ratio for cork can be taken as equal to zero, while the value for concrete is in the region 0.033-0.125. Further, Krynin and Juad(7) give the following values of Poisson's Ratio for various rock types: Granite 0.18-0.24, limestone 0.18-0.23, schist 0.08-0.20, marble 0.22-0.30; and, from isolated tests, the value for granite is 0.11, monzonite 0.17, sandstone 0.17 and tuff 0.11.

CHAPTER 4

POISSON'S RATIO IN RELATION TO ELASTIC STATES OF STRESS AND STRAIN

4.1 Introduction

For a body in equilibrium under the action of external forces, 6 stress components are necessary (3.2) to define the state of stress at any point in the body completely. With reference to a rectangular system of coordinates Ox, Oy and Oz , these stresses are the normal stresses $\sigma_x, \sigma_y, \sigma_z$, and the shearing stresses $\tau_{xy} = \tau_{yx}, \tau_{xz} = \tau_{zx}, \tau_{yz} = \tau_{zy}$. Similarly also, 6 strain components are necessary (3.3) to define the state of strain at any point of the body completely. These are the unit strains in the three perpendicular directions $\epsilon_x, \epsilon_y, \epsilon_z$, and the unit shear strains $\gamma_{xy}, \gamma_{yz}, \gamma_{zx}$ related to the same directions.

Under two types of conditions, however, the number of stress and strain components necessary to define the states of stress and strain at a point completely reduce to only 3 in each case. These two conditions are known as a state of plane stress and a state of plane strain respectively, and in each case the stress distribution problem is reduced to a 2-dimensional problem of elasticity.

4.2 Plane Stress and Plane Strain (3.3)

If a thin plate is subjected to the action of forces applied at the boundary, parallel to the plane of the plate and distributed uniformly over its thickness (Fig. 4.1), the stress components $\sigma_y, \tau_{xy}, \tau_{yz}$ are zero on both surfaces of the plate, and without

Fig. 4.1



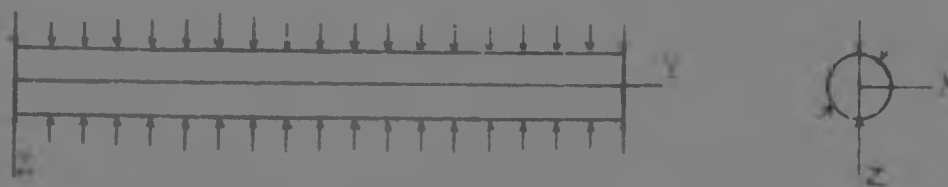
substantial error it can be assumed that these components are zero throughout the thickness of the plate. This condition constitutes a state of plane stress distribution. For its solution, a problem of plane stress therefore requires the determination of only three stress components: σ_x, σ_y and τ_{xz} . It should be noted, however, that the fact that the stresses $\sigma_y, \tau_{xy}, \tau_{yz}$ are zero on cross-sections perpendicular to the Y -axis of the plate, does not necessarily mean that the corresponding strains ϵ_y, γ_{xy} , and γ_{yz} are zero, since Poisson's Ratio effects occur as a result of the stresses which are not zero.

The same simplification of the problems in the case of thin plates is encountered when one goes to the other extreme in which the dimension of the body in the Y -direction is very large. If a long cylindrical or prismatic body be subjected to the action of forces uniformly distributed along its length and in the plane of cross-sections perpendicular to its axis (Fig. 4.2), the displacements during deformation at a considerable distance from the ends, occur only in planes perpendicular to the axis of the body, and the strain components ϵ_y, γ_{xy} , and γ_{yz} are zero. This condition is known as a state of plane strain.

Furthermore/

Furthermore, the shearing stresses τ_{xy} and τ_{yz} , which are proportional to ϵ_{xy} and ϵ_{yz} are also zero, while, since $\epsilon_z = 0$, the normal stress σ_y (which is not equal to zero) can readily be expressed in terms of σ_x and σ_z by applying basic principles of stress and strain. A problem of plane strain is therefore reduced, as in the case of problems of plane stress, to the determination of only three stress components: σ_x , σ_z and τ_{xz} , and

Fig. 4.2



hence, in both cases, the problem of stress and strain reduces to a problem in 2-dimensions. It should also be noted in the case of problems of plane strain, that conditions are not altered in any way if a uniform extension in the direction of the axis of the body is superimposed upon the state of plane strain. Furthermore, the fact that the three strains mentioned (ϵ_y , ϵ_{xy} , ϵ_{yz}) are zero, constitutes an enforced condition due to the length of the body, in which the three normal stresses σ_x , σ_y , σ_z acting over cross-sections normal to the axis of the body, serve to maintain the state of plane strain.

These two conditions of plane stress and plane strain therefore constitute 2-dimensional problems in the theory of elasticity, and in all such cases the determination of stress and strain in elastic bodies is considerably simplified.

4.3 The Moduli of Elasticity in relation to States of Plane Stress and Plane Strain

In dealing with the problem of an elastic, isotropic solid in equilibrium under given body and surface forces, Michall⁽¹⁾ treats the following two 2-dimensional cases:

- (a) That of a long cylinder with applied forces perpendicular to its length and the same at corresponding points along its length (a case of plane strain),

and (b) that of a thin plate with applied forces in its plane (a case of plane stress).

He determines the stress function which satisfies the equations of equilibrium and the boundary conditions in each case, and then shows that if the body forces are zero, the stresses in the solids are independent of the moduli of elasticity provided the resultant force on each boundary vanishes. He also points out that where there is a single boundary (such as in the case of a semi-infinite solid), this latter condition is always satisfied and the stresses are therefore always independent of the moduli of elasticity in this case, provided there is no body force. His final conclusions are that the stress distribution in elastic isotropic bodies for the cases considered (cases of plane stress and plane strain) are independent of the moduli of elasticity if, firstly, body forces are absent, and secondly, the boundary is simply connected. If the boundary is multi-connected, such as in the case of a perforated body, the stresses are independent of the moduli of elasticity only if the resultant force on each boundary separately vanishes.

It thus appears that in 2 dimensional problems (cases of plane stress and plane strain) wherein the stress distribution in a semi-infinite, elastic, isotropic solid is required (the case of a single or simply-connected boundary), the stress distribution is independent of the moduli of elasticity provided the body forces (such as the self weight of the material) are disregarded.

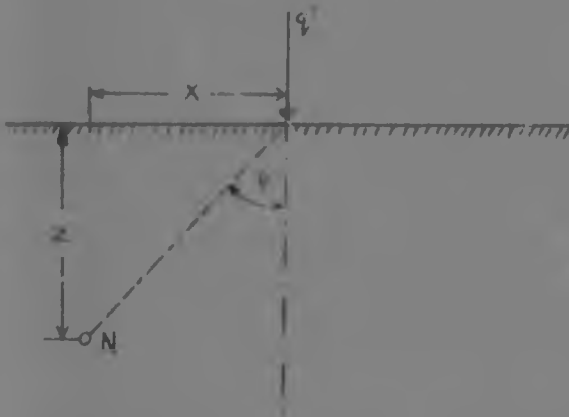
It is of interest to note (3.5) that Michell's conclusion is of great practical importance in cases where the photo-elastic method of stress analysis is used, since it enables experimental results obtained with transparent materials to be applied immediately to any other material such as steel if the external forces are the same.

4.4 Poisson's Ratio in relation to States of Stress and Strain in a Semi-infinite Elastic Solid

With a view to the later discussion of the application of the elastic theory to soils which, for such purposes, are generally considered to be semi-infinite in extent, certain 2-dimensional and 3-dimensional problems of stress and strain in a semi-infinite elastic solid will be reviewed in this Section.

Firstly, there is the case of an infinitely extended line load of constant magnitude per unit length on the surface of a semi-infinite elastic solid (Fig. 4.3). From the discussion in the previous Section, it is clear that this loading condition produces a state of plane strain in the solid, and the problem is therefore essentially a 2-dimensional one. This case was originally dealt with in a paper by Flamant (12) in which he outlines the derivation of the mathematical expressions for the stresses induced at any point in the solid due to such applied loading. These expressions have also been given in polar coordinates by Terzaghi (8.4) as follows (cf. Fig. 4.3):

Fig. 4.3



$$\sigma_z = \frac{2}{\pi} \cdot \frac{q'}{x} \cos^3 \psi \quad \dots\dots\dots 4.1$$

$$\sigma_x = \frac{2}{\pi} \cdot \frac{q'}{x} \cos^2 \psi \sin^2 \psi \quad \dots\dots\dots 4.2$$

$$\tau_{xz} = \frac{2}{\pi} \cdot \frac{q'}{x} \cos^3 \psi \sin \psi \quad \dots\dots\dots 4.3$$

where q' is the load per unit length of the straight line. It should be noted as discussed in Section 4.2, that due to the state of plane strain, only three stress components appear in this case. Furthermore, it should be noted that the equations do not contain Poisson's Ratio for the reasons discussed in Section 4.3

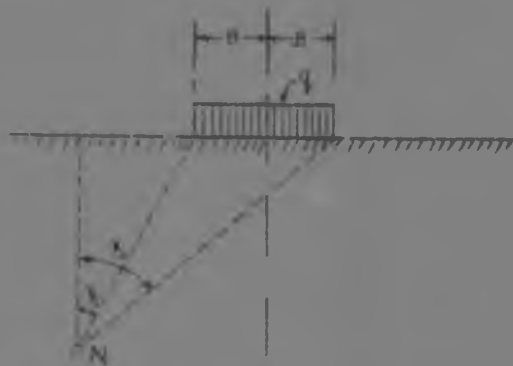
In the latter connection, it is of interest to note how Poisson's Ratio becomes eliminated from the basic expressions

of...../

of equilibrium in Flamant's original paper during his derivation of the equations 4.1, 4.2 and 4.3 given above. The actual steps in the final reduction of his mathematical expressions from which this is apparent have not been given in the paper, but are given in Appendix II of this paper.

Secondly, there is the case of a strip load of infinite extent and constant (finite) width on the surface of a semi-infinite elastic solid (Fig. 4.4). This problem was solved by Michell(13) and is actually only an extension of the problem solved by Flamant which was discussed above. It is therefore another 2-dimensional problem. The solution is obtained by integration of the basic expressions for the case of a straight line load of constant magnitude and of infinite extension on the surface of a semi-infinite solid. Terzaghi(8.4) gives these expressions for the stresses at any point in the semi-infinite solid as (cf. Fig. 4.4):

Fig. 4.4



$$\sigma_z = \frac{q}{\pi} \left[\sin \psi \cos \psi + \psi \right]_{\psi_1}^{\psi_2} \dots\dots\dots 4.4$$

$$\sigma_x = \frac{q}{\pi} \left[-\sin \psi \cos \psi + \psi \right]_{\psi_1}^{\psi_2} \dots\dots\dots 4.5$$

$$\tau_{xz} = \frac{q}{\pi} \left[\sin \psi \right]_{\psi_1}^{\psi_2} \dots\dots\dots 4.6$$

where q is the load per unit of area on the strip. It is clear that, for the same reasons as discussed in the case of the first 2-dimensional problem considered above, these expressions also only comprise 3 stress components which do not contain Poisson's Ratio.

Other 2-dimensional problems of stress and strain, such as those solved by Carothers(14) and Jurgenson(15), follow the same pattern as the two cases dealt with above, in that for the complete determination of stress and strain, expressions for only the three stress components σ_z , σ_x and τ_{xz} are required, all of which do not contain Poisson's Ratio.

However, the case of a vertical point load applied to the horizontal surface of a semi-infinite elastic solid (Fig. 4.5), which was originally solved by Boussinesq(16), is a 3-dimensional problem of stress and strain. The expressions for the stresses at any point in the solid therefore actually comprise 6 stress components in this case, but due to radial symmetry the vertical component (τ_{tz}) and the horizontal component (τ_{tr}) of shearing stress on radial planes (see Fig. 4.5) are each equal to zero and only 4 stress components are therefore involved. The relevant expressions only are given by both Taylor(1.3) and Terzaghi(8.5), but their derivation has been outlined again in full by Timoshenko(3.7). The expressions are as follows:

$$\sigma_z = \frac{Q}{2\pi} \frac{3z^3}{(r^2 + z^2)^{5/2}} = \frac{Q}{2\pi z^2} (3\cos^3\theta) \dots\dots\dots 4.7(a)$$

and. 4.7(b)

$$\sigma_r = \frac{Q}{2\pi} \left[\frac{3r^2z}{(r^2 + z^2)^{5/2}} - \frac{1 - 2\mu}{r^2 + z^2 + z\sqrt{r^2 + z^2}} \right] \dots\dots\dots 4.8(a)$$

$$= \frac{Q}{2\pi z^2} \left[3\sin^2\theta \cos^3\theta - \frac{(1-2\mu)\cos^2\theta}{1 + \cos\theta} \right] \dots\dots\dots 4.8(b)$$

$$\sigma_t = -\frac{Q}{2\pi} (1-2\mu) \left[\frac{z}{(r^2 + z^2)^{3/2}} - \frac{1}{r^2 + z^2 + z\sqrt{r^2 + z^2}} \right] \dots\dots\dots 4.9(a)$$

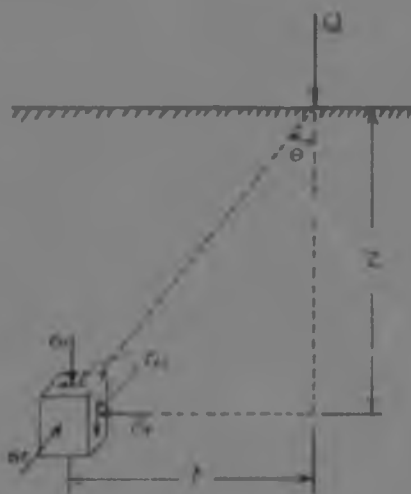
$$= -\frac{Q}{2\pi z^2} (1-2\mu) \left(\cos^3\theta - \frac{\cos^2\theta}{1 + \cos\theta} \right) \dots\dots\dots 4.9(b)$$

$$\tau_{rz} = \frac{Q}{2\pi} \frac{3rz^2}{(r^2 + z^2)^{5/2}} = \frac{Q}{2\pi z^2} (3\sin\theta \cos^4\theta) \dots\dots\dots 4.10(a)$$

and 4.10(b)

where Q in each case is the magnitude of the applied vertical point load. Poisson's Ratio does appear in the above expressions,

Fig. 1.5



although only in the case of certain stress components viz. σ_r and σ_t . This is the case since the moduli of elasticity affect the stress distribution in 3-dimensional problems.

Extensions of the abovementioned problem in the form of a uniformly distributed loading on a finite area such as a rectangular, square or circular area, also constitute 3-dimensional problems of stress and strain, and hence, the corresponding expressions for the stress components will also contain Poisson's Ratio in certain instances. Yet, according to Terzaghi(8.6), "the computation of the stresses (in such cases) are rather involved, and the results of the computation cannot be represented by a simple set of equations. However, the problem has been solved by Love(17) and the results have been compiled in tables which make it possible to determine the stresses at any point by means of a simple process of interpolation."

Both Terzaghi(8.6) and Taylor(1.3) point out, however,

that/

1000 UNITS OF FORCE

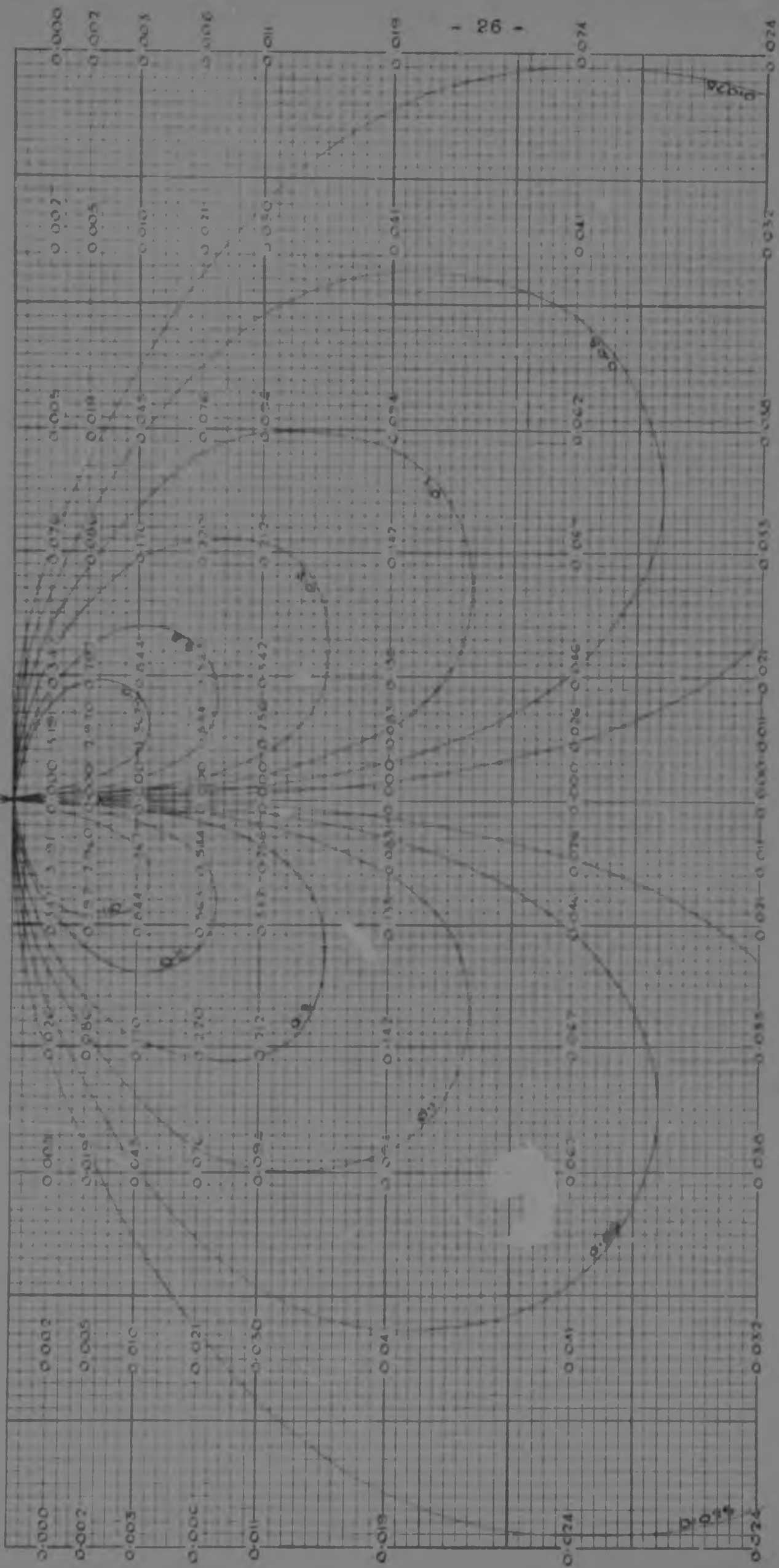
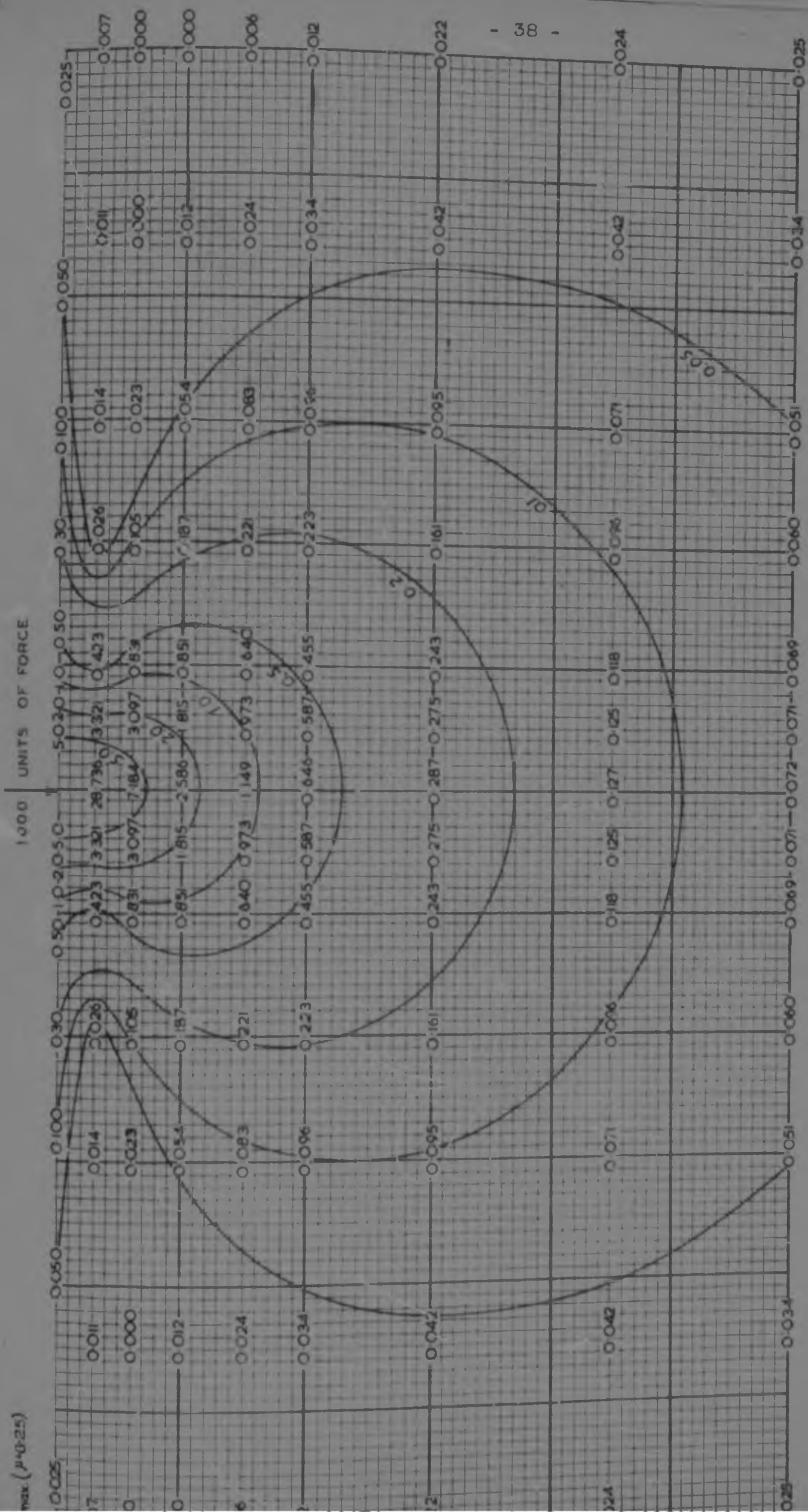
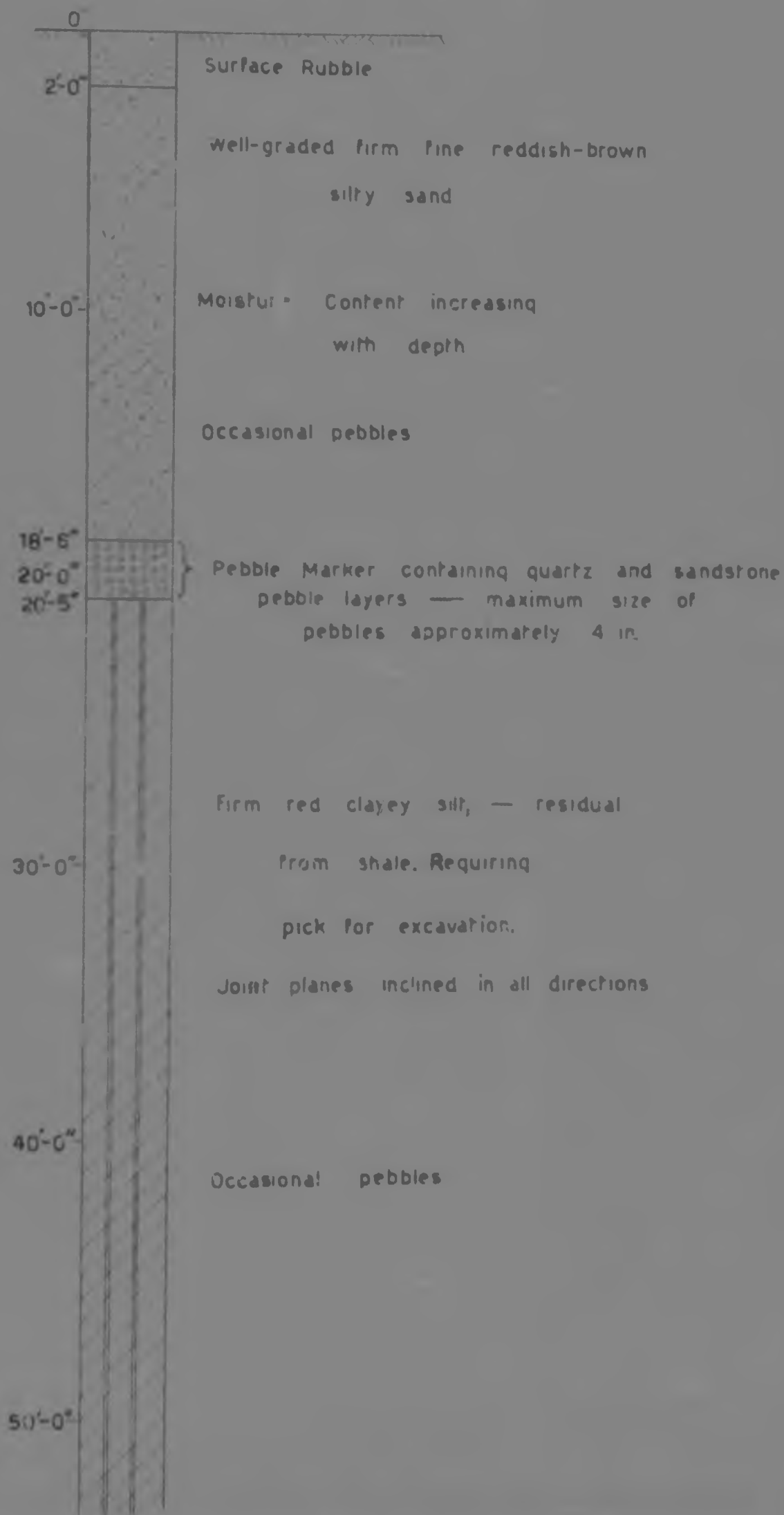


FIG. 2 - CONTOURS OF VERTICAL SHEAR STRESS (τ_{xz})

FIG. 2.



SOIL PROFILE ON THE NORTH SIDE OF JUTA ST. NEAR BICCARD ST., BRAAMFONTEIN, J'BURG.



Horizontal Radial Stress σ_r

$$\text{Equation: } \sigma_r = \frac{Q}{2H} \left[\frac{3r^2 z}{(r^2 + z^2)^{3/2}} - \frac{1 - \mu}{r^2 + z^2} \sqrt{r^2 + z^2} \right]$$

TABLE IV

Z	r	σ_r				
		$\mu = 0$	$\mu = 0.10$	$\mu = 0.20$	$\mu = 0.30$	$\mu = 0.05$
3	0	-0.412	+0.6314	-4.4210	-0.2105	0
	5	+2.1979	+2.9779	+3.7378	+1.5391	+1.3190
	10	+0.0131	+0.3024	+0.5873	+0.8722	+1.1555
	20	-0.1703	-0.0889	0	+0.0844	+0.1687
	30	-0.1017	-0.0663	-0.0271	+0.0127	+0.0532
	45	-0.0273	-0.0382	-0.0207	+0.0016	+0.0159
	60	-0.0310	-0.0281	-0.0143	-0.0032	+0.0084
5	0	-1.2107	-1.6484	-1.1045	-0.5523	0
	5	+0.7231	+1.3624	+1.7300	+2.0993	+2.4559
	10	+0.8570	+0.7486	+0.4438	+1.1364	+1.3289
	20	+0.0046	+0.0764	+0.1464	+0.2180	+0.2891
	30	-0.0485	-0.0111	+0.0258	+0.0605	+0.0932
	45	-0.0343	-0.0131	-0.0037	+0.0127	+0.0302
	60	-0.0271	-0.0175	-0.0064	+0.0032	+0.0127
10	0	-0.7988	-0.3866	-0.3979	-0.1989	0
	5	+0.0111	+0.1794	+0.3470	+0.5141	+0.6809
	10	+0.3772	+0.1734	+0.0112	+0.7273	+0.8635
	20	+0.1259	+0.1783	+0.0314	+0.2871	+0.3452
	30	+0.0144	+0.0246	+0.0742	+0.1050	+0.1353
	45	-0.0130	0	+0.0143	+0.0302	+0.0462
	60	-0.0189	-0.0084	+0.0032	+0.0111	+0.0207
15	0	-1.3113	-0.3843	-0.1769	-0.0891	0
	5	-0.1448	-0.0837	+0.0191	+0.1003	+0.1814
	10	+0.1089	+0.1731	+0.2419	+0.3088	+0.3754
	20	+0.1317	+0.1739	+0.2173	+0.2531	+0.2890
	30	+0.0041	+0.0280	+0.1035	+0.1273	+0.1512
	45	+0.0064	+0.0191	+0.0351	+0.0477	+0.0602
	60	-0.0048	+0.0032	+0.0127	+0.0207	+0.0256
20	0	-0.1249	-0.1447	-0.0977	-0.0493	0
	5	-0.1273	-0.0789	-0.0119	+0.0199	+0.0537
	10	+0.0013	+0.0435	+0.0452	+0.1150	+0.1703
	20	+0.0013	+0.1341	+0.1544	+0.1830	+0.2117
	30	+0.0037	+0.0820	+0.1035	+0.1286	+0.1416
	45	+0.0007	+0.0311	+0.0440	+0.0507	+0.0669
	60	+0.0032	+0.0111	+0.0173	+0.0235	+0.0334
30	0	-0.0001	-0.0804	-0.0446	-0.0223	0
	5	-0.0716	-0.0403	-0.0226	-0.0064	+0.0143
	10	-0.0366	-0.0182	+0.0032	+0.0239	+0.0440
	20	+0.0171	+0.0430	+0.0603	+0.0780	+0.0939
	30	+0.0014	+0.0141	+0.0604	+0.0812	+0.0939
	45	+0.0271	+0.0364	+0.0446	+0.0541	+0.0621
	60	+0.0143	+0.0207	+0.0285	+0.0318	+0.0382
45	0	-0.0348	-0.0302	-0.0191	-0.0095	0
	5	-0.0350	-0.0253	-0.0159	-0.0061	+0.0032
	10	-0.0246	-0.0191	-0.0095	0	+0.0095
	20	-0.0046	+0.0048	+0.0127	+0.0223	+0.0302
	30	+0.0111	+0.0191	+0.0285	+0.0334	+0.0414
	45	+0.0121	+0.0258	+0.0302	+0.0350	+0.0414
	60	+0.0143	+0.0191	+0.0223	+0.0271	+0.0318
60	0	-0.0223	-0.0159	-0.0111	-0.0064	0
	5	-0.0207	+0.0143	-0.0095	-0.0048	+0.0016
	10	-0.0191	-0.0127	-0.0080	-0.0032	+0.0032
	20	-0.0046	+0.0048	+0.0016	+0.0064	+0.0111
	30	-0.0000	+0.0048	+0.0095	+0.0143	+0.0191
	45	+0.0080	+0.0111	+0.0159	+0.0207	+0.0239
	60	+0.0111	+0.0143	+0.0175	+0.0207	+0.0239

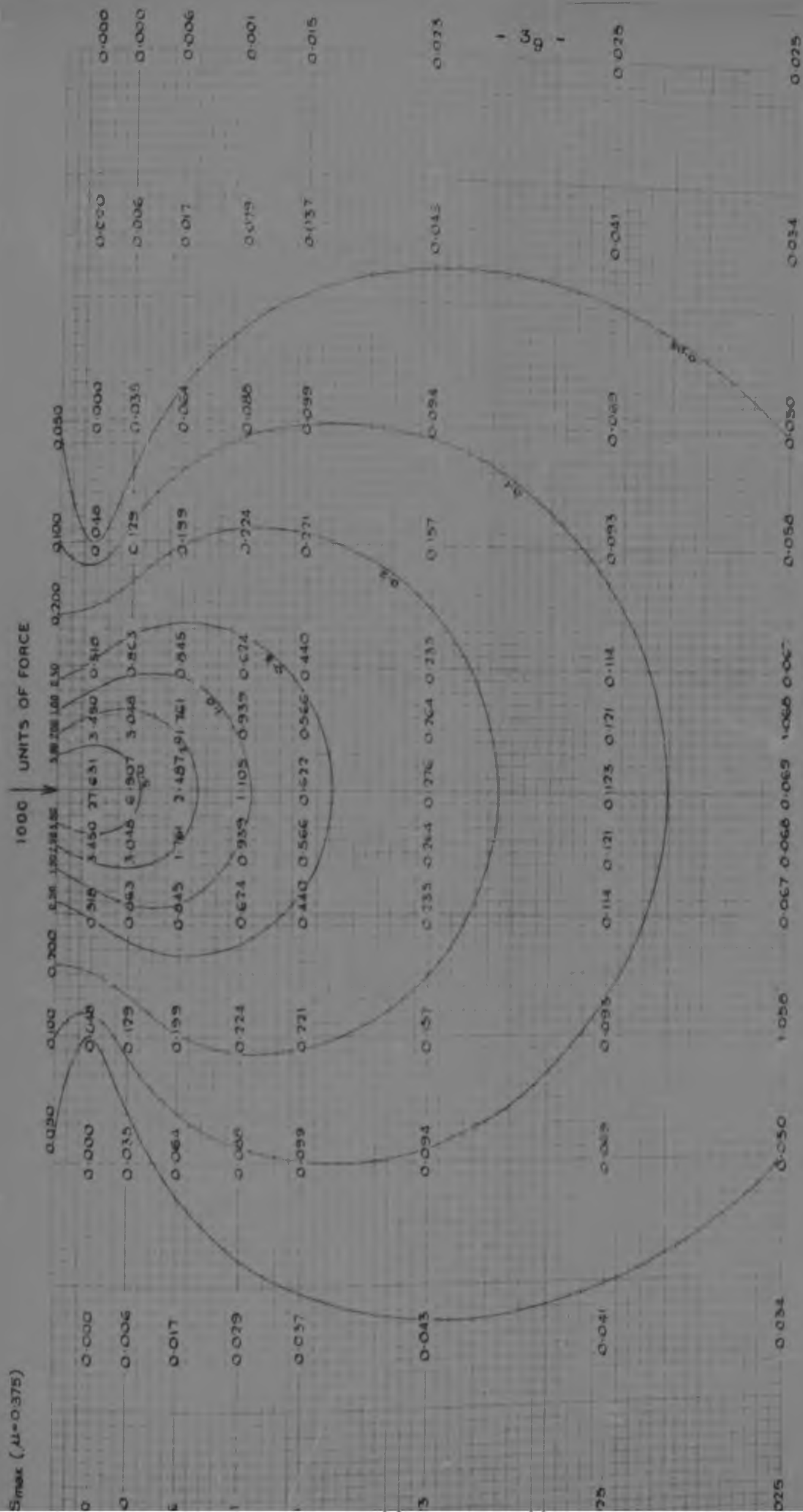


FIG 12 - CONTOURS OF MAXIMUM SHEAR STRESS (S_{\max}) FOR CONDITION $\mu = 0.375$

The results of various laboratory tests on the soil are tabulated below:

TABLE VII

Atterberg Limits	: Liquid Limit	: 25.2%
	: Plastic Limit	: 17.0%
	: Plasticity Index	: 8.2%
	: Linear Shrinkage	: 3.3%
Grading Analysis	: Gravel	: 8.5%
	: Sand	: 53.0%
	: Silt	: 30.0%
	: Clay	: 8.5%
Specific Gravity	:	2.62
Void Ratio	: (Undisturbed state):	0.70
Compression Index C_c	: " "	0.26

The soil appears to fall into the class ML of the Casagrande Airfield Soil classification and into the class A4 of the Public Roads classification. A full grading curve and a pressure : void ratio curve determined from a normal 1-dimensional consolidometer test, are shown in Figs. 17 & 18 respectively. The moisture content of the soil at the time of sampling in the field is not known, but would appear to have been approximately 30 (see Appendix IV, Fig.53), thus indicating a Degree of Saturation of approximately 11%.

7.3 Design of the Experimental Work

The aim of the experimental work was to determine Poisson's Ratio for the selected test soil by conducting a series of Consolidated Undrained Triaxial Shear Tests (C_u) with strain control on samples of the soil. The tests were to be according to British standard practice.

In view of previous discussions, this meant that the experimental work had to be designed to enable the measurement of the change in volume of a soil sample of known initial volume, due to a known change in stress within the linear range of the soil's stress:strain curve. The information thus obtained would then be used in equation 7.2 previously derived, to enable the evaluation of Poisson's Ratio for the soil.

When a soil sample is set up inside a triaxial test cell ready for test, there is a certain volume of cell fluid inside the test cell surrounding the specimen which is equal to the difference in volume between that of the soil sample and the internal volume of the test cell. Any change in volume of the soil sample must thus cause a flow of fluid either into or out of the cell, depending upon the type of volume change occurring in the sample, which is equal in volume to the change in volume of the soil sample, if the fluid is incompressible.

However, during an actual test, change in volume of the soil sample due to compressive loading is not the only cause of cell fluid entering or leaving the test cell. Entry of the loading spindle into the test cell causes a flow of fluid out of the test cell, while leakage from the test cell, usually where the loading spindle enters the test cell, causes a flow of fluid into the cell from the fluid reservoir.

If the flow of fluid either into or out of the test cell during test be accurately measured, this flow measurement will

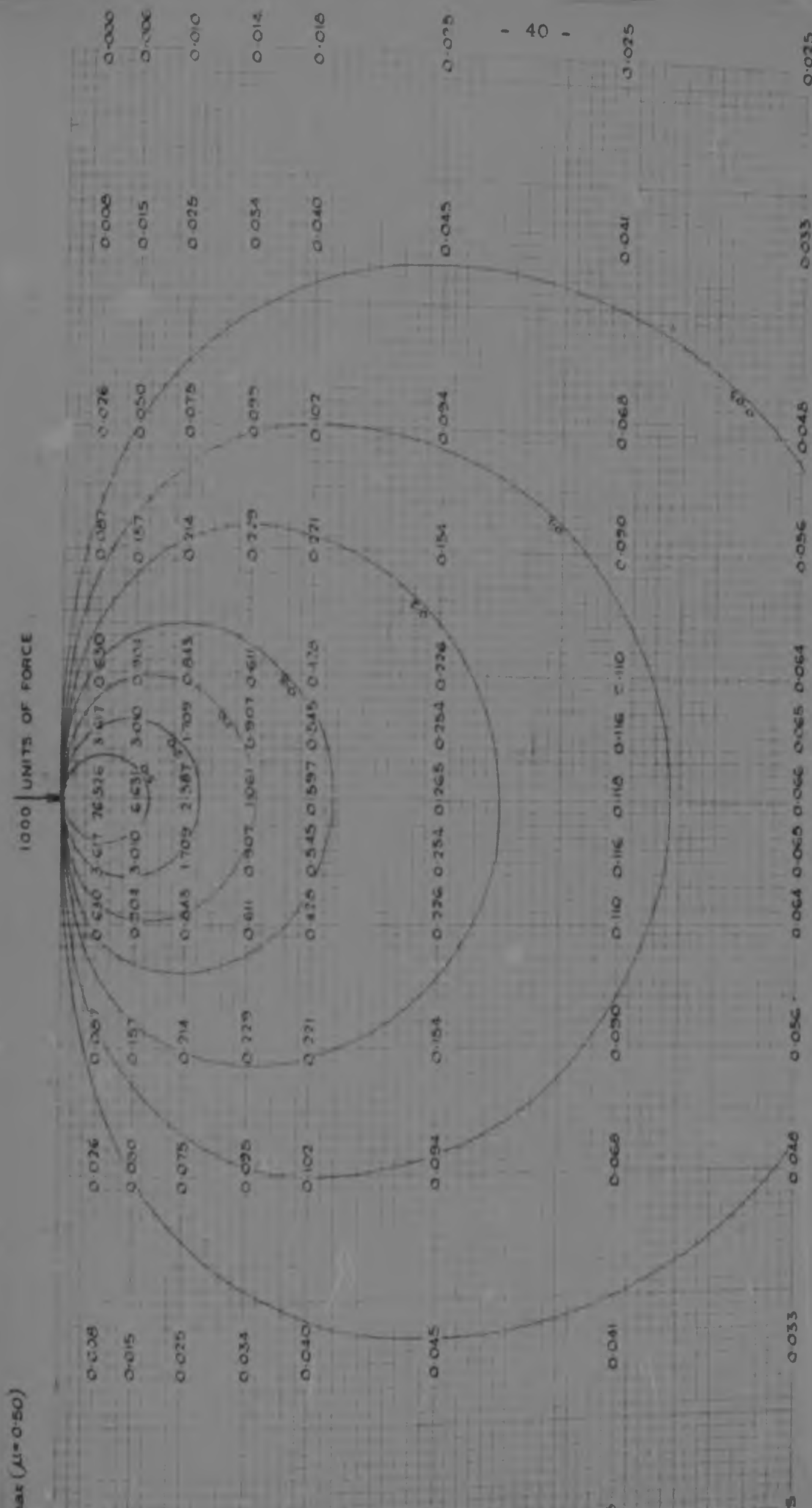


FIG 13 - CONTOURS OF MAXIMUM SHEAR STRESS (S_{max}) FOR CONDITION ($\mu=0.50$)

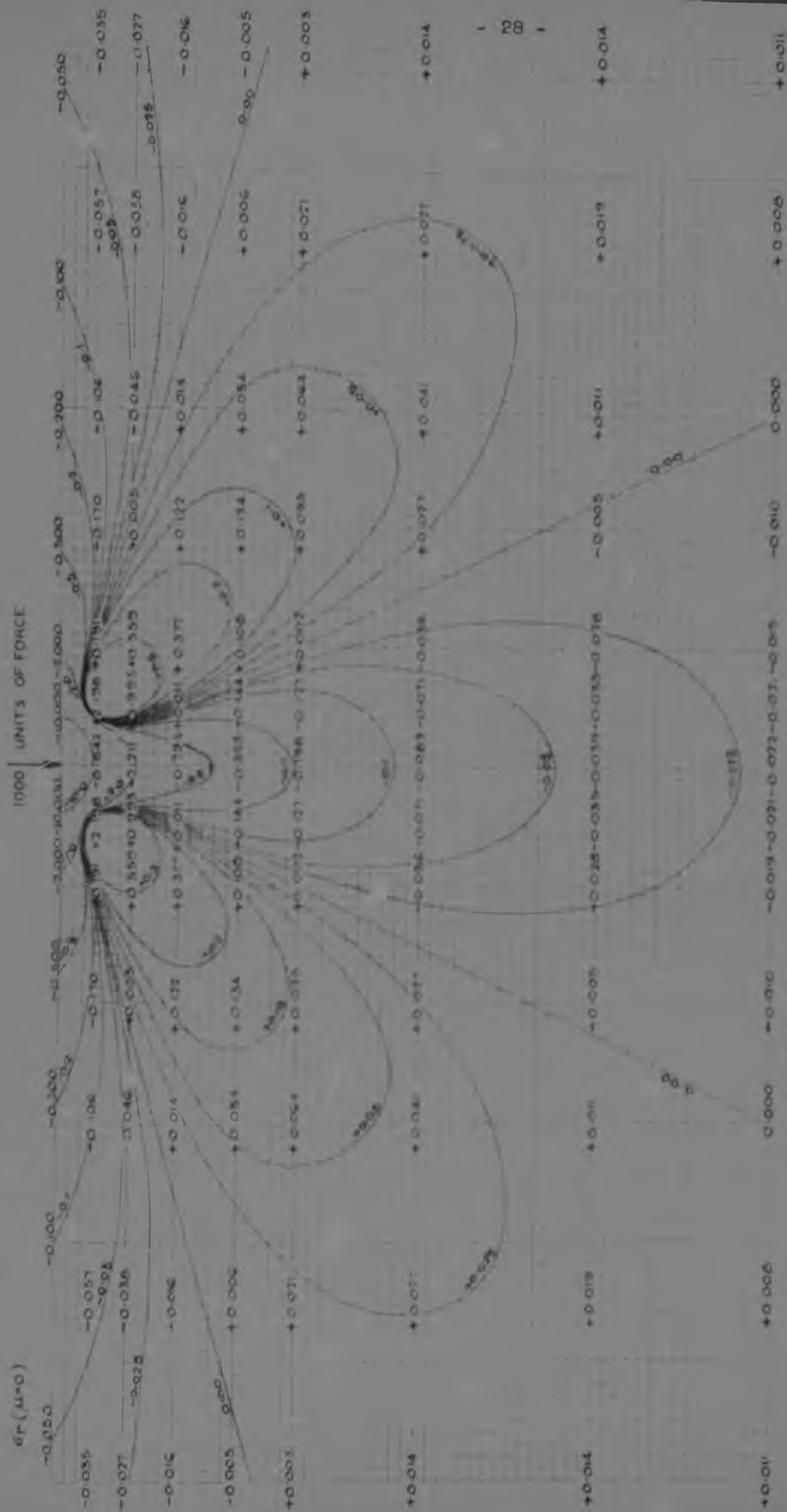
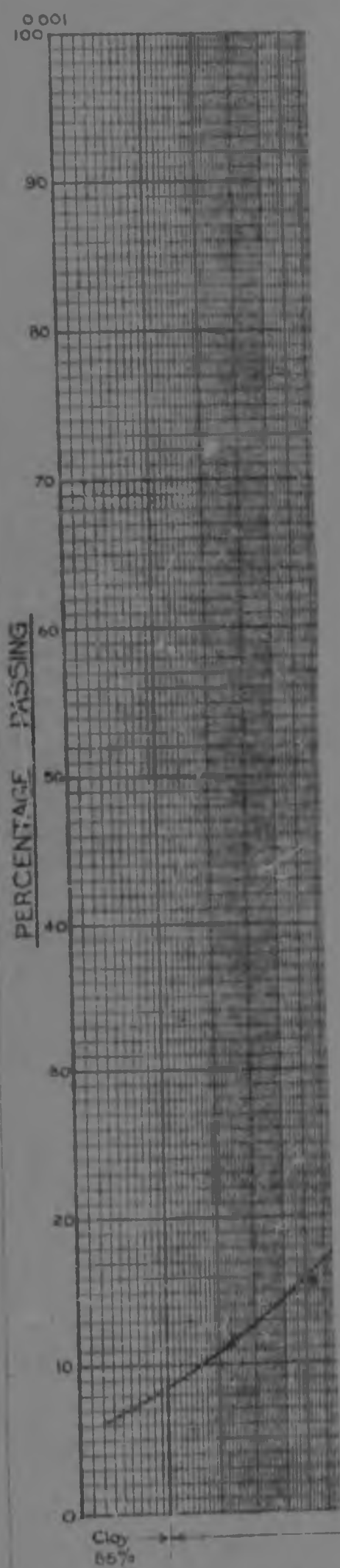


FIG. 3 - CONTOURS OF HORIZONTAL RADIAL STRESS (σ_r) FOR CONDITION $\mu=0$



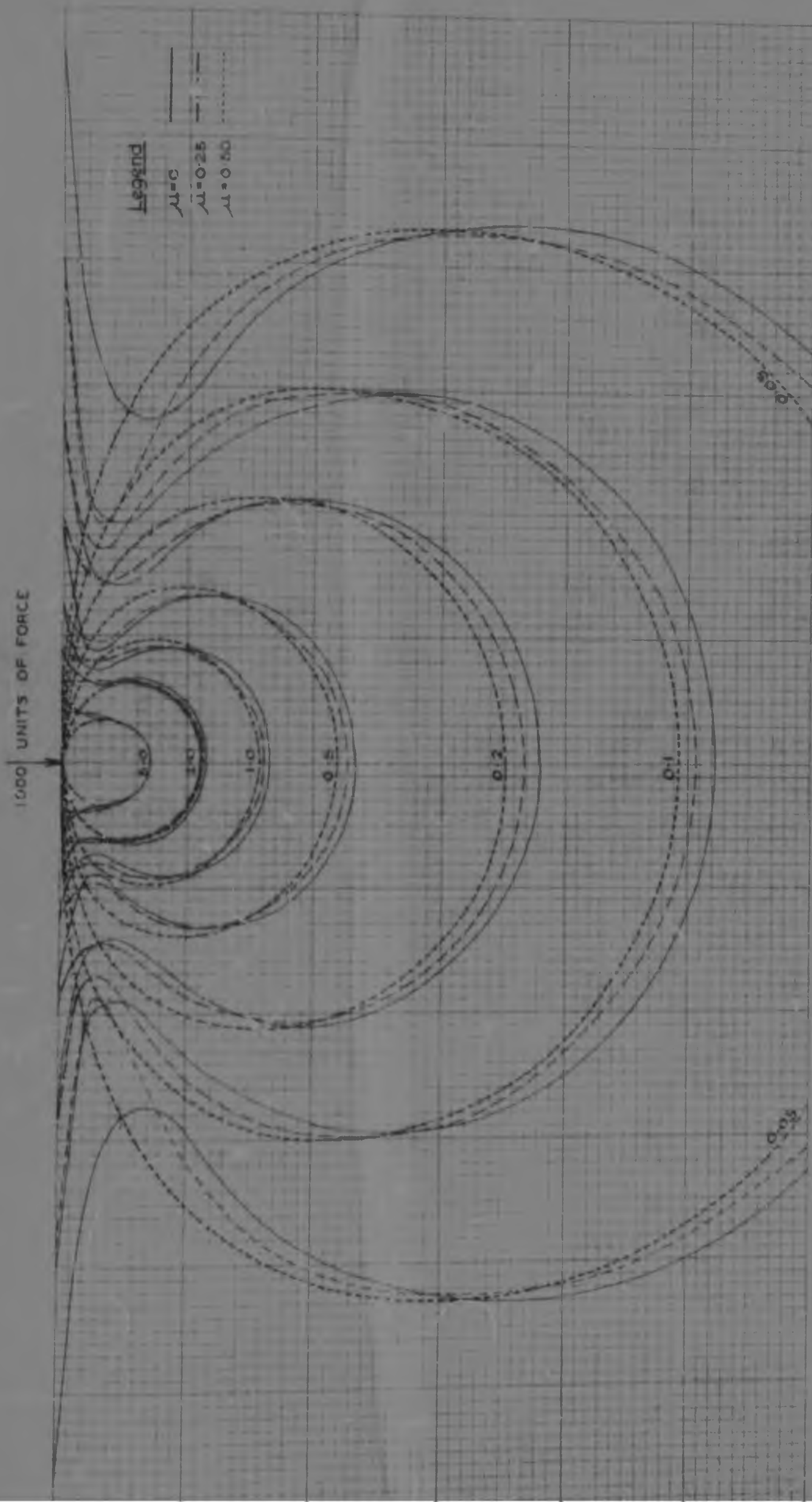


FIG 14 - COMBINED CURVES OF MAXIMUM SHEAR STRESS CONTOURS (S_{max}) FOR CONDITION $\mu=0, 0.25, 0.50$

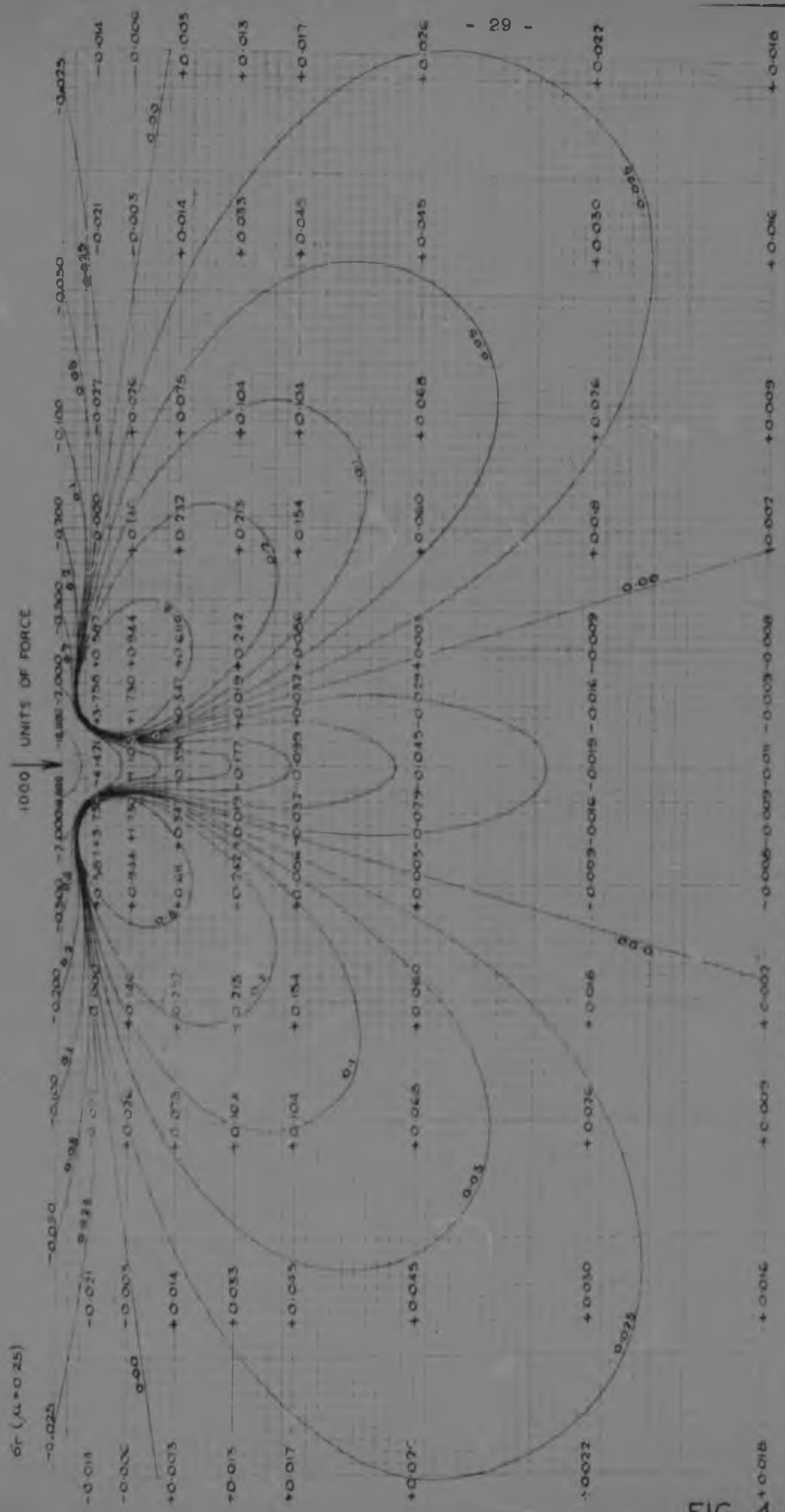


FIG. 4 - CONTOURS OF HORIZONTAL RADIAL STRESS (σ_r) FOR CONDITION $A_1=0.25$

be as a result of these three combined effects, and for any one of them to be known independently, both the other two effects need to be determined.

In this case, the flow of fluid as a result of volume change of the test sample only needs to be known, so that it is necessary to determine the flow of fluid during test resulting from the effect of leakage from the test cell and entry of the loading spindle into the test cell.

The latter effect mentioned can be determined by calculation from a knowledge of the cross-sectional area of the loading spindle and the distance advanced into the test cell. If leakage effects can be totally eliminated, there would be no further difficulty in determining the nett flow of fluid as a result of volume change of the sample only.

However, if leakage cannot be eliminated completely, as is more likely to be the case, a separate determination of the fluid flow into the test cell to replace leakage will be necessary.

Thus, the experimental work was designed to enable accurate measurements of the flow of fluid into or out of the test cell during test, due to the combined effects of leakage, spindle entry and sample volume change as well as independent measurements of the flow of fluid due to the effects of leakage and spindle entry only.

7.4 The Test Apparatus

This consisted of a standard model Triaxial Compression Test Machine designed for testing 1 1/2" dia. x 3" length samples in a 3" dia. cell. The cell fluid was a mixture of glycerine and water in the ratio 30% : 70% by volume. Besides the usual pressure gauge on which the chamber pressure developed by pumping the for pump could be read off directly, an adjustable head of mercury was connected to the bottom of a second 3" dia. cell, which was connected in series with the test cell and the fluid reservoir at the base of the machine, and was acting as an intermediate fluid reservoir. Hence, by measuring the height of the mercury column, a more accurate determination of the particular pressure selected for a test could be made.

The triaxial machine was operated by an electric motor through a variable speed gearbox, thus enabling the selection of one of several different rates of loading for any particular test. Values of applied load and deflection could be read off the respective dial deflection gauges provided for the purpose.

To enable the measurement of fluid flow into or out of the test cell during test, a circuit containing a small diameter capillary tube (approx. 1.6mm), fixed to a scale graduated in millimeters and containing a mercury slug of about 13mm. length, was connected in parallel with the main test cell fluid supply line between the intermediate fluid reservoir and the test cell. Suitable stopcocks were provided so that either of or both the capillary tube circuit and the main fluid supply circuit could be put into use as desired. Fluid flow measurements could then be effected by cutting in only the capillary tube circuit, whence any movement of fluid into or out of the test cell, would be directly indicated by the movement of the slug, excepting that the fluid is incompressible. The arrangement of the various circuits in the test set up is shown in Fig. 19.

The arrangement of the test system was such that it was

found/

2. Vertical Shear Stress τ_{rz} : (a) and (b) as above in (1).
3. Horizontal Radial Stress σ_r : (a) Stress data for 5 values of μ in tabular form.
(b) Stress contour diagrams for conditions: $\mu=0$, 0.25 and 0.50.
4. Horizontal Tangential Stress σ_t : (a) as above in (3).
(b) Stress contour diagrams for conditions: $\mu=0$, 0.25 and 0.375.
5. Curves of horizontal stresses σ_r and σ_t versus Depth on the Axis of Loading, for conditions: $\mu=0$, 0.125, 0.25, 0.375 and 0.50.
6. Maximum Shear Stress (S_{\max}): (a) as above in (3).
(b) Stress contour diagrams for conditions: $\mu=0$, 0.25, 0.375 and 0.50.
7. Combined curves of Maximum Shear Stress contours for conditions: $\mu=0$, 0.25 and 0.50.
8. Curves of Maximum Shear Stress (S_{\max}) versus Depth on the Axis of Loading, for conditions: $\mu=0$, 0.25 and 0.50.

The following points with regard to the various diagrams should, however, be noted. Firstly, in the case of item (4) above, stress contour diagrams for three values of Poisson's Ratio ($\mu=0$, 0.25 and 0.375) are given in this section — but for the condition $\mu=0.50$, $\sigma_t = \sigma_r$ (see also Discussion: Section 2.3) and hence, the stress contour diagram vanishes for $\mu = 0.50$. Secondly, regarding item (5), the values of the horizontal stresses σ_r and σ_t are equal on the axis of loading for the same values of Poisson's Ratio (and Section 2.3), and hence the curves shown in Fig. 9 are the same for both σ_r and σ_t versus depth on the axis of loading. Further, it needs to be mentioned that in the case of the stress contour diagrams for σ_r , σ_t and S_{\max} , contour lines were frequently found to intersect the horizontal surface $z = 0$ of the semi-infinite solid. In these cases it was possible to calculate the exact position of the point of intersection of any stress contour line with the surface $z = 0$ from equations obtained by rewriting in each case the relevant stress component expression in a suitable form and at the same time applying the condition $z = 0$. The procedure and actual calculations are detailed in full in Appendix III Item 2.

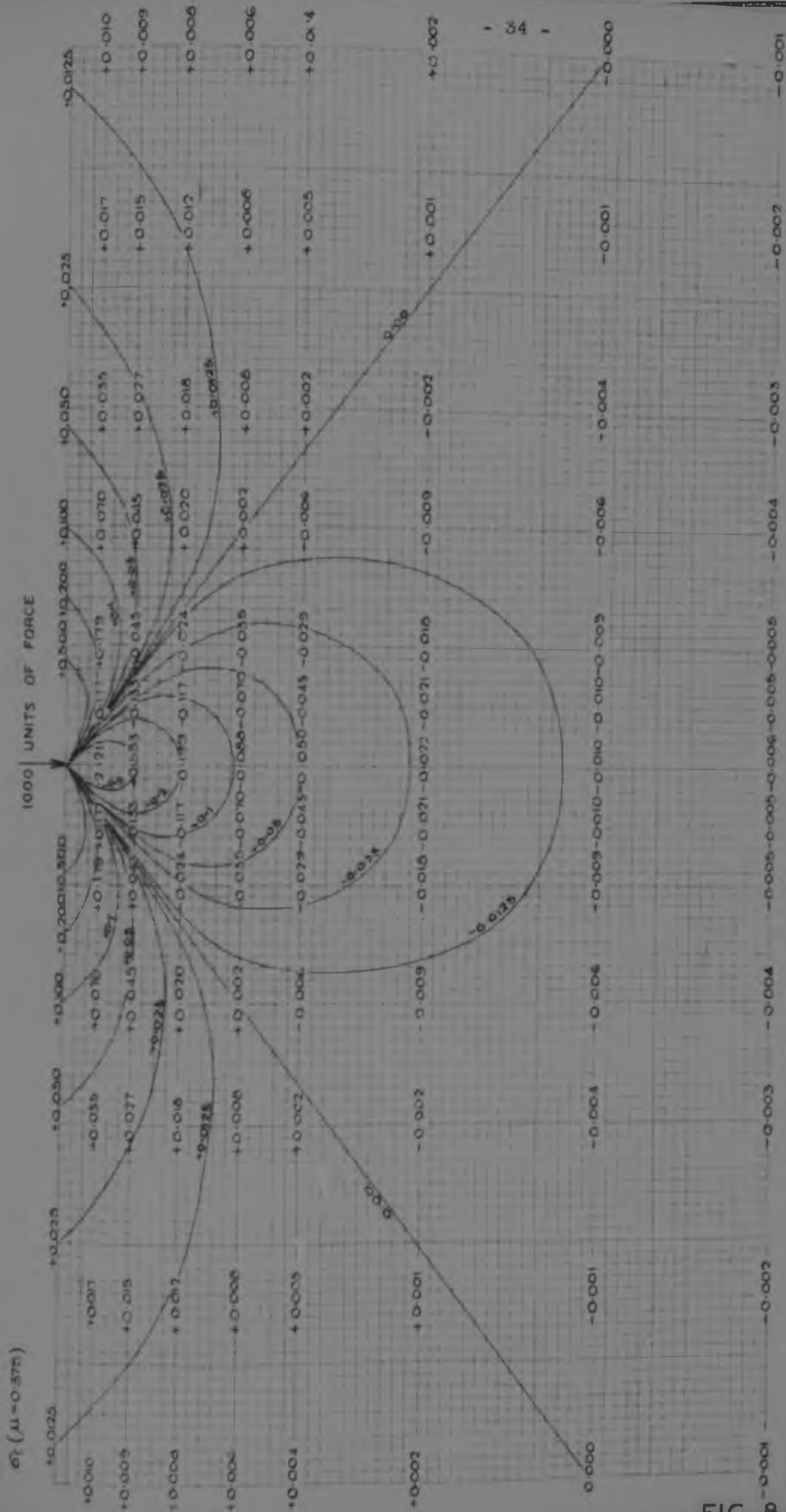


FIG 8 - CONTOURS OF HORIZONTAL TANGENTIAL STRESS (σ_t) FOR CONDITION $\mu=0.375$

extrusion of some of the pore water from the clay (and hence with volume decrease).

It should be noted that it is generally recognized (5) that due to the low compressibility of clay soils, the consolidation process does not proceed immediately after the application of loading and that during this time delay the soil is subjected to lateral expansion. However, the statement that the lateral expansion of the soil occurs without change in water content is the case of a saturated soil, on a broader basis, actually implies that there is no loss of water from the soil while the settlement occurs, i.e., the soil experiences no change of void ratio, strain, or loss of mass or otherwise (see Section 2).

On this basis, namely, the low degree of settlement in the case considered is assumed to be of a lateral nature, and is calculated by using the equation derived from the theory of elasticity, which is in agreement with previously given and discussed in Section 1.11

$$\Delta = \frac{q_0 B}{E} \frac{1-\mu^2}{1-\mu} \cdot \frac{1}{\rho} \dots\dots\dots 4.11$$

where, in this case, q_0 is the initial pressure, B is the width of the foundation, E is Young's modulus of the soil, μ is Poisson's ratio, and ρ is the radius of curvature pertaining to settlement and with reference to the center of the foundation and the balance of the supporting soil.

In the case of saturated soils, the change in moisture content during the course of lateral settlement, is considered to imply no change in volume of the soil, since both the pore water and soil grains are assumed to be incompressible. Hence, for this condition $\mu = 0.5$ and the lateral expansion value in the above equation for calculation of the lateral settlement of foundation.

As mentioned in the case of the settlement due to lateral expansion, the soil is assumed to be incompressible, i.e., the void ratio remains constant, and in which the lateral expansion of the soil is assumed to be immediate after the application of loading. The question thus arises as to whether the assumption of immediate settlement is reasonable or not. It is noted in the case of the soil, the case of partially saturated soils is usually closely linked up with the process of consolidation process in such soils, in which void ratio is known to change. If, in the case of saturated consolidated soils, this assumption can still be considered to be valid, it is also valid for the case of partially saturated soils, as described above in the case of clay soils.

1.3 The Lateral Expansion

In the present lateral expansion problem, the soil is assumed to be incompressible, i.e., the void ratio remains constant, and in which the lateral expansion of the soil is assumed to be immediate after the application of loading. The question thus arises as to whether the assumption of immediate settlement is reasonable or not. It is noted in the case of the soil, the case of partially saturated soils is usually closely linked up with the process of consolidation process in such soils, in which void ratio is known to change. If, in the case of saturated consolidated soils, this assumption can still be considered to be valid, it is also valid for the case of partially saturated soils, as described above in the case of clay soils.

According to the assumption of Poisson's ratio, $\mu = 0.5$, wherein no horizontal stresses are the result of applied loading, the condition of $\mu = 0$ is in this case an assumption of $\mu = 0$ condition.

Vertical Normal Stress σ_z

Equation: $\sigma_z = \frac{Q}{2\pi} \frac{3z^3}{(r^2+z^2)^{5/2}}$

TABLE II

z	r	σ_z
3	0	53.0516
	5	1.9152
	10	0.1040
	20	0.0037
	30	0.0005
	45	0.0003
	60	0.0000
6	0	13.2674
	5	3.4523
	10	0.4775
	20	0.0255
	30	0.0037
	45	0.0000
	60	0.0000
10	0	4.7747
	5	0.7343
	10	0.8435
	20	0.0855
	30	0.0143
	45	0.0016
	60	0.0000
15	0	2.1211
	5	1.4313
	10	0.8467
	20	0.1615
	30	0.0382
	45	0.0064
	60	0.0016
20	0	1.1027
	5	1.0250
	10	0.6828
	20	0.2117
	30	0.0521
	45	0.0127
	60	0.0032
30	0	0.7300
	5	0.4885
	10	0.4074
	20	0.2117
	30	0.0839
	45	0.0286
	60	0.0095
45	0	0.4156
	5	0.2922
	10	0.2085
	20	0.1496
	30	0.0939
	45	0.0414
	60	0.0191
60	0	0.1321
	5	0.1305
	10	0.1241
	20	0.1019
	30	0.0764
	45	0.0430
	60	0.0239

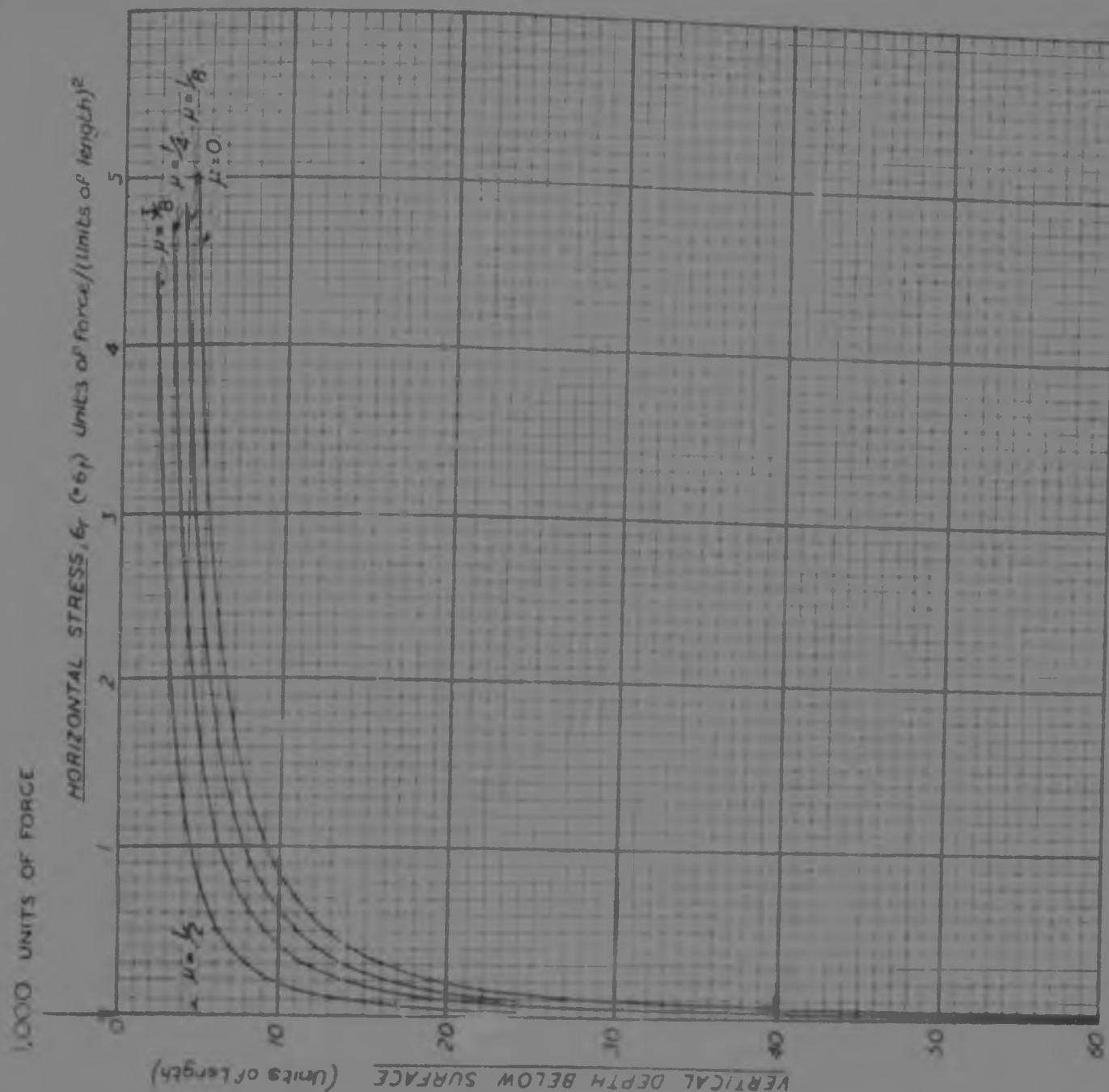


FIG. 9
CURVES
of
HORIZONTAL STRESSES σ_r & σ_t
versus
DEPTH on AXIS of LOADING
for
VARIOUS VALUES OF μ .

Hence, in terms of the discussion in Section 6.2, if any saturated soil be subjected to an oedometer test, it can experience no elastic settlement as a result of the applied loading, since, in the case of a saturated soil, such settlement is essentially that which takes place without change in moisture content, i.e., no loss of mass, and if soil grain and pore water are assumed to be incompressible and in addition lateral strain be prevented, no such settlement can occur. Alternatively also, if soil grain and pore water are considered to be incompressible, there can be no volume decrease in a saturated soil without the extrusion of pore water, i.e., without consolidation taking place, which therefore implies that for calculating the elastic (or immediate) settlement of any type of saturated soil, a value of $\mu = 0.5$ only is applicable. This statement thus also verifies the statement at the end of the previous Section regarding the value of μ applicable to saturated cohesionless soils.

As a result of the above discussion, the question arises as to what the nature of the initial compression (1.6) in the case of a consolidation test on a saturated soil may be. It is considered that it may possibly be due to the combined effects of very slight yield in the confining test ring (which was assumed to be zero above), and bulging down of the porous plates and other parts of the test set-up. However, for a final answer, a more detailed investigation may be warranted.

6.4 The Westergaard Equations

The Westergaard equations (1.6) are based on a condition which is to be discussed in detail, viz., that of anisotropy (2.20), in which strata of compressible material contain thin lenses of material of great lateral rigidity which are, in effect, of infinite rigidity. This type of soil structure greatly accentuates the non-isotropic condition in these soils, and is also the cause of a greatly increased resistance to lateral strain.

Westergaard's equations constitute a solution based on the elastic theory, in which extreme non-isotropic conditions of this type are assumed. In the derivation, an elastic material is assumed to be laterally reinforced by numerous, closely spaced, horizontal sheets of negligible thickness but of infinite rigidity, which prevent the mass as a whole from undergoing lateral strain. In his mathematical expression (containing some of Poisson's Ratio) for the vertical stress caused by a point load, Westergaard finds that the stresses at points directly below the load have minimum value when Poisson's Ratio has the minimum value of zero, and considers that for the case of large lateral restraint, this yields the most realistic result (see also ref. 22). Hence, his final expressions for the vertical stress caused by point loading and uniform area loading, are thus obtained by substituting $\mu = 0$.

Taylor (1.6) in comparing the Boussinesq and Westergaard expressions, mentions that within certain limits (as discussed) both point loading and uniform area loading give values of vertical stresses which are approximately equal to two-thirds of the values given by the Boussinesq equations. He considers that the values given by the Boussinesq equations, which are based on the stratified condition under which the Westergaard solution is based, is certainly nearer to the conditions existing in sedimentary soils than the isotropic condition assumed by Boussinesq. Furthermore, he points out that estimates of (consolidation) settlements obtained by use of the Boussinesq equations for determination of (vertical) stresses, are in the great majority of cases larger than observed settlements, which possibly indicates that the Boussinesq equations give stress values which are too large, although admittedly, such a result could also be due to other assumptions used in settlement estimates. However, the view was also expressed that the Westergaard equations tend to

Maximum Shear Stress S_{max}

Equation: $S_{max} = \frac{1}{2} \sqrt{(S_x - S_y)^2 + 4\tau_{xy}^2}$

TABLE VI

z	r	S_{max}				
		$\mu = 0$	$\mu = 0.125$	$\mu = 0.25$	$\mu = 0.375$	$\mu = 0.50$
3	0	30.1912	29.8115	29.7363	27.4311	26.5258
	5	3.1912	3.2351	3.3214	3.4502	3.5166
	10	0.3195	0.3610	0.4229	0.5176	0.6299
	20	0.0310	0.0520	0.0264	0.0483	0.0865
	30	0.0132	0.0336	0.0138	0	0.0260
	45	0.0088	0.0152	0.0105	0	0.0078
	60	0.0175	0.0178	0.0071	0	0
6	0	7.7365	7.1604	7.1835	6.9073	6.6312
	5	3.2860	3.1563	3.0974	3.0781	3.0096
	10	0.7963	0.8089	0.8308	0.8627	0.9039
	20	0.0869	0.0897	0.1051	0.1291	0.1570
	30	0.0316	0.0712	0.0229	0.0350	0.0502
	45	0.0103	0.0100	0	0.0063	0.0151
	60	0.0132	0.0057	0	0	0.0063
10	0	2.7352	2.6257	2.5963	2.4868	2.3973
	5	1.2295	1.9709	1.8149	1.7612	1.7091
	10	0.3751	0.4214	0.4514	0.4454	0.4434
	20	0.1724	0.1776	0.1865	0.1990	0.2140
	30	0.0477	0.0471	0.0541	0.0636	0.0751
	45	0.0132	0.0100	0.0122	0.0173	0.0245
	60	0.0050	0	0	0.0055	0.0103
15	0	1.2374	1.1929	1.1491	1.1053	1.0607
	5	1.0416	1.0072	0.9726	0.9393	0.9065
	10	0.2786	0.2860	0.2995	0.2643	0.26107
	20	0.2201	0.2196	0.2208	0.2239	0.2286
	30	0.0767	0.0787	0.0829	0.0882	0.0948
	45	0.0209	0.0212	0.0240	0.0287	0.0335
	60	0.0032	0	0.0055	0.0095	0.0135
20	0	0.6462	0.6717	0.6462	0.6215	0.5968
	5	0.6462	0.6044	0.5872	0.5658	0.5446
	10	0.4684	0.4684	0.4551	0.4402	0.4271
	20	0.2254	0.2252	0.2228	0.2214	0.2209
	30	0.0935	0.0913	0.0960	0.0955	0.1018
	45	0.0301	0.0316	0.0339	0.0367	0.0403
	60	0.0100	0.0112	0.0122	0.0150	0.0180
30	0	0.3085	0.2884	0.2873	0.2761	0.2750
	5	0.2752	0.2845	0.2747	0.2641	0.2543
	10	0.2200	0.2213	0.2432	0.2346	0.2262
	20	0.1222	0.1650	0.1607	0.1567	0.1535
	30	0.0475	0.0960	0.0947	0.0941	0.0938
	45	0.0113	0.0115	0.0421	0.0433	0.0445
	60	0.0000	0.0206	0.0218	0.0230	0.0245
45	0	0.1377	0.1329	0.1272	0.1225	0.1177
	5	0.1347	0.1301	0.1254	0.1207	0.1161
	10	0.1271	0.1226	0.1182	0.1139	0.1095
	20	0.1022	0.0987	0.0950	0.0925	0.0898
	30	0.0780	0.0728	0.0712	0.0694	0.0678
	45	0.0427	0.0421	0.0415	0.0412	0.0412
	60	0.0215	0.0214	0.0244	0.0250	0.0255
60	0	0.0772	0.0740	0.0716	0.0692	0.0660
	5	0.0763	0.0731	0.0707	0.0683	0.0652
	10	0.0744	0.0712	0.0691	0.0667	0.0636
	20	0.0648	0.0628	0.0602	0.0581	0.0561
	30	0.0543	0.0526	0.0512	0.0497	0.0482
	45	0.0361	0.0353	0.0343	0.0335	0.0331
	60	0.0255	0.0250	0.0245	0.0245	0.0245

CHAPTER 7

LABORATORY TESTS

7.1 Theoretical Considerations

The basis on which a soil can be considered to approximate the elastic state of stress, was discussed in Section 6.1. As was mentioned in that Section and as was also implied by the discussions in Chapter 2, Poisson's Ratio only has a rational meaning within the linear range of loading of a soil's stress:strain curve. In this Chapter and in those to follow, a determination of Poisson's Ratio from the observed behaviour of a soil within its linear range of loading during a triaxial compression test, will be described and discussed.

Since the elastic constants are related to volumetric strains, (see Chapter 3) it is convenient to evaluate Poisson's Ratio for a soil by measuring the change in volume of the soil resulting from a certain measured increase in loading within the linear range. This is based on the assumption of the three-dimensional stress relation given by equation 3.3, in the conditions of a triaxial compression test.

$$\text{Dilation } (\Delta) = \frac{\delta V}{V} = \frac{1}{E} (\sigma_1 + \sigma_2 + \sigma_3) (1 - 2\mu) \dots\dots\dots 3.3$$

In the derivation of this equation, the principal stresses σ_1 , σ_2 and σ_3 were considered to act in an outward direction on the cube of unit side, with a sign convention such that this direction is taken to be positive. Hence, the volume change δV , (a volume increase) caused by the action of this system of principal stresses, is considered to be positive, so that the Dilation $[\Delta]$ is positive for principal stresses acting in an outward direction.

However, in the case of a triaxial compression test, the direction of the principal stresses is opposite to that just considered and in addition, the lateral principal stresses are of equal magnitude. Hence, for convenience, the sign convention is altered so that compressive principal stresses are considered to be positive and hence, the Dilation $[\Delta]$ is positive for a reduction in volume. Furthermore, σ_2 in equation 3.3 is replaced by σ_3 , the allround chamber pressure in the test cell, and hence, equation 3.3 becomes:

$$\text{Dilation } (\Delta) = \frac{\delta V}{V} = \frac{1}{E} (\sigma_1 + 2\sigma_3) (1 - \mu) \dots\dots\dots 3.4$$

However, σ_1 is the sum of a σ_3 pressure due to the allround chamber pressure, so that if σ_d (known as the Deviator Stress), is the net applied pressure in the Z-direction, we have that:

$$\sigma_1 = \sigma_3 + \sigma_d \dots\dots\dots 7.1$$

and hence

$$\frac{\delta V}{V} = \frac{1}{E} (\sigma_3 + \sigma_d + 2\sigma_3) (1 - \mu)$$

$$\text{i.e. } \frac{\delta V}{V} = \frac{1}{E} (3\sigma_3 + \sigma_d) (1 - \mu) \dots\dots\dots 7.2$$

If triaxial shear tests are conducted wherein the sample of initial volume V_1 is allowed to consolidate under the action of an allround chamber pressure during the pre-shear condition, then this chamber pressure causes volumetric strains in the test sample, which at the end of the consolidation process have been completely effected, thereby resulting in a new sample volume V_2 . Hence, when the actual triaxial test is commenced with the application of the Deviator Stress (σ_d), the volumetric strains then produced (which constitute the δV measured during the test), are relative to the sample volume V_2 attained at the end of consolidation, and furthermore, are caused by the action of σ_d only,

Vertical Shear Stress τ_{rz}

$$\text{Equation: } \tau_{rz} = \frac{Q}{2\pi} \frac{3r^2}{(n^2 + 2)^{3/2}}$$

TABLE III

z	r	τ_{rz}
3	0	0.0
	5	3.1911
	10	0.3470
	20	0.0256
	30	0.0049
	45	0.0016
	60	0.0000
6	0	0.0
	5	7.9603
	10	0.7274
	20	0.0859
	30	0.0191
	45	0.0049
	60	0.0016
10	0	0.0
	5	1.3671
	10	0.4435
	20	0.1703
	30	0.0446
	45	0.0098
	60	0.0032
15	0	0.0
	5	0.7443
	10	0.2544
	20	0.1158
	30	0.0764
	45	0.0207
	60	0.0064
20	0	0.0
	5	0.5588
	10	0.3487
	20	0.1117
	30	0.0939
	45	0.0302
	60	0.0111
30	0	0.0
	5	0.3888
	10	0.1883
	20	0.1416
	30	0.0939
	45	0.0414
	60	0.0181
45	0	0.0
	5	0.1215
	10	0.0462
	20	0.0161
	30	0.0081
	45	0.0014
	60	0.0000
60	0	0.0
	5	0.0111
	10	0.0207
	20	0.0334
	30	0.0382
	45	0.0318
	60	0.0239

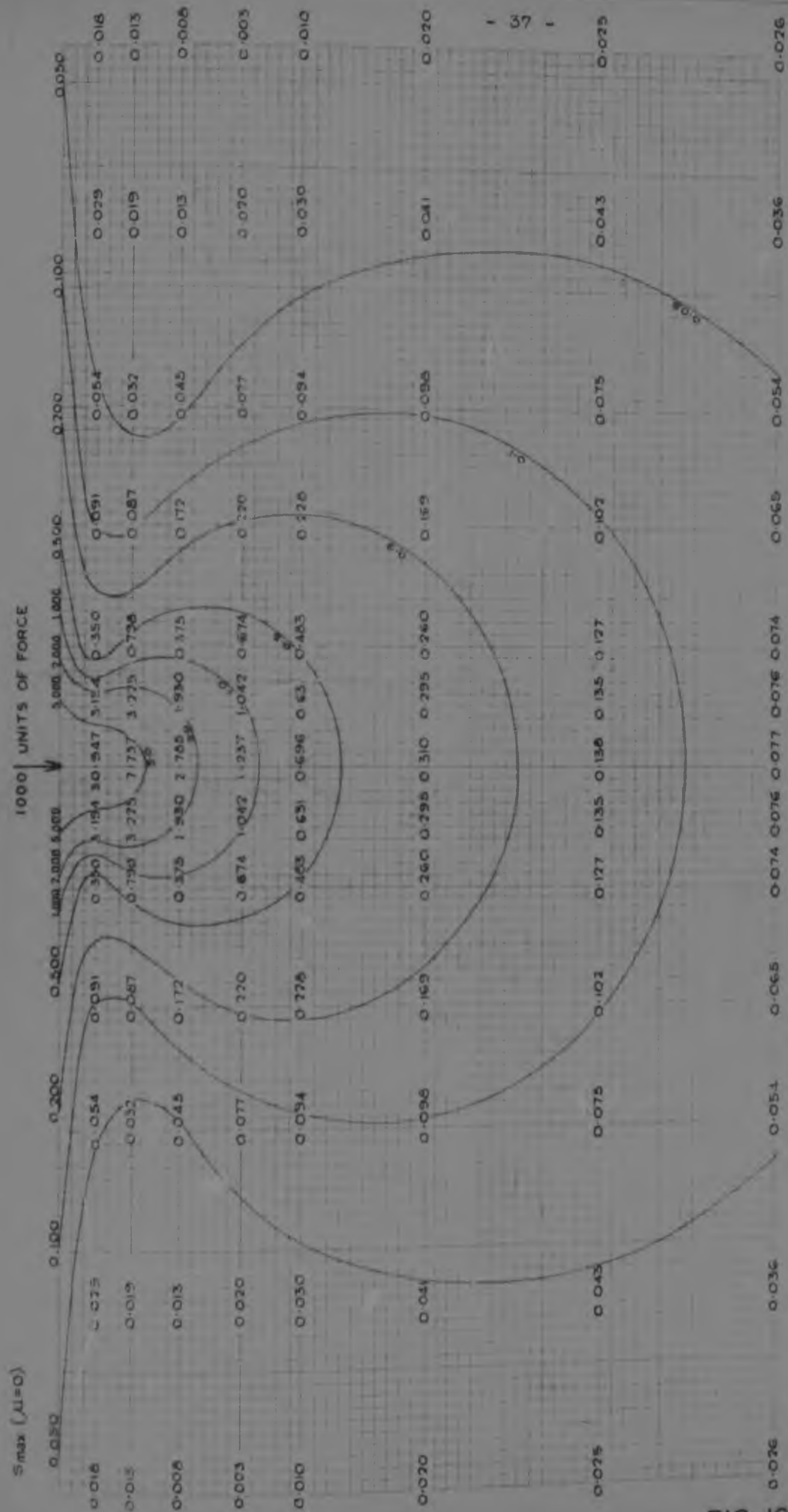


FIG 10 - CONTOURS OF MAXIMUM SHEAR STRESS (S_{max}) FOR CONDITION $\mu=0$

FIG. 10.

the chamber pressure σ_3 merely acting as a static allround pressure with no effect in so far as causing volumetric strain during test is concerned, i.e. the test conditions are similar to those of conducting a test under an allround constant air pressure, say, atmospheric pressure. In effect σ_3 thus has zero value and equation 7.3 above should be amended accordingly.

It should be pointed out, however, that the σ_3 chamber pressure controls the measured value of the volumetric strain produced by σ_d (δV as measured during the test), i.e., for different values of σ_3 , the same range of σ_d results in a different measured value of δV , so that indirectly, although in the equation σ_3 has zero value, its effect is included in the calculation of Poisson's Ratio. Further, it should be borne in mind that the change in volume during the pre-shear condition resulting from the action of the σ_3 chamber pressure, is mainly as a result of consolidation effects, while the change in volume within the linear range resulting from the application of σ_d is considered to be due to elastic effects, and as such forms the valid basis of the determination of Poisson's Ratio from an equation applying to the elastic state only (cf. Chapter 2).

Hence, as it was intended to conduct Unconsolidated Undrained shear test, σ_3 , in equation 7.3, has zero value and the sample volume V_1 is actually the sample volume V_2 referred to in the above discussion.

Equation 7.3 thus becomes:

$$\frac{\delta V}{V} = \frac{1}{E} (\sigma_d) (1 - 2\mu) \dots\dots\dots 7.4$$

From this relationship Poisson's Ratio (μ) can be solved for by rewriting the equation as follows:-

$$\begin{aligned} (1 - 2\mu) &= \frac{\delta V}{V} \cdot \frac{E}{\sigma_d} \\ - 2\mu &= \frac{\delta V}{V} \cdot \frac{E}{\sigma_d} - 1 \\ \mu &= \frac{1}{2} \left[1 - \frac{\delta V}{V} \cdot \frac{E}{\sigma_d} \right] \dots\dots\dots 7.5 \end{aligned}$$

The values of all the unknowns on the right hand side of this equation can be obtained experimentally from a triaxial compression test, and hence, the value of μ can be calculated.

Thus, the experimental work was designed to enable the measurement during a triaxial test, of the unknowns δV , E and σ_d in the right hand side of equation 7.5, V being the volume of the test sample at the end of the consolidation process during the pre-shear condition. The method by which this volume was determined, is discussed fully in Section 4.4.

7.2 The Test Soil

The soil used for the tests was a well-graded, firm, fine, reddish-brown, silty sand, taken from a depth of 15ft. from a site on the North side of Juta Street neariscard Street, Braamfontein, Johannesburg. The full soil profile on the site was measured down to a depth of 55ft. and is shown on the next page. (Fig. 16).

As the test soil occurs above a 1ft. thick layer of pebbles which is commonly known as the "pebble marker", it is probably of a transported origin.

that the application to practical problems of the expressions for the stress components in 3-dimensional cases, generally requires the expression for the vertical normal stress (σ_z). Hence, the expressions for stress components containing Poisson's Ratio are seldom used. This is especially so in the case of surface loadings, since, as discussed by both the references just mentioned, an area load is very often replaced by an equivalent point load without introducing very significant errors.

An expression for the vertical normal stress distribution below a corner of a uniform rectangular area loading on the surface of a semi-infinite elastic solid, was derived by Melanek (10) by integrating Boussinesq's expression for the vertical normal stress in such a solid due to a point load (equations 4.7 (a) and (b)). This expression is given by both Terzaghi (8.7) and Taylor (1.4), and is frequently used in soils work. As is the case with Boussinesq's equation 4.7 above, Newmark's expression therefore also does not contain Poisson's Ratio.

Expressions for the displacements in a semi-infinite elastic solid in 3-dimensional problems of stress and strain, also contain terms of Poisson's Ratio, since displacements are directly related to stress distribution. Boussinesq (16) computed the vertical, horizontal and radial displacements produced by a vertical point load applied to the horizontal surface of a semi-infinite elastic solid. These expressions have also been given by Terzaghi (8.6). Using the basic expressions of Boussinesq, Schiele (19) obtained by integration an expression for the settlement of the corners of a uniformly loaded rectangular area of width B and length L. His expression is given by Terzaghi (8.9), who subsequently writes it in the form:

$$\Delta s = qB \cdot \frac{1-\mu^2}{E} \cdot I_F \dots\dots\dots 4.11$$

where q is the intensity of the uniformly distributed loading, and I_F is a pure number known as the settlement influence value. Its value depends on the ratio L/B of the sides of the loaded area. This is another expression which is frequently used in soils work as will be seen in Section 6.2.

It is thus clear that with regard to the determination of stress and strain in a semi-infinite, elastic, isotropic solid due to applied surface forces, Poisson's Ratio only enters in 3-dimensional problems of stress and strain, since as was shown in Section 4.3, the moduli of elasticity do not affect the stress distribution and hence also the strains in 2-dimensional problems. It should be noted that in the case of a semi-infinite elastic solid wherein all loadings are applied vertically on its surface (as is generally the case in soils work), a 2-dimensional problem of stress and strain is therefore also one wherein the applied loading occurs in only 2-dimensions, and similarly in the case of 3-dimensional problems.

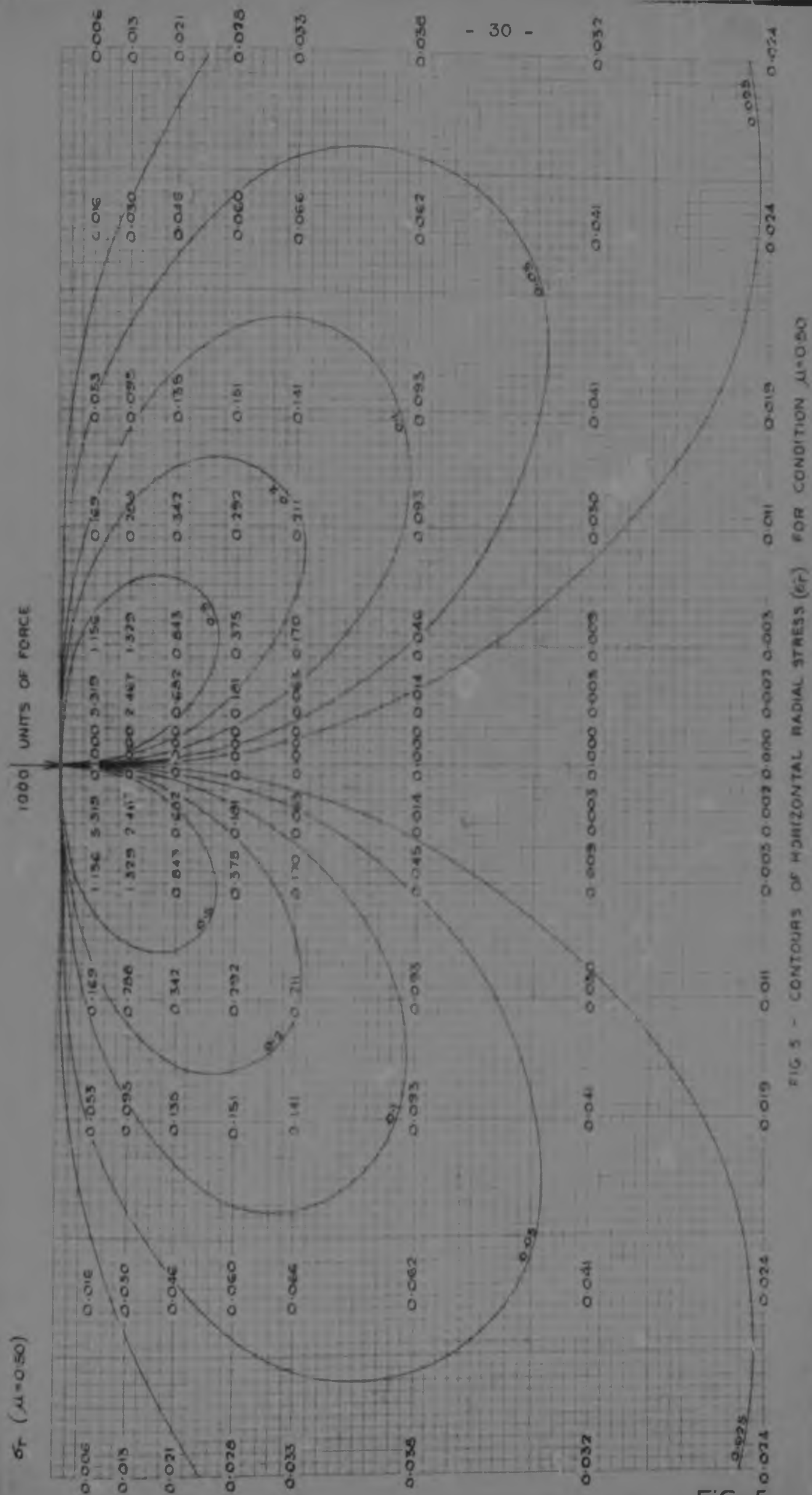


FIG. 5 - CONTOURS OF HORIZONTAL RADIAL STRESS (σ_r) FOR CONDITION $\mu=0.50$

FIG. 5.

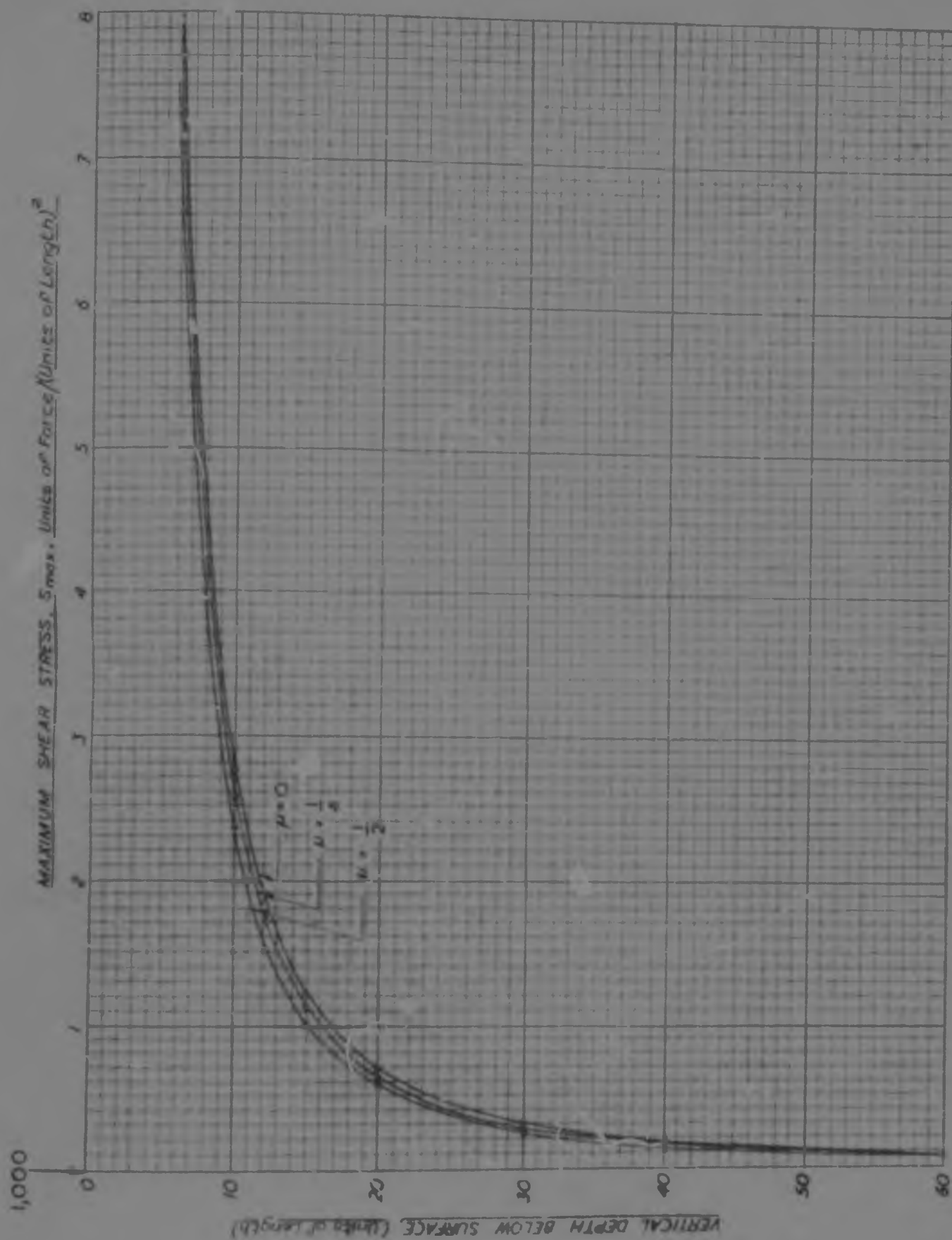


Fig.15
 CURVES
 OF
 MAXIMUM SHEAR STRESS,
 S_{max}
 VERSUS
 DEPTH ON LOADING AXIS
 FOR
 VARIOUS VALUES OF μ

that the application to practical problems of the expressions for the stress components in 3-dimensional cases, generally only requires the expression for the vertical normal stress (σ_z). Hence, the expressions for stress components containing Poisson's Ratio are seldom used. This is especially so in the case of finite area loadings, since, as discussed by both the references just mentioned, an area load is very often replaced by an equivalent point load without introducing very significant errors.

An expression for the vertical normal stress distribution below a corner of a uniform rectangular area loading on the surface of a semi-infinite elastic solid, was derived by Newmark(18) by integrating Boussinesq's expression for the vertical normal stress in such a solid due to a point load (equations 4.7 (a) and (b)). The expression is given by both Terzaghi(9.7) and Taylor(11.3), and is frequently used in soils work. In the case with Boussinesq's equation 4.7, i.e., Newmark's expression therefore also does not contain Poisson's Ratio.

Expressions for the displacements in a semi-infinite elastic solid in 3-dimensional problems of stress and strain, also contain terms of Poisson's Ratio, since displacements are directly related to stress distribution. Boussinesq(16) computed the vertical, horizontal and radial displacements produced by a vertical point load applied to the horizontal surface of a semi-infinite elastic solid. These expressions have also been given by Terzaghi(8.6). Using the basic expressions of Boussinesq, Schleicher(19) obtained by integration an expression for the settlement of the corners of a uniformly loaded rectangular area of width B and length L. His expression is given by Terzaghi(8.9) who subsequently writes it in the form:

$$\Delta s = qB \frac{1-\mu^2}{E} \cdot I_F \quad \dots \dots \dots 4.11$$

where q is the intensity of the uniformly distributed loading, and I_F is a pure number known as the settlement influence value. Its value depends on the ratio L:B of the sides of the loaded area. This is another expression which is frequently used in soils work as will be seen in Section 5.2.

It is thus clear that with regard to the determination of stress and strain in a semi-infinite, elastic, isotropic solid due to applied surface forces, Poisson's Ratio only enters in 3-dimensional problems of stress and strain, since as was shown in Section 4.3, the moduli of elasticity do not affect the stress distribution and hence also the strains in 2-dimensional problems. It should be noted that in the case of a semi-infinite elastic solid where in all loadings are applied vertically on its surface (as is generally the case in soils work), a 2-dimensional problem of stress and strain is therefore also one where in the applied loading occurs in only 2-dimensions, and similarly in the case of 3-dimensional problems.

Horizontal Force at the Str. base

$$\text{Equation: 6.} = -\frac{Q}{2H}(1-2\mu)\left[\frac{z}{(r^2+z^2)^{3/2}} - \frac{1}{z^2+z^2+z\sqrt{r^2+z^2}}\right]$$

TABLE V

z	r	δt				
		μ = 0	μ = 0.125	μ = 0.25	μ = 0.375	μ = 0.50
5	0	-0.0014	-0.0014	-1.1910	-0.0014	0
	5	+0.7098	+0.3323	+0.3549	+0.1774	0
	10	+0.7162	+0.1871	+0.3381	+0.1790	0
	20	+0.2817	+0.2113	+0.1489	+0.0769	0
	30	+0.1412	+0.1002	+0.0709	+0.0355	0
	45	+0.0584	+0.0513	+0.0340	+0.0171	0
	60	+0.0308	+0.0303	+0.0199	+0.0100	0
10	0	-0.0107	-1.0500	-1.1031	-0.1127	0
	5	-0.1382	-0.5082	-0.2843	-0.1383	0
	10	+0.1703	+0.1873	+0.0812	+0.0424	0
	20	+0.1708	+0.1430	+0.0891	+0.0400	0
	30	+0.1002	+0.1011	+0.0581	+0.0271	0
	45	+0.0584	+0.0642	+0.0295	+0.0147	0
	60	+0.0335	+0.0382	+0.0173	+0.0088	0
15	0	-0.7083	-0.3858	-0.3099	-0.1900	0
	5	-0.4879	-0.3809	-0.2380	-0.1170	0
	10	-0.0871	-0.0785	-0.0482	-0.0243	0
	20	+0.0700	+0.0383	+0.0390	+0.0191	0
	30	+0.0700	+0.0323	+0.0386	+0.0175	0
	45	+0.0401	+0.0442	+0.0250	+0.0115	0
	60	+0.0202	+0.0287	+0.0181	+0.0079	0
20	0	-0.5133	-0.2880	-0.1788	-0.0883	0
	5	-0.2781	-0.2080	-0.1380	-0.0688	0
	10	-0.1380	-0.1030	-0.0700	-0.0380	0
	20	+0.0801	+0.0348	+0.0380	+0.0016	0
	30	+0.0380	+0.0380	+0.0180	+0.0083	0
	45	+0.0310	+0.0313	+0.0179	+0.0060	0
	60	+0.0233	+0.0193	+0.0100	+0.0050	0
30	0	-0.1708	-0.1442	-0.0895	-0.0497	0
	5	-0.1012	-0.1369	-0.0880	-0.0430	0
	10	-0.1380	-0.0871	-0.0891	-0.0400	0
	20	-0.0873	-0.0179	-0.0180	-0.0050	0
	30	+0.0000	+0.0001	+0.0049	+0.0024	0
	45	+0.0191	+0.0143	+0.0086	+0.0047	0
	60	+0.0191	+0.0131	+0.0086	+0.0044	0
45	0	-0.0873	-0.0886	-0.0489	-0.0439	0
	5	-0.0843	-0.0832	-0.0421	-0.0431	0
	10	-0.0700	-0.0836	-0.0350	-0.0175	0
	20	-0.0380	-0.0088	-0.0175	-0.0088	0
	30	-0.0088	+0.0091	+0.0049	+0.0024	0
	45	+0.0088	+0.0056	+0.0088	+0.0017	0
	60	+0.0088	+0.0060	+0.0046	+0.0020	0
60	0	-0.0380	-0.0200	-0.0191	-0.0195	0
	5	-0.0380	-0.0200	-0.0191	-0.0036	0
	10	-0.0380	-0.0200	-0.0175	-0.0088	0
	20	-0.0288	-0.0191	-0.0128	-0.0064	0
	30	-0.0143	-0.0107	-0.0078	-0.0037	0
	45	-0.0048	-0.0036	-0.0024	-0.0012	0
	60	-0.0000	0	0	0	0
60	0	-0.0223	-0.0167	-0.0111	-0.0056	0
	5	-0.0207	-0.0155	-0.0101	-0.0052	0
	10	-0.0207	-0.0165	-0.0104	-0.0052	0
	20	-0.0173	-0.0131	-0.0088	-0.0044	0
	30	-0.0127	-0.0095	-0.0063	-0.0032	0
	45	-0.0064	-0.0048	-0.0032	-0.0016	0
	60	-0.0032	-0.0024	-0.0016	-0.0008	0

1000 UNITS OF FORCE

$\sigma_z (\mu=0)$

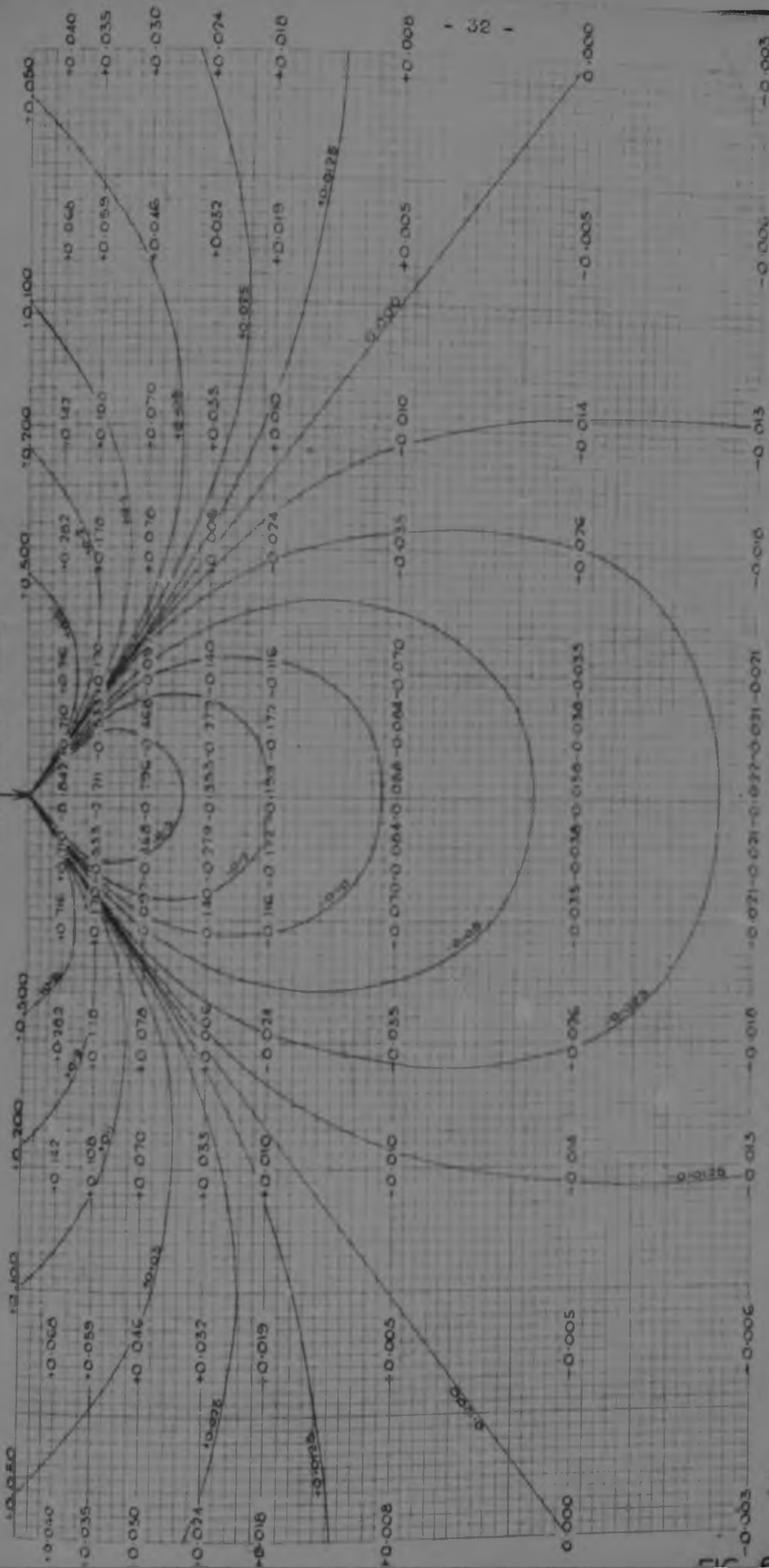


FIG 6 - CONTOURS OF HORIZONTAL TANGENTIAL STRESS (σ_z) FOR CONDITION $\mu=0$

CHAPTER 5

THE AFFECT OF VARIOUS VALUES OF POISSON'S RATIO ON THE STRESS DISTRIBUTION IN A SEMI-INFINITE ELASTIC SOLID DUE TO AN APPLIED VERTICAL POINT LOAD

5.1 Introduction

In this Chapter the effect of various values of Poisson's Ratio within the range -0.1 range on the stresses calculated from Boussinesq's equations in the basic 3-dimensional case, will be outlined. The equations referred to are the equations 4.7-4.10 given in the previous Chapter.

5.2 Stress Calculations and Curves

For the purposes under consideration, the value of the vertical point load Q in Boussinesq's equations was assumed to be 1000 units of force. No specific units of either force or length were adopted, as it was intended to render the results adaptable to any system of units. The units of the stresses calculated are therefore simply : units of force/(units of length)², the numerical value of the stress calculated being the same for any units of force and length. That this is the case, can be seen from a consideration of the form of any of Boussinesq's equations, for example, equation 4.7(a) of previously:

$$\sigma_z = \frac{Q}{2\pi} \cdot \frac{3z^3}{(r^2+z^2)^{5/2}} \dots\dots\dots 4.7(a)$$

Whatever the units of length may be, the numerical value of the term $3z^3/(r^2+z^2)^{5/2}$ will in each case be the same, and has dimensions : (units of length)⁻², while the numerical value of the term $Q/2\pi$ is also the same whatever units of force may be used. Hence σ_z , as the product of these two terms, has a numerical value which is independent of the particular units of force and length used. The only effect is that with the later presentation of the results in the form of curves, stress contour diagrams, the scale of any diagram depends on the particular units of length used, but this is of no consequence for the purposes considered herein. For this reason also, no scales are given with any of the diagrams.

For each stress component, i.e. σ_z , σ_r , σ_t and τ_{rz} , the values of the stresses have been calculated for a grid of points extending 60 units of length horizontally on either side of the axis of loading of the vertical point load, and to a depth of 60 units of length below the horizontal surface of the semi-infinite solid. Furthermore, for the grid of points just detailed, stresses were calculated for each of the stress components σ_r and σ_t (which contain terms of Poisson's Ratio) using five different values of μ , viz. $\mu = \text{zero}$, 0.125, 0.25, 0.375 and 0.50. Stresses were in all cases evaluated by direct calculation from the relevant equations and the results have been presented, as mentioned above, mainly in the form of stress contour diagrams. The actual results of the calculations for each grid of points have been compiled in tabular form and appear in each case on the page immediately before the corresponding curves.

For the Maximum Shear Stress (S_{max}), the standard equation for 2-dimensional cases was used, although the problem being considered is essentially a 3-dimensional one. The reason for this is that the 3-dimensional case has proved to be almost insoluble (as pointed out by Kenty and Herr(20)), and the only known solution is that of Jurgenson(15) for the special case of a uniformly loaded circular area. Even in this case the solution is so complicated that Jurgenson does not give his

formulas,/

have a constant ratio to one another, and that the stresses for the condition $\mu = 0$ are a constant 75% of the corresponding stresses for the condition $\mu = 0.575$. Furthermore it is clear that the extreme difference in the stress values is given by the conditions $\mu = 0$ and $\mu = 0.575$ and is 0.50 inasmuch as the axis of loading.

In the case of the Maximum Shear Stress (S_{max}), the most serious effect of variation in μ on the stress contour diagrams appears to be only in the near vicinity of the horizontal surface $x = 0$, i.e., immediately in the region which is less than 5 units or less below the surface. This can best be seen in Fig. 14, in which the stress contour lines for the three conditions $\mu = 0$, 0.25 and 0.50 are shown superimposed. Fig. 14 shows that the variation in values of S_{max} on the axis of loading as a result of variation in μ is appreciably insignificant throughout. A consideration of the actual numerical values of S_{max} corresponding to the five values of Poisson's ratio considered (Table VI), shows in the first instance that at any depth on the axis of loading the five stress values are all very constant ratios to one another, and further, that in the case of the extreme conditions $\mu = 0$ and $\mu = 0.575$, the corresponding difference in the values of S_{max} is only a constant 12.5% at all depths on the axis of loading.

On the whole, therefore, it appears that S_{max} is not very critically affected by variation in Poisson's Ratio throughout the limits of its range for elastic materials. This is a very important conclusion especially as it can be seen from a study of the numerical values of the various stresses at points in the axis of loading (where the greatest stress values occur), that second only to the vertical normal stress σ_z , S_{max} is the largest stress values and as a design stress it may therefore be a critical factor in design. Hence from the axis of loading the values of S_{max} are quite frequently larger than the corresponding σ_z values. On the axis of loading the values of S_{max} for the condition $\mu = 0.575$ are 50% of the corresponding values of σ_z , while for the condition $\mu = 0$ this figure is 41.6%.

The horizontal stresses σ_x and σ_y and their extreme sensitivity to variations in the value of Poisson's Ratio are therefore possibly not so important in design as would appear at first sight, and it seems that S_{max} is a more important design factor with, in addition, the important property that its value is not seriously affected by Poisson's Ratio over the complete range of values applicable to elastic materials.

FIG 7 - CONTOURS OF HORIZONTAL TANGENTIAL STRESS (σ_t) FOR CONDITION $\mu = 0.25$

formulas, since "they contain functions of derivatives of the solid angle subtended by the loaded circle at the point under consideration which are of interest to the mathematician only". The use of the formula for 2-dimensional cases is therefore frequently resorted to in 3-dimensional cases; especially as according to Kintoy and Barr, it introduces an additional factor of safety which may be as high as 1.25.

As previously discussed (Chapter 4), 2-dimensional cases are either problems of plane stress or plane strain. In the case of plane stress (and referring now to the same orientation of coordinate axes as in Chapter 4), σ_z , τ_{xz} and τ_{yz} are zero, while in the case of plane strain, τ_{xz} and τ_{yz} are zero, but σ_y is not zero. If the normal and shearing stresses acting on the two perpendicular planes containing the OX and OZ axes are combined to give the maximum Shearing Stress, the resulting 2-dimensional formula is:

$$\tau_{max} = \frac{1}{2} \sqrt{(\sigma_z - \sigma_x)^2 + 4\tau_{xz}^2} \dots\dots\dots 5.1$$

For this equation to hold, it therefore does not necessarily signify the assumption that $\sigma_y = \text{zero}$, i.e. the equation is valid even if the third principal stress is not zero since in the case of plane strain, which is a 2-dimensional problem, σ_y is not equal to zero. Hence also, if the normal and shearing stresses acting on the two perpendicular planes containing the OY and OZ axes be combined, the following 2-dimensional relationship is obtained:

$$S_{max} = \frac{1}{2} \sqrt{(\sigma_z - \sigma_y)^2 + 4\tau_{yz}^2} \dots\dots\dots 5.2$$

In the case of the Tresca stress equations of stress, the equations 5.1 and 5.2 given above therefore become (cf. Fig. 4.5, Chapter 4):

$$S_{max} = \frac{1}{2} \sqrt{(\sigma_z - \sigma_r)^2 + 4\tau_{rz}^2} \dots\dots\dots 5.3$$

$$\text{and } S_{max} = \frac{1}{2} \sqrt{(\sigma_z - \sigma_t)^2 + 4\tau_{tz}^2} \dots\dots\dots 5.4$$

but, since $\tau_{tz} = 0$, equation 5.4 above becomes:

$$S_{max} = \frac{1}{2}(\sigma_z - \sigma_t) \dots\dots\dots 5.5$$

Although equation 5.3 (or basically equation 5.1) is the generally accepted expression for determining S_{max} , S_{max} was evaluated from both the equations 5.3 and 5.5 above for the purposes of comparison. Since S_{max} in both equations contains either the stress component σ_r or the stress component σ_t , both of which contain terms of Poisson's Ratio, S_{max} was also evaluated for the five conditions: $\mu = \text{zero}$, 0.125, 0.25, 0.375 and 0.50. A tabular comparison of the results is given in Appendix III, Item 1. It was found that equation 5.3 gave, according to the generally accepted equation 5.1 for 2-dimensional cases, gave the larger values of S_{max} in all cases except a few very isolated instances.

On the following pages the results of all the abovementioned calculations and the corresponding curves are presented. These appear in the following sequence:

1. Vertical Normal Stress σ_z : (a) Stress data in tabular form.
(b) Stress contour diagram.

2. Vertical/

CHAPTER 4

GENERAL CONCEPTS OF ELASTICITY AND POISSON'S RATIO IN SOILS WORK

4.1 Applicability of the Elastic Theory to Soils

The basic and validity of the application of the elastic theory to soils has been discussed in detail by various Authors (see for example Ref. 1, p. 200-204; p. 230 and p. 241-244, and Ref. 2, p. 3-4 and p. 107), and still deserves not to be discussed again herein.

It need only be mentioned here that the theory of elasticity has been used for estimating stresses and settlements induced in soil masses by externally applied loads, with the important provision that the induced stresses must be of a moderate order and well clear of the state of stress tending to produce failure conditions if the results are to be of any real significance. In this connection, Terzaghi's opinion (Ref. 3, p. 304) that: "If the factor of safety of a mass of soil with respect to failure by plastic flow exceeds a value of about 3, the state of stress in the soil is likely to be more or less similar to the state of stress computed on the assumption that the soil is perfectly elastic. Hence, the state of stress in a mass of soil

under the influence of external stresses can be estimated by means of the theory of elasticity. The magnitude of the error associated with the results of the computation depends chiefly on the extent to which the soil compressibility deviates from Hooke's Law."

In practice, the concept of elasticity in soils is based on the fact that with moderate stresses: strains curves derived from tests such as triaxial compression tests and field bearing tests, show a certain range, or at least the start, over which stress and strain are approximately linear, and it is said to exhibit elastic behavior over that range of loading. In terms of the discussion in Chapter 3, the elastic theory is thus strictly only applicable to a soil mass within this so-called linear range of loading (which is usually a stress less than Terzaghi's provision of a factor of safety of about 3 against shear failure), and therefore also Terzaghi's analysis of the soil mass only has a rational meaning within this range of loading.

In the next 3 chapters of this Chapter, some aspects of Poisson's Ratio in relation to externally applied analytical and limit procedures will be briefly reviewed, while in subsequent chapters, a determination of Poisson's Ratio from the observed behavior of a soil within the linear range of loading, derived from triaxial compression test, will be described and discussed.

4.2 Settlement Analysis for saturated Clay

In discussing a development of the existing methods of calculating settlements of structures founded on clay, Skempton, Peck and Macdonald (21) commence by describing the principles on which such settlement analysis is based.

It is accepted that the total settlement (i.e., that resulting from the increase in net foundation pressure) at any end of construction is made up of two parts: the immediate settlement which results from deformation of soil mass without change in water content (and hence without volume change in a saturated clay); and the consolidation settlement arising from

SKETCH SHOWING ARRANGEMENT OF THE VARIOUS CIRCUITS IN THE TEST SET-UP.

- 55 -

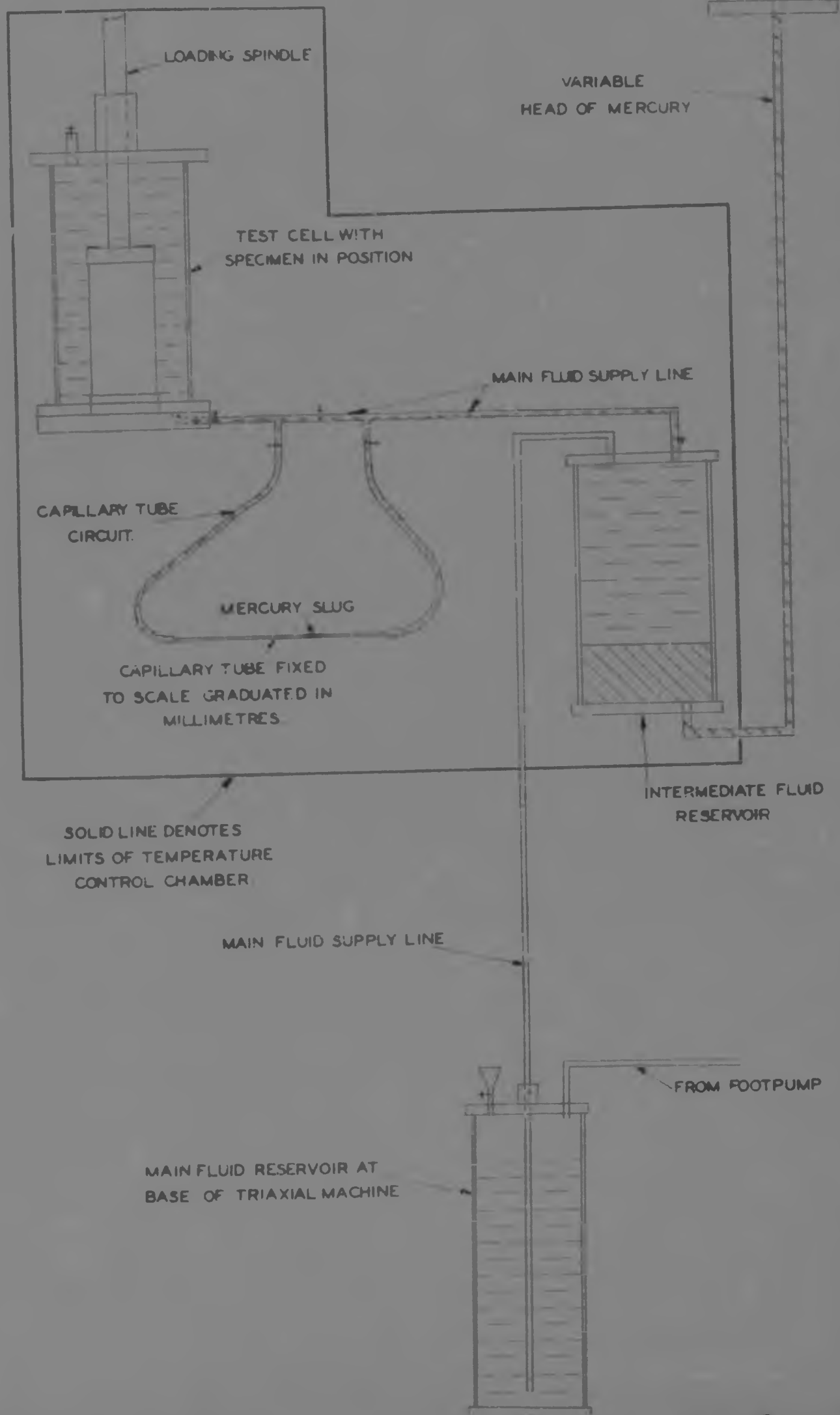


FIG. 10

found most convenient to use a tube of about 32cms. graduated length clear between end connections. In selecting a suitable tube diameter, two main factors had to be considered:

- (a) The diameter would have to be small enough to enable the slug to fill the whole bore and not only part of it, otherwise it would leave a gap between its top surface and the top of the capillary tube through which fluid could flow without causing movement of the slug.
- (b) The slug movement during test would have to be of a reasonable magnitude, i.e. preferably over as much of the graduated length of the tube as possible, but preferably not more than this.

A suitable balance was eventually obtained by trying out capillary tubes of different diameters in a few trial tests with the test soil.

Due consideration was given to the following matters:-

- (a) Air in the test system: As the presence of air in the confining fluid system would adversely affect the flow measurements due to its compressibility it was very important to ensure that all entrapped air be expelled from the system before any test be commenced. It proved to be a very difficult matter to get the capillary tube circuit filled with fluid and its mercury slug in position with all air bubbles expelled from the circuit. However, once this was done at the commencement of the main test series, matters were so arranged by handling the stopcocks, that the circuit would remain filled with its fluid and with its slug in position over the whole series of tests.
- (b) Leakage from the test cell: Leakage from the test cell was an undesirable effect for the purpose of this investigation and hence an attempt was made to eliminate it completely. However, it was found that this was not readily accomplished and hence, all that could be done was to reduce the leakage as much as possible by keeping all leakage points well greased, especially where the loading spindle enters the test cell.
- (c) Temperature changes during test: Due consideration was given to the elimination of temperature changes during test as this would affect the fluid flow measurements made, and would introduce a further variable into an already complex system of test variables. For this reason the whole test had was enclosed in a wooden box with glass windows in its access doors and a heating element and fan installed so as to enable a uniform, constant temperature to be maintained within, during test. However, it was later found that temperature conditions inside the laboratory were not very variable and that with the added protection of the wooden box against possible draughts, no significant temperature changes were liable to occur within the temperature control chamber during the comparatively short duration of a test. The heating element and fan were thus never used.

Figs. 20 to 23 inclusive are photographs showing various aspects of the test apparatus.

The test procedure would then be as follows:-

Having positioned the sample in the test cell and with the capillary tube circuit cut out, fluid is pumped from the main fluid reservoir at the base of the machine via the intermediate fluid reservoir and the main fluid supply line into the test

cell,...../

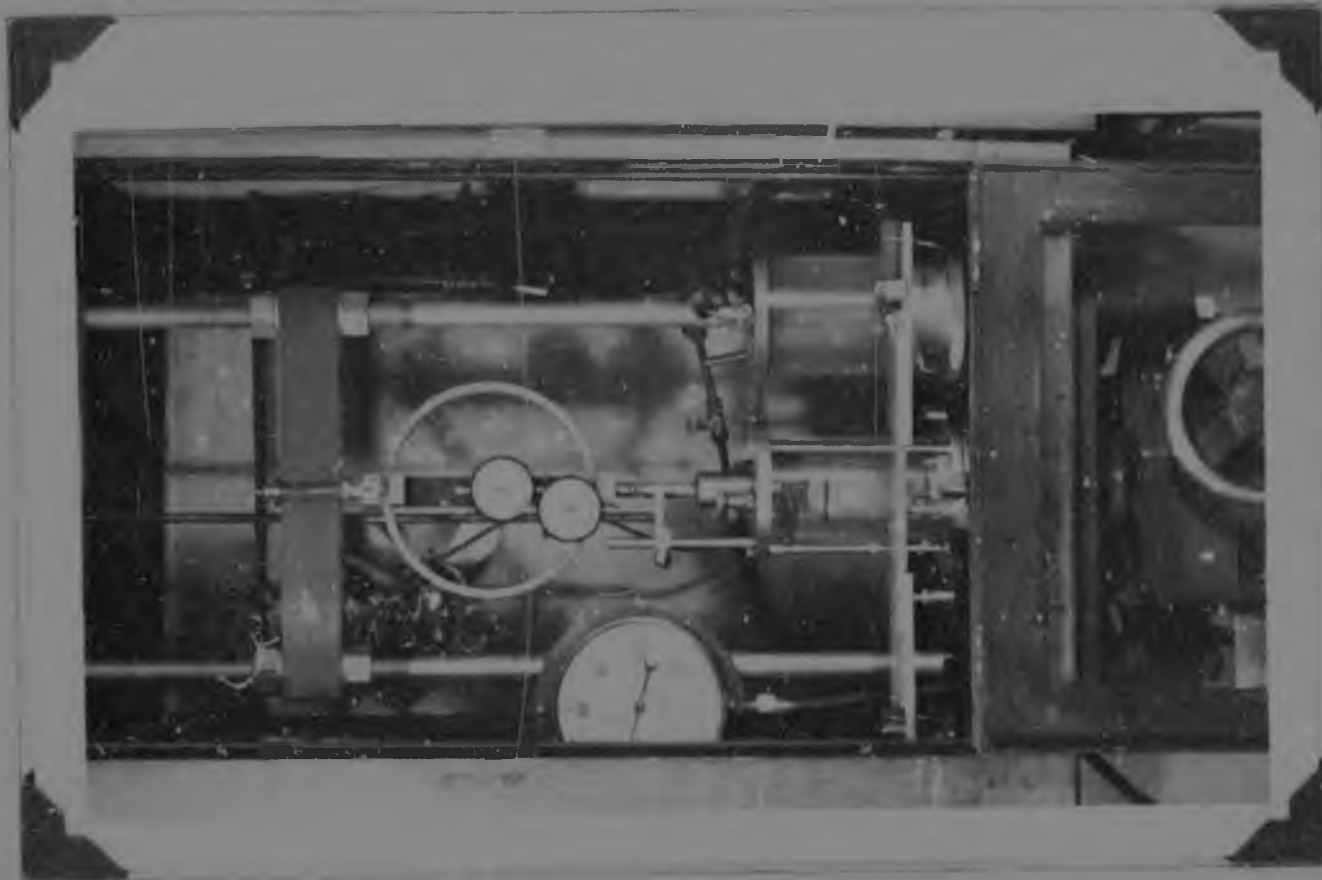


FIG. 21 - ARRANGEMENT WITHIN TEMPERATURE
CONTROL CHAMBER



FIG. 20 - OUTSIDE VIEW OF TEMPERATURE
CONTROL CHAMBER ENCLOSING THE TEST BED

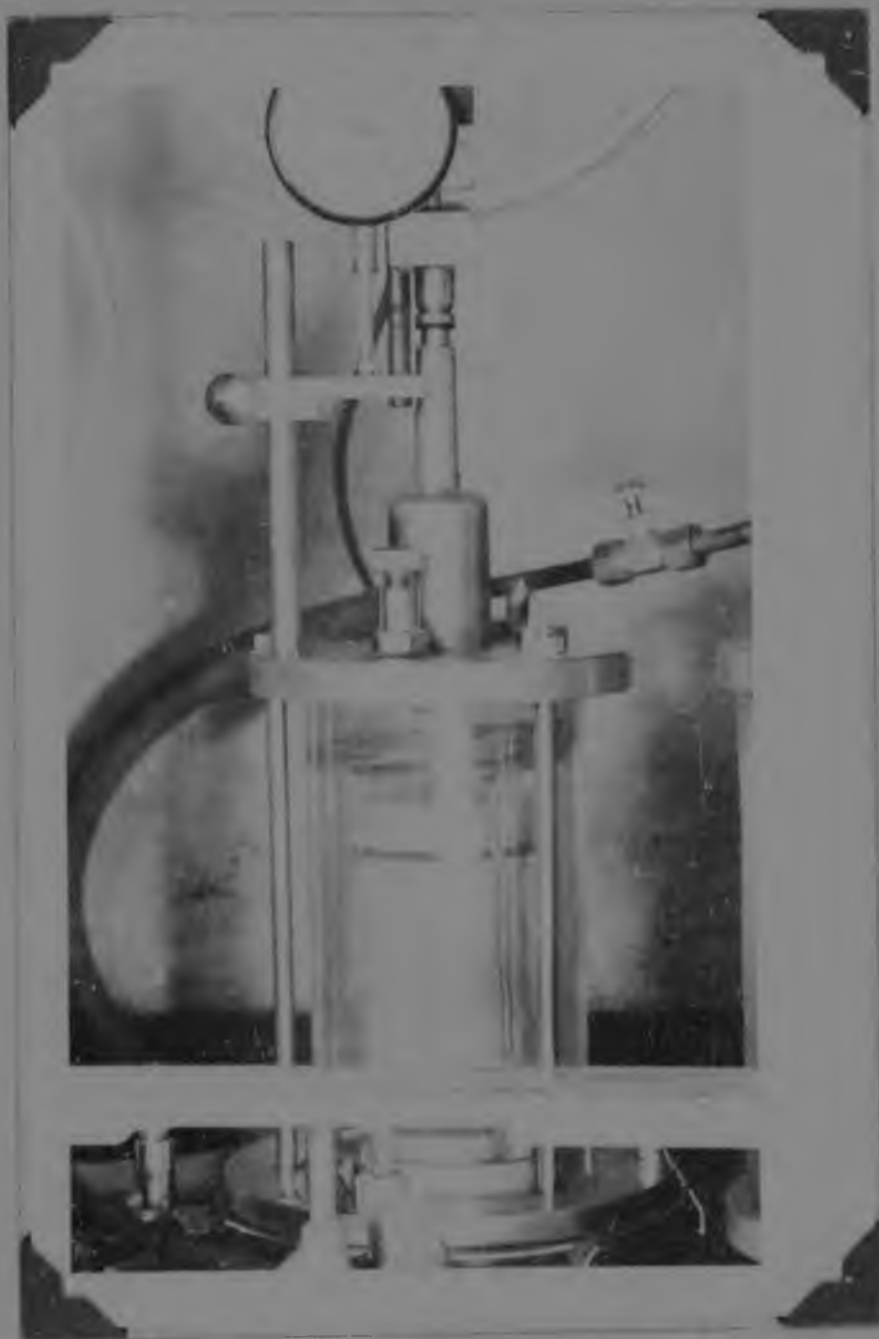


FIG 22 - TRIAXIAL TEST CELL WITH
SAMPLE IN POSITION



FIG 23 - CAPILLARY TUBE (WITH SLUG) FIXED TO GRADUATED SCALE

cell, as is usual procedure with triaxial tests. Having attained the preselected chamber pressure, as indicated on the pressure gauge, the variable head of mercury is suitably adjusted, if necessary, and an accurate head measurement made.

Immediately prior to testing the sample, the capillary tube circuit is opened as well, so as to produce equilibrium conditions in all circuits throughout the whole test system. Under this condition it is possible to move the mercury slug in the capillary to any desired position along the tube, by simply tilting it up or down at one end as required. Movement of the slug is made possible by the fluid moving round in the continuous closed circuit formed by the main fluid supply line in parallel with the capillary tube circuit. This knowledge serves a very useful purpose in cases where it happens that during a test the slug tends to move off the scale, as by opening the main fluid supply circuit and tilting the tube, the slug can be readily reset to the desired position without stopping the test to do so. After the test, each gap in the recording can easily be bridged by plotting several points on either side of a particular gap on a large scale and then, by knowing what the change in deflection during the reset interval had been, arranging, by a little trial and error, that the two sets of points be linked with a common smooth curve which thus also straddles the gap.

At the commencement of the test the main fluid supply line is closed off so that only the capillary tube circuit is cut in, and the following effects take place:

The loading spindle advances downwards into the test cell causing the displacement of cell fluid back into the fluid reservoir via the capillary tube circuit, thus causing a slug movement from left to right. Superimposed on this, is a movement of fluid into the test cell from the fluid reservoir via the capillary tube circuit if a decrease in volume of the sample occurs as a result of the loading, (thereby causing a slug movement from right to left), or vice-versa in the event of a volume increase of the sample. Furthermore, superimposed on these two effects is an additional fluid movement into the test cell via the capillary tube circuit, to replace any leakage from the test cell (which usually occurs when the loading spindle enters the cell), thus also causing a slug movement from right to left. Hence, during a test, the slug movement in the capillary tube is thus the net movement resulting from three combined effects, and in order to determine the slug movement due to volume change of the sample only, it is necessary to separate out the slug movement which has taken place due to the other two effects.

As previously mentioned, slug movement due to entry of the loading spindle into the test cell can be calculated from a knowledge of the diameter of the capillary tube and from a determination of the volume of fluid displaced by the movement of the spindle. The latter can be found from a knowledge of the diameter of the spindle and the distance the spindle has travelled into the test cell, which corresponds to the deflection of the sample as read on the relevant dial deflection gauge.

The value of slug movement as a result of leakage from the test cell during an actual test, cannot be determined directly as during the test it is not possible to eliminate the effects of slug movement due to spindle entry and sample volume change. The only circumstances under which slug movement due to leakage only can be measured is under the steady conditions existing immediately before or after test. This measurement may thus not be truly representative of the actual slug movement due to leakage occurring during a test, as the rate of leakage may be

affected/

affected by the disturbed conditions during test. However, as this serves as a means of obtaining some idea of the leakage during test, these measurements were taken and in each case with the full particular chamber pressure acting and only the capillary tube circuit cut in.

To obtain some idea of the leakage under disturbed conditions similar to those existing during a test, a measurement of slug movement due to the combined effects of leakage and spindle entry only was contemplated, from which, by knowing from calculation the value of slug movement due to spindle entry only, the value of slug movement due to leakage only could be determined. As such measurements would only be possible provided no sample volume change effects were present, it was considered most suitable to carry out this determination immediately after completion of a test in the following manner:

With the capillary tube circuit closed off and the main supply circuit cut in, the spindle is raised to a convenient height above its previous position on the top end plate in contact with the failed sample. With the relevant chamber pressure still acting and with only the capillary tube circuit cut in, the machine is again started and a series of slug movement : deflection readings taken. This slug movement recording is now inclusive of both spindle entry and leakage effects, but exclusive of sample volume change effects. This combined measurement would be carried out directly after the leakage measurement at the completion of the test, as discussed above.

Finally, to round off these measurements of slug movement due to leakage and spindle entry effects, a further leakage measurement is made immediately after this measurement of slug movement due to the combined effects of leakage and spindle entry.

7.5 The Test Series

As previously mentioned (Section 7.3), the type of triaxial compression test selected for the test series was the Consolidated Undrained Shear Test (Su) with strain control. In order to obtain some information about the possible effect of rate of strain and chamber pressure on the value of Poisson's Ratio determined for the soil, it was decided that the test series should comprise three tests at a comparatively fast speed, and three tests at a much slower speed. Each set of three tests would then be done at three different chamber pressures which were to be 10lb/sq.in., 20lb/sq.in., and 30lb/sq.in., thus six tests in all. The chamber pressures of 10lb/sq.in. corresponded approximately to the overburden pressure of a 13ft. depth of soil, to which the test soil had been subjected in the field.

Two convenient rates of strain, one fast and one slow, were obtained by using suitable gearbox settings. An initial determination of the resulting rates of strain was made by running the machine at each of the selected gearbox settings in turn, and taking deflection/time readings. While recording, the spindle would be entering the test cell against the resistance of the cell fluid only, which was at an arbitrarily selected chamber pressure of 30lb/sq.in. It was realized that the values determined might be dependent on the particular chamber pressure used, and might also be affected by the resistance of a sample to loading during an actual test. Hence, it was decided to refer to them as the nominal rates of strain. For the fast speed this was found to be 0.0125 inches per minute and for the slow speed 0.00256 inches per minute.

As all samples were to be consolidated in the triaxial cell under the respective chamber pressures selected, it was necessary to know within what length of time such consolidation would be completed. Hence, in conducting a consolidation test on an undisturbed sample of the test soil, settlement:time readings were taken in each case immediately after placing the loading increments corresponding to chamber pressures of 30lb/sq.in., 20lb/sq.inches, and 10lb/sq.in., respectively, i.e. approximately 2Ton/sq.ft., 1.5Ton/sq.ft. and 0.7Ton/sq.ft. respectively. These curves are shown on the next page. It was found that 90% consolidation would be reached within less than 24 hours in all cases and hence it was decided to consolidate all samples for about 24 hours before testing.

The following is a description of a typical test performed. A 3" length x 1 1/2" dia., cylindrical sample was cut from an undisturbed block sample of the soil, using the cutting cylinder provided for the purpose. To standardise the volume of all test samples cut, the same cutting cylinder was used throughout. An intermittent check was kept on the initial moisture content of test samples by using cuttings from the particular test sample being trimmed.

The sample was then placed in the triaxial machine and allowed to consolidate with drainage for about 24 hours under the particular chamber pressure selected.

When consolidation was completed, the drainage cock was closed and after noting the temperature inside the closing wooden box, a leakage measurement was made by recording slug movement: time readings every 15 seconds for 5 minutes, according to the procedure already described in the previous Section.

The slug was then reset to a convenient position along the scale and the main fluid supply line closed off to leave only the capillary tube circuit cut in. After noting the time and again the test temperature, the test was commenced. Using deflection as a basis, accurate readings of load, slug movement, and time together with intermittent temperature readings were taken over the whole duration of the test, until definite shear failure of the sample had occurred. At the end of the test, the time as well as the temperature were recorded and a sketch of the failed sample made. On occasion, it may have been necessary to reset the slug during a test and this was then done on the lines previously described. In the initial tests, only deflection, load and slug movement were recorded, two observers being required in the case of fast tests. Continuous time recordings were initially not considered necessary, in view of the acceptance of a constant rate of strain during test, and in addition would have required a third observer which was not readily available. However, the need for continuous time recordings throughout any test (see Section 2.3) in order to determine the actual rate of strain was realised once the fact of an uneven rate of strain during test had been noticed, and it was thus necessary to call in the assistance of a third observer. Although time readings were thus not taken in some tests, it was, however, possible to utilise the information obtained from other tests in which time readings were taken to cover such cases.

Immediately after completion of the test and with the sample and loading spindle in the same position as when the machine was stopped, the slug in the capillary was reset to a convenient position and a leakage measurement made similar to the one carried out immediately before the commencement of the test. Temperature and time were appropriately recorded.

This/

SETTLEMENT--TIME CURVES

(FROM NORMAL 1-DIMENSIONAL CONSOLIDATION TEST.)

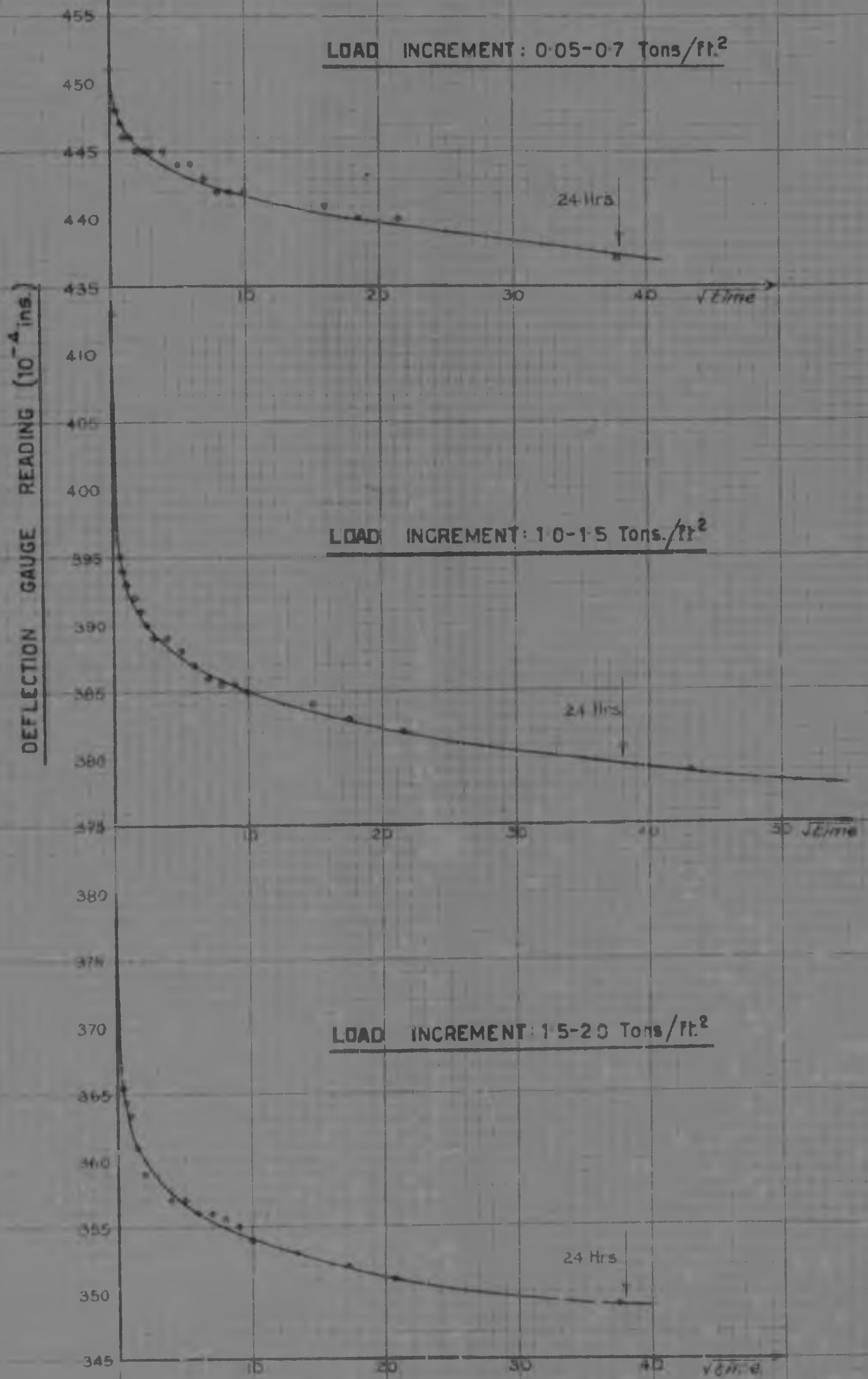


FIG. 24

SETTLEMENT-TIME CURVES

(FROM NORMAL 1-DIMENSIONAL CONSOLIDATION TEST.)

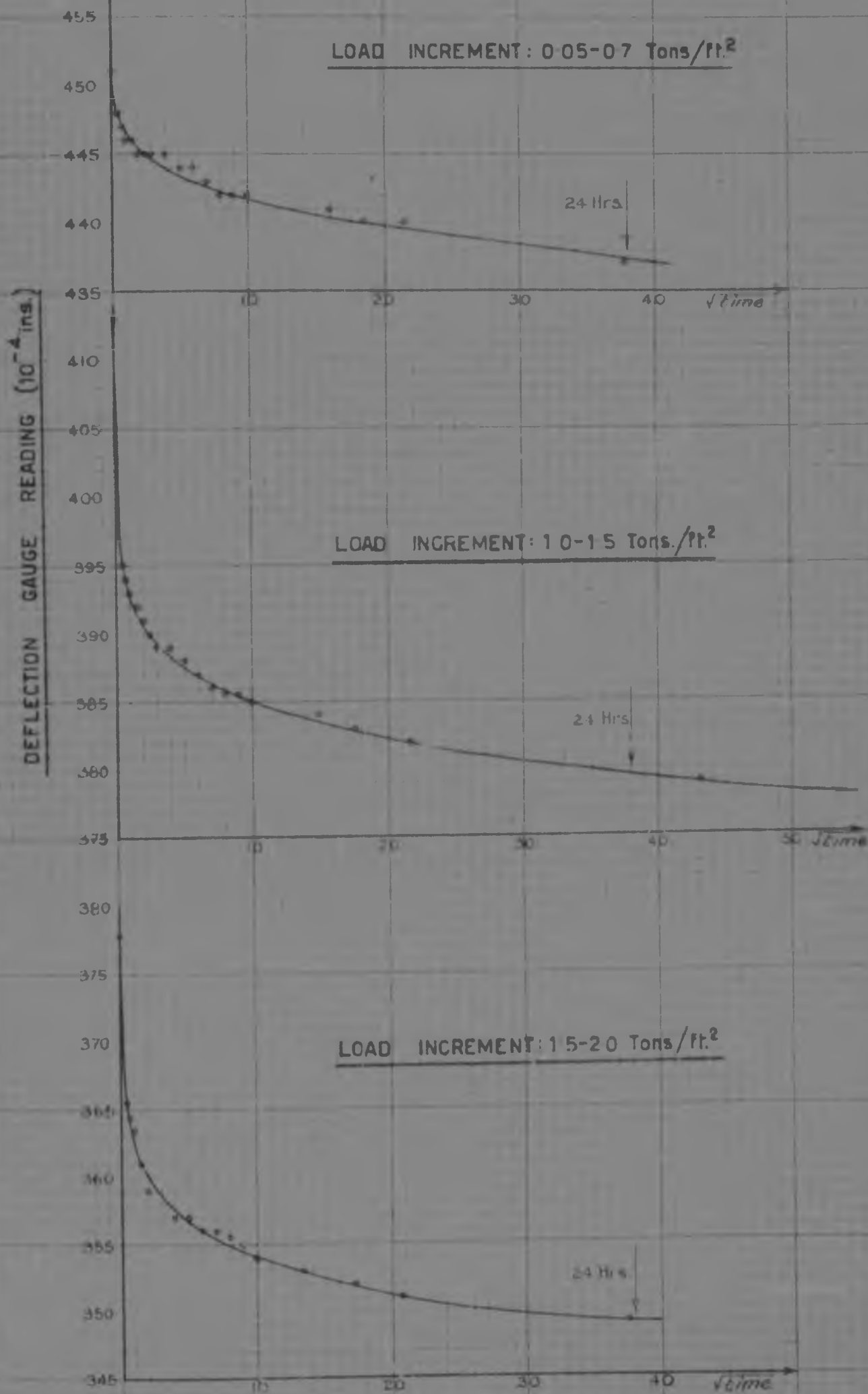


FIG. 24

This having been done, a recording of slug movement due to the combined effects of leakage and spindle entry was carried out according to the procedure described under "Test Apparatus". In addition, however, time readings were also taken in order to determine the rate of strain under these circumstances and so to ascertain the possible effect of the particular chamber pressure used on the nominal rate of strain previously established. Rate of strain was determined in this manner for each test and will hereafter be referred to as the Calibrated rate of strain.

After this combined recording, a further leakage measurement was finally made, similar to the ones previously carried out.

Then with the capillary tube circuit cut out and only the main fluid supply circuit left in, the chamber pressure was released and the oil fluid allowed to drain back into the fluid reservoirs. The failed sample was carefully removed and a moisture content determination carried out.

According to this procedure, tests falling into each of the six type categories previously mentioned were carried out. Their strength values for tests in the same speed category were plotted in the form of Mohr diagrams and any that showing poor fit was discarded and a repeat test subsequently performed.

At the completion of the test series it was necessary to determine the cross-sectional area of the capillary tube used. This was done by obtaining the weight of mercury required to fill the tube exactly over its whole length and measuring the length of the tube accurately. From these measurements the volume of mercury required to fill the tube and hence the volume of the tube and its average cross-sectional area could be calculated. (See Item 1, Appendix V).

7.6 Test Observations and Curves

On the following pages, test observations and curves are given for the results of six tests. The results of each test appear in the following sequence:

1. Tabular presentation of the following data:
 - (a) Leakage measurement immediately before test.
Denoted: "Before test".
 - (b) Leakage measurement immediately after test.
Denoted: "After test (1)".
 - (c) Combined leakage + spindle entry measurement (after test).
 - (d) Further leakage measurement. Denoted: "After test (2)".
2. Presentation of the curves for the above data.
3. Tabular presentation of the main test observations under suitable headings, with selection of their observations.
4. Graphical presentation. Rate of Strain determinations:
 - (a) After test: spindle entry against resistance of relevant pressure only, i.e. Calibrated Rate of Strain.
 - (b) During test: spindle entry against resistance of relevant pressure as well as resistance of sample to compression, i.e. actual Rate of Strain during test.
5. (a) Stress:Strain curve.
(b) Young's Modulus:Strain Curve.
6. Tabular presentation: Calculation of Instantaneous values of Young's Modulus as a secant modulus over the initial range of the Stress:Strain curve.

7. Slug/

7. Slug movement : Deflection curve for the three combined effects during an actual test. This curve is headed: "Main slug movement : deflection curve".

Then, following on these sets of test results for each of the six tests performed, are:

8. Summary in Tabular Form of the six Triaxial Test results, i.e., the Shear Strength results required for constructing the Mohr Circles for each test.
9. Two sets of Mohr Circles, corresponding to the results of tests within the same soil categories.

The following points should, however, be especially noted:

(1) Triaxial chamber pressure values could be read on the pressure gauge provided for this purpose, but, as a check and for more accuracy, the height of a mercury column balanced by the chamber pressure was measured in each case. This pressure as a head of mercury was then converted to an equivalent pressure in lb/sq.in. The observed pressure value read on the triaxial pressure gauge will hereafter be referred to as the "Nominal" chamber pressure and the value obtained from the measured head of mercury will be referred to as the "Actual" chamber pressure.

(2) With regard to the lateral stress calculation in item (3) mentioned above: The initial sample area used was taken to be the cross-sectional area of the cutting cylinder, i.e., the area of a circle 1.0" in diameter. This gave a figure of 1.77 sq.in. The actual cross-sectional area of a sample may have been slightly less than this, thus leading to slightly greater stresses, but this is considered to be of little consequence for the purposes of these tests. However, the effect of lateral sample strain during compression, i.e., an increase in sample diameter and hence cross-sectional area, was taken into account by applying a factor:

$$1 - (\text{longitudinal strain}), \text{ i.e., } 1 - \epsilon$$

The "corrected stress" was thus obtained by using the initial sample area of 1.77 sq.in. divided by the appropriate value of this factor in each case.

(iii) Stress:Strain Curves (item 3(i)) and Main Slug Movement:Deflection Curves (item 7): These curves were, in the first instance drawn fully according to the data observed during the tests. In most cases the presence of "bedding-in" effects at the start of tests was clearly revealed by both these curve types. In the case of Stress:Strain curves, the strain due to "bedding-in" effects was determined by producing the initial approximately linear portion of the curve backwards to intersect the strain axis. The intercept on this axis then represents the strain due to "bedding-in" effects. This information was subsequently used for constructing the Young's Modulus:Strain curves. In the case of the Main Slug Movement:Deflection curves, the unusual peak-shaped "bedding-in" effect observed in some instances, is fully discussed in Section 7 of this Chapter. With the final presentation of test results (see Chapter 8, Figs. 43, 44, 45 and 46) "bedding-in" effects have been ignored.

(iv) Young's Modulus:Strain Curves (item 3(ii)): These curves are based on instant moduli values of Young's Modulus calculated as a secant modulus, i.e., working from point to point along the Stress:Strain curves but always from the corrected start of the curves, i.e., as obtained after eliminating "bedding-in" effects. For this reason the start of all Young's Modulus:Strain curves is displaced to the right of the actual start of the corresponding Stress:Strain curves.

TEST NO. 1

DATE PERFORMED 16/2/57

SAMPLE CONSOLIDATED FOR 22^{HR} 15^{MIN} PRIOR TO TEST

TIME START OF TEST 4/30 PM TEMPERATURE 27.5°C

TIME END OF TEST 5/54 PM TEMPERATURE 27.25°C

NOMINAL σ_3 CHAMBER PRESSURE 30 LB/30 IN

HEAD OF MERCURY 58 $\frac{1}{2}$ INCHES (FULL)

ACTUAL σ_3 CHAMBER PRESSURE 26.015 LBS/IN²

STRAIN RATE OF STRAIN 0.00256 IN/IN/MIN

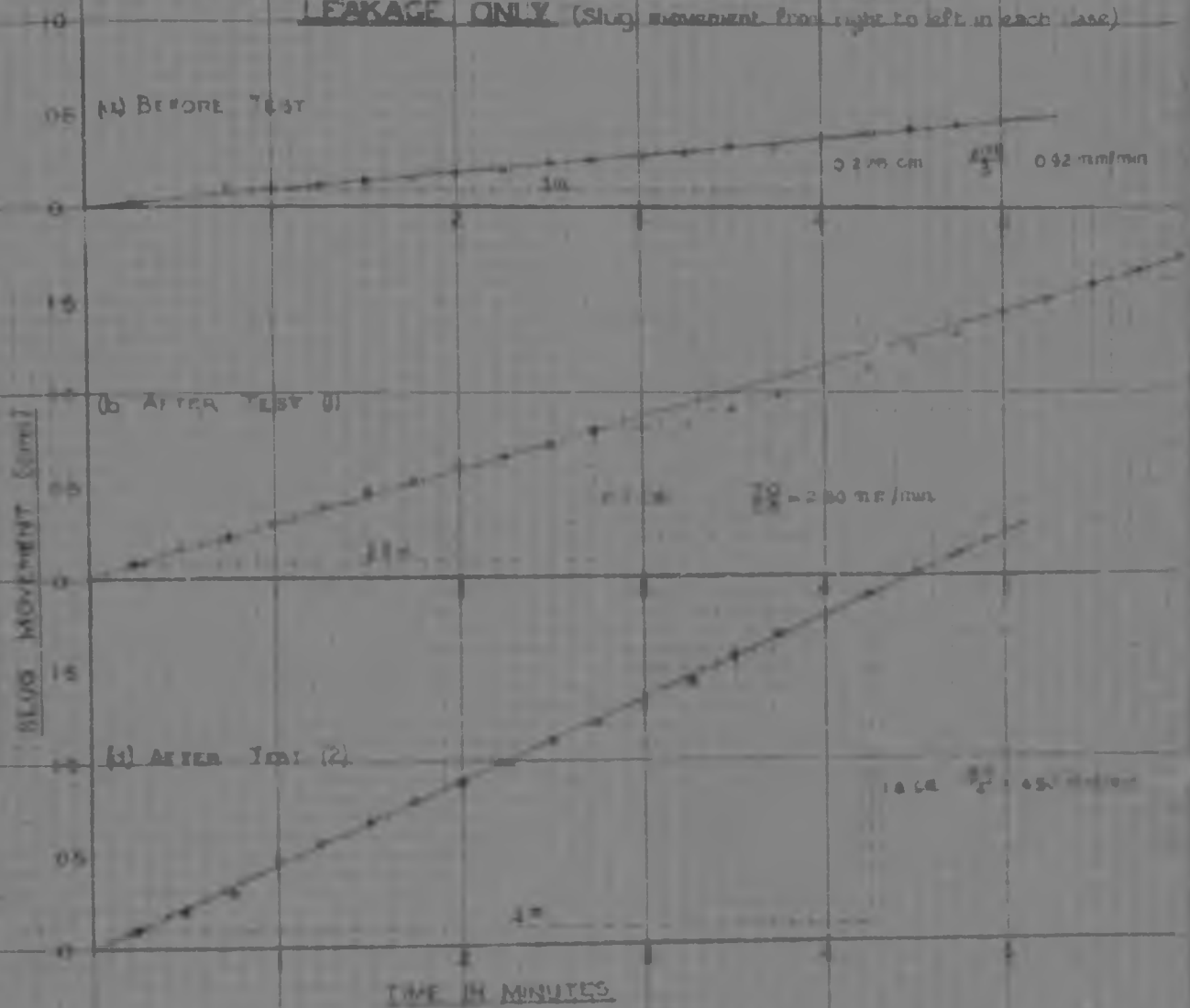
TEST NO 1 LEAKAGE MEASUREMENTS

(A) MEASUREMENT OF SLUG MOVEMENT DUE TO LEAKAGE ONLY BEFORE TEST TEMP 27.50°C TIME 4/25 P.M.			(B) MEASUREMENT OF SLUG MOVEMENT DUE TO LEAKAGE ONLY. AFTER TEST (1) TEMP 27.25°C TIME 5/55 P.M.		(C) MEASUREMENT OF SLUG MOVEMENT DUE TO COMBINED EFFECTS OF LEAKAGE & SPINDLE ENTRY (AFTER TEST) TEMPERATURE 27.25°C TIME 6/05 P.M.			(D) MEASUREMENT OF SLUG MOVEMENT DUE TO LEAKAGE ONLY AFTER TEST (2) TEMP 27.25°C TIME 6/05 P.M.	
TIME	VOLUME		TIME	VOLUME	DEFLECT	VOLUME	TIME	TIME	VOLUME
min. sec.	SCALE		min. sec.	SCALE	GAUGE	SCALE	min. sec.	min. sec.	SCALE
				cm	mm	cm			cm
0 00	21.60		0 00	8.90	40	7.40	0 00	00	6.60
15	21.575		15	8.825	41	7.35	15	15	6.50
30	21.525		30	8.725	42	7.30	30	30	6.40
45	21.50		45	8.675	43	7.30	45	45	6.30
1 00	21.50		1 00	8.60	44	7.30	1 00	00	6.125
15	21.475		15	8.50	45	7.275	15	15	6.025
30	21.475		30	8.425	46	7.225	30	30	5.925
45	21.45		45	8.375	47	7.185	45	45	5.825
2 00	21.425		2 00	8.30	48	7.185	2 00	00	5.725
15	21.40		15	8.25	49	7.15	15	15	5.625
30	21.375		30	8.20	50	7.175	30	30	5.50
45	21.35		45	8.125	51	7.175	45	45	5.40
3 00	21.325		3 00	8.10	52	7.15	3 00	00	5.30
15	21.30		15	8.075	53	7.125	15	15	5.275
30	21.275		30	8.00	54	7.10	30	30	5.05
45	21.275		45	7.90	55	7.10	45	45	4.975
4 00	21.225		4 00	7.825	56	7.075	4 00	00	4.875
15	21.20		15	7.75	57	7.05	15	15	4.75
30	21.175		30	7.65	58	7.025	30	30	4.675
45	21.15		45	7.575	59	7.00	45	45	4.475
5 00	21.125		5 00	7.475	60	7.00	5 00	00	4.375
			55	7.40	61	6.975			
			30	7.350	62	6.975			
			45	7.25	63	6.95			
			6 00	7.175	64	6.925			
					65	6.90			
					66	6.90			
					67	6.90			
					68	6.90			
					69	6.85			
					70	6.85			
					71	6.825			
					72	6.80			
					73	6.80			
					74	6.80			
					75	6.80			
					76	6.775			
					77	6.775			
					78	6.75			
					79	6.725			
					80	6.725			
					81	6.75			

TEST NO. 1 LEAKAGE MEASUREMENTS

DETERMINATIONS OF RATE OF SLUG MOVEMENT DUE TO

LEAKAGE ONLY (Slug movement from right to left in each case)



(c) DETERMINATION OF RATE OF SLUG MOVEMENT DUE TO COMBINED EFFECTS OF LEAKAGE & SPINDLE ENTRY



FIG. 25.

TEST No 1 MAIN TEST OBSERVATIONS

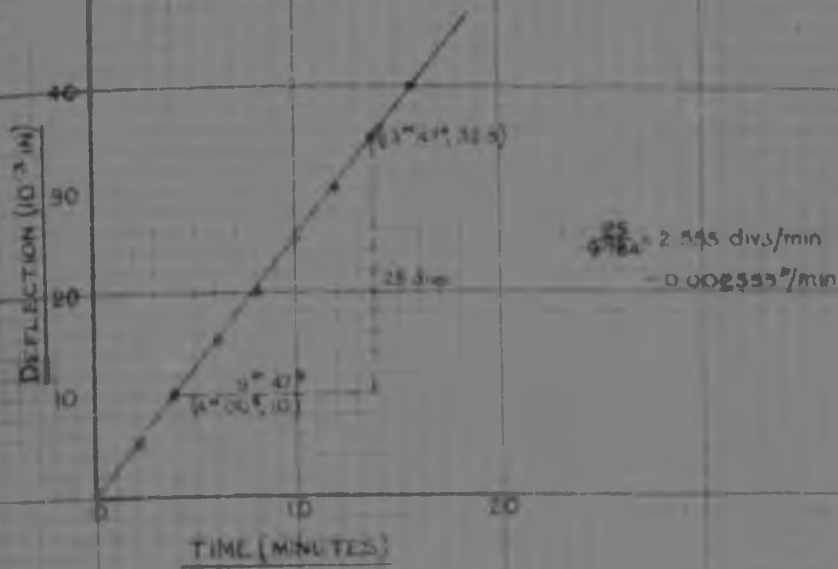
DEFLEC- TION GAUGE	LOAD GAUGE	SLUG SCALE	TIME	TEMPER- TURE	CORRECTED SLUG SCALE cm	CORRECTED LOAD lb	CORRECTED DEFLECT 10 ⁻³ in.	STRAIN ε percent	CORRECTED STRESS (G-C) 64 10 ³ psi
00 30	20	10.70	00 00	27.2	0	0	0	0	0
31	24.5	10.70	00 27		0	4.2	1	0.035	3.64
32	27.5	10.70	00 55		0.028	2.2	2	0.047	4.23
33	32	10.30	01 32		0.40	12.2	3	0.100	8.97
34	37.5	10.70	07 27		0.18	12.8	4	0.133	10.04
35	44.5	10.6	08 40		0.10	24.2	5	0.182	14.00
36	49.5	10.5	09 21		0.40	24.8	6	0.200	16.80
37	52.1	24.325	10 11		0.375	35.1	7	0.213	19.78
38	59.5	23.345	10 38		0.875	38.5	8	0.247	22.43
39	64.5	20.5	11 38		1.40	44.3	9	0.300	25.21
40	69.0	21.30	12 08		0.40	48.0	10	0.333	27.60
41	73.5	20.30	12 42		0.40	52.0	11	0.387	29.75
42	77.5	18.50	13 12		10.70	56.0	12	0.400	31.04
43	81.5	17.505	13 48		11.472	60.2	13	0.411	32.72
44	86.5	17.572	14 23		10.500	64.2	14	0.425	34.08
45	90.5	17.175	14 52		10.300	68.2	15	0.437	35.67
46	95.5	17.04	15 30		14.44	73.2	16	0.453	37.35
47	97.5	14.770	16 03		13.415	77.0	17	0.467	38.21
48	100.5	14.7	16 37		16.40	81.2	18	0.480	40.24
49	104.0	14.50	17 12		16.40	84.0	19	0.483	41.14
50	107.0	13.875	17 42		13.000	87.2	20	0.487	42.77
51	110.6	13.50	18 17		14.00	91.2	21	0.490	44.33
52	113.4	12.70	18 40		20.70	93.2	22	0.492	45.40
53	116.4	8.80	19 23		11.05	96.4	23	0.494	46.33
54	119.5	7.8	19 58		12.70	100.2	24	0.497	47.41
55	122.5	6.95	20 31		12.70	104.2	25	0.493	48.49
56	124.5	6.10	21 00		23.6	108.0	26	0.487	49.8
57	127.5	5.35	21 32		24.35	112.2	27	0.480	50.82
58	130.0	4.5	22 00		25.10	116.2	28	0.453	51.4
59	131.5	3.5	22 30		25.80	121.2	29	0.457	52.4
60	134.5	2.5	22 57		26.50	124.1	30	0.450	53.4
61	136.3	1.80	23 31		27.2	128.3	31	0.443	54.4
62	138.4	1.5	24 17		28.00	132.2	32	0.437	55.71
63	140.5	1.2			28.00	136.2	33	0.430	56.83
64	142.5	0.8	24 58		28.00	140.2	34	0.423	57.94
65	144.5	0.5	25 25		27.00	144.1	35	0.417	59.02
66	146.5	0.2	25 56		27.00	148.2	36	0.410	60.10
67	147.7	7.375	26 24		27.00	152.2	37	0.403	61.2
68	149.5	4.272	26 48		11.115	156.2	38	0.397	62.3
69	150.5	3.222	27 14		11.225	160.2	39	0.390	63.4
70	152.5	2.272	27 31		11.225	164.2	40	0.383	64.5
71	154.5	1.4	28 00		11.225	168.2	41	0.376	65.6
72	156.5	0.4	28 30		30.55	172.2	42	0.370	66.7
73	158.5	0.2	29 00		30.55	176.2	43	0.363	67.8
74	160.5	0.2	29 31		30.55	180.2	44	0.356	68.9
75	162.5	1.800	30 43		30.55	184.2	45	0.350	70.0
76	164.5	1.5			30.55	188.2	46	0.343	71.1
77	166.5	1.2			30.55	192.2	47	0.336	72.2
78	168.5	0.8			30.55	196.2	48	0.330	73.3
79	170.5	0.5			30.55	200.2	49	0.323	74.4
80	172.5	0.2			30.55	204.2	50	0.316	75.5
81	174.5	0.2			30.55	208.2	51	0.310	76.6
82	176.5	0.2			30.55	212.2	52	0.303	77.7
83	178.5	0.2			30.55	216.2	53	0.296	78.8
84	180.5	0.2			30.55	220.2	54	0.290	79.9
85	182.5	0.2			30.55	224.2	55	0.283	81.0
86	184.5	0.2			30.55	228.2	56	0.276	82.1
87	186.5	0.2			30.55	232.2	57	0.270	83.2
88	188.5	0.2			30.55	236.2	58	0.263	84.3
89	190.5	0.2			30.55	240.2	59	0.256	85.4
90	192.5	0.2			30.55	244.2	60	0.250	86.5
91	194.5	0.2			30.55	248.2	61	0.243	87.6
92	196.5	0.2			30.55	252.2	62	0.236	88.7
93	198.5	0.2			30.55	256.2	63	0.230	89.8
94	200.5	0.2			30.55	260.2	64	0.223	90.9
95	202.5	0.2			30.55	264.2	65	0.216	92.0
96	204.5	0.2			30.55	268.2	66	0.210	93.1
97	206.5	0.2			30.55	272.2	67	0.203	94.2
98	208.5	0.2			30.55	276.2	68	0.196	95.3
99	210.5	0.2			30.55	280.2	69	0.190	96.4
100	212.5	0.2			30.55	284.2	70	0.183	97.5
101	214.5	0.2			30.55	288.2	71	0.176	98.6
102	216.5	0.2			30.55	292.2	72	0.170	99.7
103	218.5	0.2			30.55	296.2	73	0.163	100.8
104	220.5	0.2			30.55	300.2	74	0.156	101.9
105	222.5	0.2			30.55	304.2	75	0.150	103.0
106	224.5	0.2			30.55	308.2	76	0.143	104.1
107	226.5	0.2			30.55	312.2	77	0.136	105.2
108	228.5	0.2			30.55	316.2	78	0.130	106.3
109	230.5	0.2			30.55	320.2	79	0.123	107.4
110	232.5	0.2			30.55	324.2	80	0.116	108.5
111	234.5	0.2			30.55	328.2	81	0.110	109.6
112	236.5	0.2			30.55	332.2	82	0.103	110.7
113	238.5	0.2			30.55	336.2	83	0.096	111.8
114	240.5	0.2			30.55	340.2	84	0.090	112.9

TEST 1 MAIN TEST OBSERVATIONS (Cont.)

DEFLECTION GAUGE	LOAD GAUGE	SLUG SCALE	TEMPERATURE	CORRECTED SLUG SCALE	CORRECTED LOAD	CORRECTED DEFLECT	STRAIN ϵ	CORRECTED STRESS (G/IN ²)
				cm	lb	10 ⁻³ in	%	10 ⁴ psi
117	183.9	5.425	24	41.45	163.2	87	2.410	82.55
120	183.4	5.425	31	41.45	163.4	90	2.400	82.50
123	183.5	5.425	41	41.45	163.5	93	2.400	82.51
126	183.5	5.4	50	41.475	163.5	96	2.400	82.48
129	183.5	5.425	59	41.35	163.5	99	2.390	82.38
132	183.5	5.425	68	41.25	163.5	102	2.400	82.23
135	183.4	5.4	80	41.475	163.4	105	2.390	82.29
138	183.3	5.40	85	40.975	163.1	109	2.380	82.03
141	183.0	5.405	90	40.90	163.0	111	2.380	82.00
144	182.8	5.40	94	40.825	162.7	114	2.380	81.48
147	182.4	5.395	98	40.55	162.4	117	2.380	81.17
150	182.1	5.425	103	40.45	162.1	120	2.380	80.70
153	181.9	5.40	108	40.175	161.8	124	4.100	80.72
156	181.5	5.4	113	40.075	161.5	126	4.200	80.41
159	181.2	7.000	118	39.80	161.2	129	4.300	80.18
162	181.1	7.95	123	39.625	161.1	132	4.400	80.01
165	180.9	7.475	128	39.40	160.8	135	4.500	80.76
168	180.7	7.000	133	39.25	160.5	138	4.600	80.40
171	180.5	7.95	138	39.025	160.2	141	4.700	80.18
174	179.8	5.005	143	38.80	159.8	144	4.800	80.00
177	179.5	5.35	148	38.675	159.5	147	4.900	81.58
180	179.4	5.475	153	38.40	159.4	150	5.000	80.86
183	179.1	5.62	158	38.225	159.1	153	5.100	82.80
186	178.8	5.4	163	38.075	158.8	156	5.200	82.11
189	178.7	5.60	168	37.875	158.7	159	5.300	81.91
192	178.7	5.050	173	37.85	158.7	160	5.343	

TEST NO. 1 RATE OF STRAIN DETERMINATIONS

(a) CALIBRATED RATE OF STRAIN ($G_s = 30 \text{ lb/sq. in.}$)



(b) ACTUAL RATE OF STRAIN DURING TEST ($G_s = 30 \text{ lb/sq. in.}$)

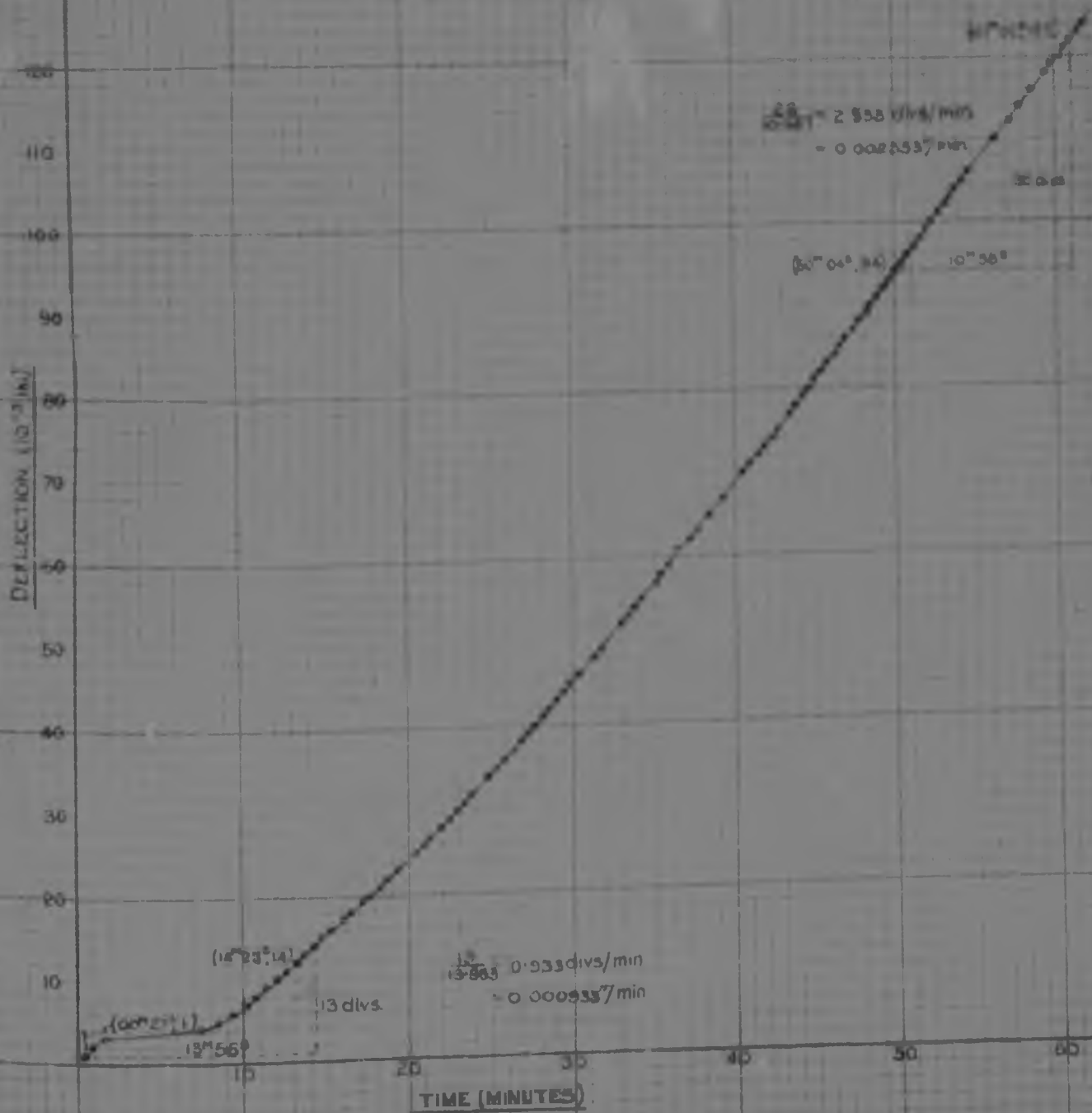


FIG. 26

STRESS STRAIN CURVE



(b) YOUNG'S MODULUS STRAIN CURVE

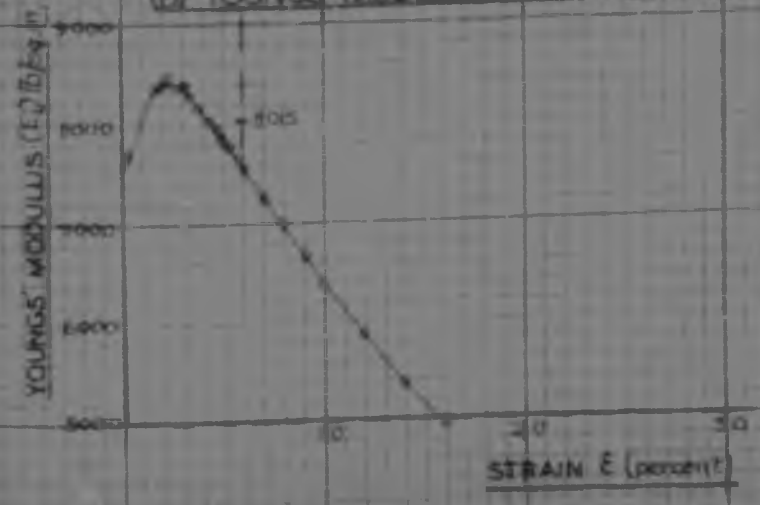


FIG. 27

TEST No. 1
CALCULATION OF INSTANTANEOUS VALUES
OF YOUNGS' MODULUS (E)

CORRECTED STRESS = $\frac{P}{A}$ lb./sq. in.	STRAIN percent	STRAIN DUE TO BEDDING - IN EFFECTS percent	CORRECTED STRAIN = $\frac{S}{1 - \frac{S}{100}}$ percent	YOUNGS MODULUS (E) = $\frac{P}{\Delta L}$ lb./sq. in.
2.54	0.083	0	0.083	7697
4.23	0.167	0	0.167	6313
6.77	0.100	0	0.100	677
10.04	0.133	0	0.133	7549
14.00	0.167	0	0.167	8383
16.20	0.200	0	0.200	8400
18.75	0.233	0	0.233	8499
22.43	0.267	0	0.267	8401
25.23	0.300	0	0.300	8401
27.20	0.333	0	0.333	8286
29.95	0.367	0	0.367	8161
32.64	0.400	0	0.400	8160
34.82	0.433	0	0.433	8042
37.33	0.467	0	0.467	7977
39.79	0.500	0	0.500	7853
41.53	0.533	0	0.533	7792
43.20	0.567	0	0.567	7619
45.38	0.600	0	0.600	7563
47.16	0.633	0	0.633	7450
48.88	0.667	0	0.667	7319
50.83	0.700	0	0.700	7261
52.66	0.733	0	0.733	7184
54.33	0.767	0	0.767	7083
55.90	0.800	0	0.800	6990
60.02	0.833	0	0.833	6669
63.80	1.000	0	1.000	6382
67.33	1.100	0	1.100	6121
70.33	1.200	0	1.200	5861
72.77	1.300	0	1.300	5598
75.09	1.400	0	1.400	5364
76.91	1.500	0	1.500	5127
78.11	1.600	0	1.600	4944
80.60	1.700	0	1.700	4713
82.61	1.800	0	1.800	4529
83.80	1.900	0	1.900	4410
85.04	2.000	0	2.000	4252

MAIN SLUG MOVEMENT DEFLECTION CURVE

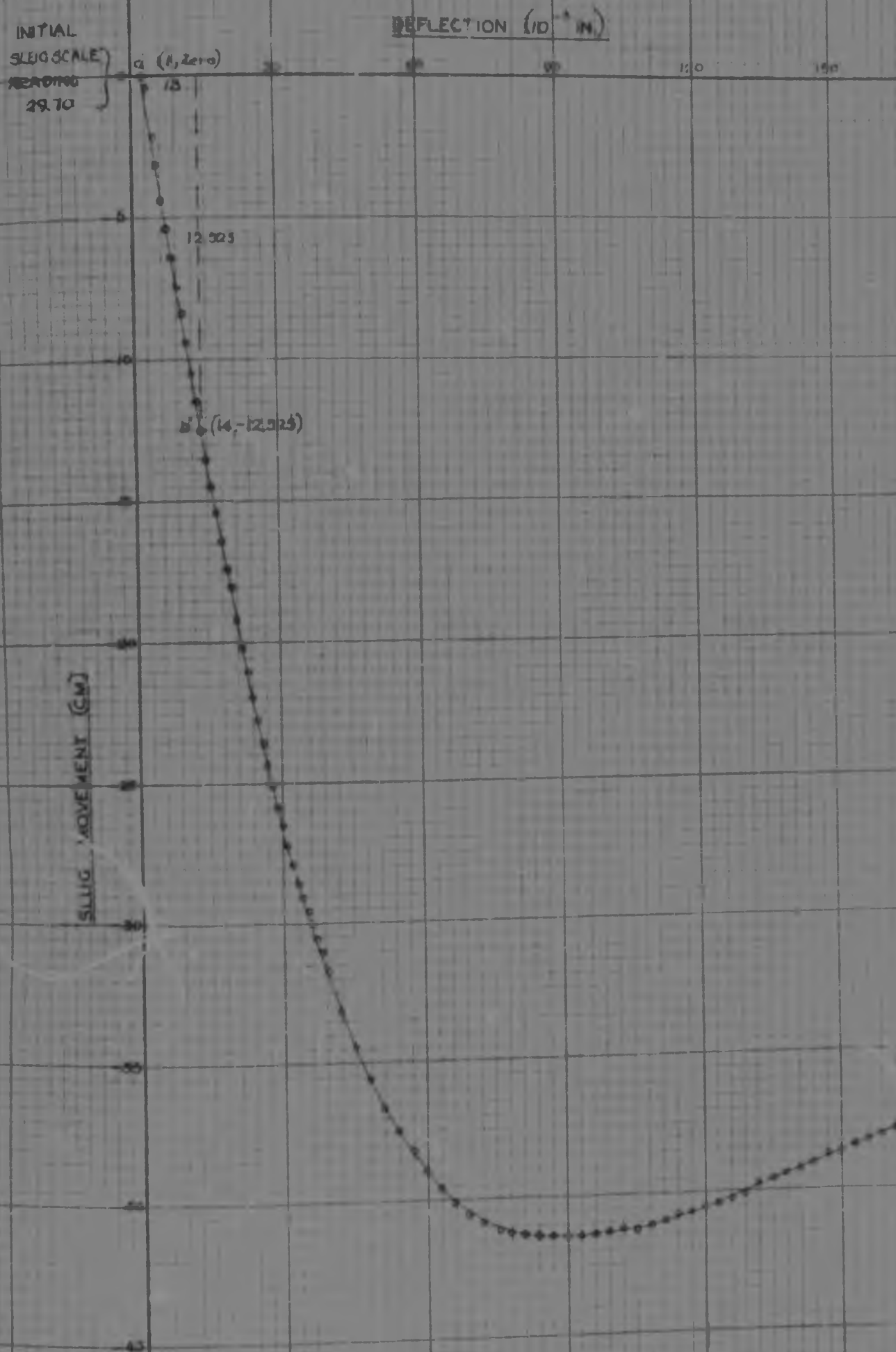


FIG. 28

TEST NO 2

DATE PERFORMED 22/1/57

SAMPLE CONSOLIDATED FOR 24^{hrs} 30^{min} PRIOR TO TEST

TIME START OF TEST 2/55 PM TEMPERATURE 25.25°C

TIME END OF TEST 3/10 PM TEMPERATURE 25.25°C

NOMINAL σ_3 CHAMBER PRESSURE 30 LB./SQ IN

HEAD OF MERCURY 58.9% INCHES, HENCE

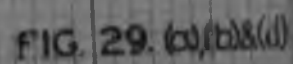
ACTUAL σ_3 CHAMBER PRESSURE 28.738 LB./SQ IN

NOMINAL RATE OF STRAIN 0.0125 INCHES/MINUTE

TEST NO 2 LEAKAGE MEASUREMENTS.

(A) MEASUREMENT OF SLUG MOVEMENT DUE TO LEAKAGE ONLY BEFORE TEST TEMP 25.5°C TIME 2/25p.m.		(B) MEASUREMENT OF SLUG MOVEMENT DUE TO LEAKAGE ONLY. AFTER TEST (1) TEMP 25.25°C TIME 3/15p.m.		(C) MEASUREMENT OF SLUG MOVEMENT DUE TO COMBINED EFFECTS OF LEAKAGE & SPINDLE ENTRY (AFTER TEST) TEMPERATURE: 25.5°C TIME 3/25p.m.		(D) MEASUREMENT OF SLUG MOVEMENT DUE TO LEAKAGE ONLY. AFTER TEST (2) TEMP 25.0°C TIME 3/35p.m.	
TIME min sec	VOLUME SCALE cm	TIME min sec	VOLUME SCALE cm	DEFLECT GAUGE 10	VOLUME SCALE cm	TIME min sec	TIME min sec VOLUME SCALE cm
0 00	26.00	0 00	28.00	00 50	1.60	0 00	23.7
15	25.975	15	27.95	52.5	1.80	15	23.575
30	25.95	30	27.925	55	2.05	30	23.425
45	25.925	45	27.75	57.5	2.30	45	23.3
1 00	25.90	1 00	27.65	60	2.55	1 00	23.175
15	25.85	15	27.55	62.5	2.825	15	23.075
30	25.825	30	27.45	65	3.075	30	23.00
45	25.8	45	27.325	67.5	3.40	45	22.90
2 00	25.775	2 00	27.225	70	3.65	2 00	22.80
15	25.75	15	27.125	72.5	3.90	15	22.70
30	25.70	30	27.025	75	4.20	30	22.60
45	25.675	45	26.95	77.5	4.50	45	22.475
3 00	25.675	3 00	26.85	80	4.80	3 00	22.35
15	25.625	15	26.75	82.5	5.00	15	22.225
30	25.55	30	26.65	85	5.35	30	22.10
45	25.525	45	26.55	87.5	5.65	45	22.00
4 00	25.50	4 00	26.45	90	5.95	4 00	21.80
15	25.475	15	26.325	92.5	6.20	15	21.675
30	25.45	30	26.225	95	6.50	30	21.525
45	25.40	45	26.125	97.5	6.80	45	21.40
5 00	25.375	5 00	26.00	100	7.05	5 00	21.275
				102.5	7.35		
				105	7.60		
				107.	7.85		
				110	8.20		
				112.5	8.45		
				115	8.75		
				117.5	9.05		
				120	9.325		
				122.5	9.525		
				125	9.925		
				127.5	10.125		
				130	10.525		
				132.5	10.825		
				135	11.125		
				137.5	11.40		
				140	11.70		
				142.5	12.00		
				145	12.30		
				147.5	12.55		
				150	12.85		

(Slug movement from right to left in each case)



TEST NO. 2. LEAKAGE MEASUREMENTS (CONTINUED)

(c) DETERMINATION OF RATE OF SLUG MOVEMENT DUE TO COMBINED EFFECTS OF LEAKAGE & SPINDLE ENTRY

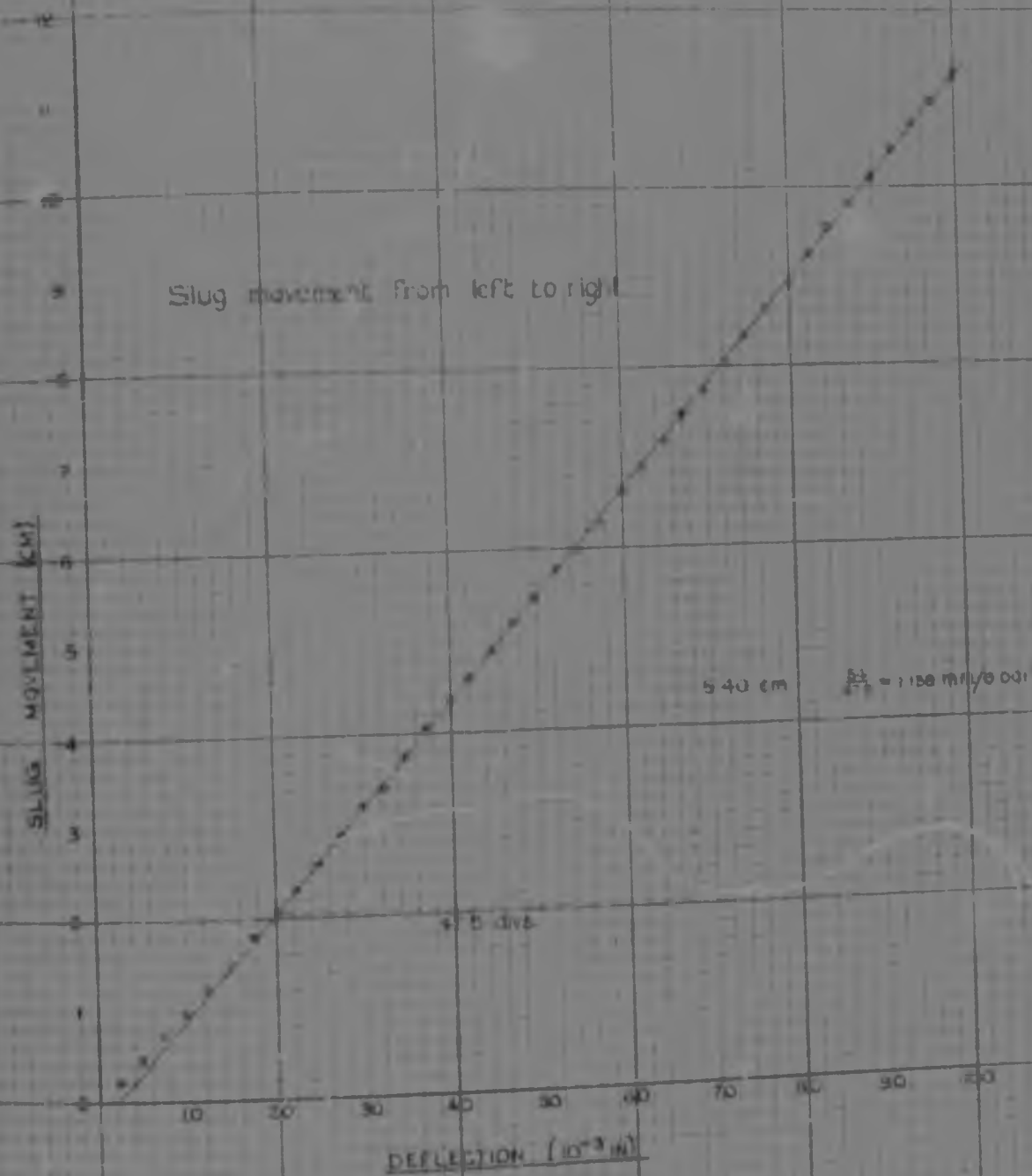
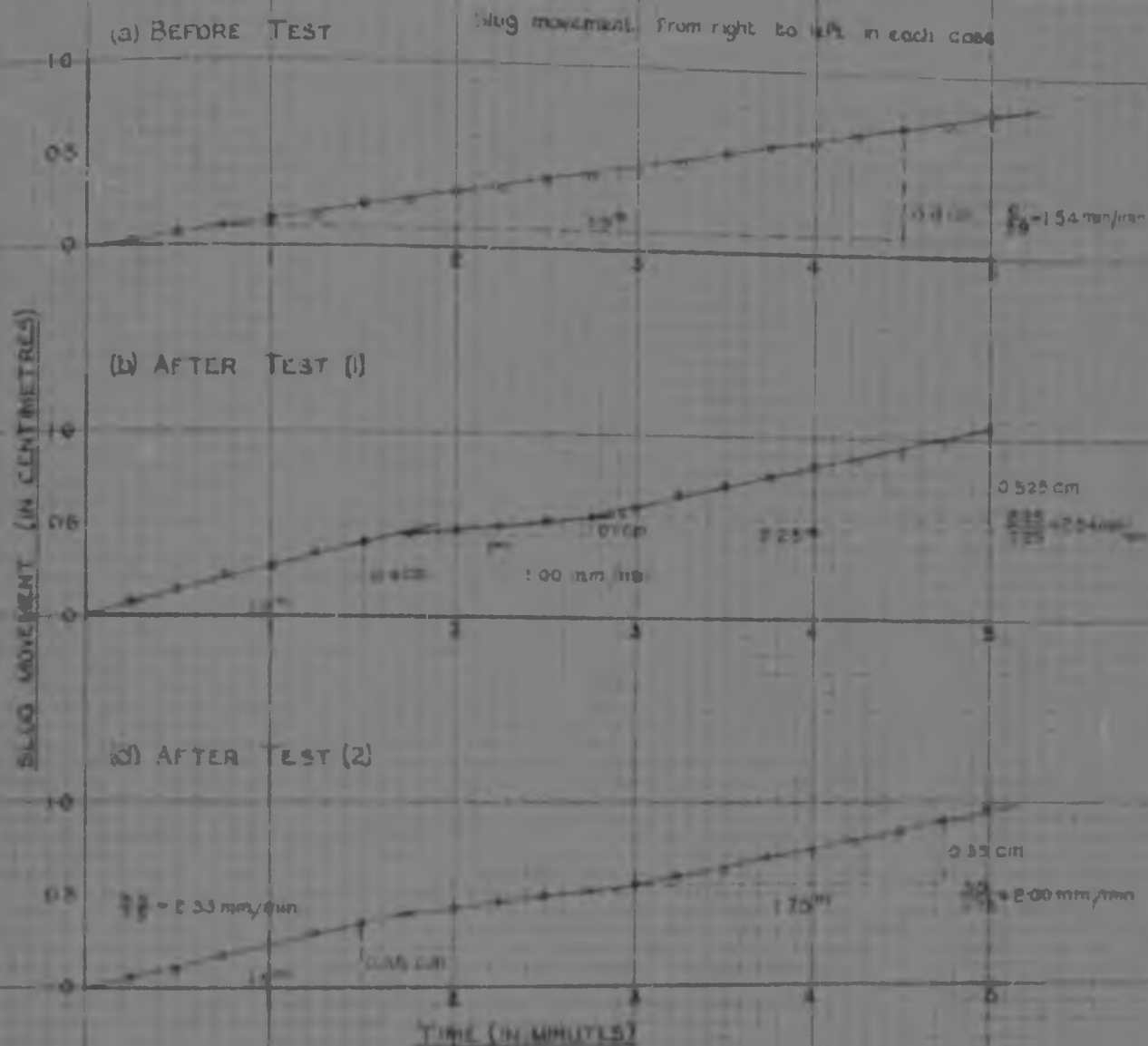


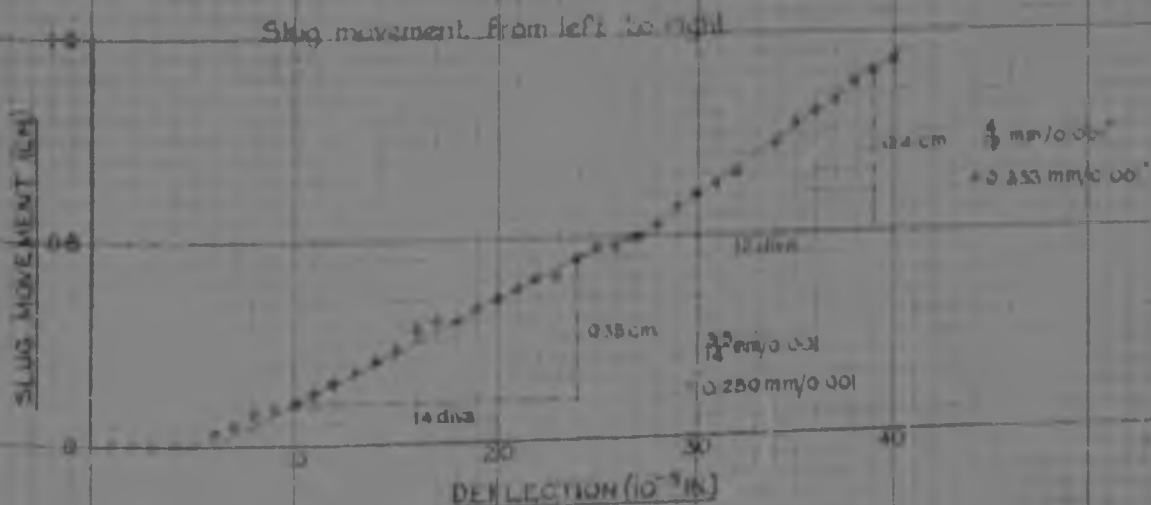
FIG 29(C)

- 83 -
TEST NO3 LEAKAGE MEASUREMENTS

DETERMINATION OF RATE OF SLUG MOVEMENT DUE TO LEAKAGE ONLY



(d) DETERMINATION OF RATE OF SLUG MOVEMENT DUE TO COMBINED EFFECTS OF LEAKAGE & SPINDLE ENTRY



TEST NO 6 : LEAKAGE MEASUREMENTS

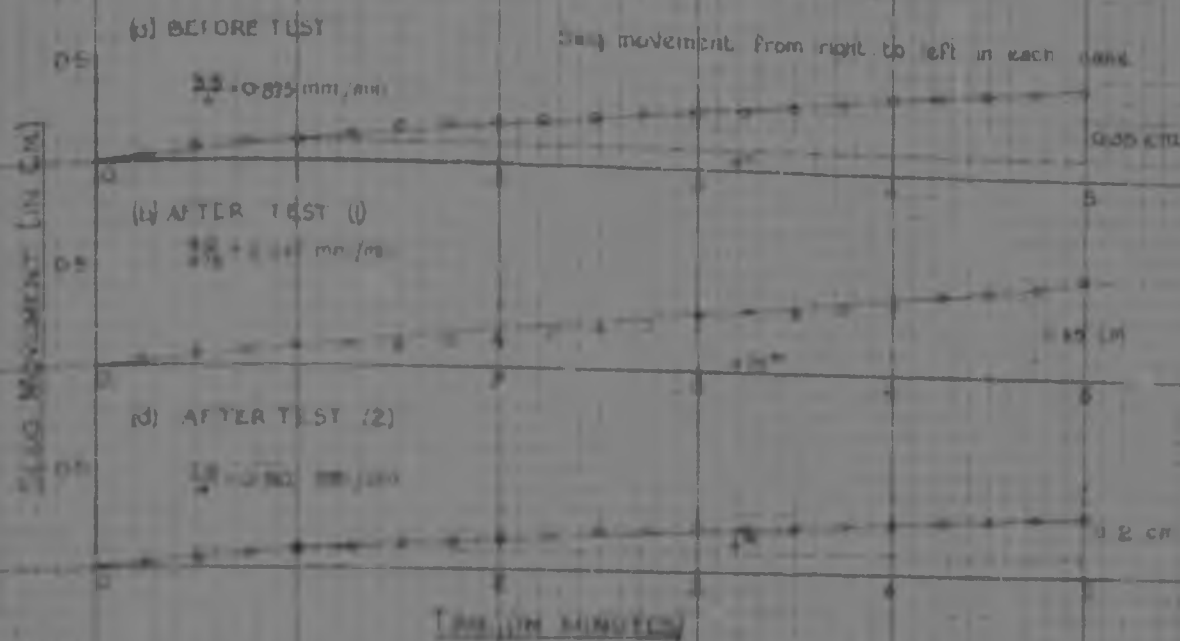
(A) MEASUREMENT OF SLUG MOVEMENT DUE TO LEAKAGE ONLY. BEFORE TEST TEMP 20.25°C TIME 11.14.30		(B) MEASUREMENT OF SLUG MOVEMENT DUE TO LEAKAGE ONLY AFTER TEST (1) TEMP 20.74°C TIME 12/15.45		(C) MEASUREMENT OF SLUG MOVEMENT DUE TO COMBINED EFFECTS OF LEAKAGE & SPINDLE ENTRY (AFTER TEST) TEMPERATURE 20.72°C TIME 12/15.45			(D) MEASUREMENT OF SLUG MOVEMENT DUE TO LEAKAGE ONLY AFTER TEST (2) TEMP 20.72°C TIME 12/15.45	
TIME mm: sec	VOLUME SCALE cm ³	TIME mm: sec	VOLUME SCALE cm ³	DEFLECT GAUGE 10 ⁻³	VOLUME SCALE cm ³	TIME mm: sec	TIME mm: sec	VOLUME SCALE cm ³
0 00	21.40	0 00	21.40	40	18.00	0 00	0 00	18.00
15	21.405	15	21.405	41	18.00		15	18.00
30	21.410	30	21.410	42	18.00		30	18.00
45	21.415	45	21.415	43	18.00		45	18.00
1 00	21.420	1 00	21.420	44	18.00		1 00	18.00
15	21.425	15	21.425	45	18.00	1 58	1 15	18.00
30	21.430	30	21.430	46	18.00		30	18.00
45	21.435	45	21.435	47	18.00		45	18.00
2 00	21.440	2 00	21.440	48	18.00		2 00	18.00
15	21.445	15	21.445	49	18.00		15	18.00
30	21.450	30	21.450	50	18.00	3 58	3 30	18.00
45	21.455	45	21.455	51	18.00		45	18.00
3 00	21.460	3 00	21.460	52	18.00		3 00	18.00
15	21.465	15	21.465	53	18.00		15	18.00
30	21.470	30	21.470	54	18.00		30	18.00
45	21.475	45	21.475	55	18.00	5 58	45	18.00
4 00	21.480	4 00	21.480	56	18.00		4 00	18.00
15	21.485	15	21.485	57	18.00			
30	21.490	30	21.490	58	18.00			
45	21.495	45	21.495	59	18.00		45	18.00
5 00	21.500	5 00	21.500	60	21.00	6 00	5 00	21.00
				61	21.00			
				62	21.00			
				63	21.00			
				64	21.00			
				65	21.00			
				66	21.00			
				67	21.00			
				68	21.00			
				69	21.00			
				70	21.00			
				71	21.00			

TEST NO 3 MAIN TEST OBSERVATIONS.

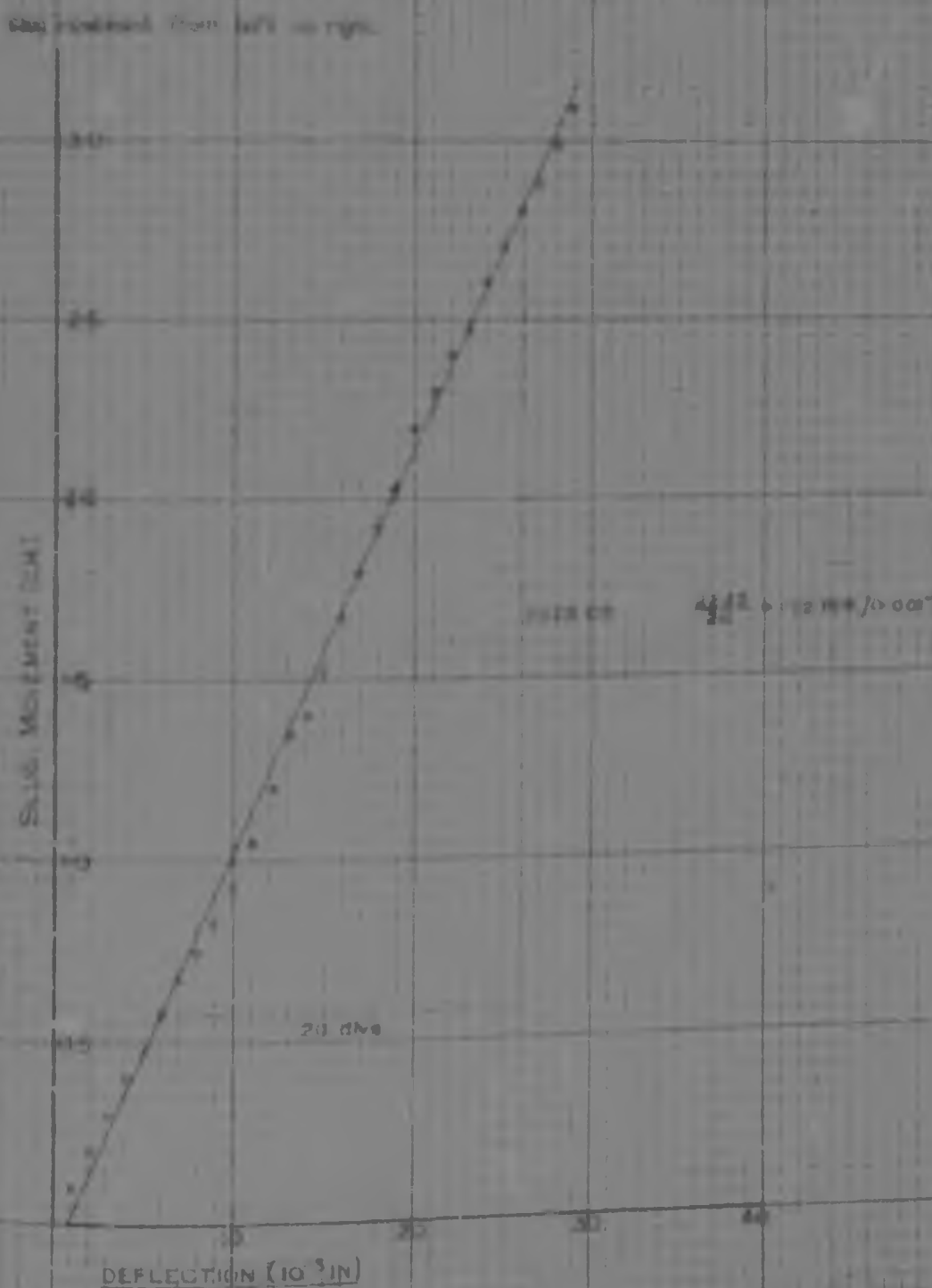
DEFLEC- TION GAUGE	LOAD GAUGE	SLUG SCALE	TIME	TEMPERA- TURE	CORRECTED SLUG SCALE	CORRECTED LOAD	CORRECT DEFLECT	STRAIN E	CORRECTED STRESS (61-63) Gd
					cm	lb	10 ⁻³ in	percent	lb/in ²
00 35	15	23.30	00 00	23.25	0	0	0	0	0
36	17.25	23.55			-0.25	2.25	1	0.033	
37	19.5	23.525			-0.025	4.5	2	0.067	
38	20.5	23.30			0	5.8	3	0.100	3.3
39	24.0	23.10			+0.20	9.0	4	0.133	5.1
40	26.7	22.90	02 35		0.50	11.7	5	0.167	6.8
41	29.0	22.10	03 15		1.20	13.0	6	0.200	7.34
42	33.25	20.75	08 07		2.55	19.25	7	0.233	10.29
43	37.8	20.2			3.10	27.5	8	0.267	12.68
44	42.5	19.5			4.10	27.8	9	0.300	16.66
45	43.2	17.96			5.45	33.2	10	0.333	18.70
46	52.5	16.9	11 19		6.40	37.3	11	0.367	21.00
47	56.9	15.7	11 57		7.50	41.5	12	0.400	23.58
48	60.6	14.7			8.60	41.6	13	0.433	25.65
49	64.6	13.65	13 08		9.65	49.1	14	0.467	27.92
50	65.2	12.7	13 41		10.60	53.2	15	0.500	29.91
51							16	0.533	
52	75.2	10.0	14 46		12.50	60.2	17	0.567	33.52
53	78.5	9.05			13.35	63.2	18	0.600	35.49
54	81.5	8.0			14.10	65.2	19	0.633	37.33
55	84.5	7.0			15.00	69.6	20	0.667	39.06
56	87.4	6.0	15 57		15.80	72.4	21	0.700	40.82
57	90.5	5.7			16.60	75.5	22	0.733	42.74
58	93.2	5.35			17.35	78.2	23	0.767	44.54
59	95.9	5.2			18.10	80.8	24	0.800	46.28
60	98.0	4.35	16 06		18.75	83.0	25	0.833	46.50
61	100.7	3.775			19.525	85.7	26	0.867	48.29
62	102.7	3.3			20.00	87.7	27	0.900	49.10
63	104.0	2.775			20.625	89.7	28	0.933	49.82
64	106.0	2.775			21.025	91.0	29	0.967	50.21
65	107.4	2.775	21 24		21.425	92.0	30	1.000	51.90
66	110.0	2.7.8			22.75	97.0	33	1.100	54.20
67	113.0	27.45			23.10	98.4	34	1.133	54.96
70	114.7	27.15	23 41		23.40	99.7	35	1.167	55.67
71	116.5	26.0			23.75	100.5	36	1.200	56.10
72	116.5	26.55			24.00	101.5	37	1.233	56.64
73	117.3	26.85			24.30	102.5	38	1.267	57.18
74	118.3	26.75			24.55	103.2	39	1.300	57.35
75	119.0	25.775	25 51		24.775	104.1	40	1.333	57.97
80	121.8	24.5	27 51		25.65	106.8	42	1.367	58.43
88	124.5	24.375	09 57		26.175	109.2	50	1.667	60.85
90	125.5	24.175	31 53		26.475	110.8	55	1.933	61.4
91	126.5	24.00	33 53		26.55	111.8	60	2.000	61.3
100	127.3	24.00	35 53		26.55	112.3	65	2.167	62.1
105	129.1	24.10	37 52		26.45	113.1	70	2.333	62.5
110	130.2	24.05			26.30	114.2	75	2.500	63.0
115	130.4	24.475	41 51		26.075	115.4	80	2.667	63.5
120	131.2	24.725	43 49		25.825	116.2	85	2.833	63.9
125	131.7	24.975	45 49		25.675	116.7	90	3.000	63.9
130	132.1	21.175	47 45		25.40	117.1	95	3.167	64.0
135	132.5	20.45	49 45		25.125	117.2	100	3.333	64.1
140	132.7	25.875	51 41		24.70	117.7	105	3.500	64.1
145	133.0	26.475	53 41		24.15	118.0	110	3.667	64.2
150	133.2	27.025	55 40		23.885	118.2	115	3.833	64.4
155	134.1	27.6	57 39		23.975	119.1	120	4.000	64.6
160	134.8	28.5	59 32		23.875	119.2	125	4.167	64.8
165	135.1	28.5	61 38		21.775	120.1	130	4.333	64.91
168	135.5	22.10			21.475	120.2	133	4.500	65.10
170	135.7	2.50			21.275	120.7	135	4.533	
181	135.8	2.70			21.175	120.8	136	4.533	

TEST NO. 6: LEAKAGE MEASUREMENTS

DETERMINATIONS OF RATE OF SLUG MOVEMENT DUE TO LEAKAGE ONLY



(c) DETERMINATION OF RATE OF SLUG MOVEMENT DUE TO COMBINED EFFECTS OF LEAKAGE & SPINDLE ENTRY



TEST NO 3 MAIN TEST OBSERVATIONS (Cont.)

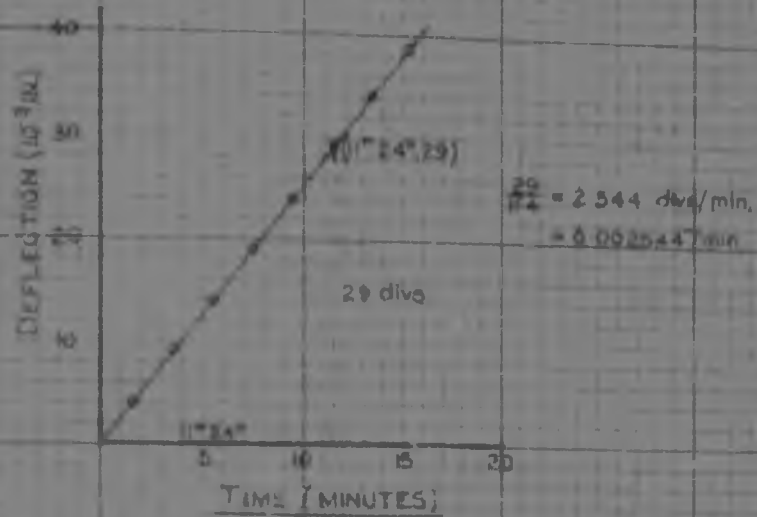
DEFLECTION GAGE	LOAD GAUGE	SLUG SCALE	TIME	TEMPERATURE	CORRECTED SLUG SCALE	CORRECTED LOAD	CORRECTED DEFLECTION	STRAIN E	CORRECTED STRESS (G/CS/64)
172	135.9	3.80			21.075	120.9	137	4.567	
173	135.9	3.90			20.975	120.9	138	4.600	
174	136.0	4.00			20.875	121.0	139	4.633	
175	136.0	4.10	65 34		20.775	121.0	140	4.667	65.16
180	136.2	4.60	67 26		20.275	121.2	145	4.833	65.16
185	136.7	5.20	69 28		19.675	121.7	150	5.000	65.50
190	136.9	5.75	71 17	24.0	19.125	121.9	155	5.167	65.50
195	137.1	6.325	73 17		18.550	122.2	160	5.333	65.50
200	137.2	6.90	75 13		17.975	122.2	165	5.500	65.24
205	137.2	7.50	77 11		17.375	122.2	170	5.667	65.12
210	137.2	8.20	79 11		16.675	122.2	175	5.833	65.01
215	137.2	8.90	81 04		16.075	122.2	180	6.000	64.79
220	137.2	9.475	83 00		15.40	122.2	185	6.167	64.77
225	137.2	10.075	84 56		14.80	122.2	190	6.333	64.60
230	137.2	10.7	86 51		14.175	122.2	195	6.500	64.55
235	137.2	11.35	88 48		13.525	122.2	200	6.667	64.43
240	137.2	11.90	90 43		12.975	122.2	205	6.833	64.31
245	137.2	12.50	92 39	24.0	12.375	122.2	210	7.000	64.21

TEST NO. 2 MAIN TEST OBSERVATIONS

DEFLECTION GAUGE	LOAD GAUGE	SLUG SCALE	TIME	TEMPERATURE	DEFLECTED SLUG SCALE	CORRECTED LOAD	CORRECTED DEFLECTION	STRAIN	STRESS
OC 35	15.0	15.10	00	70.0	0	0	0	0	0
36	16.0	16.00	01 09		0.001	1.0	1	0.001	1.0
37	16.4	16.00	01 54		0.002	1.4	2	0.002	1.4
38	17.3	17.00	01 59		0.003	1.7	3	0.003	1.7
39	18.0	18.00	02 00		0.004	1.8	4	0.004	1.8
40	18.7	18.00	02 40		0.005	1.8	5	0.005	1.8
41	23.4	23.00	03 00		0.011	2.3	6	0.011	2.3
42	29.2	29.00	04 08		1.00	12.0	7	0.012	12.0
43	30.3	30.00	09 15		2.00	24.0	8	0.024	24.0
44	36.0	36.00	10 40		3.00	36.0	9	0.036	36.0
45	43.0	43.00	11 00		4.00	43.0	10	0.043	43.0
46	46.0	46.00	12 20		5.00	46.0	11	0.046	46.0
47	51.0	51.00	13 00		6.00	51.0	12	0.051	51.0
48	58.0	58.00	13 40		7.00	58.0	13	0.058	58.0
49	61.0	61.00	14 10		8.00	61.0	14	0.061	61.0
50	68.0	68.00	14 30		9.00	68.0	15	0.068	68.0
51	71.0	71.00	15 34		10.00	71.0	16	0.071	71.0
52	72.0	72.00	16 12		11.00	72.0	17	0.072	72.0
53	75.0	75.00	16 40		12.00	75.0	18	0.075	75.0
54	84.0	84.00	17 00		13.00	84.0	19	0.084	84.0
55	85.0	85.00	17 30		14.00	85.0	20	0.085	85.0
56	85.0	85.00	18 04		15.00	85.0	21	0.085	85.0
57	85.0	85.00	18 09		16.00	85.0	22	0.085	85.0
58	101.0	101.00	19 47		17.00	101.0	23	0.101	101.0
59	104.0	104.00	20 21		18.00	104.0	24	0.104	104.0
60	107.0	107.00	20 51		19.00	107.0	25	0.107	107.0
61	110.0	110.00	21 01		20.00	110.0	26	0.110	110.0
62	111.0	111.00	21 06		21.00	111.0	27	0.111	111.0
63	111.0	111.00	21 08		22.00	111.0	28	0.111	111.0
64	111.0	111.00	21 10		23.00	111.0	29	0.111	111.0
65	110.0	110.00	21 21		24.00	110.0	30	0.110	110.0
66	109.0	109.00	21 30		25.00	109.0	31	0.109	109.0
67	121.0	121.00	24 12		26.00	121.0	32	0.121	121.0
68	120.0	120.00	24 41		27.00	120.0	33	0.120	120.0
69	120.0	120.00	25 07		28.00	120.0	34	0.120	120.0
70	123.0	123.00	25 14		29.00	123.0	35	0.123	123.0
71	123.0	123.00	25 24		30.00	123.0	36	0.123	123.0
72	123.0	123.00	25 34		31.00	123.0	37	0.123	123.0
73	123.0	123.00	26 00		32.00	123.0	38	0.123	123.0
74	123.0	123.00	27 04		33.00	123.0	39	0.123	123.0
75	123.0	123.00	28 00		34.00	123.0	40	0.123	123.0
76	123.0	123.00	28 00		35.00	123.0	41	0.123	123.0
77	123.0	21.0	28 12		36.00	123.0	42	0.123	123.0
78	121.0	20.0	28 34		37.00	121.0	43	0.121	121.0
79	121.0	22.0	28 44		38.00	121.0	44	0.121	121.0
80	121.0	24.0	29 14		39.00	121.0	45	0.121	121.0
81	119.0	24.1	29 36		40.00	119.0	46	0.119	119.0
82	119.0	25.0	29 57		41.00	119.0	47	0.119	119.0
83	117.0	26.0	30 19		42.00	117.0	48	0.117	117.0
84	116.0	28.5	30 40		43.00	116.0	49	0.116	116.0
85	116.0	30.0	31 02		44.00	116.0	50	0.116	116.0
86	114.0	31.0	31 23		45.00	114.0	51	0.114	114.0
87	112.0	31.0	31 44		46.00	112.0	52	0.112	112.0

TEST NO 3 RATE OF STRAIN DETERMINATIONS.

(a) CALIBRATED RATE OF STRAIN ($\sigma_s = 20 \text{ lb/sq in.}$)



(b) ACTUAL RATE OF STRAIN DURING TEST ($\sigma_s = 20 \text{ lb/sq in.}$)

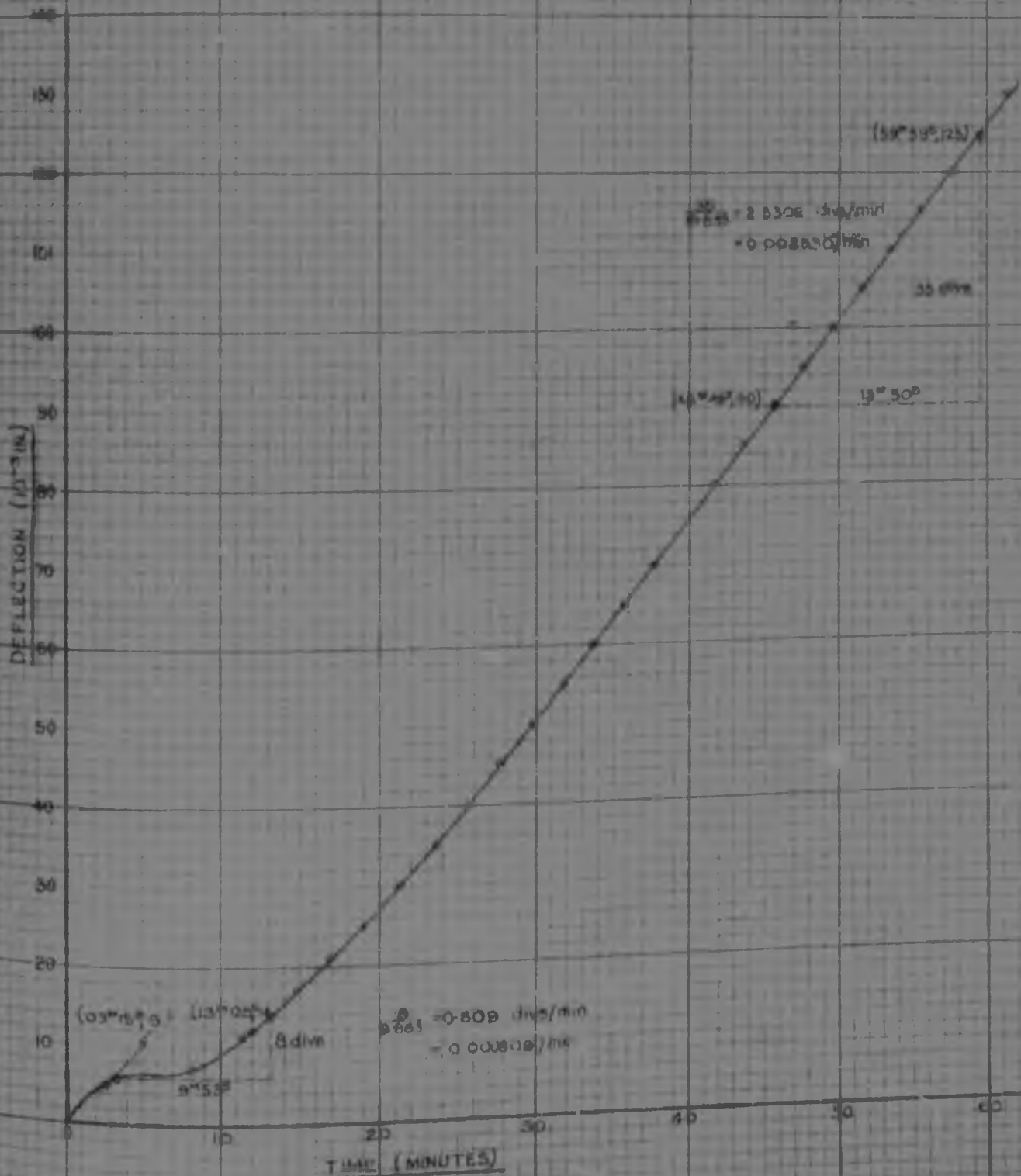
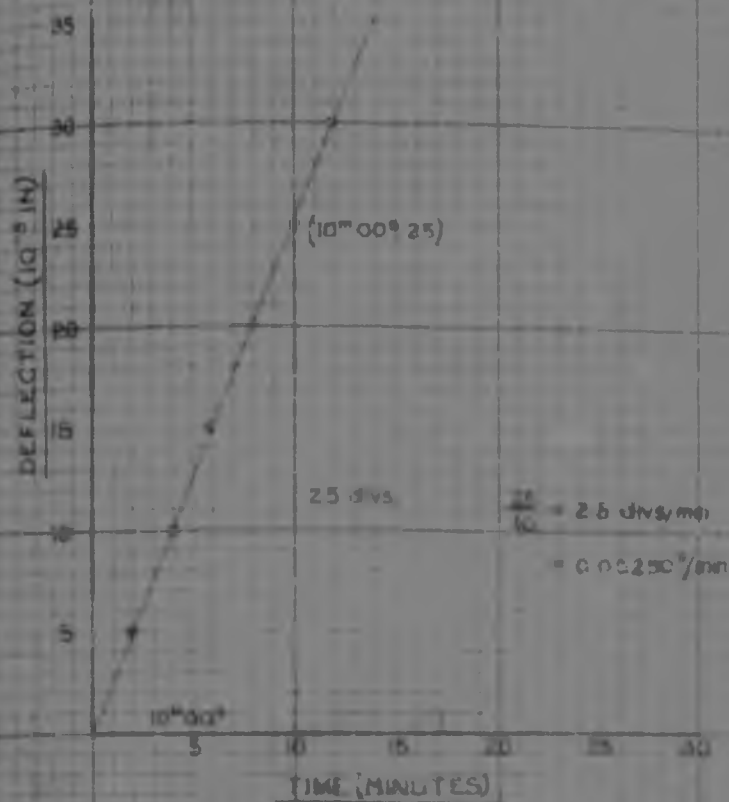


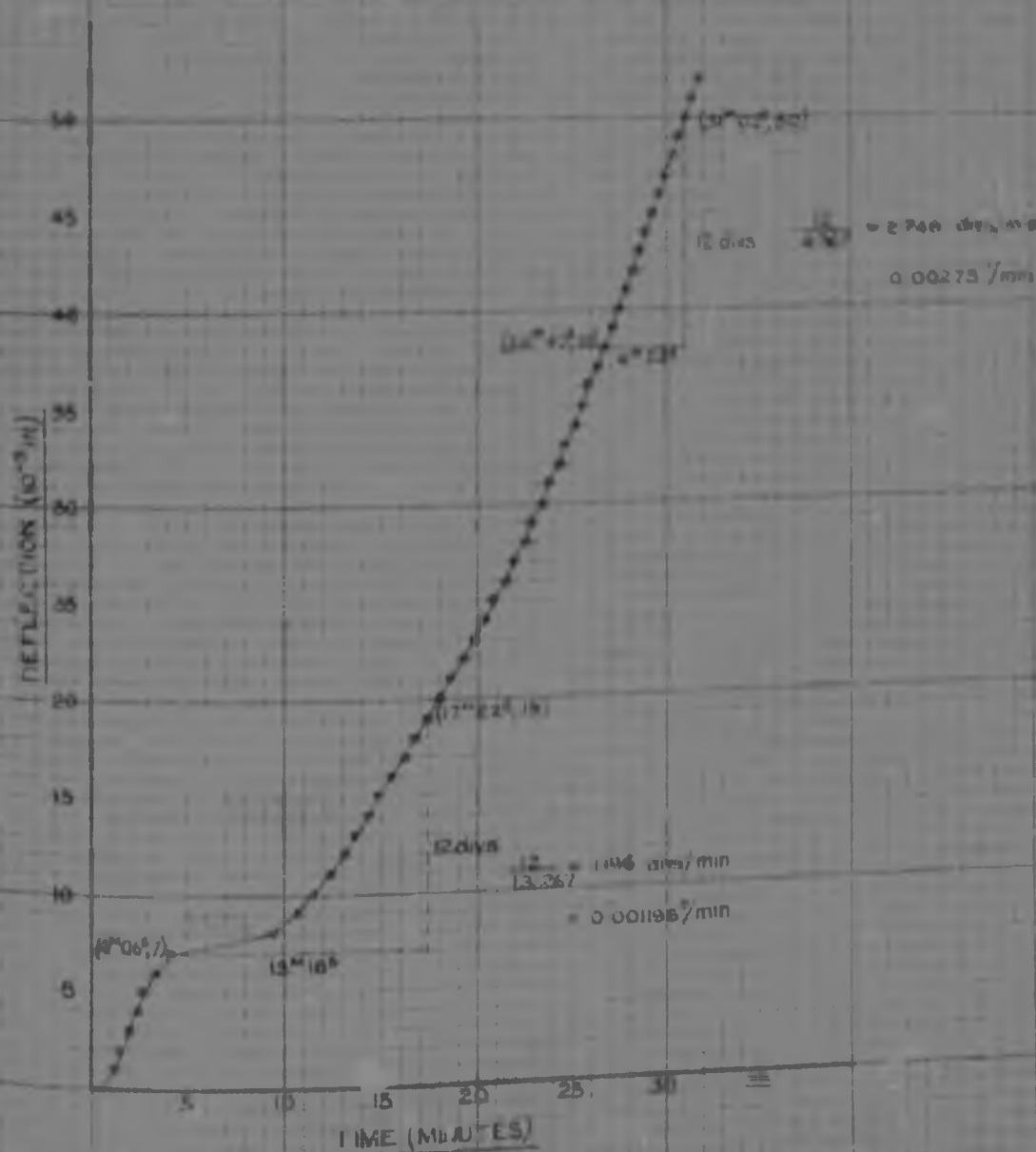
FIG. 33.

TEST No 8 RATE OF STRAIN DETERMINATIONS

(a) CALIBRATED RATE OF STRAIN ($\sigma_3 = 1016 \text{ lb/sq in}$)



(b) ACTUAL RATE OF STRAIN DURING TEST ($\sigma_3 = 1016 \text{ lb/sq in}$)



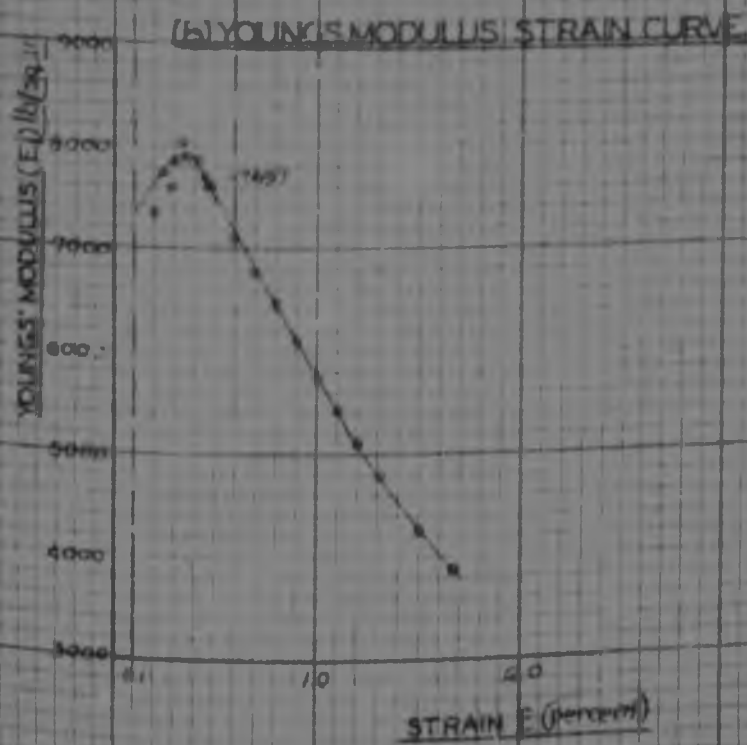
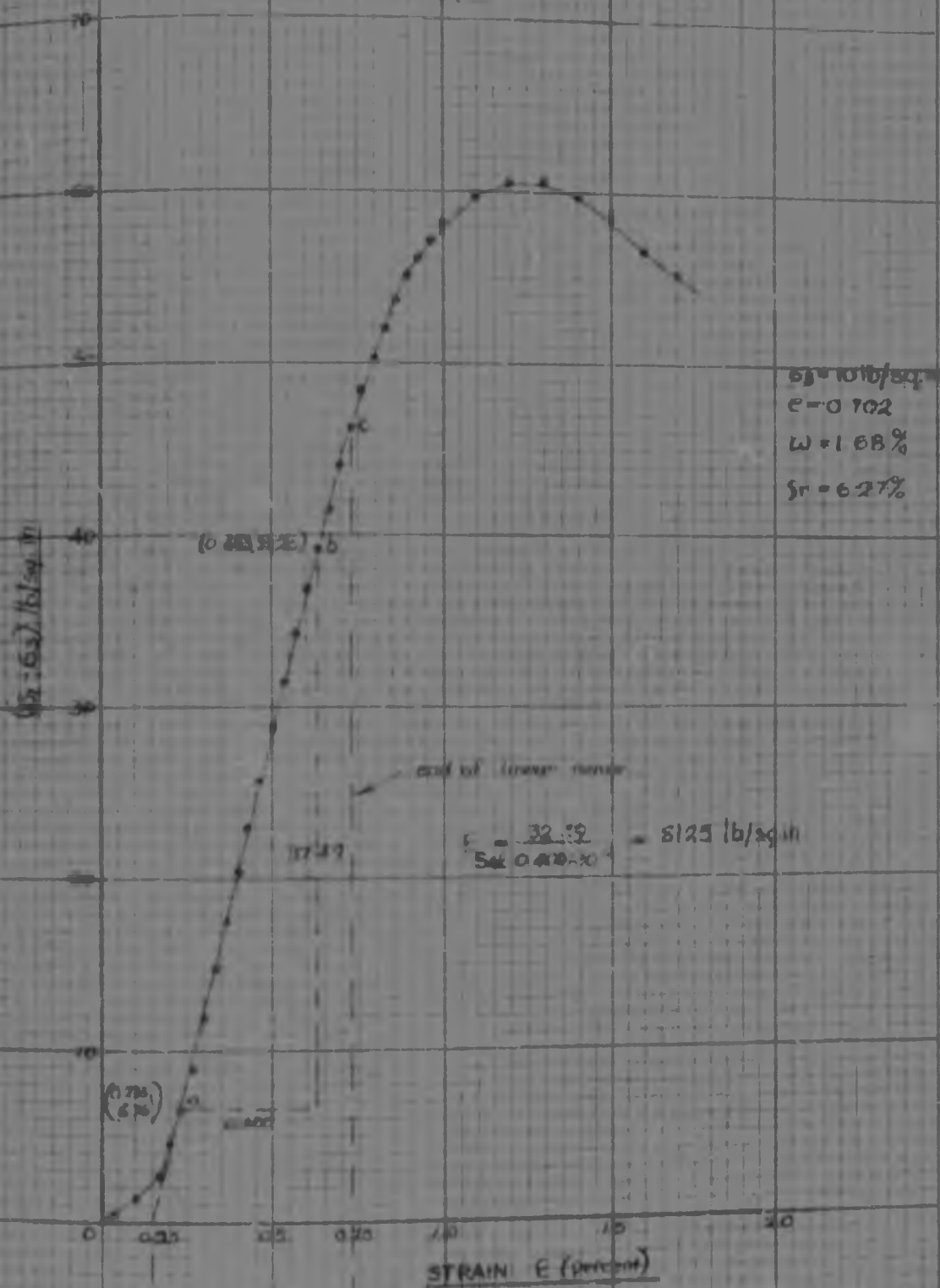


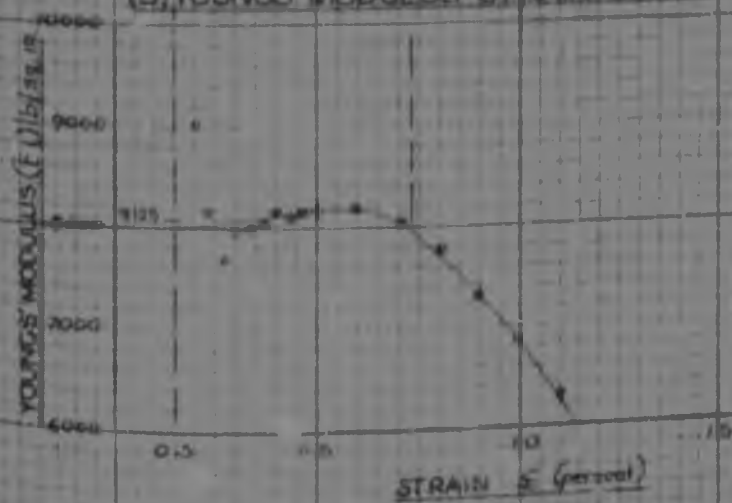
FIG. 34.

- 111 -
TEST NO 6

(a) STRESS-STRAIN CURVE



(b) YOUNG'S MODULUS-STRAIN CURVE



TEST No 3

CALCULATION OF INSTANTANEOUS VALUES
OF YOUNGS MODULUS (E)

CORRECTED STRESS = S lb / sq in.	STRAIN percent	STRAIN DUE TO BEDDING - IN EFFECTS percent	CORRECTED STRAIN = S percent	YOUNGS MODULUS (E) = S/E lb / sq in.
7.34	0.200	0.100	0.100	7340
10.29	0.233	"	0.133	7737
12.68	0.267	"	0.167	7593
15.66	0.300	"	0.200	7830
18.90	0.333	"	0.233	8026
21.00	0.367	"	0.267	7856
23.50	0.400	"	0.400	7860
26.00	0.433	"	0.333	7703
27.84	0.467	"	0.367	7599
29.91	0.500	"	0.400	7478
33.80	0.567	"	0.467	7242
35.12	0.600	"	0.500	7098
37.33	0.633	"	0.533	7004
39.06	0.667	"	0.567	6899
42.00	0.700	"	0.600	6770
42.34	0.733	"	0.633	6689
43.94	0.767	"	0.667	6573
45.28	0.800	"	0.700	6468
46.50	0.833	"	0.733	6344
48.00	0.867	"	0.767	6258
49.10	0.900	"	0.800	6139
49.92	0.933	"	0.833	5993
50.91	0.967	"	0.867	5872
51.90	1.000	"	0.900	5767
54.50	1.100	"	1.000	5420
54.96	1.133	"	1.033	5320
56.67	1.167	"	1.067	5217
58.10	1.200	"	1.100	5100
56.64	1.233	"	1.133	4999
57.18	1.267	"	1.167	4900
57.55	1.300	"	1.200	4798
57.97	1.333	"	1.233	4702
59.43	1.367	"	1.300	4545
60.56	1.400	"	1.367	4371

TEST No 6

CALCULATION OF INSTANTANEOUS VALUES
OF YOUNGS' MODULUS (E)

CORRECTED STRESS = a lb/sq in	STRAIN percent	STRAIN DUE TO BEDDING - IN EFFECTS percent	CORRECTED STRAIN = b percent	YOUNGS MODULUS (E) = a/b lb/sq in
4.51	0.200	0.150	0.050	9020
6.74	0.233	"	0.083	8144
8.96	0.267	"	0.117	7659
11.93	0.300	"	0.150	7953
14.63	0.333	"	0.183	7994
17.45	0.367	"	0.217	8041
20.38	0.400	"	0.250	8152
23.04	0.433	"	0.283	8141
25.21	0.467	"	0.317	8142
28.63	0.500	"	0.350	8196
31.42	0.533	"	0.383	8214
34.25	0.567	"	0.417	8213
37.93	0.600	"	0.450	8200
39.28	0.633	"	0.483	8126
41.53	0.667	"	0.517	8033
44.11	0.700	"	0.550	8027
46.18	0.733	"	0.583	7918
49.51	0.767	"	0.617	7969
50.33	0.800	"	0.650	7743
51.99	0.833	"	0.683	7617
53.65	0.867	"	0.717	7482
54.92	0.900	"	0.750	7323
56.08	0.933	"	0.783	7162
57.12	0.967	"	0.817	6991
58.11	1.000	"	0.850	6836
59.17	1.033	"	0.883	6661
59.42	1.067	"	0.917	6481
59.88	1.100	"	0.950	6299

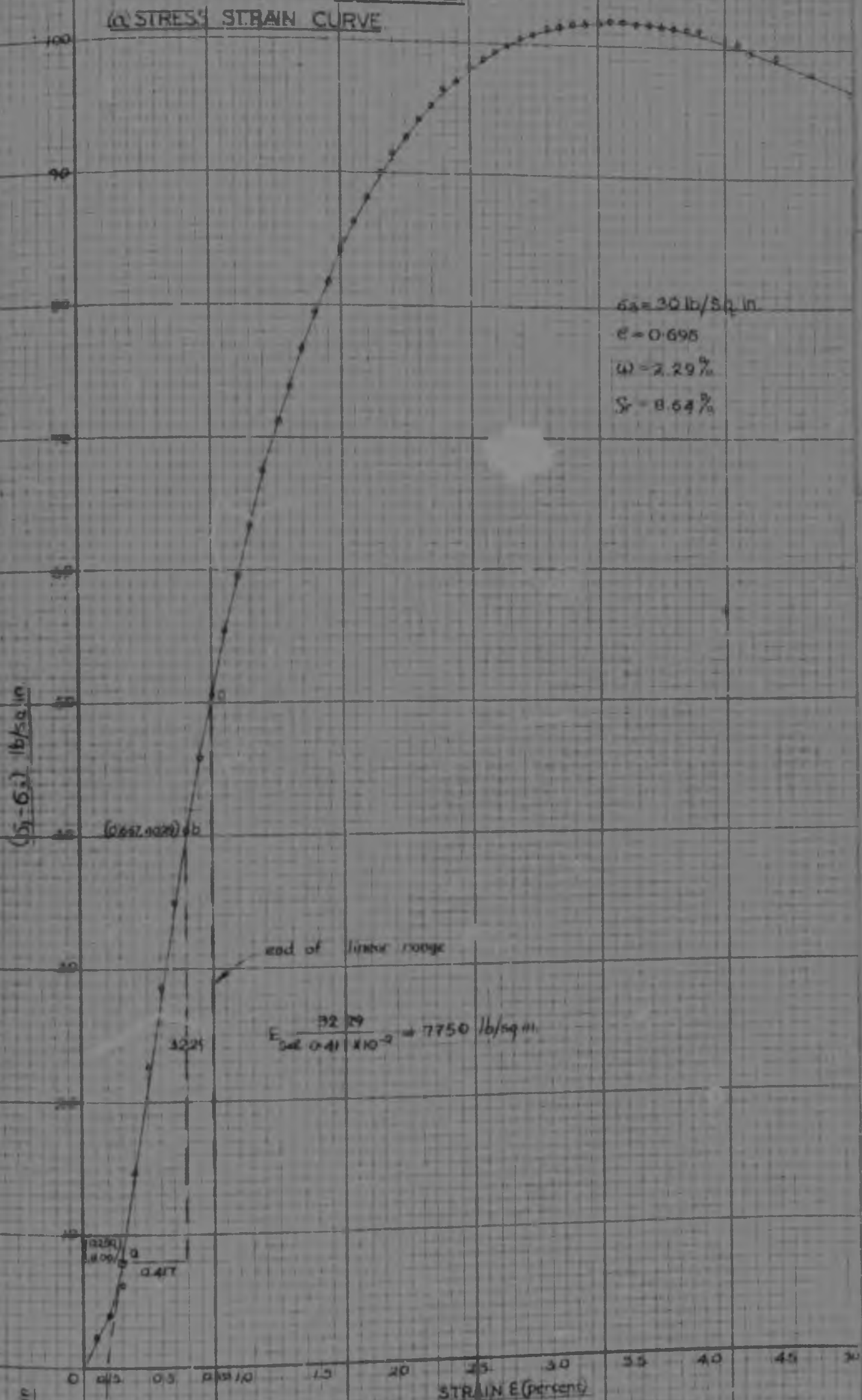
TEST N° 2 MAIN TEST OBSERVATIONS.

DEFLEC- TION GAUGE	LOAD GAUGE	SLUG SCALE	TIME	TEMPERA- TURE	CORRECTED SLUG SCALE	CORRECTED LOAD	CORRECT DEFLECT	STRAIN E	CORRECTED STRESS (G) 43-6
					cm	lb	10 ⁻³ in.	percent	10 ⁴ psi
00.50	12.7	25.5		85.25	0	0	0	0	0
52.5	17.0	25.65			- 0.12	4.3	2.2	0.183	1.83
55	17.2	25.75			- 0.25	7.2	5	0.167	4.08
57.5	23.8	25.7			- 0.30	11.1	7.5	0.250	8.28
59 pronounced time-lag sets in.									
62	32.0	25.7			- 1.8	24.3	10	0.333	14.41
62.5	33.0	25.7			- 4.2	40.3	17.5	0.417	20.67
65	64	25.8			- 6.7	53.3	25	0.500	24.73
67.5	75	16.45			- 7.05	62.3	27.5	0.583	24.73
70	84.3	14.55			- 10.05	71.3	30	0.600	40.24
72.5	84.2	17.40			- 13.10	82.3	32.5	0.750	45.07
75	103	10.22			- 14.05	90.3	35	0.833	50.54
77.5	112	8.75			- 15.71	94.3	37.5	0.917	54.14
80	119	7.20			- 16.34	100.3	40	1.000	59.45
82.5	125.5	5.55			- 18.95	104.3	42.5	1.083	63.22
85	131.0	4.05			- 21.45	109.3	45	1.167	67.42
87.5	140	2.55			- 25.00	124.3	57.5	1.250	71.1
90	141					129.7	60	1.333	75.7
92.5	150.3					139.4	62.5	1.417	78.7
95	155.3	25.8			27.12	143.1	65	1.500	79.4
97.5	160	25.7			27.35	147.3	67.5	1.583	81.7
100	164.5	27.7			28.35	151.2	70	1.667	84.2
102.5	168.7	26.25			29.1	155.4	72.5	1.750	86.3
105	171.7	26.15			29.8	159.0	75	1.833	88.1
107.5	175	22.45		85.5	30.6	162.3	77.5	1.917	90.0
110	178	22.00			31.05	165.3	80	2.000	91.6
112.5	180.4	24.55			31.50	167.7	82.5	2.083	93.6
115	183	24.50			31.95	170.3	85	2.167	94.1
117.5	185	22.075			32.35	172.3	87.5	2.250	95.3
120	187.2	20.25			32.8	174.6	90	2.333	96.4
122.5	189.1	27.40			33.25	176.7	92.5	2.417	97.1
125	191.0	23.325			33.7	178.1	95	2.500	98.1
127.5	192.0	23.575			34.05	179.3	97.5	2.583	98.8
130	193.5	23.825			34.425	180.0	100	2.667	99.4
132.5	194.5	23.275			34.825	181.9	102.5	2.750	99.9
135	195.5	23.30			35.25	183.9	105	2.833	100.4
137.5	196.5	23.45			35.65	185.9	107.5	2.917	100.9
140	197.5	23.55			36.05	187.3	110	3.000	101.2
142.5	198.5	23.65			36.45	188.3	112.5	3.083	101.5
145	199.5	24.05			36.85	189.3	115	3.167	101.8
147.5	199.0	24.30			37.25	190.3	117.5	3.250	101.9
150	199.1	24.55			37.65	191.4	120	3.333	101.9
152.5	199.5	25.15			38.05	192.3	122.5	3.417	102.0
155	199.2	25.70			38.40	193.3	125	3.500	102.0
157.5	199.5	26.20			38.80	194.1	127.5	3.583	101.9
160	199.5	26.80			39.20	195.1	130	3.667	101.7
162.5	197.5	27.40			39.60	195.7	132.5	3.750	101.5
165	197.5	28.00			39.95	196.0	135	3.833	101.5
167.5	198.7	28.65			40.40	197.0	137.5	3.917	101.5
170	198.7	28.30			40.80	198.0	140	4.000	101.5
172.5	198.7	30.75			41.25	198.0	142.5	4.083	100.7
175	198.7	31.40			41.70	198.3	145	4.167	100.7
177.5	198.7					199.3	147.5	4.250	100.7
180	198.7					199.3	150	4.333	100.7
182.5	198.7					199.3	152.5	4.417	100.7
185	198.7					199.3	155	4.500	100.7
187.5	198.7					199.3	157.5	4.583	100.7
190	198.7					199.3	160	4.667	100.7

TEST NO. MAIN TEST OBSERVATIONS

DEFLEC- TION GAUGE	LOAD GAUGE	SLUG SCALE	TIME	TEMPERA- TURE	ORIGINAL SLUG SCALE	CORRECTED LOAD	CORRECT DEFLECT	STRAIN E	CORRECTED STRESS (lb./sq. in.)
							10 ⁻³	Percent	
00.30	15	78.4		24.0	0	0	0	0	0
32.5	15.0	27.3			- 0.20	1.0	0.2	0.002	1.56
35	15.6	24.4			- 0.20	1.6	0	0.004	2.09
37.5	15.1	24.5			- 0.20	1.5	0	0.004	2.12
40	21.3	2.2			- 1.20	0.3	10	0.001	3.17
41	Broke in 20 time-lag sets in.								
42.5	24.0	27.45			0.2	10.5	10.5	0.001	11.40
45	40.0	14.05			0.25	31	10	0.001	17.91
47.5	20.0	7.50			0.40	41	10.5	0.001	18.00
50	64.0	15.10			0.70	49	20	0.001	24.0
52.5	73.0	14.70			0.70	50.5	20.5	0.001	24.50
55	80.4	12.80			0.9	62.4	25	0.001	26.94
57.5	87.0	11.70		24.0	11.00	72.5	27	0.001	40.15
60	93.8	11.35			11.51	74.5	30	0.002	43.43
62.5	97.0	11.11			11.55	81.0	30.5	0.002	47.01
65	101	11.10			11.5	86.0	35	0.002	49.07
67.5	104.0	11.78			12.48	89.0	38.5	0.002	49.7
70	108.1	11.60			12.50	91.1	40	0.002	51.7
72.5	108.1	12.80			12.50	91.1	40	0.002	51.7
75	109.0	14.10			12.50	91.1	40	0.002	51.7
77.5	110.1	16.55			12.50	91.1	40	0.002	51.7
80	110.0	16.70			12.50	91.1	40	0.002	51.7
82.5	110.0	16.70			12.50	91.1	40	0.002	51.7
85	110.0	16.70			12.50	91.1	40	0.002	51.7
87.5	110.0	16.70			12.50	91.1	40	0.002	51.7
90	110.0	16.70			12.50	91.1	40	0.002	51.7
92.5	109.8	17.00			12.50	91.1	40	0.002	51.7
95	109.8	17.00			12.50	91.1	40	0.002	51.7
97.5	109.8	17.00			12.50	91.1	40	0.002	51.7
100	109.8	17.00			12.50	91.1	40	0.002	51.7
102.5	109.8	17.00			12.50	91.1	40	0.002	51.7
105	109.8	17.00			12.50	91.1	40	0.002	51.7
107.5	109.8	17.00			12.50	91.1	40	0.002	51.7
110	109.8	17.00			12.50	91.1	40	0.002	51.7
112.5	109.8	17.00			12.50	91.1	40	0.002	51.7
115	109.8	17.00			12.50	91.1	40	0.002	51.7
117.5	109.8	17.00			12.50	91.1	40	0.002	51.7
120	109.8	17.00			12.50	91.1	40	0.002	51.7
122.5	109.8	17.00			12.50	91.1	40	0.002	51.7
125	109.8	17.00			12.50	91.1	40	0.002	51.7
127.5	109.8	17.00			12.50	91.1	40	0.002	51.7
130	109.8	17.00		24.0	12.50	91.1	40	0.002	51.7

(a) STRESS STRAIN CURVE



(b) YOUNG'S MODULUS STRAIN CURVE

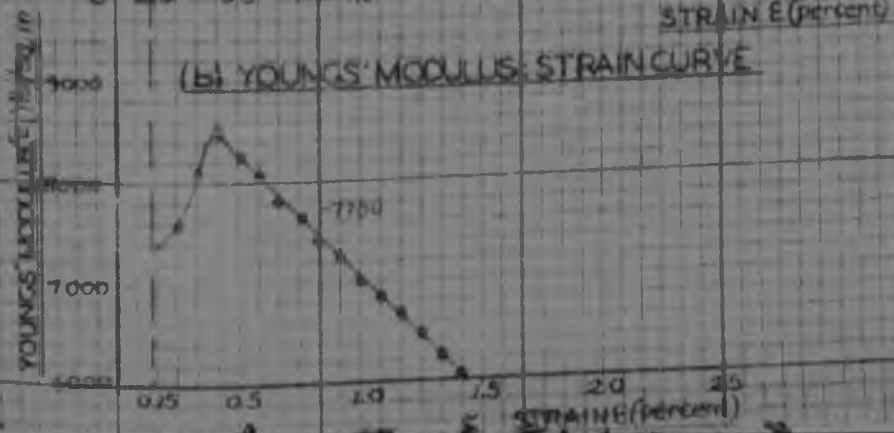
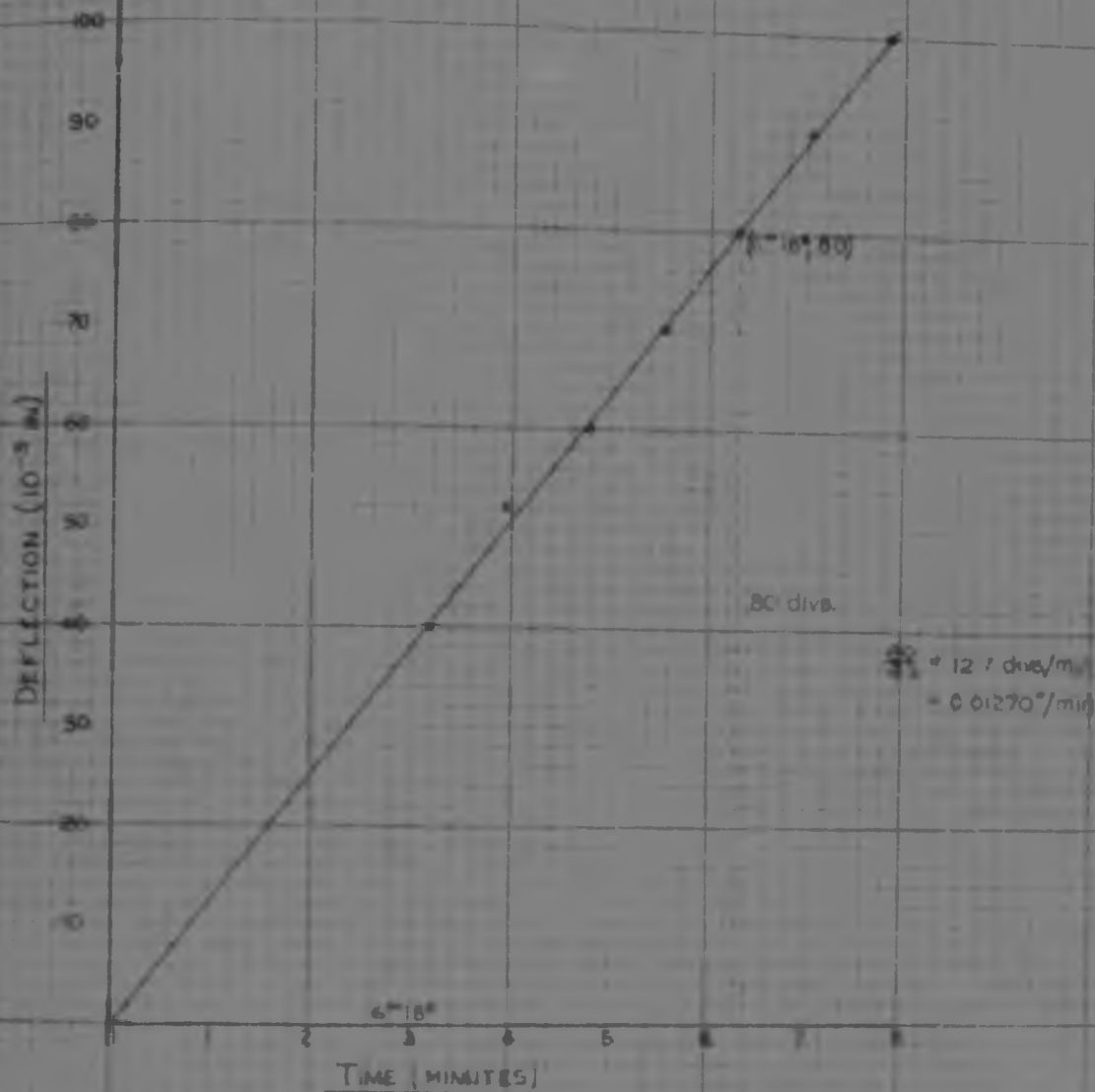


FIG. 30

TEST NO 5 RATE OF STRAIN DETERMINATION

FIG 4 CALIBRATED RATE OF STAIN ($\sigma_s = 10 \text{ lb/sq in}$)



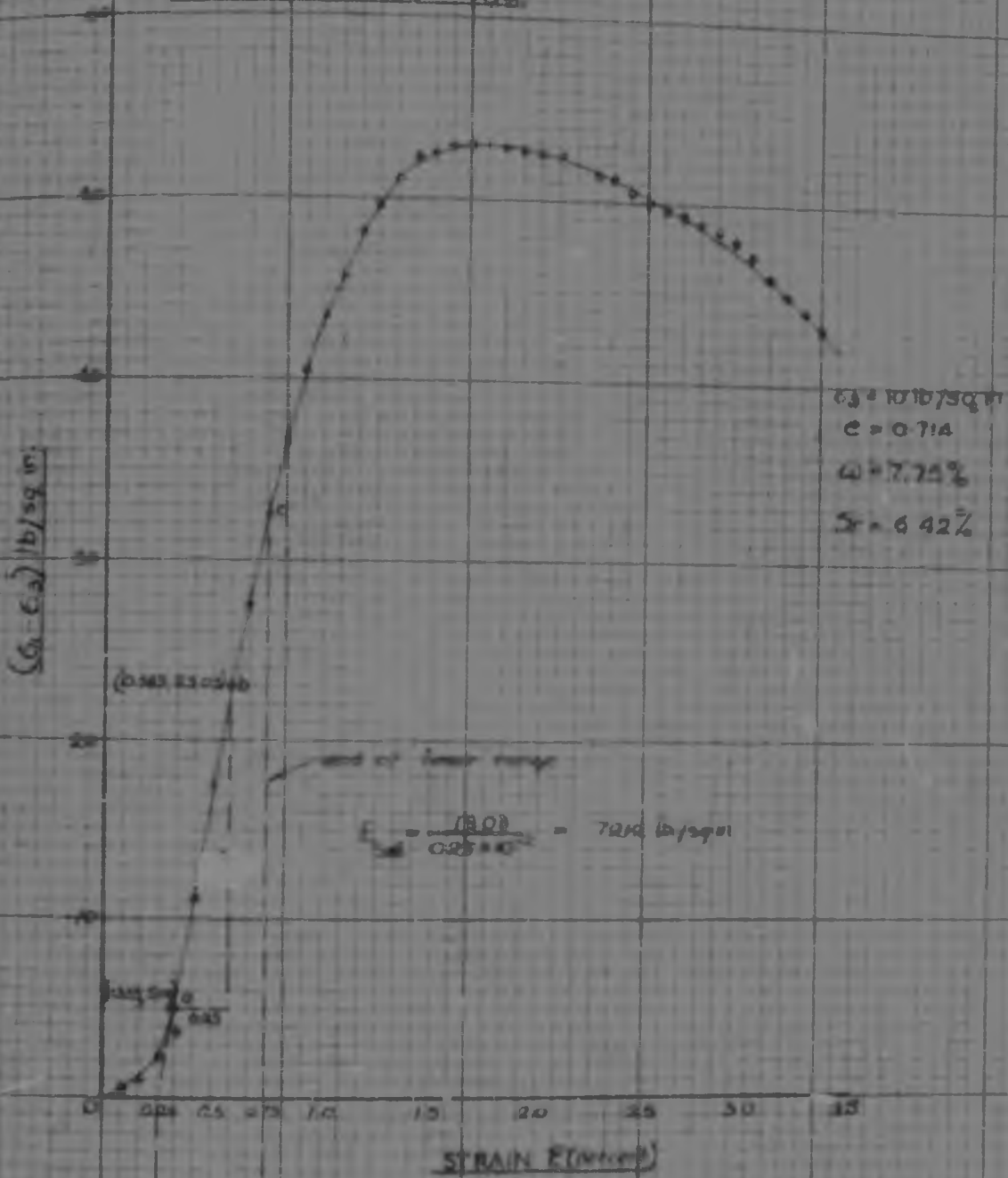
NOTE: NO CURVE FOR DETERMINATION OF ACTUAL RATE OF STRAIN DURING TEST, DUE TO CONTINUOUS TIME MEASUREMENTS NOT HAVING BEEN TAKEN

TEST No 2

CALCULATION OF INSTANTANEOUS VALUES
OF YOUNGS' MODULUS (E)

CORRECTED STRESS = a lb/sq in	STRAIN percent	STRAIN DUE TO BEDDING - IN EFFECTS percent	CORRECTED STRAIN = b percent	YOUNGS' MODULUS (E) = $\frac{a}{b}$ lb/sq in
5.00	0.216	0.150	0.066	7575
14.91	0.333	"	0.183	8092
22.67	0.417	"	0.267	8492
28.84	0.500	"	0.350	8240
34.99	0.583	"	0.433	8081
40.29	0.667	"	0.517	7793
45.87	0.750	"	0.600	7645
50.59	0.833	"	0.683	7407
55.59	0.917	"	0.767	7248
59.45	1.000	"	0.850	6994
63.62	1.083	"	0.933	6819
67.45	1.167	"	1.017	6632
71.02	1.250	"	1.100	6456
73.75	1.333	"	1.183	6234
76.64	1.417	"	1.267	6049
79.63	1.500	"	1.350	5898

A STRESS STRAIN CURVE



B YOUNG'S MODULUS STRAIN CURVE

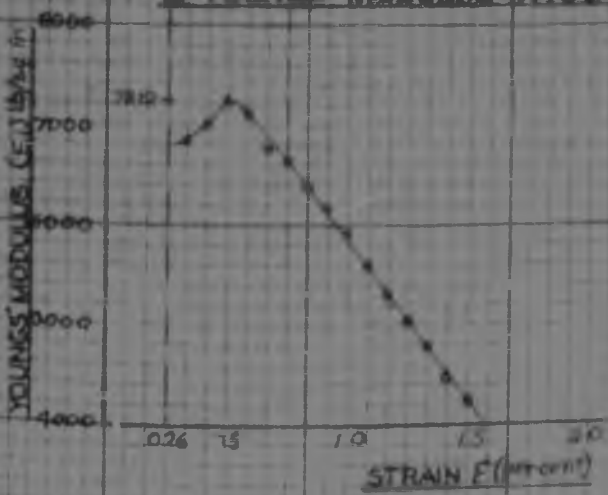


FIG 42

TEST NO 2

MAIN SLUG MOVEMENT DEFLECTION CURVE

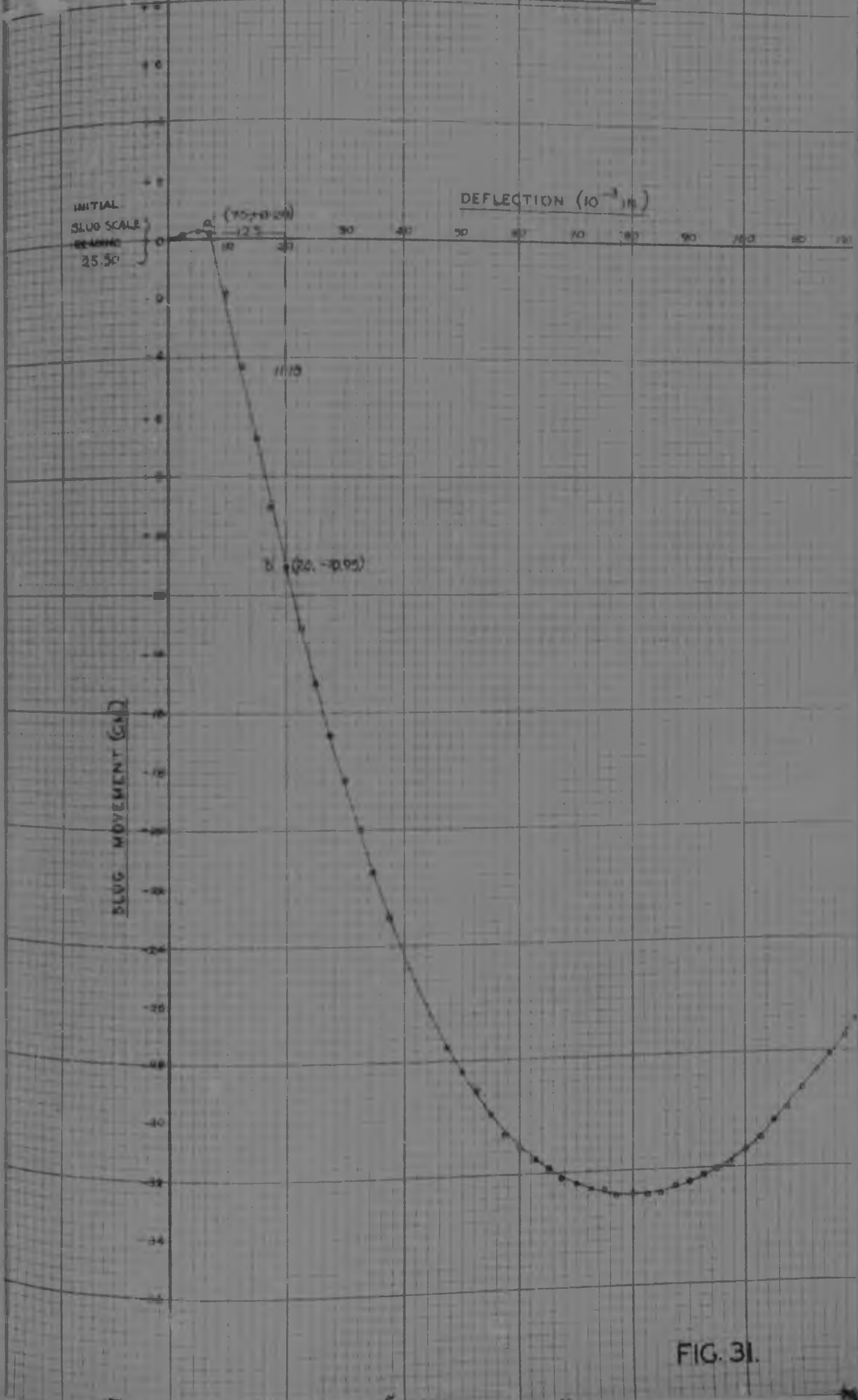


FIG. 31.

TEST No. 5
CALCULATION OF INSTANTANEOUS VALUES
OF YOUNG'S MODULUS (E)

CORRECTED STRESS P lb./sq. in.	STRAIN PERCENT	STRAIN DUE TO BEDDING IN EFFECTS percent	CORRECTED STRAIN percent	YOUNG'S MODULUS (E) $E = \frac{P}{\epsilon}$ lb./sq. in.
5.000	0.333	0.267	0.073	6849
10.97	0.417	"	0.157	5967
17.45	0.500	"	0.240	7288
23.03	0.583	"	0.323	7130
27.50	0.667	"	0.407	6757
32.52	0.750	"	0.490	6637
36.64	0.833	"	0.573	6394
40.58	0.917	"	0.657	6177
43.63	1.000	"	0.740	5898
45.83	1.083	"	0.823	5583
48.02	1.167	"	0.907	5294
49.85	1.250	"	0.990	5018
51.01	1.333	"	1.073	4754
52.08	1.417	"	1.157	4501
52.64	1.500	"	1.240	4245

MAIN SLUG MOVEMENT DEFLECTION CURVE



TEST NO 3

DATE PERFORMED: 29/1/57

SAMPLE CONSOLIDATED FOR 24 HRS PRIOR TO TEST

TIME START OF TEST 12/32 PM TEMPERATURE 23.2°C

TIME END OF TEST 2/03 PM TEMPERATURE 24.0°C

NOMINAL STRESS, DIAMETER, PRESSURE 20 LB/30 IN

HEAD OF MERCURY 38% ALLOY, 10 IN

ACTUAL STRESS, DIAMETER, PRESSURE 18.8 LB/30 IN

NOMINAL STRESS, DIAMETER, PRESSURE 20 LB/30 IN

TEST NO 5 LEAKAGE MEASUREMENTS.

(A) MEASUREMENT OF SLUG MOVEMENT DUE TO LEAKAGE ONLY BEFORE TEST TEMP 24.0°C TIME 12/12/54		(B) MEASUREMENT OF SLUG MOVEMENT DUE TO LEAKAGE ONLY AFTER TEST (1) TEMP 24.0°C TIME 2/00/54		(C) MEASUREMENT OF SLUG MOVEMENT DUE TO COMBINED EFFECTS OF LEAKAGE & SPINDLE ENTRY (AFTER TEST) TEMPERATURE 24.0°C TIME 2/10/54			(D) MEASUREMENT OF SLUG MOVEMENT DUE TO LEAKAGE ONLY AFTER TEST (2) TEMP 24.0°C TIME 2/12/54	
TIME	VOLUME	TIME	VOLUME	DEFLECT	VOLUME	TIME	TIME	VOLUME
MIN	SCALE	MIN	SCALE	GAUGE	SCALE	MIN	MIN	SCALE
0 00	20.20	0 00	11.80	00 11	20.70	00 00	0 00	10.20
15	20.25	15	11.825	01 22	10.70		15	11.25
30	20.30	30	11.85	02 33	10.70		30	12.30
45	20.35	45	11.875	03 44	10.70		45	13.35
1 00	20.40	1 00	11.90	04 55	10.70	01 34	1 00	14.40
15	20.45	15	11.925	05 06	10.725		15	15.45
30	20.50	30	11.95	06 17	10.75		30	16.50
45	20.55	45	11.975	07 28	10.775		45	17.55
2 00	20.60	2 00	12.00	08 39	10.80	03 38	2 00	18.60
15	20.65	15	12.025	09 50	10.825		15	19.65
30	20.70	30	12.05	10 01	10.85		30	20.70
45	20.75	45	12.075	11 12	10.875		45	21.75
3 00	20.80	3 00	12.10	12 23	10.90	05 33	3 00	22.80
15	20.85	15	12.125	13 34	10.925		15	23.85
30	20.90	30	12.15	14 45	10.95		30	24.90
45	20.95	45	12.175	15 56	10.975		45	25.95
4 00	21.00	4 00	12.20	16 07	11.00	07 32	4 00	26.00
15	21.05	15	12.225	17 18	11.025		15	27.05
30	21.10	30	12.25	18 29	11.05		30	28.10
45	21.15	45	12.275	19 40	11.075		45	29.15
5 00	21.20	5 00	12.30	20 51	11.10		5 00	30.20
				21 02	11.125			
				22 13	11.15			
				23 24	11.175	09 30		
				24 35	11.20			
				25 46	11.225			
				26 57	11.25			
				27 08	11.275			
				28 19	11.30	11 34		
				29 30	11.325			
				30 41	11.35			
				31 52	11.375			
				32 03	11.40	13 36		
				33 14	11.425			
				34 25	11.45			
				35 36	11.475			
				36 47	11.50			
				37 58	11.525			
				38 09	11.55	15 14		
				39 20	11.575			
				40 31	11.60			

TEST No 6

DATE PERFORMED 31 / 1 / 57

SAMPLE CONSOLIDATED FOR 24^{hrs} 00^{min} PRIOR TO TEST

TIME START OF TEST 11 12 0 AM TEMPERATURE 20 75°C

TIME END OF TEST 12 00 NOON TEMPERATURE 20 75°C

NOMINAL 6₃ CHAMBER PRESSURE 10 LB / SQ IN

HEAD IN WITH 10

ACTUAL 6₃ CHAMBER PRESSURE 8 825 LB / SQ IN

NOMINAL RATE OF STRAIN 0 00256 PER MINUTE

- 80 -
TEST NO3

MAIN SLUG MOVEMENT, DEFLECTION CURVE

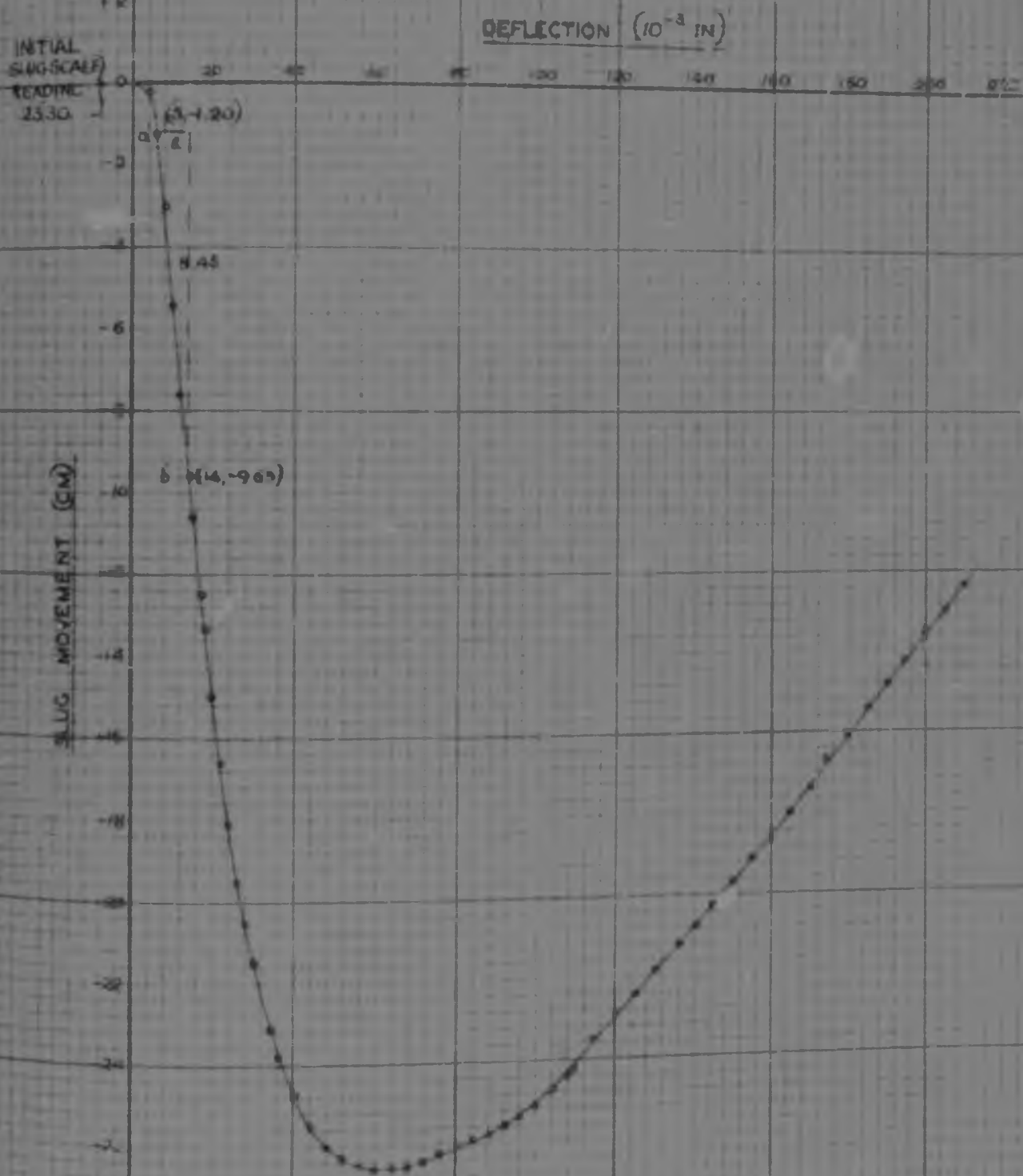


FIG. 35

TEST NO 4.

DATE PERFORMED 15 / 2 / 57

SAMPLE CONSOLIDATED FOR 23^{HR} 40^{MIN} PRIOR TO TEST

TIME START OF TEST 8 40 A M TEMPERATURE 24 0°C

TIME END OF TEST 8 58 A M TEMPERATURE 24 25°C

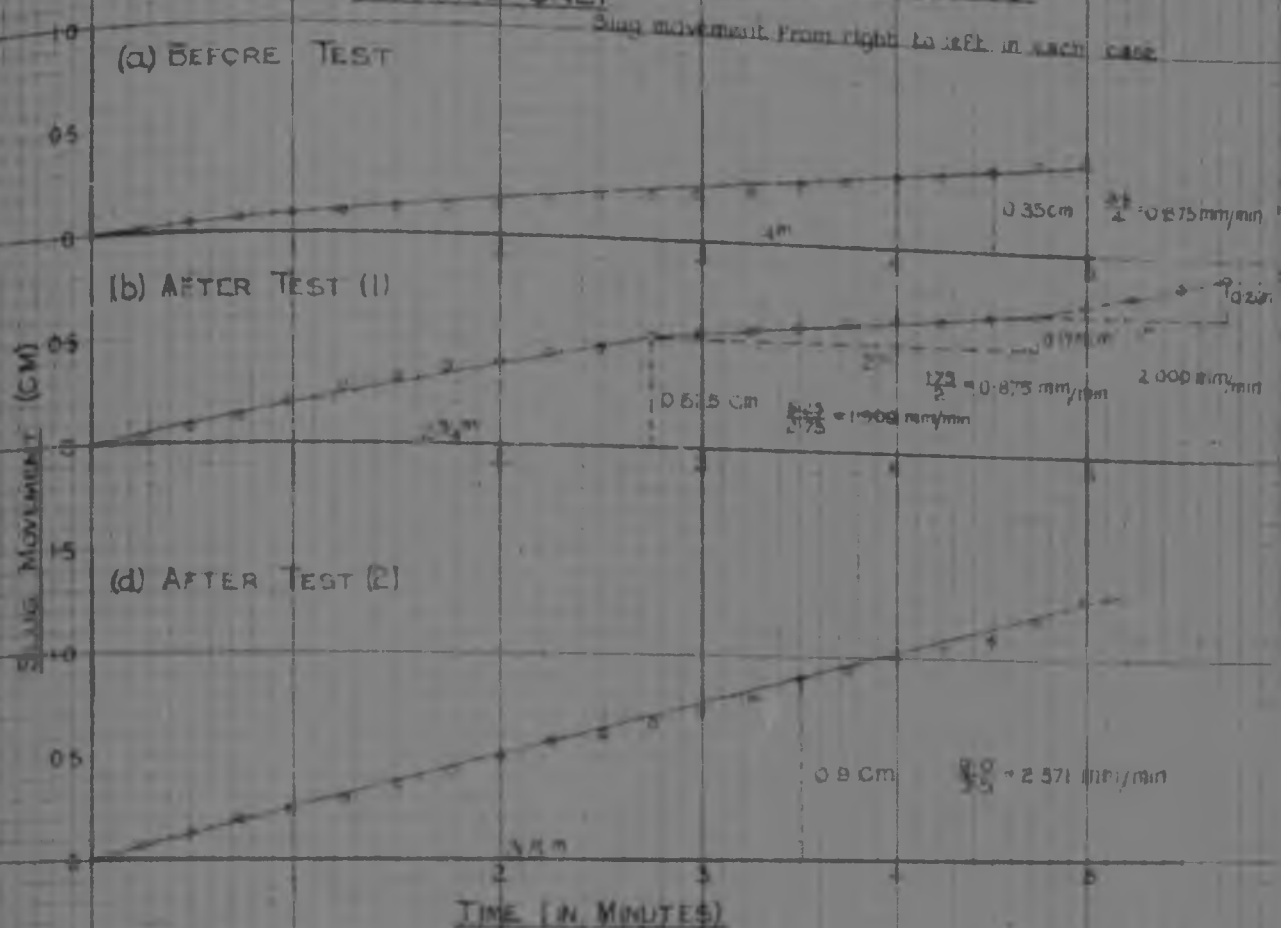
NOMINAL G_3 CHAMBER PRESSURE 20 LB / SQ IN

HEAD OF MERCURY 38½ INCHES, HENCE

ACTUAL G_3 CHAMBER PRESSURE 18 750 LB / SQ IN

NOMINAL RATE OF STRAIN 0 0125 INCHES / MINUTE

TEST NO. 4: LEAKAGE MEASUREMENTS DETERMINATION OF RATE OF SLUG MOVEMENT DUE TO LEAKAGE ONLY



(c) DETERMINATION OF RATE OF SLUG MOVEMENT DUE TO COM- BINED EFFECTS OF LEAKAGE AND SPINDLE ENTRY

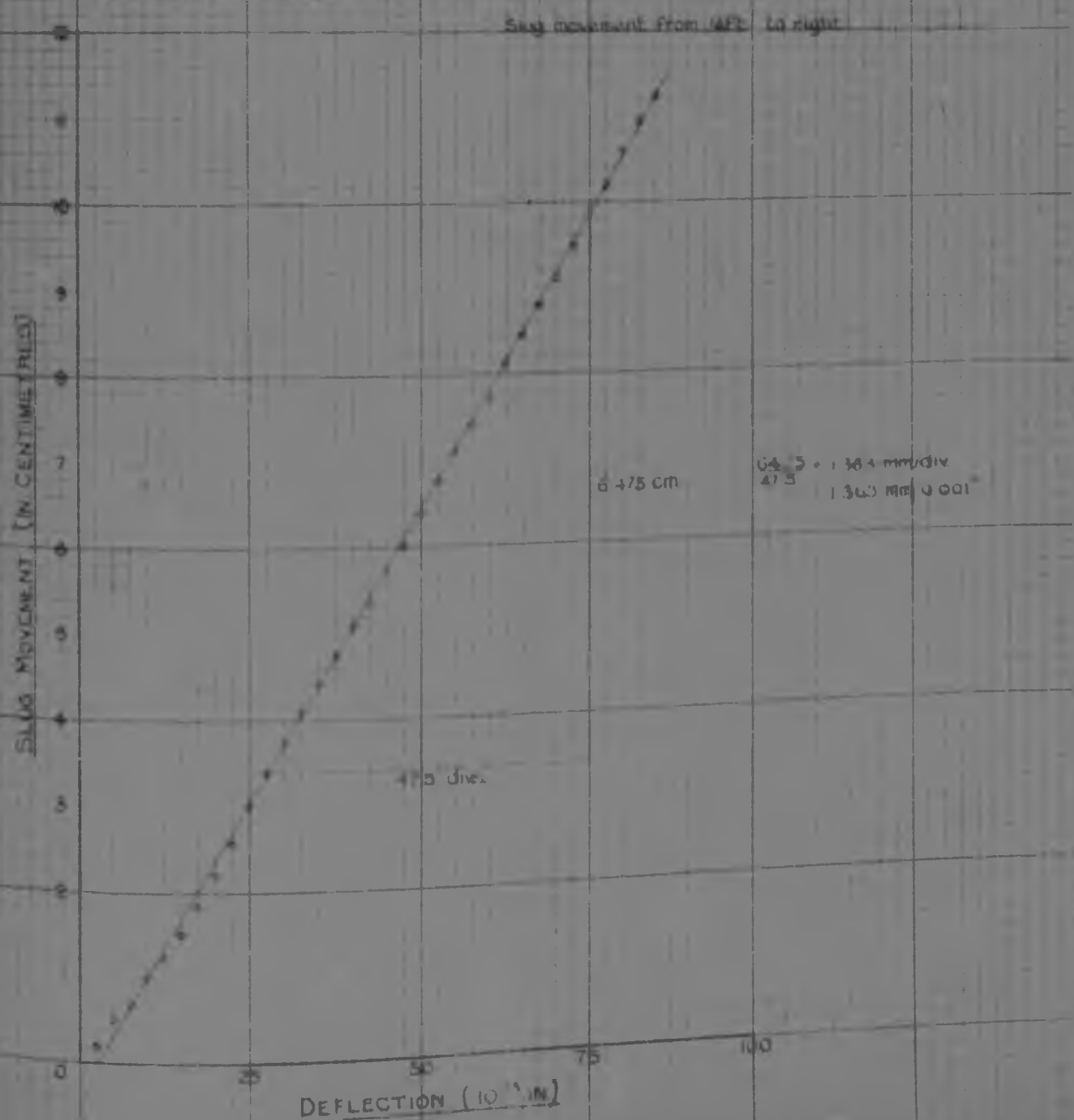
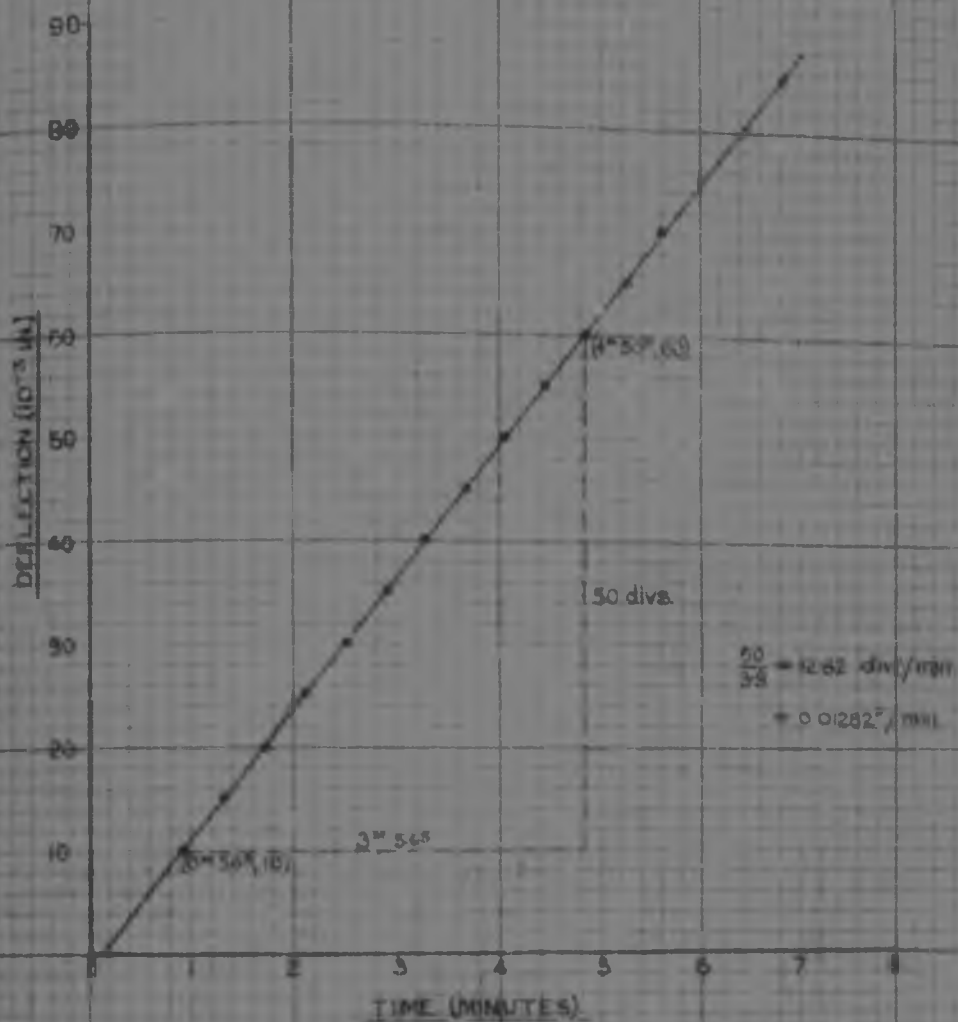


FIG. 36.

TEST NO4 RATE OF STRAIN DETERMINATIONS

(a) CALIBRATED RATE OF STRAIN ($\sigma_s = 20 \text{ lb/Sq. in.}$)



(b) ACTUAL RATE OF STRAIN DURING TEST ($\sigma_s = 20 \text{ lb/Sq. in.}$)

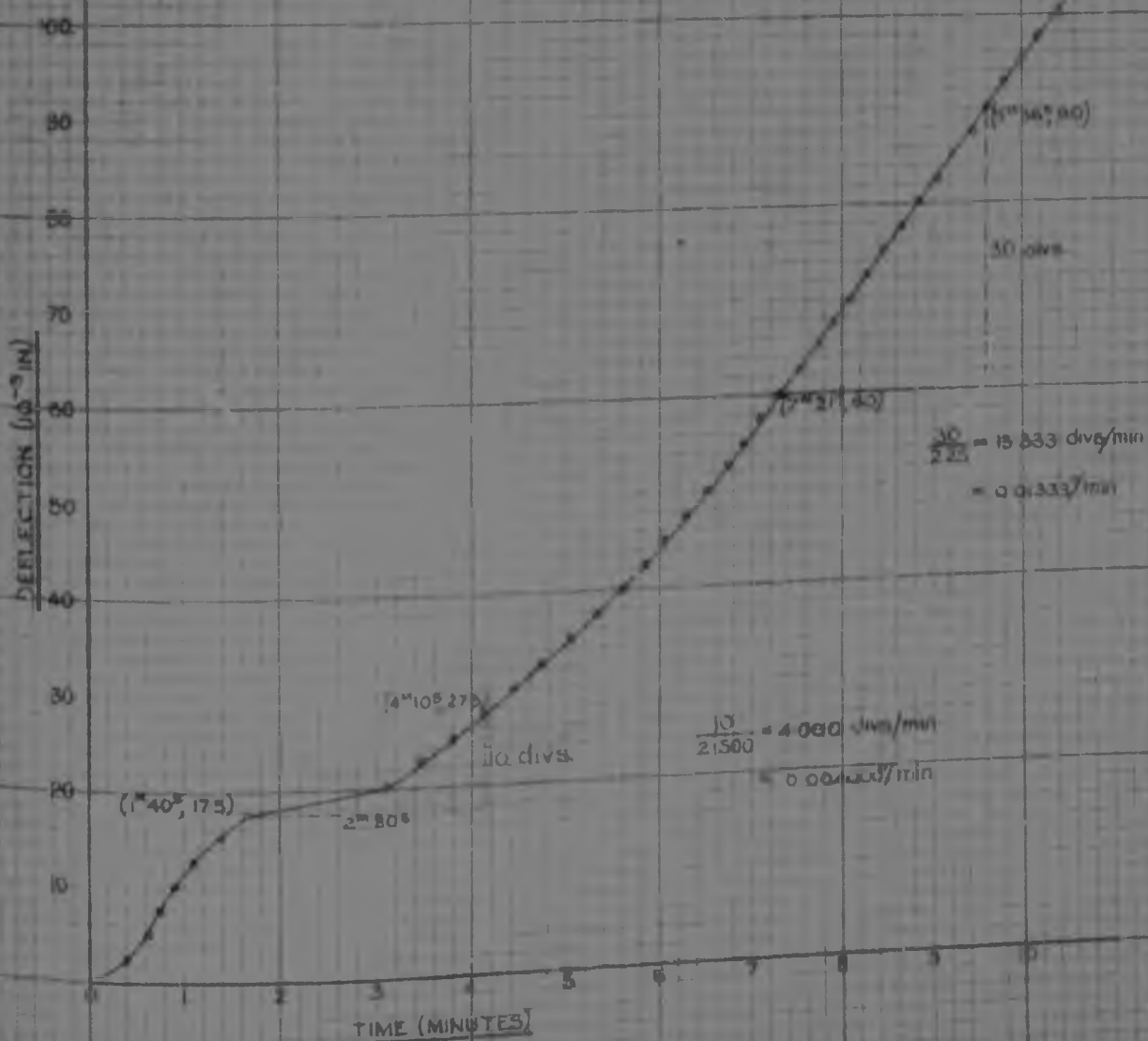
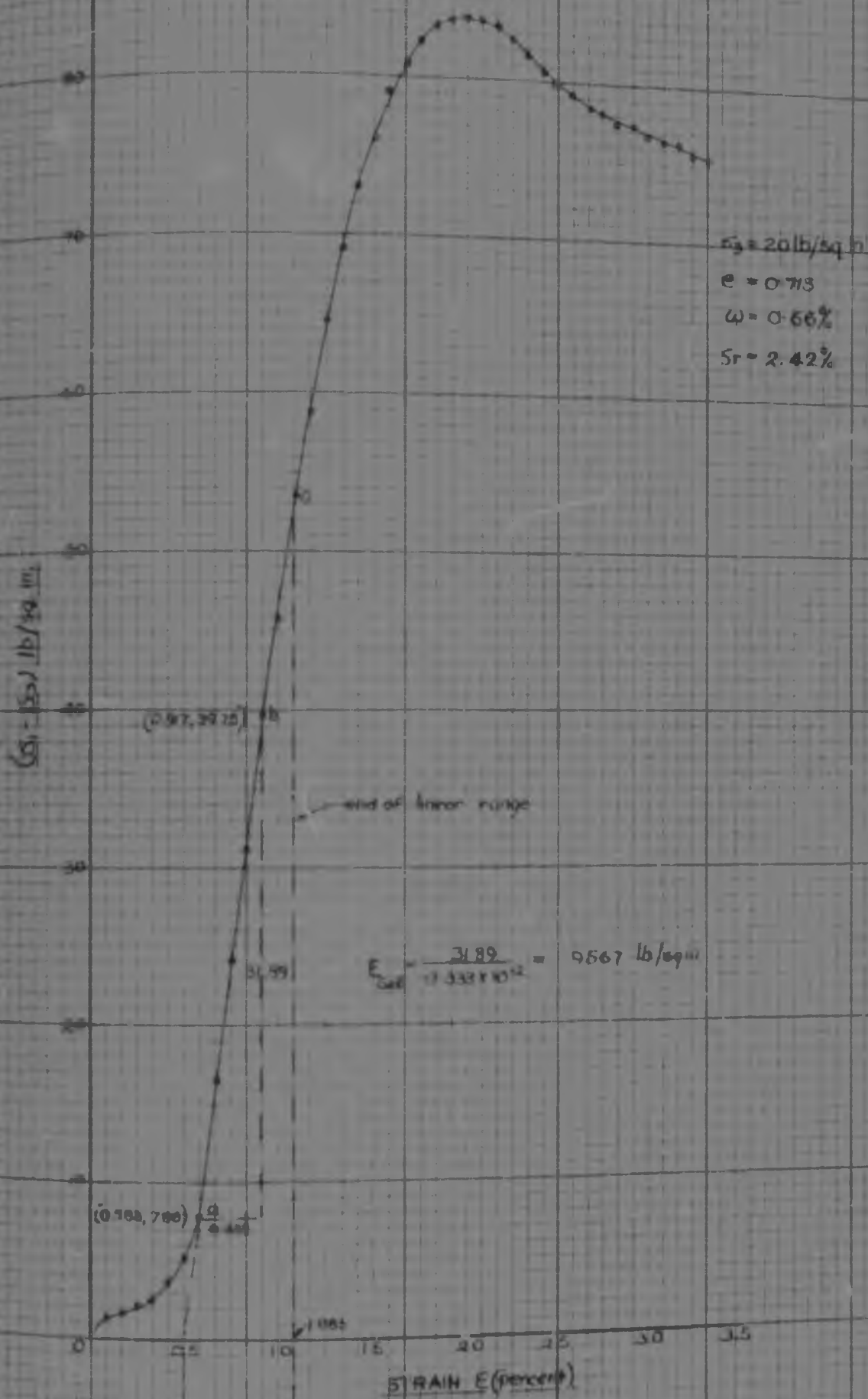


FIG. 37

- 95 -
TEST N°4

(a) STRESS - STRAIN CURVE



(b) YOUNG'S MODULUS STRAIN CURVE

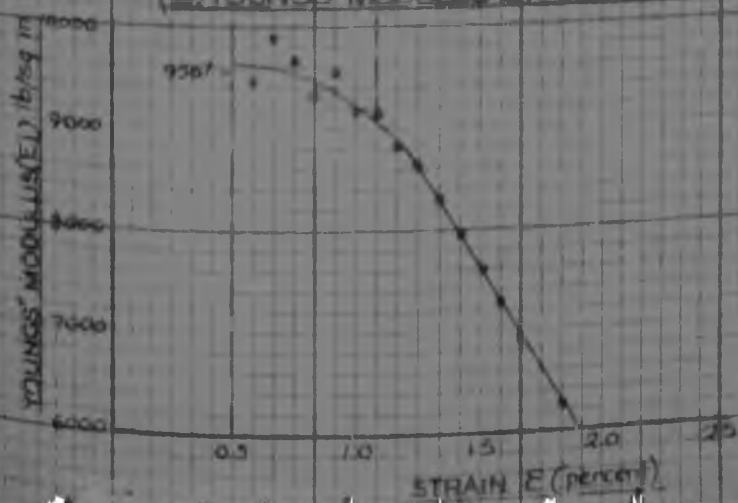


FIG 38

TEST No 4

CALCULATION OF INSTANTANEOUS VALUES
OF YOUNGS MODULUS (E)

CORRECTED STRESS = a lb/sq. in.	STRAIN percent	STRAIN DUE TO BEDDING - IN EFFECTS percent	CORRECTED STRAIN = b percent	YOUNGS MODULUS (E) = a/b lb/sq.
7.86	0.883	0.500	0.083	9470
16.16	0.867	"	0.167	9916
24.12	1.750	"	0.25	9648
31.10	0.833	"	0.233	9330
39.75	0.917	"	0.417	9532
45.87	1.000	"	0.500	9174
53.37	1.083	"	0.583	9154
58.85	1.167	"	0.667	8823
64.72	1.250	"	0.750	8629
69.12	1.333	"	0.833	8293
75.36	1.417	"	0.917	7956
78.96	1.500	"	1.000	7596
78.96	1.583	"	1.083	7291
80.83	1.667	"	1.167	6926
82.15	1.750	"	1.250	6572
83.15	1.833	"	1.333	6241
83.67	1.917	"	1.417	5905
83.88	2.000	"	1.500	5592

TEST No 4

MAIN SLUG MOVEMENT DEFLECTION CURVE

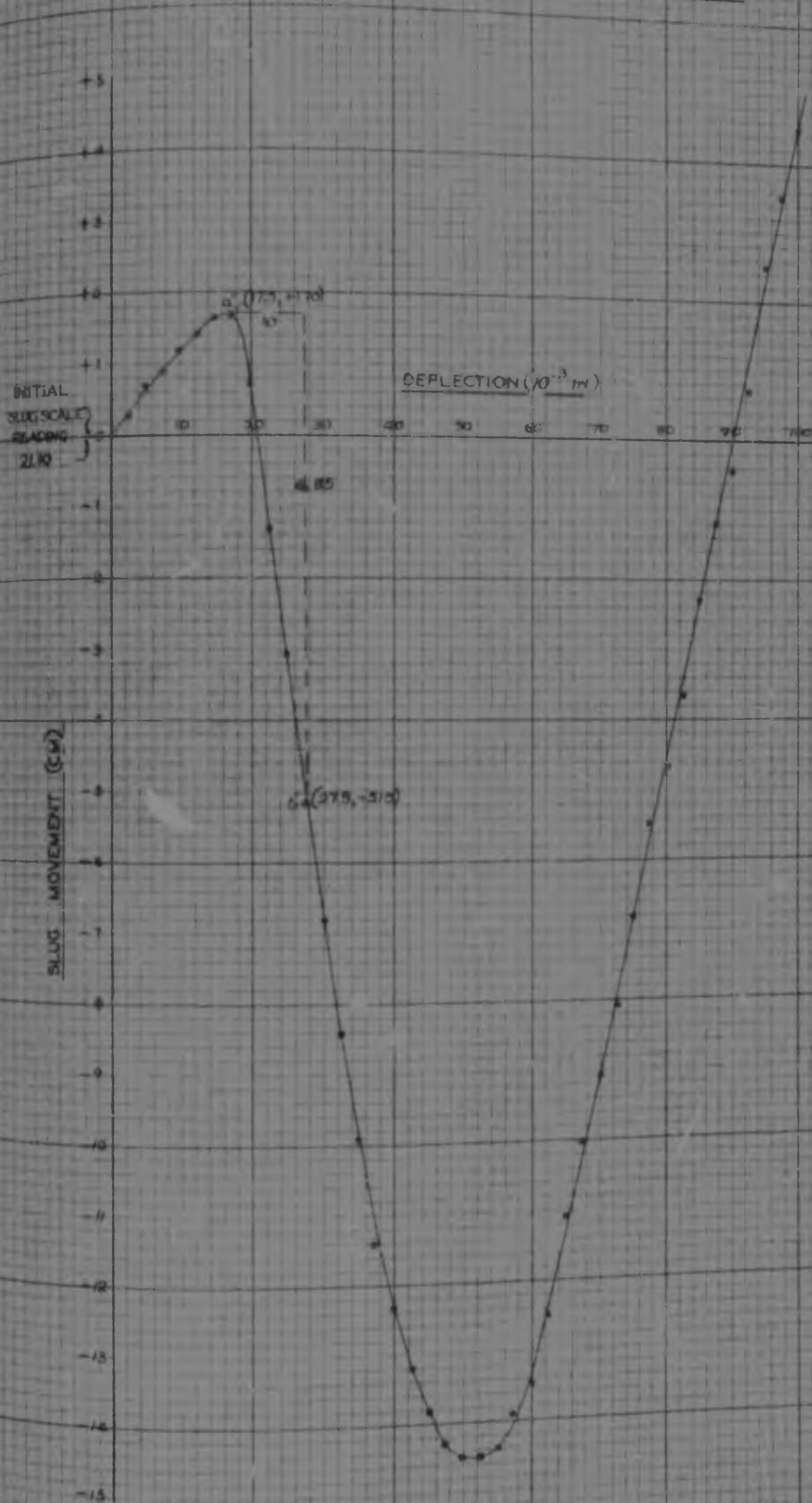


FIG. 39.

TEST NO 5.

DATE PERFORMED 30/1/57

SAMPLE CONSOLIDATED FOR 23^{HR} 15^{MIN} PRIOR TO TEST

TIME START OF TEST: 4/33 PM TEMPERATURE 24.0°C

TIME END OF TEST 4/43 PM TEMPERATURE 24.0°C

NOMINAL σ_3 CHAMBER PRESSURE 10 LB/SQ IN

HEAD OF MERCURY 18 INCHES, HENCE

ACTUAL σ_3 CHAMBER PRESSURE 8.825 LB/SQ IN

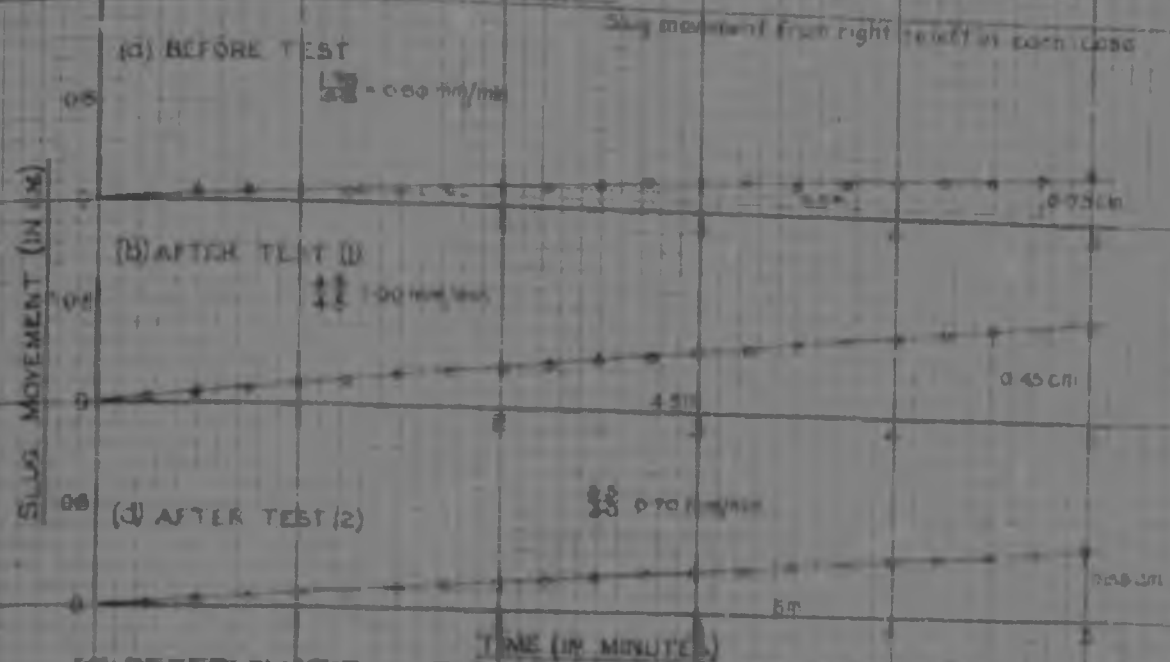
NOMINAL RATE OF STRAIN 0.0125 INCHES/MINUTE

TEST NO 5: LEAKAGE MEASUREMENTS.

(A) MEASUREMENT OF SLUG MOVEMENT DUE TO LEAKAGE ONLY BEFORE TEST TEMP 22.75°C TIME 4/20 D.M.		(B) MEASUREMENT OF SLUG MOVEMENT DUE TO LEAKAGE ONLY. AFTER TEST (1) TEMP 24.0°C TIME 4/45 D.P.		(C) MEASUREMENT OF SLUG MOVEMENT DUE TO COMBINED EFFECTS OF LEAKAGE & SPINDLE ENTRY (AFTER TEST) TEMPERATURE 24.0°C TIME 4/55 D.P.		(D) MEASUREMENT OF SLUG MOVEMENT DUE TO LEAKAGE ONLY AFTER TEST (2) TEMP 24.25°C TIME 5/10 D.M.	
TIME min sec	VOLUME SCALE cm ³	TIME min sec	VOLUME SCALE cm ³	DEFLECT GAUGE 10 ⁻² in	VOLUME SCALE cm ³	TIME min sec	VOLUME SCALE cm ³
0 00	22.75	0 00	18.60	00 10	2.30	0 00	18.70
15	22.725	15	17.975	12.5	2.45	15	18.675
30	22.70	30	17.95	15	3.00	30	18.675
45	22.70	45	17.925	17.5	3.30	45	18.65
1 00	22.70	1 00	17.90	20	3.425	1 00	18.625
15	22.70	15	17.875	22.5	3.80	15	18.625
30	22.675	30	17.85	25	4.25	30	18.60
45	22.675	45	17.825	27.5	4.60	45	18.575
2 00	22.65	2 00	17.80	30	4.925	2 00	18.575
15	22.65	15	17.775	32.5	5.30	15	18.55
30	22.625	30	17.75	35	5.60	30	18.525
45	22.60	45	17.725	37.5	5.975	45	18.50
3 00	22.60	3 00	17.70	40	6.30	3 00	18.475
15	22.60	15	17.675	42.5	6.70	15	18.475
30	22.60	30	17.65	45	7.025	30	18.45
45	22.575	45	17.625	47.5	7.50	45	18.45
4 00	22.575	4 00	17.60	50	7.90	4 00	18.425
15	22.55	15	17.575	52.5	8.25	15	18.40
30	22.55	30	17.55	55	8.70	30	18.375
45	22.525	45	17.55	57.5	9.20	45	18.375
5 00	22.50	5 00	17.525	60	9.60	5 00	18.35
		15	17.50	62.5	9.85		
				65	10.25		
				67.5	10.675		
				70	11.10	4 46	
				72.5	11.425		
				75	11.70		
				77.5	12.275		
				80	12.625	5 32	
				82.5	12.95		
				85	13.30		
				87.5	13.65		
				90	14.05	6 18	
				92.5	14.40		
				95	14.80		
				97.5	15.20		
				100	15.475	7 03	
				102.5	16.00		
				105	16.40		
				107.5	16.775		
				110	17.15	7 51	

TEST NO 5 LEAKAGE MEASUREMENTS

DETERMINATIONS OF RATE OF SLUG MOVEMENT DUE TO LEAKAGE ONLY



DETERMINATION OF RATE OF SLUG MOVEMENT DUE TO COMBINED EFFECTS OF LEAKAGE & SPINDLE ENTRY

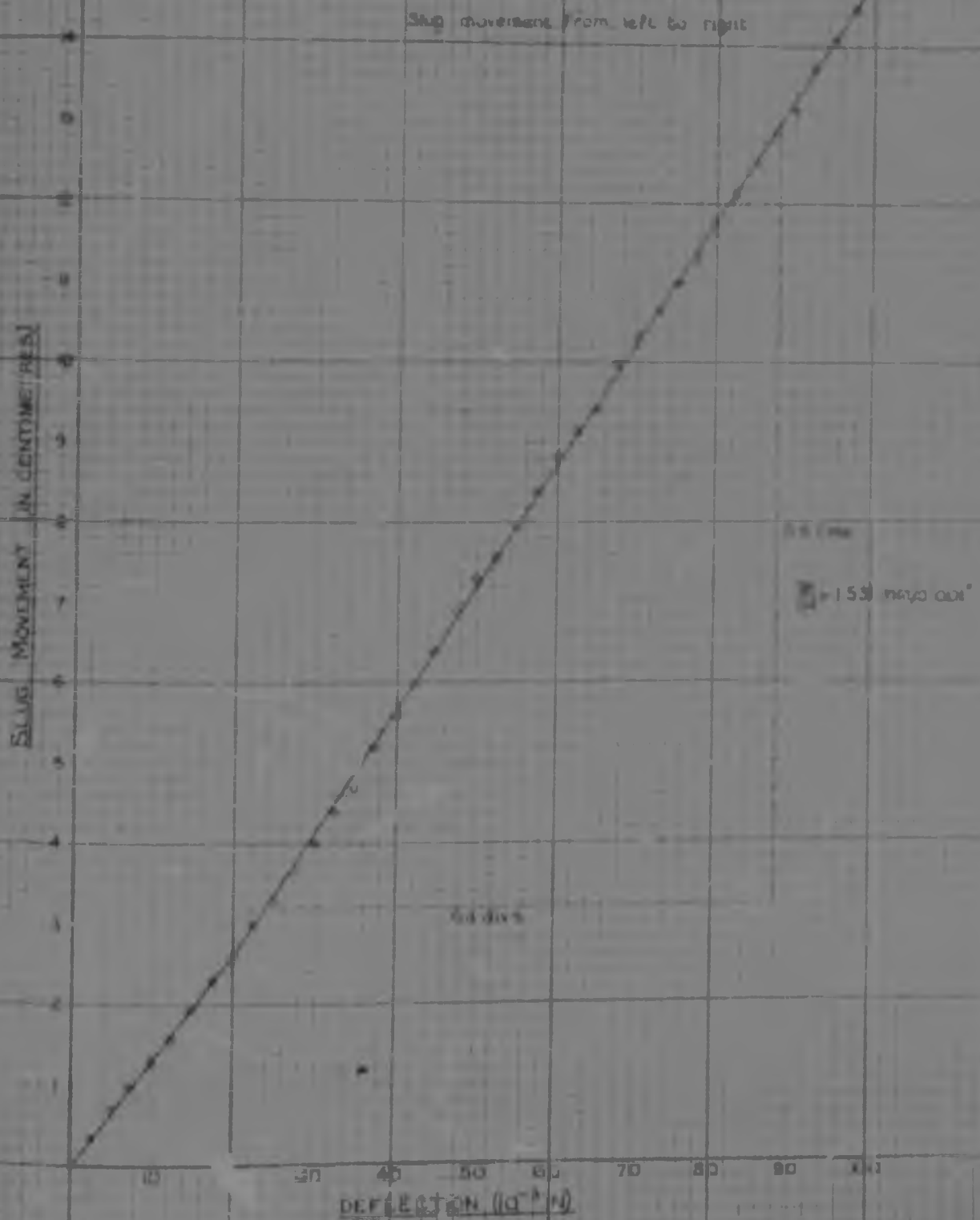


FIG. 40.

TEST NO 4. LEAKAGE MEASUREMENTS

(A) MEASUREMENT OF SLUG MOVEMENT DUE TO LEAKAGE ONLY BEFORE TEST TEMP 24.0°C TIME 8.55 A.M.		(B) MEASUREMENT OF SLUG MOVEMENT DUE TO LEAKAGE ONLY AFTER TEST(1) TEMP 24.25°C TIME 8.59 A.M.		(C) MEASUREMENT OF SLUG MOVEMENT DUE TO COMBINED EFFECTS OF LEAKAGE & SPINDLE ENTRY (AFTER TEST) TEMPERATURE 24.25°C TIME 9.07 A.M.			(D) MEASUREMENT OF SLUG MOVEMENT DUE TO LEAKAGE ONLY. AFTER TEST(2) TEMP 24.25°C TIME 9.16 A.M.	
TIME	VOLUME SCALE	TIME	VOLUME SCALE	DEFLECT GAUGE	VOLUME SCALE	TIME	TIME	VOLUME SCALE
MIN	SEC	MIN	SEC	10 ⁻³ IN	CM	MIN	SEC	10 ⁻³ IN
0 00	21.70	0 00	24.70	00 30	10.40	00 00	1 30	17.30
15	21.675	15	24.675	35.5	10.60		15	16.875
30	21.65	30	24.60	35	10.90		30	15.975
45	21.625	45	24.575	37.5	11.125		45	15.30
1 00	21.60	1 00	24.50	40	11.40	00 56	1 00	15.00
15	21.60	15	24.425	42.5	11.60		15	14.80
30	21.60	30	24.40	45	11.925	12 20	30	14.725
45	21.575	45	24.375	47.5	12.15		45	14.475
2 00	21.55	2 00	24.30	50	12.60	01 44	2 00	14.60
15	21.525	15	24.25	50.5	12.975		15	14.325
30	21.50	30	24.225	55	13.40	02 08	30	14.00
45	21.50	45	24.175	57.5	13.80		45	13.425
3 00	21.475	3 00	24.15	60	14.125	02 32	3 00	13.375
15	21.45	15	24.125	62.5	14.50		15	13.30
30	21.40	30	24.10	65	14.875	03 50	30	13.20
45	21.375	45	24.075	67.5	15.15		45	13.15
4 00	21.35	4 00	24.05	70	15.50	03 19	4 00	13.10
15	21.325	15	24.05	72.5	15.775		15	13.05
30	21.30	30	24.025	75	16.125	03 42	30	13.00
45	21.25	45	24.00	77.5	16.425		45	12.90
5 00	21.225	5 00	23.95	80	16.80	04 04	5 00	12.80
		15	23.90	82.5	17.15			
		30	23.85	85	17.50	04 28		
		45	23.80	87.5	17.80			
		6 00	23.775	90	18.15	04 50		
		15	23.705	92.5	18.50			
		30	23.70	95	18.85	05 14		
				97.5	19.20			
				100	19.575	05 37		
				102.5	19.975			
				105	20.375	06 01		
				107.5	20.80			
				110	21.20	06 26		
				112.5	21.65			
				115	22.05	06 50		

TEST NO 4 MAIN TEST OBSERVATIONS

DEFLEC- TION GAUGE	LOAD GAUGE	SLUG SCALE	TIME	TEMPERA- TURE	CORRECTED SLUG SCALE	CORRECTED LOAD	CORRECT DEFLECT	STRAIN ε	CORRECTED STRESS (6) C3 C4
							10 ⁻³ in.	percent	10 ³ psi
00 30	19	21.10	00 00	24.25	0	0	0	0	0
32.5	17.5	21.375	00 24		- 0.275	2.8	2.5	0.083	1.4
35	18	21.90	00 37		- 0.70	3.0	5	0.167	1.7
37.5	18.7	22.00	00 45		- 0.90	3.7	7.5	0.250	2.1
40	19.2	22.30	00 56		- 1.20	4.2	10	0.333	2.4
42.5	21.5	22.525	01 07		- 1.485	6.5	12.5	0.417	3.7
45	24.1	22.75	01 24		- 1.65	9.1	15	0.500	5.1
47.5	29.0	22.90	01 40		- 1.70	14.0	17.5	0.583	7.86
50	44.5	21.85	03 07		- 0.75	29.5	20	0.667	16.56
52.5	58	19.80	03 30		- 1.30	43.9	22.5	0.750	24.12
55	70.5	18.05	03 48		3.05	55.5	25	0.833	31.10
57.5	86	15.95	04 10		5.15	71.0	27.5	0.917	39.75
60	97	14.30	04 26		6.80	82.0	30	1.000	45.87
62.5	110.5	12.70	04 46		8.40	95.5	32.5	1.083	53.57
65	120.4	11.20	05 03		9.90	105.4	35	1.167	58.85
67.5	131.0	9.70	05 21		11.40	116.0	37.5	1.250	64.72
70	139.0	8.775	05 35		12.325	124.0	40	1.333	69.12
72.5	146.0	7.90	05 50		13.20	131.0	42.5	1.417	72.90
75	151.5	7.30	06 04		13.80	136.5	45	1.500	75.96
77.5	157.0	6.825	06 19		14.275	142.0	47.5	1.583	78.26
80	160.5	6.625	06 33		14.475	145.5	50	1.667	80.23
82.5	163.0	6.625	06 45		14.475	148.0	52.5	1.750	82.15
85	165.0	6.70	06 56		14.40	150.0	55	1.833	83.19
87.5	166.0	7.20	07 08		13.90	151.0	57.5	1.917	83.87
90	166.5	7.625	07 21		13.475	151.5	60	2.000	83.80
92.5	166.5	8.575	07 33		15.525	151.5	62.5	2.083	85.4
95	165.8	10.00	07 45		11.10	160.8	65	2.167	83.3
97.5	164.7	11.05	07 56		10.05	142.7	67.5	2.250	82.7
100	163.4	12.025	08 06		9.075	148.4	70	2.333	81.9
102.5	161.5	13.025	09 16		8.075	146.5	72.5	2.417	80.8
105	160.2	14.275	08 27		6.825	146.2	75	2.500	80.0
107.5	158.8	15.625	08 40		5.475	143.5	77.5	2.583	78.1
110	158.0	16.40	08 51		4.70	143.0	80	2.667	78.0
112.5	157.0	17.45	09 04		3.55	142.0	82.5	2.750	78.1
115	156.2	18.75	09 13		2.55	141.2	85	2.833	77.5
117.5	156.0	19.90	09 27		1.90	141.0	87.5	2.917	77.4
120	155.3	20.65	09 36		0.45	140.3	90	3.000	76.9
122.5	154.8	21.00	09 47		- 0.70	139.6	92.5	3.083	76.5
125	154.2	22.70	09 59		- 1.50	139.0	95	3.167	76.3
127.5	153.5	23.60	10 10		- 1.80	138.5	97.5	3.250	75.8
130	153.2	24.60	10 24	24.25	- 1.80	138.2	100	3.333	75.8

MAIN SLUG MOVEMENT DEFLECTION CURVE

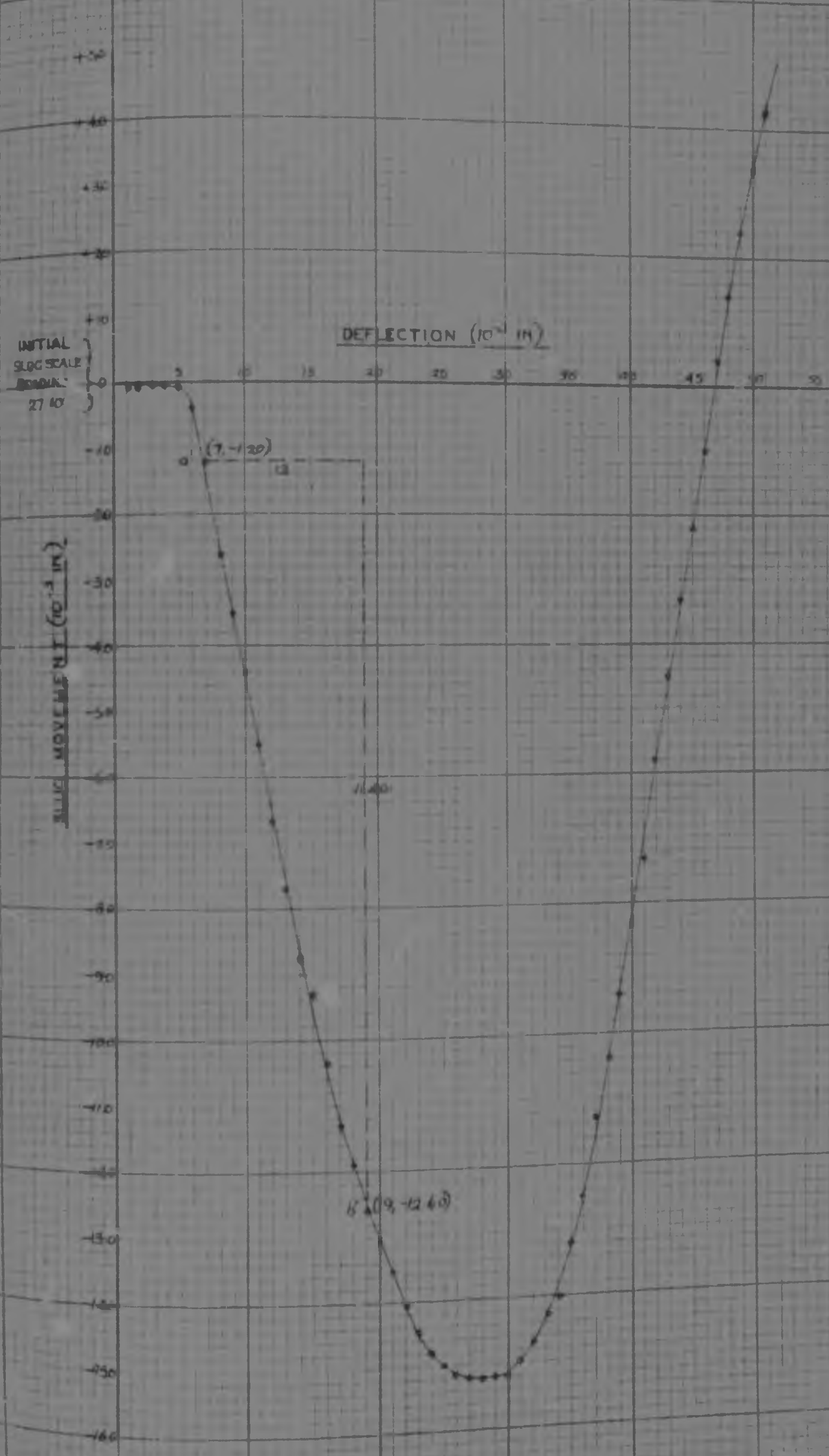


FIG. 47.

SUMMARY OF TRIAXIAL TEST RESULTS.

TABLE VIII

TEST NUMBER	NOMINAL RATE OF STRAIN INCHES/ MINUTE	ACTUAL CHAMBER PRESSURE (σ_3) LB/SQ. IN.	DEVIATOR STRESS AT FAILURE $(\sigma_1 - \sigma_3)_f$ LB/SQ. IN.	HENCE: NORMAL STRESS AT FAILURE $(\sigma_1)_f$ LB/SQ. IN.
1	0.00256	28.6	89.6	118.2
3	0.00256	18.7	85.3	104.0
6	0.00256	8.8	60.6	69.4
2	0.0125	28.7	102.0	130.7
4	0.0125	18.8	83.9	102.7
5	0.0125	8.8	53.0	61.8

Fig 48 (a)

NOMINAL RATE OF STRAIN 0.00256 inches/min

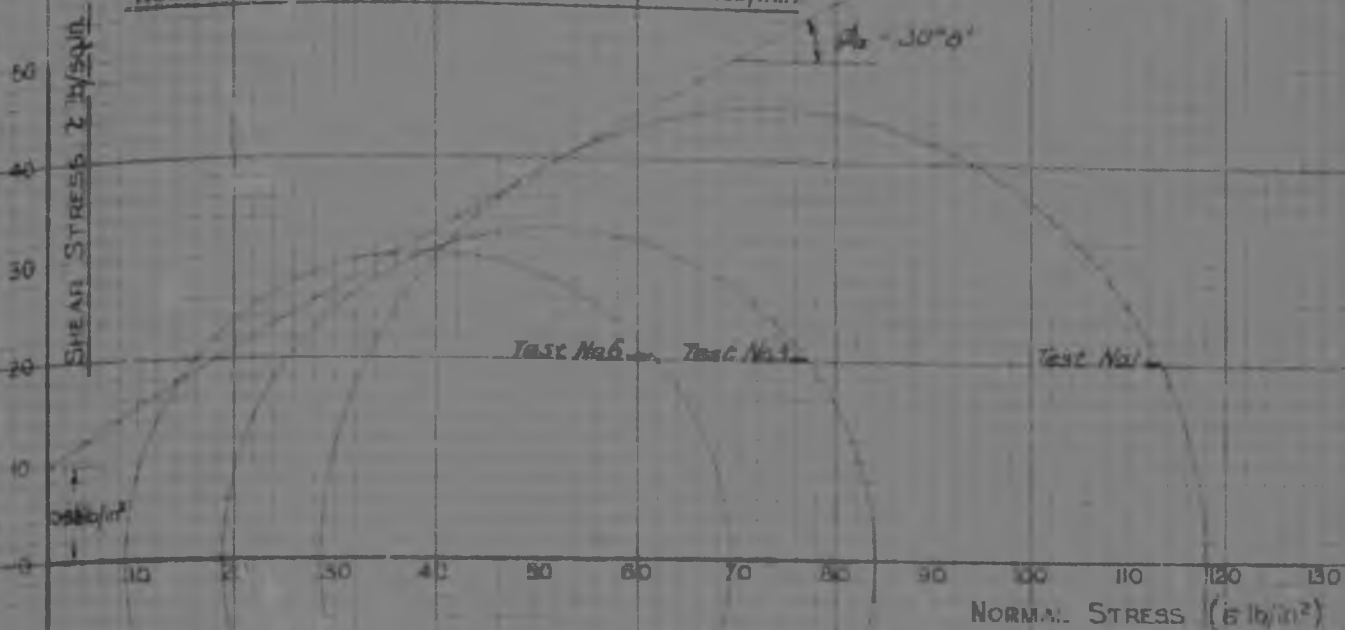
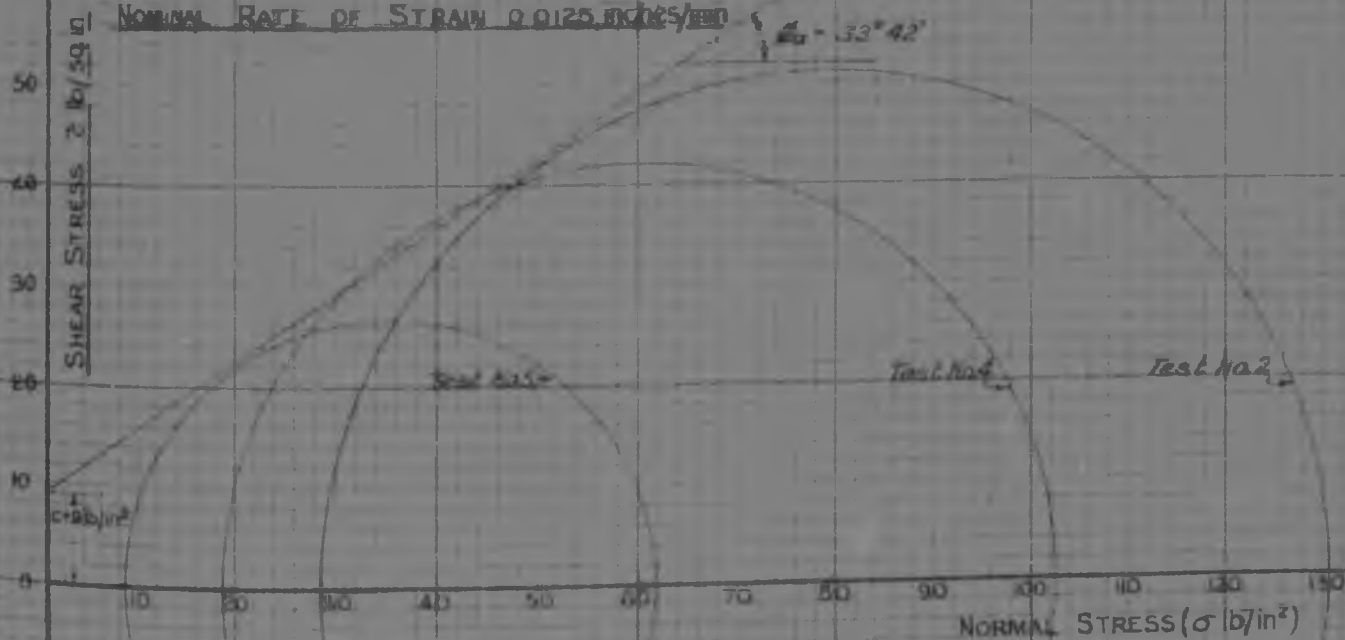


Fig 48 (b)

NOMINAL RATE OF STRAIN 0.0125 inches/min



7.7 Discussion

A study of the recorded data for each test shows that the variation in temperature inside the enclosing wooden box was insignificant during test in all cases, the greatest variation being 0.75°C in the case of Test No.3 which lasted for 92 min. 38 sec. It also appears that the test series as a whole was conducted within a temperature range of 20.75°C - 27.5°C , i.e., a maximum variation in test temperature between any two tests of 6.75°C (Tests No.1 and No.6.)

The actual time allowed for consolidation in the triaxial test cell was in each case very close to 24 hours if not exactly so, except in the case of Test No.1 in which consolidation was allowed for only 22hrs.15min. However, this probably had very little bearing (if any) on the results of the tests. The test samples were apparently so dry in each case, that no moisture was ever found in the bowl below the open drainage cock after the completion of consolidation.

From the moisture content measurements taken, it appears that:

- (a) over the duration of the test series, (which lasted for about 4 weeks excluding the time taken for trial tests), the initial moisture content of test samples decreased in value from about 2.5% to 0.5%, thus indicating that drying out had been taking place in the laboratory while handling the block sample. The various values of initial moisture content:time have been plotted (Fig.53, Appendix IV) and seem to indicate that the rate of decrease in moisture content was approximately uniform during this period.
- (b) the final (after test) moisture content of test samples was always slightly greater than the corresponding initial moisture content. In each case this was probably mainly due to leakage through the walls of the rubber membrane enclosing the test sample, as no special provisions were made to prevent this from happening. An additional cause may have been that some of the moisture adhering to the surface of the rubber membrane after test was imparted to the sample on removal of the membrane. It is rarely possible to prevent this from happening. Table XX, Appendix IV is a summary in tabular form of the moisture content before and after test of each test sample.

Regarding the Void Ratio and Degree of Saturation figures shown alongside the various stress-strain curves, it needs to be mentioned that they were obtained (See Table XXI, Appendix IV) by using the oven-dry weight of each test sample after test and a sample volume of 93.0cc, which is slightly less than the volume of the cutting cylinder used. A full discussion giving reasons for this procedure is given later in Section 8.4. The moisture content figure shown is in each case the initial moisture content of the particular test sample. With some tests no initial moisture content determination was made (see Table XX, Appendix IV). In such cases an estimated figure was used which was obtained by reading off the initial moisture content value corresponding to the date of the test on Fig. 53, Appendix IV.

The curves of slur movement due to leakage only as well as the curves of slur movement due to the combined effects of leakage and spindle entry only, show in some instances that leakage from the test cell could be erratic at times. In such cases more than one value of the rate of leakage was determined as shown. The results of all leakage determinations are presented

in/

in summarised form in Table IX, Section 8.2. In the same Section these results as well as the factors affecting the rate of leakage from the test cell are discussed in more detail.

The stress:strain curves generally show a well defined linear range which commences at or close to the start of the curve depending on the magnitude of the bedding-in effects. Some mention about "bedding-in" effects was already made in section 7.6. It was mentioned that the corrected start of the stress:strain curve was obtained by producing the approximately linear portion of the curve backwards to intersect the strain axis. In order to determine the point at which proportionality between stress and strain ceases, i.e., the end of the linear range, the curve of Young's Modulus versus strain was prepared. This curve is considered to serve as a very useful guide to the selection of the point mentioned, since, while stress and strain are proportional, Young's Modulus has a constant value (independent of strain), and therefore, under these conditions, the curve of Young's Modulus versus strain is a horizontal straight line. Hence, in the ideal case, the strain at which the Young's Modulus:strain curve starts to slope downward after the initial horizontal straight line portion, demarcates the point at which proportionality between stress and strain ceases, i.e., demarcates the end of the linear range. The actual plotted curves, however, show that this horizontal straight line portion of the ideal Young's Modulus:strain curve was seldom perfectly realised. Nevertheless, these curves were of considerable assistance in judging by careful inspection where the linear range ceased in each case. The point eventually decided on, is shown marked by the letter c.

Having determined the end of the linear range of the stress:strain curve for each test in the manner just described the "best" portion of this range in the sense of being the closest representation of truly linear conditions, was selected, and the terminal points of this selected range marked by the letters a and b. Hereafter, this range will be referred to only as the "Selected Range". The value of Young's Modulus was then determined for each selected range and denoted by the symbols E_{sel} .

The Main Slug Movement:Deflection curves generally show a well defined linear range, usually falling closely within the same range of strain as the linear range of the relevant stress:strain curve. The points corresponding to the limits of the Selected Range are in each case shown marked a' and b'. This information is later used in the evaluation of Poisson's Ratio (Section 8.5). These linear ranges in all cases terminate in the development of trough-shaped turning points in the curves, which demarcate the commencement of the phenomenon of sample expansion on approaching failure conditions.

The curves again reveal the presence of "bedding-in" effects, generally by an initially flat portion immediately before the main steep linear portion of the curve commences, but in some instances, (see Figs. 35 and 43), by a pronounced peak-shaped portion before the main curve commences. The phenomenon in this case can be explained as follows: During the "bedding-in" period, only portion of the applied loading is taken up by the test sample, the remainder being used up in causing the bedding-in movements in the test set-up. Hence, during the bedding-in period at the start of a test, sample compression is small and therefore the tendency for fluid flow into the test cell due to this cause is small. In contrast, the loading spindle during the same period has a partially unrestrained and hence comparatively rapid advance into the test cell with a tendency to cause fluid flow out of the test cell. It appears that during

the/

the bedding-in period, this latter effect outweighs the combined effects of an initial small sample compression and leakage from the test cell (which both tend to cause fluid flow into the test cell), and results in a net fluid flow out of the test cell i.e. increasing slug scale readings and hence the initial upward trend of the curve.

Subsequently, however, when the test set-up is firmly bedded down, all the applied loading is taken by the test sample causing it to compress considerably and at the same time severely restraining the advance of the loading spindle into the test cell. As soon as this happens, the combined effects of sample compression and leakage from the test cell start to outweigh the effect of spindle entry into the test cell, and thus, result in a net inflow of fluid into the test cell, i.e., decreasing slug scale readings and hence the commencement of a downward trend in the curve and the formation of the peak observed.

The argument presented above is strengthened by the actual calculation of Sample Dilation ($\delta V/V$) during test (Section 8.5). These calculations show that over the bedding-in range, sample compression is small compared with subsequent sample compression when bedding-in is complete. (See, for example, the calculation of Sample Dilation for Test No. 4.) The pronounced peak-shaped bedding-in effect would thus occur in cases where the effect of the initial advance of the loading spindle into the test cell considerably exceeds the opposite effects caused by sample compression and leakage. This is probably only possible in the case of an initially very loosely bedded sample.

Mention was previously made about the possible effect of chamber pressure on the Calibrated Rate of Strain, i.e. the rate of strain obtained from the calibration of loading spindle entering the test cell against the resistance of the relevant chamber pressure only. (See end of Section 7.8) Table IX Section 8.2, shows the values of calibrated rate of strain, obtained at the various chamber pressures for the same nominal rates of strain. The values apparently show that the calibrated rate of strain decreases as the chamber pressure increases. This is contrary to expectation and is possibly due to insufficient values being available. This suspicion is based on the fact that in the case of Test No. 55 (not included in the test series being reported on herein), a calibrated rate of strain of 0.003690 inches/min. for a chamber pressure of 1015.4 sq. in. was obtained. It is considered that the calibrated rate of strain would possibly increase with decreasing chamber pressure.

Where detailed time measurements were taken, the resulting deflection:time curves show clearly that the actual rate of strain during test is very uneven, especially during the initial stages of the test. A very pronounced time lag is obtained at a point corresponding approximately to the start of the linear range of the stress:strain curve. The phenomenon is revealed by the nearly horizontal portion of the curve soon after its commencement, indicating a negligible increase in deflection during this period. In contrast, there is a rapid increase in loading during the same period. In most cases, it will also be noted (from the curves of Young's Modulus versus Strain), that Young's Modulus has a maximum value just about at the point where the time lag occurs. Subsequently the actual rate of strain steadily increases until, when sample failure is approached, it tends to take on the value of the calibrated rate of strain.

Careful investigation seems to show that the pronounced time lag occurs at the completion of the bedding-in period. It

is/

is possibly due to a back-lock in the loading system once the bedding down is complete and the applied loading is directed in full at overcoming the resistance of the sample to deformation, which, at this point happens to be a maximum. The subsequent steady increase in the actual rate of strain is due to a steady decrease in the value of Young's Modulus (See Young's Modulus: Strain curves). This continues until, at sample failure, the rate of strain is approximately the same as the calibrated rate of strain, which, notably, was determined for the condition of loading spindle advancing into the test cell against the resistance of the relevant chamber pressure only. The disturbing thought is that the tests were intended to have been conducted as tests subject to strain control.

Finally, it is necessary to consider reasons for the peaks in the Young's Modulus:Strain curves which occur in most cases. The basic cause of this phenomenon is the shape of the stress: strain curve. Careful inspection shows that within the accepted extent of the linear range of the stress: strain curve, the curve usually makes a slight S-shaped bend, i.e., according to actual points plotted. (See, for instance, Test No. 1, Fig. 27.) The curve of Young's Modulus: Strain was prepared by calculating instantaneous values of Young's Modulus as a secant modulus, i.e., working from point to point along the curve but always from the start of the curve, which in this case, is the 'corrected' start as obtained after elimination of bedding-in effects. With an S-shaped curve and this secant modulus method of calculation, the result is clearly a peak-shaped variation of Young's Modulus.

It is considered that the slight S-shape of the curve is at its lower end probably due to the inclusion of bedding-in effects, and, at the upper end, due to a natural slight curving over to the right of the actual stress: strain curve (this being the case even within the extent of the linear range). In the absence of bedding-in effects the portion of the Young's Modulus: Strain curve to the left of its peak would probably have been much nearer horizontal and thereby would have conformed closer to the requirements of the ideal Young's Modulus: Strain curve as previously discussed in this Section. The fact that the respective values of E_{SEL} (Young's Modulus for the Selected Range) are in all cases lower than the corresponding peak values of Young's Modulus as indicated by the Young's Modulus: Strain curves, is due to the fact that in each case the Selected Range is in effect the straight line joining the ends of a slightly S-shaped curve. This clearly leads to a lower value of Young's Modulus than the maximum value obtainable by the other method.

In the following Chapter, Poisson's Ratio (μ) has for each test been calculated using both instantaneous values of Young's Modulus (yielding instantaneous values of μ , denoted μ_i) and the value of Young's Modulus obtained from the Selected Range (the corresponding μ value being denoted μ_{SEL}).

CHAPTER 8

REDUCTION OF TEST RESULTS AND THE DETERMINATION OF POISSON'S RATIO

8.1 Introduction

Before the evaluation of Poisson's Ratio for each test can finally be commenced, it is necessary to discuss in more detail some important factors relating to the evaluation, some of which have already been briefly discussed. These discussions follow in Sections 8.2, 8.3 and 8.4 hereafter.

8.2 Rate of Slug Movement due to Leakage only during Actual Test

For the evaluation of Poisson's Ratio, the rate of slug movement due to leakage from the test cell during actual test needs to be known. As previously discussed (Section 7.4), this measurement cannot be made directly, since it is not possible to isolate the effects of slug movement due to entry of the loading spindle into the test cell and change in volume of the test sample during test.

To enable some idea of the rate of leakage during actual test, the only circumstances under which slug movement due to leakage only can be measured directly, viz., under the steady cell conditions existing immediately before and after test, were resorted to. As the rate of leakage measured under these circumstances was likely to be different to the rate of leakage occurring under the disturbed cell conditions of an actual test, a further indirect measurement of the rate of leakage was made from a test which it was hoped simulated the disturbed cell conditions of an actual test.

Thus, having observed values of the rate of leakage under the steady cell conditions existing before and again after test, as well as having determined the rate of leakage under disturbed cell conditions similar to those of an actual test although possibly not identical, it is necessary to consider in some detail the possible value of the rate of leakage occurring under the disturbed cell conditions of an actual test.

For this purpose, it is in the first instance necessary to study carefully the results of all the various leakage measurements made during the test series. These are presented in summarised form in Table IX on the next page. Table X on the same page, shows the determination of slug movement due to leakage only under the disturbed cell conditions of the test simulating the conditions of an actual test. The basis of this determination was discussed in Section 7.4 (pages 39 and 40). Table X also shows a comparison of these results with the maximum observed slug movement due to leakage only measured under the steady cell conditions existing before and again after test. In Table IX, where more than one value appears under the same heading in some instances, this happens as a result of a definite change in value having been observed during test due to entry of the loading spindle into the test cell. The determination of the rate of slug movement due to entry of the loading spindle into the test cell, is given in Appendix V, item 2.

From the data shown in the Tables, it is evident that:

- (1) The rate of slug movement due to leakage measured immediately after any triaxial test is generally higher than

that/

TABULAR SUMMARY OF ALL LEAKAGE MEASUREMENTS

NOTE AN ARROW THUS \leftarrow ABOVE A FIGURE DENOTES SLUG MOVEMENT FROM RIGHT TO LEFT.
AN ARROW THUS \rightarrow ABOVE A FIGURE DENOTES SLUG MOVEMENT FROM LEFT TO RIGHT.

TABLE IX

TEST NUMBER	NOMINAL CHAMBER PRESSURE LB./SQ. IN.	NOMINAL RATE OF STRAIN inches/minute	OBSERVED SLUG MOVEMENT DUE TO LEAKAGE ONLY UNDER STEADY CELL CONDITIONS.			CALCULATED SLUG MOVEMENT DUE TO SPINDLE ENTRY ONLY = N mm./div. deflect	OBSERVED SLUG MOVEMENT DUE TO COMBINED EFFECTS OF LEAKAGE & SPINDLE ENTRY = M mm./div. deflect	CALIBRATED RATE OF STRAIN = S inches/minute
			BEFORE TRIAxIAL TEST mm./minute	AFTER TRIAXIAL TEST				
				1. mm./minute	2 mm./minute			
1	30	0.00256	0.92 	2.80 2.867 1.00 2.34	4.500 	1.614 	0.173 0.250 0.333	0.002555 0.002544
3	20	0.00256	1.54 	0.947 	0.50 	1.614 	1.112 	0.002500
6	10	0.00256	0.875 	0.947 	0.50 	1.614 	1.112 	0.002500
2	30	0.0125	1.27 	4.00 3.89 5.238	5.238 	1.614 	1.138 	—
4	20	0.0125	0.875 	1.909 0.875 2.000	2.571 	1.614 	1.363 	0.01282
5	10	0.0125	0.500 	1.000 	0.700 	1.614 	1.531 	0.01270

NOTE THE MAXIMUM VALUES OF SLUG MOVEMENT DUE TO LEAKAGE FOR EACH TEST, ARE SHOWN UNDERLINED IN RED

DETERMINATION OF SLUG MOVEMENT DUE TO LEAKAGE ONLY UNDER DISTURBED CELL CONDITIONS, AND COMPARISON WITH MAXIMUM OBSERVED SLUG MOVEMENT DUE TO LEAKAGE UNDER STEADY CELL CONDITIONS

TABLE X

TEST NUMBER	M = OBSERVED SLUG MOVEMENT DUE TO COMBINED EFFECTS OF LEAKAGE & SPINDLE ENTRY <small>mm./div. deflect</small>	S = CALIBRATED RATE OF STRAIN <small>inches/minute</small>	HENCE SLUG MOVEMENT DUE TO COMBINED EFFECTS OF LEAKAGE & SPINDLE ENTRY = M X S <small>mm./minute</small>	N = CALCULATED SLUG MOVEMENT DUE TO SPINDLE ENTRY ONLY. <small>mm./div. deflect</small>	HENCE CALCULATED SLUG MOVEMENT DUE TO SPINDLE ENTRY ONLY. = N X S = h <small>in./minute</small>	HENCE RESULTANT SLUG MOVEMENT DUE TO LEAKAGE ONLY UNDER DISTURBED CELL CONDITIONS <small>mm./div. deflect</small>	MAXIMUM OBSERVED SLUG MOVEMENT DUE TO LEAKAGE UNDER STEADY CELL CONDITIONS <small>mm./minute</small>	DIFFERENCE <small>mm./minute</small>
1	\leftarrow 0.173	2.555	\leftarrow 0.442	\rightarrow 1.614	\rightarrow 4.124	\leftarrow 4.586	\leftarrow 4.500	0.086
3	\leftarrow 0.333	2.544	\leftarrow 0.847	\rightarrow 1.614	\rightarrow 4.106	\leftarrow 3.259	\leftarrow 2.867	0.392
6	\rightarrow 1.112	2.500	\rightarrow 2.780	\rightarrow 1.614	\rightarrow 4.035	\rightarrow 1.255	\leftarrow 0.947	0.308
2	\rightarrow 1.138	12.50*	\rightarrow 14.225	\rightarrow 1.614	\rightarrow 20.175	\rightarrow 5.950	\leftarrow 5.238	0.712
4	\rightarrow 1.363	12.82	\rightarrow 17.474	\rightarrow 1.614	\rightarrow 20.691	\rightarrow 3.217	\leftarrow 2.571	0.646
5	\rightarrow 1.531	12.70	\rightarrow 19.444	\rightarrow 1.614	\rightarrow 20.498	\rightarrow 1.054	\leftarrow 1.000	0.054

* NOMINAL RATE OF STRAIN USED HERE, AS CALIBRATED RATE OF STRAIN WAS NOT DETERMINED FOR THIS TEST

TABULAR SUMMARY OF ALL LEAKAGE MEASUREMENTS

NOTE: AN ARROW THUS: \leftarrow ABOVE A FIGURE DENOTES SLUG MOVEMENT FROM RIGHT TO LEFT.
AN ARROW THUS: \rightarrow ABOVE A FIGURE DENOTES SLUG MOVEMENT FROM LEFT TO RIGHT.

TABLE IX

TEST NUMBER	NOMINAL G ₃ CHAMBER PRESSURE LB/SQ IN	NOMINAL RATE OF STRAIN. Inches/minute	OBSERVED SLUG MOVEMENT DUE TO LEAKAGE ONLY UNDER STEADY CELL CONDITIONS.			CALCULATED SLUG MOVEMENT DUE TO SPINDLE ENTRY ONLY = N mm/div deflect	OBSERVED SLUG MOVEMENT DUE TO COMBINED EFFECTS OF LEAKAGE & SPINDLE ENTRY = M mm/div deflect	CALIBRATED RATE OF STRAIN = S inches/minute
			BEFORE TRIAxIAL TEST mm/minute	AFTER TRIAXIAL TEST				
				1. mm/minute	2 mm/minute			
1	30	0.00256	\leftarrow 0.92 \leftarrow	\leftarrow 2.80 \leftarrow 2.667 \leftarrow 1.00 \leftarrow 2.34	\leftarrow 4.500 \leftarrow 2.00 \leftarrow 2.33	\rightarrow 1.614 \rightarrow 1.614	\leftarrow 0.173 \leftarrow 0.250 \leftarrow 0.333	0.002555 0.002544
6	10	0.00256	\leftarrow 0.875	\leftarrow 0.947	\leftarrow 0.50	\rightarrow 1.614	\rightarrow 1.112	0.002500
2	30	0.0125	\leftarrow 1.27	\leftarrow 4.00 \leftarrow 1.909 \leftarrow 0.875 \leftarrow 2.000	\leftarrow 3.85 \leftarrow 5.238 \leftarrow 2.571	\rightarrow 1.614 \rightarrow 1.614	\leftarrow 1.138 \leftarrow 1.363	— 0.01262
5	10	0.0125	\leftarrow 0.500	\leftarrow 1.000	\leftarrow 0.700	\rightarrow 1.614	\leftarrow 1.531	0.01270

NOTE: THE MAXIMUM VALUES OF SLUG MOVEMENT DUE TO LEAKAGE FOR EACH TEST, ARE SHOWN UNDERLINED IN RED

DETERMINATION OF SLUG MOVEMENT DUE TO LEAKAGE ONLY UNDER DISTURBED CELL CONDITIONS, AND COMPARISON WITH MAXIMUM OBSERVED SLUG MOVEMENT DUE TO LEAKAGE UNDER STEADY CELL CONDITIONS

TABLE X

TEST NUMBER	M = OBSERVED SLUG MOVEMENT DUE TO COMBINED EFFECTS OF LEAKAGE & SPINDLE ENTRY mm/div deflect	S = CALIBRATED RATE OF STRAIN inches/minute	HENCE SLUG MOVEMENT DUE TO COMBINED EFFECTS OF LEAKAGE & SPINDLE ENTRY = M x S = N mm/minute	N = CALCULATED SLUG MOVEMENT DUE TO SPINDLE ENTRY ONLY mm/div deflect	HENCE CALCULATED SLUG MOVEMENT DUE TO SPINDLE ENTRY ONLY = N x S = b mm/minute	HENCE RESULTANT SLUG MOVEMENT DUE TO LEAKAGE ONLY UNDER DISTURBED CELL CONDITIONS = a mm/minute	MAXIMUM OBSERVED SLUG MOVEMENT DUE TO LEAKAGE UNDER STEADY CELL CONDITIONS mm/minute	DIFFERENCE
1	\leftarrow 0.173	2.555	\leftarrow 0.442	\rightarrow 1.614	\leftarrow 4.124	\leftarrow 4.586	\leftarrow 4.500	0.086
3	\leftarrow 0.333	2.544	\leftarrow 0.847	\rightarrow 1.614	\leftarrow 4.106	\leftarrow 3.259	\leftarrow 2.667	0.592
6	\leftarrow 1.112	2.500	\leftarrow 2.780	\rightarrow 1.614	\leftarrow 4.035	\leftarrow 1.255	\leftarrow 0.947	0.308
2	\leftarrow 1.138	12.50*	\leftarrow 14.225	\rightarrow 1.614	\leftarrow 20.175	\leftarrow 5.950	\leftarrow 5.238	0.712
4	\leftarrow 1.363	12.82	\leftarrow 17.474	\rightarrow 1.614	\leftarrow 20.691	\leftarrow 3.217	\leftarrow 2.571	0.646
5	\leftarrow 1.531	12.70	\leftarrow 19.444	\rightarrow 1.614	\leftarrow 20.498	\leftarrow 1.054	\leftarrow 1.000	0.054

* NOMINAL RATE OF STRAIN USED HERE, AS CALIBRATED RATE OF STRAIN WAS NOT DETERMINED FOR THIS TEST

that measured immediately before the test. (Table IX)

- (ii) Comparing the two leakage measurements made after the tri-axial test (Table IX), it appears that they are different to one another, but of more or less the same order of magnitude.
- (iii) As regards the comparison of leakage measurements made under steady conditions and those derived from the test simulating the disturbed conditions of an actual tri-axial test, the values in Table X show clearly that the leakage occurring under the disturbed conditions caused by the loading spindle advancing into the test cell, is greater than even the maximum value of leakage measured at any time under steady cell conditions.

In trying to establish the causes of these experimental observations, it was necessary to examine more closely the factors affecting leakage and variations in the rate of leakage from the test cell:

Before commencement of any tri-axial test, steady conditions exist in the test cell. These conditions are maintained only by the action of the particular chamber pressure selected for the test. Any leakage occurring usually takes place from the point where the loading spindle enters the test cell. This point was greased prior to positioning the test sample in order to reduce leakage during the test as much as possible. The rate of leakage under these steady cell conditions is indicated by the leakage measurement immediately before commencement of the test.

Then the test is commenced, the advance of the loading spindle into the test cell results in an increased chamber pressure which causes a tendency for fluid flow out of the test cell, as has been previously fully discussed (Section 7.4). Simultaneously however, the volume of the test sample is reduced (initially) due to the compressive loading, which results in a reduction in the chamber pressure and hence a tendency for a resulting inflow of fluid into the test cell. The net effect may be either an increase or decrease in the chamber pressure depending on which effect is the greater, and hence, there is a consequent increase or decrease in the rate of leakage from the test cell (usually however, a decrease). As failure of the test sample is approached, the compressive loading causes an expansion of the sample, resulting in an increased chamber pressure and a tendency for fluid flow out of the test cell. The net effect then becomes a definite increase in chamber pressure giving rise to a sharp increase in the rate of leakage from the test cell. Grease conditions in the test cell are seriously disturbed at the point where the loading spindle enters the test cell and hence steady conditions again exist at the end of the test, the rate of leakage is usually higher than that which existed before the test was commenced. This means that the effect of the increased cell pressure at sample failure is usually greater than any initial reduction in cell pressure which could have occurred while the sample volume was decreasing. Hence, the phenomenon observed as mentioned in (i) above.

Following on the first leakage measurement immediately after the tri-axial test, the test for determining the leakage under disturbed cell conditions simulating those existing during an actual test was carried out. Raising the loading spindle in preparation for this test and then subsequently the advance of the loading spindle into the test cell, again disturbs the grease conditions at the point where the loading spindle enters

the/

the test cell, showing the leakage measured after this test to be different to the previous two measurements, but apparently of the same order of magnitude as the leakage measured immediately after the triaxial test. This is the phenomenon observed as mentioned in (ii) above.

Further, Table X shows clearly that the value of leakage determined from this test, is in every case greater than even the maximum value of leakage measured under steady conditions before and after this test. The reason is clearly that during the test an increased rate of leakage results due to the increased chamber pressure caused by the advance of the loading spindle. The fact that the two leakage measurements after the triaxial test generally show little agreement with the measurement carried out before the triaxial test, is due to the former two measurements not being relatively affected by any sample volume change effects.

Hence, it is also clear that the test which it was hoped would simulate the disturbed cell conditions of an actual triaxial test, was not a good representation, as it did not cater for the phenomenon of an initially reduced and then increased chamber pressure due to decrease and increase in sample volume respectively.

However, although the main problem of determining the rate of leakage under the disturbed cell conditions of an actual test has thus not been solved by the information obtained from the leakage measurements that were carried out, it is nevertheless possible, as a result of the foregoing discussion, to obtain a better understanding of the problem which is likely to enable a more reliable estimation of the rate of leakage during an actual test based on the data that was obtained.

The main conclusions from the above discussions are that:

- (i) as long as there is a flow of fluid into the test cell (which is indicated by a slug movement in the capillary tube from right to left, i.e., decreasing slug scale readings), there is a pressure deficiency in the test cell giving rise to this flow, and hence, the rate of leakage from the test cell is less than under the steady cell conditions existing immediately before the start of the test.
- (ii) Immediately the fluid flow starts to be out of the test cell (as indicated by a reversal in the direction of the slug movement in the capillary tube, i.e., increasing slug scale readings), there is a pressure excess in the test cell giving rise to this flow and hence, there is an increase in the rate of leakage from the test cell.

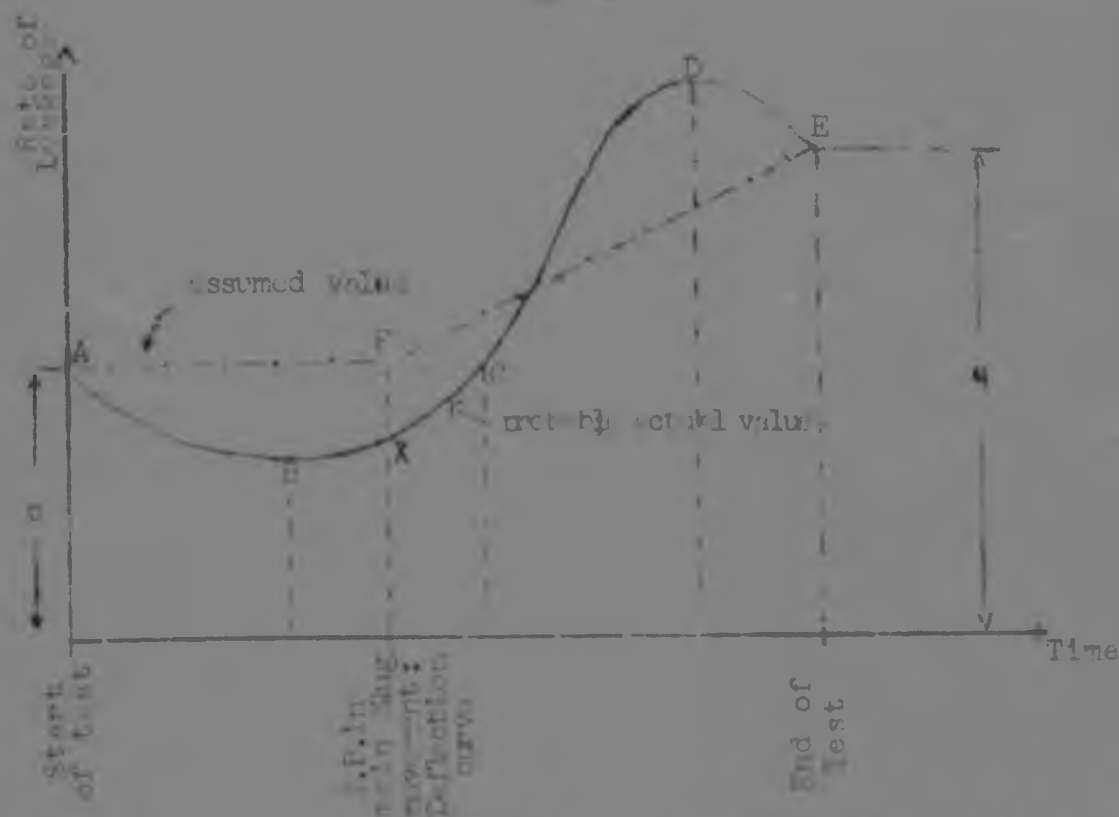
With regard to the main slug movement/reflection curves, this means that in cases over the portion of the curve to the left of the trough-shaped turning point, (i.e. the portion resulting from decreasing slug scale readings), there is a pressure deficiency in the test cell, while over the portion to the right of this turning point, (i.e. the portion resulting from increasing slug scale readings), there is a pressure excess in the test cell. This statement ignores the possible small pressure increase close to the start of the curve resulting from the small peak due to bedding-in effects, which is observed in some cases immediately before the main downward portion of the curve commences — an effect which was fully discussed in Section 7.7.

Hence, it is considered that subsequent to the rate of

leakage/

leakage existing under the steady cell conditions immediately before the start of a test, the rate of leakage varies approximately according to the relationship shown in the diagram below:

Fig. 3.1



In this diagram, p represents the measured value of the rate of leakage under steady cell conditions immediately before test, while c represents the measured value of the rate of leakage under steady cell conditions immediately after test. As soon as the test commences there is a pressure deficiency in the test cell and therefore a resulting decrease in the rate of leakage. This pressure deficiency continues, but gradually decreases as the turning point of the Main Slug Movement: Deflection curve is approached, thereby tending to restore steady pressure conditions in the test cell. At the turning point when steady conditions exist and there is neither inflow nor outflow from the test cell, the rate of leakage would probably be a value which is greater than the minimum value obtained (ordinate at B) while the pressure deficiency existed, but probably less than the value before commencement of the test (ordinates at A and C), i.e., some value between points B and D as shown (ordinate at X).

As soon as the turning point in the Main Slug Movement: Deflection curve is passed, there is a pressure excess in the test cell and hence a small increase in the rate of leakage to some maximum value as indicated by the ordinate at D. When the test is stopped, steady conditions again set in (pressure excess then reduced to zero), and the corresponding rate of leakage which is the value measured immediately after the test, is somewhat less than the maximum rate, according to actual measurements, somewhat greater than the value for the steady conditions existing immediately before test (ordinates at A and C) i.e., possibly as represented by the ordinate at E.

Hence, as an approximation to the curve ABCDE shown, it was decided to assume that the initial measured value of the rate of leakage under the steady cell conditions before test (ordinate at A), remains constant until the turning point in the Main Slug Movement: Deflection curve is reached (which is a known point with regard to time), and then to assume that the rate of leakage increases uniformly to the value measured under the steady cell conditions immediately after test. In

cases where more than one value was obtained for the rate of leakage after test (see Table IX), the maximum value was used, as it is considered that this value would be closer to the actual maximum value attained at the end of the test, which is represented by the ordinate at D.

The above procedure was followed in all calculations relating to the determination of instantaneous values of Sample Dilation ($\delta V/V$) and Poisson's Ratio (μ_i). Although the results obtained in this way may not have been strictly accurate, it is considered that they were sufficiently accurate for the purposes required, as in actual fact, the proportion of slug movement due to leakage only in the overall measured value of slug movement due to the three combined effects is small (see calculation sheets, Section 8.5). Hence, an error in the value of slug movement due to leakage only, does not cause a serious error in the value of Sample Dilation or Poisson's Ratio.

However, in order to demonstrate this fact, the calculation of Poisson's Ratio for the Selected Range of each stress:strain curve was carried out, using both the measured value of leakage under the steady cell conditions existing before test, as well as the (maximum) measured value of leakage under the steady cell conditions existing immediately after test. The results show an insignificant difference in the value of μ_i obtained (see Section 9.5).

The values of μ_i based on the value of the rate of leakage under steady cell conditions immediately before test, are considered to be more reliable, as the actual rate of leakage during test over the Selected Range corresponds closer to this value than the one relating to conditions at the end of the test. The reason for this is that the Selected Range of the stress:strain curve always falls within that range of the Main Slug Movement: Deflection curve which is to the left of its turning point, i.e., the range over which there is a pressure deficiency in the test cell. Therefore, the actual rate of leakage over the Selected Range is in each case a value which is lower than the value measured under the steady cell conditions immediately before the start of the test.

8.3 Time Effects during Test

The reduction in rate of strain during test, (the causes of which were discussed at the end of Section 7.7), has a very important bearing on the subsequent reduction of test results.

This statement is made, mainly as a result of the effect of a reduction in rate of strain on the calculated value of actual slug movement due to change in volume of the test sample only. The original intention with regard to the latter determination, was merely to combine:

- (i) whatever value of rate of leakage during test (as a slug movement in millimetres/minute) be decided on, with
- (ii) either the nominal or calibrated rate of strain (in units of divisions deflection/minute, i.e., units of 10^{-3} inches/minute), both of which were considered to be constant throughout the duration of a test.

Item (i) divided by item (ii) would give the rate of leakage from the test cell as a slug movement in millimetres/division deflection, which would then be in the same units as obtained for the calculated value of slug movement due to entry of the loading spindle into the test cell (see Appendix V, Item 2),

as well as in the same units as the measured value of total slug movement due to the three combined effects during test (Section 7.3). The subsequent combination of these three rate of slug movement values in order to determine the actual slug movement in millimetres due to volume change of the test sample only over any particular range of strain, would then present no difficulty.

If the rate of strain during test remains constant, this procedure is in order. However, leakage from the test cell is in the first instance independent of time. Hence, with the method discussed above, this determination may be seriously in error if, while the determination of rate of slug movement due to leakage only (in units of mm./div. deflection) is based on some rate of strain which is considered to be constant throughout the test, the actual rate of strain during part of the test be considerably lower than the value used. The reason for this is that, the lower the rate of strain, the greater is the proportion of actual slug movement due to leakage only in the measured value of total slug movement due to the three combined effects, the values of slug movement due to spindle entry and sample volume change only being independent of time.

Hence, it was necessary to express all measured rates of slug movement (whether they be in units of millimetres/minute or millimetres/division deflection), as actual slug movements in millimetres over the particular range of strain considered. For slug movements measured in millimetres/minute it was thus necessary to determine the actual time interval corresponding to the particular range of strain considered, in order to obtain an actual slug movement in millimetres. Hence also, the need for continuous time recordings during test mentioned in Section 7.5.

In cases where continuous time recordings during test were taken, the actual time interval corresponding to any particular range of strain could be directly obtained. In these cases it was therefore possible to evaluate Sample Dilation ($\delta V/V$) and Poisson's Ratio (μ) for each increase in strain (working from the same starting point each time - usually the corrected start of the stress:strain curve - as previously discussed in Section 7.7), and so to obtain curves of instantaneous Sample Dilation:Strain ($\delta V/V : \epsilon$) and instantaneous Poisson's Ratio : Strain ($\mu : \epsilon$).

In cases where continuous time recordings during test had not been taken, (see remarks in this respect in Section 7.1), this was not possible, and it was only possible to determine the value of Sample Dilation and Poisson's Ratio corresponding to the Selected Range of the Stress:Strain curve in each case. To enable even these determinations, it was necessary to estimate the value of the actual rate of strain over the Selected Range, in order to obtain the time interval corresponding to the duration of the Selected Range. The basis on which this estimate could be made, is discussed in the following paragraphs.

Careful investigation of the deflection:time curves for the tests in which detailed time recordings were taken (Nos. 1, 3, 4 and 6), revealed the facts shown in Table XI on the following page:

TABLE XI/

as well as in the same units as the measured value of total slug movement due to the three combined effects during test (Section 7.3). The subsequent combination of these three rate of slug movement values in order to determine the actual slug movement in millimetres due to volume change of the test sample only over any particular range of strain, would then present no difficulty.

If the rate of strain during test remains constant, this procedure is in order. However, leakage from the test cell is in the first instance dependent on time. Hence, with the method discussed above, this determination may be seriously in error if, while the determination of rate of slug movement due to leakage only (in units of mm./div. deflection) be based on some rate of strain which is considered to be constant throughout the test, the actual rate of strain during part of the test be considerably lower than the value used. The reason for this is that, the lower the rate of strain, the greater is the proportion of actual slug movement due to leakage only in the measured value of total slug movement due to the three combined effects, the values of slug movement due to spindle entry and sample volume change only being independent of time.

Hence, it was necessary to express all measured rates of slug movement (whether they be in units of millimetres/minute or millimetres/division deflection), as actual slug movements in millimetres over the particular range of strain considered. For slug movements measured in millimetres/minute it was thus necessary to determine the actual time interval corresponding to the particular range of strain considered, in order to obtain an actual slug movement in millimetres. Hence also, the need for continuous time recordings during test mentioned in Section 7.5.

In cases where continuous time recordings during test were taken, the actual time interval corresponding to any particular range of strain could be directly obtained. In these cases it was therefore possible to evaluate Sample Dilation ($\delta V/V$) and Poisson's Ratio (μ) for each increase in strain (working from the same starting point each time - usually the corrected start of the stress:strain curve as previously discussed in Section 7.7), and so to obtain curves of instantaneous Sample Dilation:Strain ($\delta V/V : \epsilon$) and instantaneous Poisson's Ratio : Strain ($\mu : \epsilon$).

In cases where continuous time recordings during test had not been taken, (see remarks in this respect in Section 7.5), this was not possible, and it was only possible to determine the value of Sample Dilation and Poisson's Ratio corresponding to the Selected Range of the Stress:Strain curve in each case. To enable even these determinations, it was necessary to estimate the value of the actual rate of strain over the Selected Range, in order to obtain the time interval corresponding to the duration of the Selected Range. The basis on which this estimate could be made, is discussed in the following paragraphs.

Careful investigation of the duration:time curves for the tests in which detailed time recordings were taken (Nos. 1, 3, 4 and 6), revealed the facts shown in Table XI on the following page:

TABLE XI/

TABLE XI

Test No.	RATE OF STRAIN		AVERAGE RATE OF STRAIN DURING TEST OVER SELECTED RANGE (=a) inch/min.	REDUCTION IN RATE OF STRAIN OVER SELECTED RANGE (=b/a) percent	REMARKS
	NOMINAL inch/min.	CALIBRATED(=a) inch/min.			
1	0.00256	0.001551	0.000933	36.5%	Selected Range for each test includes the pronounced time-lag effects soon after test commencement.
3	0.00256	0.001414	0.000905	31.8%	
6	0.00256	0.002500	0.000903	36.2%	
4	0.01250	0.012500	0.004000	31.2%	
				$\bar{a}=33.9$	

It was also observed that the Selected Range for each of the four tests listed above, included the range over which the pronounced time-lag effects occurred (discussed in Section 7.7). In the case of the two tests during which continuous time recordings had not been taken (Tests No. 2 and 5), the strain at which the pronounced time-lag effects commenced had been noted down during the original test observations, and hence it was known that their Selected Ranges (as chosen), also included these effects.

It therefore seemed reasonable to conclude that approximately the same reduction in rate of strain had occurred over their respective Selected Ranges, as was found to be the case with Tests No. 1, 3, 4 and 6. As the latter tests had shown an average reduction in rate of strain over their Selected Ranges of 33.9% (calculated with respect to the calibrated rate of strain in each case) with very little variation among individual values, it was decided to adopt a value of 33% of the calibrated rate of strain, or, where this was not available, simply 33% of the nominal rate of strain, as the actual rate of strain during test over the Selected Range for the two tests concerned.

8.4 Initial Volume of test samples

Under this heading, a clear definition is in the first instance considered to be essential. By initial volume of test samples is meant the volume of test samples as at the commencement of the actual triaxial test, i.e., the sample volume corresponding to zero strain. It is this volume, relative to which all subsequent sample volume changes during test are considered to occur, and hence, it is this volume which is required for substitution in equation 7.6 for the evaluation of Poisson's Ratio.

In approaching the problem of determining this volume, the two factors which have a direct bearing on the initial volume of test samples, need to be considered in detail. These are:

- (i) The volume of a test sample after being extruded from the cutting cylinder. (Let this volume be denoted V_1).
- (ii) the subsequent change in this volume V_1 due to consolidation of the sample in the triaxial cell during the pre-shear condition. Let the volume at the completion of the consolidation process be denoted V_2 .

With regard to item (i) above: It was previously mentioned that the test soil was a rather dry sandy soil, so that in

sliding/

TABLE XI

Test No.	RATE OF STRAIN		AVERAGE RATE OF STRAIN DURING TEST OVER SELECTED RANGE (=b) inch/min.	REDUCTION IN RATE OF STRAIN OVER SELECTED RANGE (=b/a) percent	REMARKS
	NOMINAL inch/min.	CALIBRATED(=c) inch/min.			
1	0.00250	0.002555	0.000933	36.5%	Selected Range for each test includes the pronounced time-lag effects soon after test commencement.
3	0.00250	0.002544	0.000909	31.7%	
6	0.00256	0.002500	0.000903	36.2%	
4	0.01250	0.01282	0.004000	31.8%	
				$\bar{a}=33.9$	

It was also observed that the Selected Range for each of the four tests listed above, included the range over which the pronounced time-lag effects occurred (discussed in Section 7.7). In the case of the two tests during which continuous time recordings had not been taken (Tests No. 2 and 5), the strain at which the pronounced time-lag effects commenced had been noted down during the original test observations, and hence it was known that their Selected Ranges (as chosen), also included these effects.

It therefore seemed reasonable to conclude that approximately the same reduction in rate of strain had occurred over their respective Selected Ranges, as was found to be the case with Tests No. 1, 3, 4 and 6. As the latter tests had shown an average reduction in rate of strain over their Selected Ranges of 33.9% (calculated with respect to the calibrated rate of strain in each case) with very little variation among individual values, it was decided to adopt a value of 33% of the calibrated rate of strain, or, where this was not available, simply 33% of the nominal rate of strain, as the actual rate of strain during test over the Selected Range for the two tests concerned.

8.4 Initial Volume of test samples

Under this heading, a clear definition is in the first instance considered to be essential. By initial volume of test samples is meant the volume of test samples as at the commencement of the actual triaxial test, i.e., the sample volume corresponding to zero strain. It is this volume, relative to which all subsequent sample volume changes during test are considered to occur, and hence, it is this volume which is required for substitution in equation 7.8 for the evaluation of Poisson's Ratio.

In approaching the problem of determining this volume, the two factors which have a direct bearing on the initial volume of test samples, need to be considered in detail. These are:

- (i) The volume of a test sample after being extruded from the cutting cylinder. (Let this volume be denoted V_1).
- (ii) the subsequent change in this volume V_1 due to consolidation of the sample in the triaxial cell during the pre-shear condition. Let the volume at the completion of the consolidation process be denoted V_2 .

With regard to item (i) above: It was previously mentioned that the test soil was a rather dry sandy soil, so that in

sliding/

sliding the cutting cylinder downwards while trimming a test sample end, subsequently, when extruding the test sample from the cutting cylinder, a thin layer of soil viz. that which was previously in contact with the inside face of the cutting cylinder, is loosened from the test sample and is lost. Therefore, the final sample diameter is slightly less than the actual inside diameter of the cutting cylinder and hence, the final sample volume is slightly less than the internal volume of the cutting cylinder.

Regarding item (ii): The consolidation process in the triaxial test cell which test samples are subjected to during the pre-shear condition, is a 3-dimensional effect. As yet, the change in volume of a test sample during this type of consolidation process can only be evaluated with difficulty for the case of saturated samples, but cannot be evaluated in the case of partially saturated samples such as is the case with the test samples being considered.

Thus, as both the quantities concerned cannot be readily evaluated (if at all), it is necessary to consider what arbitrary reduction in the internal volume of the cutting cylinder should be allowed in order to obtain the initial volume of a test sample. Further, as the same cutting cylinder was used throughout for trimming the test samples, it will also be assumed that the initial volume of all test samples was the same throughout.

The internal dimensions of the cutting cylinder were $1\frac{1}{2}$ " dia. x 3" length, thus giving a volume of 86.89 cub.cm. Assuming that on removal from the cutting cylinder a sample is $\frac{1}{64}$ " short in diameter, i.e. only $1\frac{31}{64}$ " in diameter, its volume would be 85.09 cub.cm., thus a reduction of 1.80 cc. As regards the additional decrease in volume due to the consolidation process during the pre-shear condition, it is considered that this reduction, as effected by the chamber pressures used viz. 10lb/sq.in., 20lb/sq.in. and 30lb/sq.in., could not have been appreciable, since, from the normal 1-dimensional consolidation test which was conducted (Section 7.5), the test soil was found to be fairly heavily preconsolidated (p_c approx. 8Ton/sq.ft. - see Fig.18), with an undisturbed compression index value of 0.26.

On the basis of this information, it was decided to adopt a value of 88.0 cub.cm. as the initial volume of all test samples used for the test series. It is considered that a slight error in this value is not likely to cause a serious error in the value of Sample Dilatation ($\Delta V/V$) or Poisson's Ratio subsequently determined.

8.5 Calculation of Poisson's Ratio

On the following pages in this Section, the calculation of Poisson's Ratio for each test has been set out in tabular form; in the first instance, the calculation of Poisson's Ratio as obtained from the selected range of each stress:strain curve (giving a value denoted by μ_{sel}), and secondly, the calculation of instantaneous values of Poisson's Ratio (denoted μ_t) for each increase in strain along the stress:strain curve, but always working from the corrected start of the curve (i.e. bedding-in effects ignored).

In both cases the calculations follow along the same lines, which are broadly as follows for each particular range of strain considered:

(1) Determination of the time elapsed over the range considered.

(ii) Determination /

- (ii) Determination of the slug movement (in mm.) due to leakage only.
- (iii) Determination of the slug movement (in mm.) due to entry of the loading spindle into the test cell - using the rate of slug movement due to spindle entry determined as shown in Appendix V, Item 2.
- (iv) Determination of the slug movement (in mm.) due to change in volume of the test sample only, by combining (ii) and (iii) above with the measured total slug movement due to the three combined effects during test.
- (v) Determination of the change in volume of the test sample (δV) in units of 10^{-3} cub.cm. - using the value of the cross-sectional area of the capillary tube employed during the test series which was determined as shown in Appendix V, Item 1.
- (vi) Calculation of the Sample Dilation ($\delta V/V$) - using the initial volume of test samples as 55.0cc. According to the discussion in Section 8.4.
- (vii) Calculation of Poisson's Ratio based on equation 7.5 and using the relevant value of Young's Modulus (i.e. either the particular instantaneous or Esel value) as well as the relevant change in deviator stress value.

More specifically, however, the first calculations appearing are those for μ_i . The calculations are accommodated in 3 pages and, for each test, deal with the various steps in the following order:

- First page: Determination of data relevant to the Selected Range of each test only, viz.: the value of Young's Modulus (Esel); the change in deflection (strain; the nett slug movement due to the three combined effects; and the time elapsed over the Selected Range.
- Second page: Items (i) to (vi) inclusive, as detailed above.
- Third page: Item (vii) above.

Then follow the calculations for μ_i . As previously discussed (Section 8.3), it was only possible to determine μ_i for tests in which continuous time recordings during test had been carried out, i.e. Tests No. 1, 3, 4 and 6. The calculations in this case are more lengthy and occupy several pages. On the first calculation pages for each test, the items (i) to (vi) inclusive appear in columns all on one page for each increase in strain being considered. On the subsequent pages, item (vii) is set out in a similar manner, using the instantaneous values of Young's Modulus shown calculated in Section 7.6. The calculation of values of μ_i was in each case not continued very far past the end of the linear range of the stress:strain curve, and particularly not past the peak, as actually Poisson's Ratio becomes a doubtful concept once the limit of the linear range has been exceeded (See Chapter 2). However, the calculation of values of Sample Dilation ($\delta V/V$) were continued over the full range of each test.

For the results of all these calculations, it was possible to prepare curves of instantaneous Sample Dilation : Strain and instantaneous Poisson's Ratio : Strain as mentioned in Section 8.3. These curves are presented in each case subsequent to the μ_i calculation sheets and are shown plotted below the relevant stress:strain curve (bedding-in effects ignored) for each test.

The/

The following more detailed points about the calculations should, however, be noted:

An arrow above figures relating to slug movement should be interpreted in accordance with the meaning given at the head of Table IX, Section 8.2. In the case of the calculations pertaining to μ_{sl} , such arrows have been omitted, and instead, algebraic signs have been inserted in front of these figures. These algebraic signs merely serve to indicate how the figures have been combined in determining the slug movement due to change in volume of the test sample only (item (iv) on the previous page), and were arrived at as follows:

- (a) Slug movement due to leakage from the test cell is from right to left in the capillary tube - denoted \leftarrow
- (b) Slug movement due to entry of the loading spindle into the test cell is from left to right in the capillary tube - denoted \rightarrow
- (c) Slug movement due to the combined effects of leakage, spindle entry and sample volume change, is from right to left generally (i.e. over the main portion of the Main Slug Movement : Deflection curve), and is denoted \leftarrow in these cases.

Thus, numerically: $(b) + (c) - (a) = M$, say,

gives the slug movement due to change in volume of the test sample only.

In cases where the slug movement (c) above is from left to right (such as sometimes happens at the start of tests), the relevant figure for item (c) has been given a negative sign.

A positive value for M denotes that the slug movement due to change in volume of the test sample only is from right to left in the capillary tube, i.e., the sample has experienced a volume decrease. Hence, also, a sample volume decrease yields a positive value for the Sample Dilatation $\delta V/V$, which is thus in accordance with the sign convention adopted as discussed in Section 7.1.

YOUNG'S MODULUS, SLUG MOVEMENT AND TIME CALCS. BASED ON THE SELECTED RANGE OF EACH STRESS-STRAIN CURVE.

TEST NO.	STRAIN (%)			DEVIATOR STRESS (σ_d)			YOUNG'S MODULUS (E_{sec})	CORRECTED DEFLECTION			CORRECTED SLUG SCALE			ELAPSED TIME			DIFFERENCE TIME ELAPSED OVER SELECTED RANGE
	AT START OF SELECTED RANGE	AT END OF SELECTED RANGE	DIFFERENCE = ΔE CHANGE IN STRAIN OVER SELECTED RANGE	AT START OF SELECTED RANGE	AT END OF SELECTED RANGE	DIFFERENCE = $\Delta \sigma_d$ CHANGE IN STRESS OVER SELECTED RANGE		AT START OF SELECTED RANGE	AT END OF SELECTED RANGE	DIFFERENCE = Δd IN REFLECTION OVER SELECTED RANGE	AT START OF SELECTED RANGE	AT END OF SELECTED RANGE	DIFFERENCE = ΔP = DIFF. SLUG MOVEMENT DUE TO EFFECTS OVER SELECTED RANGE	AT START OF SELECTED RANGE	AT END OF SELECTED RANGE	ELAPSED TIME IN MIN. SEC.	
1	0.033	0.467	0.433	2.54	37.25	34.71	8015	1	14	13	0	-125.25	-125.25	00 ^m 27 ^s	14 ^m 23 ^s		13 ^m 56 ^s
3	0.200	0.467	0.267	7.34	27.89	20.55	7697	6	14	8	-120.00	-96.50	-84.50	03 ^m 15 ^s	13 ^m 08 ^s		9 ^m 53 ^s
4	0.583	0.917	0.333	7.86	39.75	31.89	6567	17.5	27.5	10	+17.00	-51.50	-68.50	01 ^m 40 ^s	04 ^m 10 ^s		2 ^m 30 ^s
6	0.233	0.633	0.400	6.76	39.25	32.49	8125	7	19	12	-12.00	-126.00	-114.00	04 ^m 06 ^s	17 ^m 22 ^s		13 ^m 16 ^s
7	0.333	0.583	0.250	5.00	23.03	18.03	7212	10	17.5	7.5	+11.00	-54.00	-65.00	CALIBRATED RATE OF STRAIN = C inches/minute	ESTIMATED RATE OF STRAIN DURING TEST OVER SELECTED RANGE C = 0.553%/min inches/minute	AVERAGE ELAPSED TIME OVER SELECTED RANGE minutes	1.77 ^m
	0.250	0.667	0.417	8.00	40.29	32.29	7750	7.5	20	12.5	+2.00	-109.50	-111.50				

* NOMINAL RATE OF STRAIN

CALCULATION OF SAMPLE DILATION (ΔV) BASED ON THE SELECTED RANGE OF EACH STRESS-STRAIN CURVE*

TEST NUMBER	TIME ELAPSED OVER SELECTED RANGE		RATE OF SLUG MOVEMENT DUE TO LEAKAGE ONLY $\frac{cm}{min}$	RATE OF SLUG MOVEMENT OVER SELECTED RANGE DUE TO SPINDLE ENTRY ONLY $\frac{cm}{min}$	NUMBER OF DEFLECTIONS OVER RANGE CONSIDERED	HENCE SLUG MOVEMENT OVER RANGE DUE TO SPINDLE ENTRY ONLY $\frac{mm}{min}$	% ALL MEASURED SLUG MOVEMENT OVER RANGE DUE TO SPINDLE ENTRY THREE COMBINED EFFECTS $\frac{mm}{min}$	HENCE SLUG MOVEMENT DUE TO SPINDLE ENTRY ONLY $\frac{mm}{min}$	CROSS SECTIONAL AREA OF CAPILLARY TUBE $sq. mm$	HENCE CHANGE IN VOLUME ΔV OF SAMPLE OVER RANGE OF STRAIN CONSIDERED cc	INITIAL SAMPLE VOLUME V cc	SAMPLE DILATION $\frac{\Delta V}{V}$ units of 10^{-3}
	MIN	SEC										
1.	13	56	0.92 2.80	12.818 39.012	13	20.98 1614	125.25 1614	133.614 107.220	1.9935	265.96 213.74	85.0	3.13 2.51
2.	3	00	1.27 4.00	3.810 12.000	12.5	20.175 1614	111.50 1614	127.865 119.675	1.9935	254.90 198.57	85.0	3.00 2.31
3.	9	53	1.54 2.667	15.220 26.355	8	12.912 1614	84.50 1614	82.192 71.057	1.9935	163.85 141.65	85.0	1.93 1.67
4.	2	30	0.875 2.000	2.187 5.000	10	16.140 1614	68.50 1614	82.433 79.640	1.9935	164.37 158.76	85.0	1.93 1.87
5.	1	46	0.500 1.000	0.885 1.770	7.5	12.105 1614	65.00 1614	76.220 75.335	1.9935	151.94 150.18	85.0	1.79 1.77
6.	13	16	0.875 0.947	11.60 12.564	12	19.368 1614	114.00 1614	121.750 120.804	1.9935	242.73 240.82	85.0	2.86 2.83

*NOTE WHERE TWO SETS OF FIGURES ARE SHOWN (ONE BELOW THE OTHER), THESE ARE INTENDED FOR COMPARISON PURPOSES.

THE UPPER FIGURES CORRESPOND TO CALC. BASED ON THE RATE OF SLUG MOVEMENT DUE TO LEAKAGE ONLY MEASURED IMMEDIATELY BEFORE TEST

THE LOWER FIGURES CORRESPOND TO CALC. BASED ON THE RATE OF SLUG MOVEMENT DUE TO LEAKAGE ONLY MEASURED IMMEDIATELY AFTER TEST

THE UPPER FIGURES ARE CONSIDERED TO LEAD TO MORE RELIABLE VALUES OF SAMPLE DILATION ($\frac{\Delta V}{V}$) AND POISSONS RATIO (μ)

CALCULATION OF POISSONS' RATIO (μ) BASED ON THE SELECTED RANGE OF EACH STRESS-STRAIN CURVE*

TEST NUMBER	SAMPLE DILATION $\frac{\Delta V}{V}$ units of 10^{-3}	YOUNG'S MODULUS E_{sel} lb./sq. in.	$\frac{\Delta V}{V} \times E_{sel}$ lb./sq. in.	CHANGE IN DEVIATOR STRESS ($\Delta\sigma_d$) $[E \Delta(\epsilon_1 - \epsilon_2)]$ OVER SELECTED RANGE lb./sq. in.	$\frac{\frac{\Delta V}{V} \times E_{sel}}{\Delta\sigma_d} = \mu$	$1 - \mu$	POISSONS' RATIO (μ_{sel}) $= \frac{1}{2} [1 - \mu]$
1	3.13 2.31	8015	25.079 20.155	34.71	0.7225 0.5807	0.2775 0.4193	0.1367 0.2097
2	3.00 2.81	7750	23.241 21.752	32.29	0.7196 0.6736	0.2802 0.3264	0.1401 0.1632
3	1.93 1.67	7697	14.637 12.827	20.55	0.7220 0.6242	0.2780 0.3758	0.1390 0.1679
4	1.93 1.67	9567	18.500 17.669	31.89	0.5801 0.5605	0.4199 0.439	0.2099 0.2198
5	1.79 1.77	7212	12.892 12.742	18.03	0.7150 0.7067	0.2850 0.2933	0.1425 0.1466
6	2.66 2.83	8125	23.202 23.020	32.49	0.7141 0.7085	0.2859 0.2915	0.1429 0.1457

* SEE FOOTNOTE ON THE PREVIOUS PAGE

TEST No 1 : CALCULATION OF INSTANTANEOUS VALUES OF POISSONS RATIO (2)

RANGE OF STRAIN CONSIDERED	SAMPLE DILATION $\frac{\Delta V}{V}$	YOUNG'S MODULUS E	$\frac{\Delta V}{V} \times E$	CHANGE IN DEVIATOR STRESS (DEVI) OVER RANGE CONSIDERED	$\frac{\Delta V}{V} \times E$	POISSONS' RATIO (μ_1)
0.000 - 0.035	0.75	7895	0.2309	2.84	0.0909	0.4591
0.035 - 0.097	0.08	8513	0.3716	1.20	0.1998	0.4552
0.097 - 0.100	0.17	6770	1.1109	6.77	0.1710	0.4500
0.100 - 0.133	0.48	7549	1.7632	10.04	0.1609	0.4591
0.133 - 0.167	0.73	8383	6.1136	14.00	0.4351	0.4510
0.167 - 0.200	1.06	8400	6.8040	16.80	0.5300	0.4530
0.200 - 0.233	1.30	8442	11.0357	19.78	0.4579	0.4510
0.233 - 0.267	1.46	8401	13.1056	20.43	0.5843	0.4576
0.267 - 0.300	1.83	8410	11.3902	23.23	0.6100	0.4550
0.300 - 0.333	2.09	8298	17.3219	27.60	0.6276	0.4580
0.333 - 0.367	2.35	8161	19.1784	29.95	0.6403	0.4598
0.367 - 0.400	2.53	8160	21.4650	32.64	0.6575	0.4512
0.400 - 0.433	2.88	8442	23.1610	34.82	0.6652	0.4574
0.433 - 0.467	3.16	8472	25.1511	37.23	0.6766	0.4517
0.467 - 0.500	3.42	8418	26.9744	38.29	0.6840	0.4550

TEST NO 1 CALCULATION OF INSTANTANEOUS VALUES OF POISSONS RATIO(%) (Con)

RANGE OF STRAIN CONSIDERED	SAMPLE DILATION $\frac{\Delta V}{V}$	YOUNG'S MODULUS E	$\frac{\Delta V}{V} \times E$	CHANGE IN DEVIATOR STRESS(20.4) OVER RANGE CONSIDERED	$\frac{\Delta V \times E}{20.4}$	POISSONS RATIO (%) $\mu [1 - \mu]$
0.000 - 0.005	3.00	7770	13.5187	47.53	0.2857	0.1700
0.000 - 0.007	3.91	7838	29.7403	43.20	0.6896	0.2550
0.000 - 0.008	4.16	7883	31.6133	45.39	0.6984	0.1417
0.000 - 0.008	4.43	7450	33.0032	47.16	0.6998	0.1601
0.000 - 0.007	4.60	7314	33.8224	46.80	0.6896	0.1682
0.000 - 0.000	4.90	7221	36.5700	50.53	0.7250	0.1600
0.000 - 0.000	5.01	6999	39.5644	48.30	0.7018	0.1434
0.000 - 0.000	5.87	6669	41.9140	40.00	0.6167	0.1710
0.000 - 1.000	6.40	6182	43.7805	33.70	0.6270	0.1570
0.000 - 1.000	7.39	5481	40.4702	70.33	0.6034	0.1933
0.000 - 1.400	8.56	5364	46.4000	76.00	0.6054	0.1971
0.000 - 1.400	9.10	4464	40.9000	79.11	0.6037	0.2032
0.000 - 1.000	10.15	4480	40.7000	87.41	0.4610	0.2192
0.000 - 1.000	10.00	4250	40.7000	80.74	0.5010	0.2145

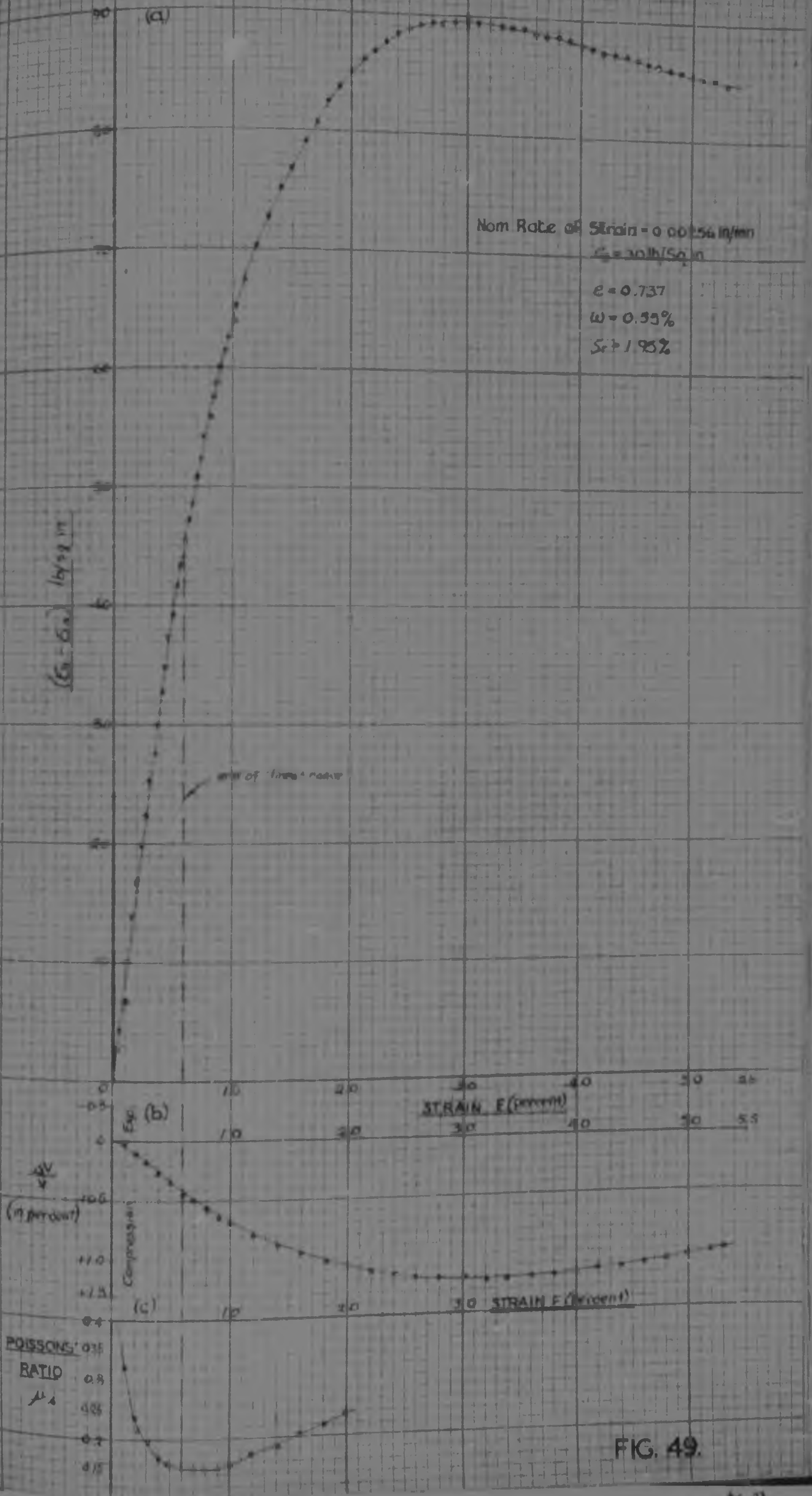


FIG. 49.

TEST NO'S : CALCULATION OF INSTANTANEOUS VALUES OF SAMPLE DILATION ($\frac{\Delta V}{V}$)

RANGE OF STRAIN CONSIDERED	TIME ELAPSED SINCE SAMPLE CONSIDERED	RATE OF SLUG MOVEMENT DUE TO LEAKAGE ONLY	RATE OF SLUG MOVEMENT DUE TO LEAKAGE ONLY	RATE OF SLUG MOVEMENT DUE TO LEAKAGE ONLY	OBSERVED SLUG MOVEMENT OVER RANGE DUE TO THREE COMBINED EFFECTS	HENCE SLUG MOVEMENT DUE TO SAMPLE COMPRESSION ONLY OVER RANGE CONSIDERED	CORRECTION-AL AREA OF CAPILLARY TUBE	HENCE CHANGE IN VOL. (ΔV) OF SAMPLE OVER RANGE OF STRAIN CONSIDERED	INITIAL SAMPLE VOLUME V	SAMPLE DILATION $\frac{\Delta V}{V}$
		mm/sec	mm/min	mm/hr	mm/hr	mm/hr	sq mm	ccm (10 ⁻⁶ cc)	ccm	ratio of 10 ⁻⁴
0.000 - 0.167	02 35	2.583	1.54	- 3.278	1.614	5 + 0.070 + 5.00	1.9935	18.12	85.0	0.21
0.000 - 0.200	03 15	3.250	1.54	- 5.005	1.614	6 + 9.604 + 12.00	1.9935	35.25	85.0	0.41
0.000 - 0.333	05 07	8.117	1.54	- 12.500	1.614	7 + 11.099 + 25.50	1.9935	49.44	85.0	0.57
0.000 - 0.367	11 19	11.317	1.54	- 17.450	1.614	11 + 17.734 + 44.00	1.9935	120.03	85.0	1.41
0.000 - 0.400	11 57	11.950	1.54	- 19.403	1.614	12 + 19.360 + 76.00	1.9935	140.45	85.0	1.60
0.000 - 0.467	13 08	13.133	1.54	- 20.225	1.614	14 + 22.595 + 96.00	1.9935	177.10	85.0	2.12
0.000 - 0.500	13 41	13.983	1.54	- 21.072	1.614	15 + 24.010 + 100.00	1.9935	217.27	85.0	2.56
0.000 - 0.567	14 46	14.767	1.54	- 22.741	1.614	17 + 27.418 + 125.00	1.9935	240.40	85.0	2.84
0.000 - 0.700	16 57	16.480	1.54	- 26.103	1.614	21 + 33.934 + 158.00	1.9935	330.50	85.0	3.89
0.000 - 0.933	19 00	19.500	1.54	- 29.260	1.614	22 + 40.350 + 197.50	1.9935	395.29	85.0	4.66
0.000 - 1.000	21 24	21.400	1.54	- 32.986	1.614	30 + 49.420 + 218.25	1.9935	457.23	85.0	5.41
0.000 - 1.167	23 41	23.683	1.54	- 36.472	1.614	35 + 56.440 + 234.00	1.9935	506.35	85.0	5.96
0.000 - 1.333	25 51	25.750	1.54	- 39.009	1.614	40 + 64.560 + 247.75	1.9935	543.03	85.0	6.39
0.000 - 1.500	27 51	27.250	1.54	- 42.499	1.614	45 + 73.730 + 268.50	1.9935	570.62	85.0	6.71
0.000 - 1.667	29 57	29.210	1.54	- 46.103	1.614	50 + 80.730 + 281.75	1.9935	600.73	85.0	7.06

TEST No. 3 CALCULATION OF INSTANTANEOUS VALUES OF SAMPLE DILATION (A_v) (Cont.)

RANGE OF STRAIN CONSIDERED	TIME ELAPSED OVER RANGE CONSIDERED		RATE OF SLUG MOVEMENT OVER RANGE CONSIDERED DUE TO LEAKAGE ONLY		RATE OF SLUG MOVEMENT OVER RANGE CONSIDERED DUE TO SPINDLE ENTRY ONLY		DETERMINED SLUG MOVEMENT OVER RANGE CONSIDERED DUE TO THREE COMBINED EFFECTS		HENCE SLUG MOVEMENT DUE TO SAMPLE COMPRESSION ONLY OVER RANGE CONSIDERED		CROSS SECTIONAL AREA OF CAPILLARY TUBE		HENCE CHANGE IN VOL. (ΔV) OF SAMPLE OVER RANGE OF STRAIN CONSIDERED		INITIAL SAMPLE VOLUME V		SAMPLE DILATION $\frac{\Delta V}{V}$	
	min	sec	min	sec	min	sec	min	sec	min	sec	Sq. mm	Sq. mm	cc/mm	(cc)	cc/mm	cc	units of 10 ⁻³	
0.000 - 5.000	60	22	52.387	2.21	155.301	1.614	150	+ 242.100	+ 190.75	+ 285.549	1.9935	569.24	88.0	8.70				
0.000 - 5.167	71	17	71.553	2.82	- 160.387	1.614	155	+ 250.170	+ 191.25	+ 261.033	1.9935	560.24	88.0	8.59				
0.000 - 5.333	73	17	73.233	2.89	- 167.818	1.614	160	+ 258.240	+ 193.60	+ 275.922	1.9935	550.05	88.0	8.47				
0.000 - 5.500	75	13	75.217	2.32	- 174.503	1.614	165	+ 265.305	+ 179.75	+ 271.852	1.9935	541.34	88.0	8.39				
0.000 - 5.667	77	11	77.283	2.36	- 182.152	1.614	170	+ 274.370	+ 173.75	+ 265.965	1.9935	530.31	88.0	8.24				
0.000 - 5.833	79	11	79.153	2.40	- 190.039	1.614	175	+ 282.435	+ 166.75	+ 259.146	1.9935	516.61	88.0	8.09				
0.000 - 6.000	81	04	81.067	2.44	- 197.603	1.614	180	+ 290.500	+ 160.75	+ 243.447	1.9935	502.22	88.0	8.04				
0.000 - 6.167	83	00	83.000	2.48	- 205.940	1.614	185	+ 298.565	+ 154.00	+ 246.785	1.9935	491.85	88.0	8.79				
0.000 - 6.333	84	56	84.833	2.32	- 214.031	1.614	190	+ 306.630	+ 147.00	+ 240.569	1.9935	479.63	88.0	8.64				
0.000 - 6.500	86	51	86.450	2.56	- 222.336	1.614	195	+ 314.695	+ 141.75	+ 234.109	1.9935	466.70	88.0	8.49				
0.000 - 7.000	92	38	92.833	2.67	- 247.330	1.614	210	+ 338.890	+ 125.75	+ 215.310	1.9935	429.22	88.0	8.05				

TEST NO. 3. CALCULATION OF INSTANTANEOUS VALUES OF POISSON'S RATIO (%)

RANGE OF STRESS CONSIDERED	SAMPLE DILATION $\frac{\Delta V}{V}$	FOUND MODULUS E	$\frac{\Delta V}{V} \times E$	CHANGE IN DEVIATION STRESS (psi) $= \Delta(\sigma - \sigma_0)$ OVER RANGE CONSIDERED	$\frac{\Delta V \times E}{V \times \Delta \sigma}$	POISSON'S RATIO μ
0.100 - 0.100	0.39	7340	2.8712	7.23	0.2312	0.0000
0.100 - 0.253	0.57	7737	4.4101	10.20	0.4282	0.0457
0.100 - 0.367	1.51	7865	11.8722	21.80	0.5407	0.0712
0.100 - 0.400	1.80	7800	14.1480	24.80	0.3100	0.0000
0.100 - 0.400	2.30	7509	17.8257	24.34	0.7310	0.1741
0.100 - 0.500	2.55	7478	19.1437	22.91	0.8300	0.1800
0.100 - 0.567	3.01	7540	22.0157	21.80	0.8320	0.1740
0.100 - 0.700	3.89	6770	26.5337	20.80	0.8483	0.1718
0.100 - 0.850	4.70	6344	29.8250	16.50	0.6556	0.1401
0.100 - 1.000	5.41	5767	31.1931	11.90	0.5011	0.1003
0.100 - 1.167	5.20	5217	31.7332	11.67	0.6209	0.0900
0.100 - 1.353	6.34	4700	30.8500	17.30	1.1163	0.1400
0.100 - 1.500	6.71	6246	39.8450	19.41	0.4793	0.0804
0.100 - 1.600	6.98	3871	26.8030	10.00	0.4435	0.0700

- 144 -
TEST NO 3.

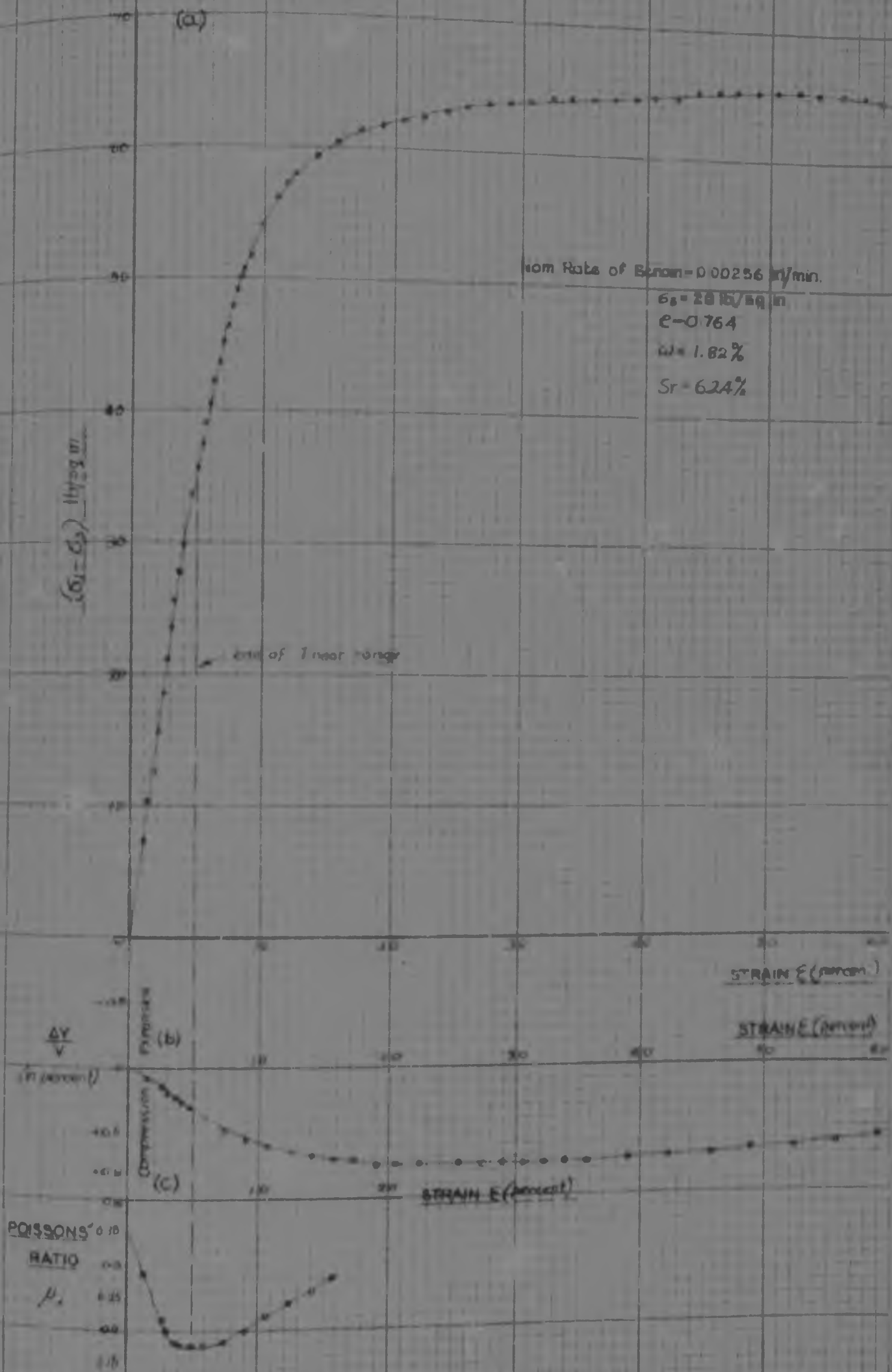


FIG. 50

TEST No. 1: CALCULATION OF INSTANTANEOUS VALUES OF SAMPLE DILATION ($\Delta V/V$)

RANGE OF STRAIN CONSIDERED	TIME ELAPSED SINCE RANGE CONSIDERED	RATE OF SLUG MOVEMENT DUE TO LEAKAGE ONLY	RATE OF SLUG MOVEMENT DUE TO LEAKAGE ONLY	RATE OF SLUG MOVEMENT DUE TO LEAKAGE ONLY	NUMBER OF SLUGS MOVED OVER RANGE	OBSERVED SLUG MOVEMENT OVER RANGE	HENCE SLUG MOVEMENT DUE TO SAMPLE COMPRESSION ONLY OVER RANGE CONSIDERED	CROSS SECTIONAL AREA OF CAPILLARY TUBE	PERCENT CHANGE IN VOL. ($\Delta V/V$) OF SAMPLE OVER RANGE OF STRAIN CONSIDERED	INITIAL SAMPLE VOLUME V	SAMPLE DILATION $\Delta V/V$
		mm/hr	mm/hr	mm/hr	mm/hr	mm/hr	mm/hr	sq. cm	cc	cc	cc
0.000 - 0.033	00 24	0.400	0.875 - 0.350	1.614	2.5	4.035	- 2.78	1.9935	1.66	85.0	0.09
0.033 - 0.167	00 37	0.617	0.875 - 0.246	1.614	5.0	8.070	- 9.36	1.9935	1.66	85.0	0.01
0.167 - 0.250	00 45	0.750	0.875 - 0.456	1.614	7.5	12.105	- 9.00	1.9935	4.85	85.0	0.06
0.250 - 0.333	00 56	0.913	0.875 - 0.516	1.614	10.0	16.140	- 12.00	1.9935	6.63	85.0	0.08
0.333 - 0.417	01 07	1.117	0.875 - 0.577	1.614	12.5	20.175	- 14.95	1.9935	9.86	85.0	0.13
0.417 - 0.500	01 24	1.400	0.875 - 1.225	1.614	15.0	24.210	- 16.50	1.9935	12.93	85.0	0.18
0.500 - 0.583	01 40	1.667	0.875 - 1.459	1.614	17.5	28.245	- 17.00	1.9935	19.51	85.0	0.23
0.583 - 0.667	03 07	3.117	0.875 - 1.727	1.614	20.0	32.280	- 7.80	1.9935	41.96	85.0	0.62
0.667 - 0.750	03 36	3.600	0.875 - 3.062	1.614	22.5	36.315	+ 13.00	1.9935	92.00	85.0	1.09
0.750 - 0.833	03 48	3.800	0.875 - 1.325	1.614	25.0	40.350	+ 30.50	1.9935	134.61	85.0	1.89
0.833 - 0.917	04 10	4.167	0.875 - 3.646	1.614	27.5	44.385	+ 51.50	1.9935	193.88	85.0	2.16
0.917 - 1.000	04 25	4.433	0.875 - 3.879	1.614	30.0	48.420	+ 68.00	1.9935	294.36	85.0	2.24
1.000 - 1.083	04 46	4.767	0.875 - 4.171	1.614	32.5	52.455	+ 84.00	1.9935	363.71	85.0	3.10
1.083 - 1.167	05 03	5.050	0.875 - 4.419	1.614	35.0	56.490	+ 92.00	1.9935	391.16	85.0	3.64
1.167 - 1.250	05 21	5.350	0.875 - 4.681	1.614	37.5	60.525	+ 114.00	1.9935	339.58	85.0	3.98

TEST NO. 6 - CALCULATION OF INSTANTANEOUS VALUES OF POISSONS RATIO (%)

RANGE OF STRAIN CONSIDERED	SAMPLE STRAIN $\frac{\Delta V}{V}$	MODULUS E 10^{10} dy/cm^2	$\frac{\Delta V}{V} \times E$ dy/cm^2	CHANGE IN DEVIATION STRESS (dy/cm ²) $\Delta(\sigma - \sigma_0)$ OVER RANGE CONSIDERED	$\frac{\Delta \sigma \times E}{V \times E_0}$	$1 - N$	POISSONS RATIO (μ_2) $\frac{1 - N}{1 - \mu_1}$
0.130 - 0.200	0.26	9070	7.2150	4.51	0.5000	0.5000	0.2510
0.150 - 0.233	0.46	9144	5.7482	6.76	0.5542	0.4458	0.2219
0.150 - 0.267	0.72	7658	5.5138	9.96	0.6154	0.3846	0.1923
0.150 - 0.300	0.94	7853	7.1758	11.23	0.6266	0.3734	0.1867
0.150 - 0.333	1.18	7934	8.4329	14.63	0.6448	0.3552	0.1776
0.150 - 0.367	1.45	8041	11.5555	17.85	0.6652	0.3348	0.1684
0.150 - 0.400	1.76	8185	14.3475	20.38	0.7040	0.2960	0.1400
0.150 - 0.433	2.02	8141	16.4448	23.04	0.7134	0.2866	0.1433
0.150 - 0.467	2.29	8142	18.6452	25.81	0.7224	0.2776	0.1388
0.150 - 0.500	2.44	8186	19.8738	28.65	0.6272	0.3728	0.1514
0.150 - 0.533	2.71	8234	22.2599	31.46	0.7076	0.2924	0.1443
0.150 - 0.567	2.96	8213	24.3105	34.26	0.7099	0.2902	0.1451
0.150 - 0.600	3.13	8200	25.5660	36.90	0.6456	0.3544	0.1525
0.150 - 0.633	3.36	8186	26.9783	38.25	0.6273	0.3727	0.1564
0.150 - 0.667	3.46	8033	27.7942	41.53	0.6692	0.3308	0.1624

CHAPTER 10

CONCLUSIONS

In conclusion, it is necessary to return to the question of the significance of Poisson's Ratio in soils work. For this purpose it is appropriate to consider in the first instance again the applicability of the elastic theory to soils, in the light now also of the information which has come to hand as a result of the practical work conducted, as was described and discussed in Chapters 7, 8 and 9.

A number of additional practical facts, besides those indicated at the beginning of Section 8.1, can now be mentioned which tend to reassure the contention that the elastic theory can be applied to soils.

Firstly, the values of Poisson's Ratio obtained from the tests conducted, were found by using a formula based on elastic theory. Without exception, all the values obtained (i.e., both μ_v and μ_{sc}) fall within the range of values applying to homogeneous, isotropic, elastic materials, viz. zero-0.5 as was discussed in Chapter 3. The values obtained also fall into line with those applying to materials other than metals, such as concrete (μ between 0.088 and 0.185 - see Section 3.3), to which the elastic theory has been applied with reasonable success. That values of Poisson's Ratio in excess of 0.5 were not obtained is due to the fact that in all cases, test samples showed a decrease in volume within the extent of the linear range of the stress-strain curve as a result of the application of compressive loading, which is a phenomenon in accordance with the requirements of the elastic state (as discussed in Section 3.2). Had values of Poisson's Ratio outside the range zero-0.5 been obtained, it would have served as a strong indication that a soil behaves more in a non-elastic manner and the application of the elastic theory to soils should be treated with reserve.

With regard to the fact that the curves of instantaneous Poisson's Ratio:Strain and instantaneous Young's Modulus:Strain showed (respectively) that both Poisson's Ratio and Young's Modulus are not constant within the linear range of the stress-strain curve as in accordance with the requirements of the elastic theory (see Chapter 2): The causes of these variations have already been fully discussed: in the case of Young's Modulus at the end of Section 7.7 and in the case of Poisson's Ratio in Chapter 9. With regard to Young's Modulus it should be remembered that in each case E was determined as a secant modulus based on actual points plotted, and not as any smooth curve drawn through the plotted points, so as to obtain the optimum conditions for enabling a constant value to be determined. It is therefore considered that the variations of both Poisson's Ratio and Young's Modulus within the extent of the linear range as obtained in the case of the tests conducted, does not necessarily tend to invalidate the application of the elastic theory to soils.

However, besides considerations of laboratory and field tests, recent results of actual practical measurements and their comparison with the results of calculations by the theory of elasticity, lend increasing evidence to the contention that the elastic theory can be applied to soils. Firstly - comparison (25) of measured and calculated vertical stresses (σ_z) developed in a uniform layer of sandy clay as a result of applied surface pressures, showed very good agreement. The applied pressures were of a transient type similar to those produced by road

traffic/

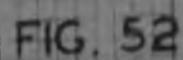
traffic. Jones (24), in this connection, expresses the view that the basic assumption of elasticity is not correct for soil when it is subjected to slowly applied loads. This is possibly because it is felt that too much consolidation effects can result under these loading conditions. It is not possible to express a view on this opinion on the basis of the tests conducted. However, the results of practical measurements under static loading conditions made by the U. S. Army Corps of Engineers, Waterways Experiment Station (26), (27), (28), which were specifically directed towards the purpose of comparing calculations by the theory of elasticity with the equivalent soil measurements, showed that much better agreement was obtained than seemed generally to have been expected.

It can therefore be concluded that although soils do not comply rigidly in all respects with the requirements of the elastic theory, there is ever-increasing evidence to strengthen the belief that the theory can be applied to soils with reasonable confidence and possibly in all cases of loading, provided (according to the discussion in Section 6.1) the induced stresses are low compared to those required to produce failure i.e. provided the induced stresses are sensibly within the elastic range of loading.

With regard to Poisson's Ratio therefore, it can be concluded that since it is primarily an elastic concept and its meaning is seldom considered other than in relation to the elastic state, it rarely enters in soils work other than in connection with applying the elastic theory to soils. Furthermore, when this is the case, Poisson's Ratio can only enter in 3-dimensional problems of stress and strain, since it was shown in Chapter 4 that the elastic constants do not affect the stress distribution in 2-dimensional cases. A 3-dimensional problem can result from any type of concentrated point loading or finite area loading, such as a rolling wheel load due to rail or road traffic or a structural foundation in the form of a rectangular, square or circular footing. However, as was pointed out in Section 4.4, in the case of stress distribution in 3-dimensional problems, Poisson's Ratio only appears in the expressions for certain of the stress components, the vertical normal stress σ_z which is most frequently used in soils work, being unaffected by it. The Maximum Shear Stress (τ_{max}) in 3-dimensional cases is also affected by Poisson's Ratio as was shown in Chapter 6. Yet, for the basic case of a vertical point load, Poisson's Ratio was in general found to be of insignificant effect below a certain comparatively shallow depth in the soil, as the stress distribution (σ_{max}) below such depth was not seriously affected by a complete range of values between zero and 0.5 (p. 14). Furthermore, on the axis of loading, which is actually of prime importance since the greatest σ_{max} values occur on the axis of loading, μ has no very great effect on the value of σ_{max} obtained at all depths, as the limits of the complete range of μ values applicable to elastic materials only caused a 14% variation in the corresponding value of σ_{max} .

As far as stress distribution in soils is therefore concerned, it appears that Poisson's Ratio is generally not of very great significance. The immediate (elastic) settlement of foundations on soils is, however, more affected by variation in the value of Poisson's Ratio, since the factor $(1 - \mu^2)$ in the equation 4.11 for the settlement of a uniformly loaded rectangular area, (a factor which also appears in the case of the expression for the settlement of the surface of a semi-infinite solid due to a vertical point load - see Ref. 9, p. 376), varies between 0.75 and unity for μ varying between zero and 0.5, and is therefore liable to cause a maximum variation of 25% in the

immediate/



immediate settlement value obtained. Yet, this effect is ultimately also not very great, since the immediate settlement only forms a part of the total settlement of any foundation, the other part being that due to consolidation effects. Therefore as far as the significance of Poisson's Ratio in the determination of both stress and settlement in soils is concerned, Poisson's Ratio is only of limited significance.

As a result of the discussions in Chapters 6 and 8, the following conclusions can be drawn with regard to the value of Poisson's Ratio applicable in various cases. In the first instance, it was shown in Sections 6.2 and 6.3 that for all types of saturated soils (i.e. both cohesive and non-cohesive), Poisson's Ratio = 0.50 should be used for all calculations by the theory of elasticity. Secondly, in the case of partially saturated soils, the following information is available from Chapter 9:

(a) D.S.I.R. findings:

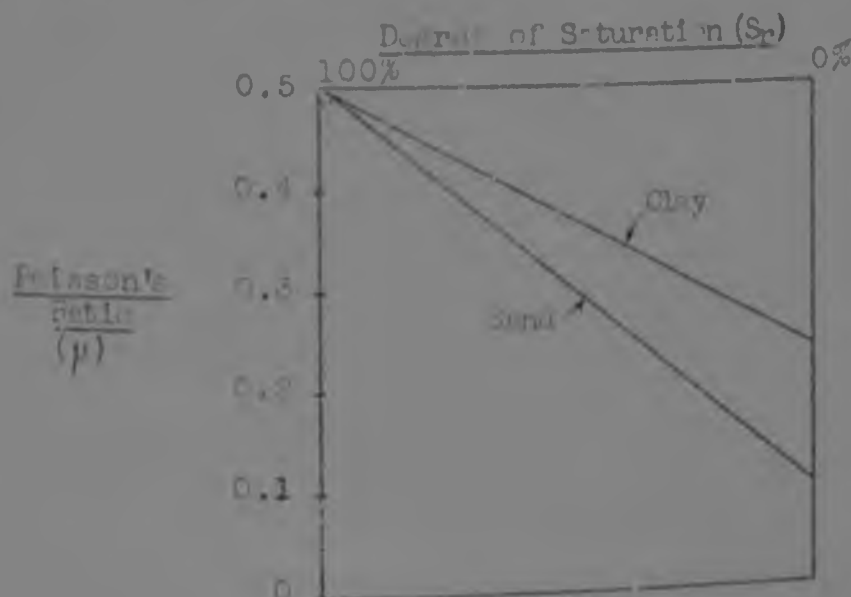
- (i) For a silty clay at a moisture content of approximately 20% (elastic limit), $\mu = 0.45$
- (ii) For the same soil at a moisture content of 5%, $\mu = 0.25$.
- (iii) No values for sands were given, but the view was expressed that the values of μ for sands were below those for clays.

(b) Findings by the U.S. Army Corps of Engineers:

- (i) For a lean clay at a moisture content near the optimum $\mu = 0.50$.
- (ii) For a dry, fairly fine, uniform sand, $\mu = 0.30$.
- (iii) Results (i) and (ii) in this case also indicate that μ values for sands are below those for clays.

(c) Findings from the laboratory work discussed in this report: For a silty sand at a moisture content of 1-2%, μ falls within the range 0.14-0.24.

From the above data it is thus clear that Poisson's Ratio is dependent on moisture content in all types of soils, i.e., according to indications so far, μ decreases with moisture content. Furthermore, it is clear that in the case of partially saturated soils, μ values for sands are below those for clays. Hence, it is suggested that the Poisson's Ratio:Degree of Saturation relationship may be of the nature shown in the diagram below:



In ...

CHAPTER 9

FINAL DISCUSSION OF TEST RESULTS

The curves of instantaneous Poisson's Ratio (μ_i): Strain (Figs. 49, 50, 51 and 52) for each of the four tests in which it was possible to prepare longer curves, show the same basic pattern in each case, viz. that of a trough-shaped curve, but with a short, approximately horizontal portion forming the turning point.

This approximately horizontal portion of the curve indicates that μ_i attains a value which is more or less constant and can be considered as such with little detrimental effect. For convenience, this constant value will be denoted $\mu_i(\text{const.})$. Its actual numerical value was for each test obtained from the relevant calculation sheets as the average of the values for the range over which μ_i can be considered to be constant. This range of values has in each case been marked on the calculation sheets by a vertical line alongside the relevant figures, which extends between arrow heads demarcating the limits of the range.

The curves show clearly that the range of strain over which μ_i is constant, does not always fall fully within that range of strain corresponding to the linear range of the stress:strain curve. In three out of four instances (Figs. 49, 50 and 51), the bulk of the range of strain over which μ_i is constant falls outside the limit of the linear range of the stress:strain curve. Furthermore, before commencement of this range of strain, μ_i decreases in each case from a value generally between 0.3 and 0.5 to the respective $\mu_i(\text{const.})$ value in the region of 0.14 - 0.24, this decrease taking place within the linear range of the stress:strain curve. Subsequent to the $\mu_i(\text{const.})$ range, μ_i again steadily increases in value.

Regarding the latter points mentioned, their causes can be explained by considering again equation 7.5 from which Poisson's Ratio was evaluated:

$$\mu = \frac{1}{2} \left[1 - \frac{\delta V}{V} \cdot \frac{E}{\delta \sigma_d} \right] \dots\dots\dots 7.5$$

or, more accurately,

$$\mu = \frac{1}{2} \left[1 - \frac{\delta V}{V} \cdot \frac{E}{\delta \sigma_d} \right] \dots\dots\dots 9.1$$

$$\text{but Young's Modulus (E)} = \frac{\delta \sigma_d}{\delta \epsilon} \dots\dots\dots 9.2$$

$$\therefore \mu = \frac{1}{2} \left[1 - \frac{\delta V}{V} \cdot \frac{\delta \sigma_d}{\delta \epsilon} \cdot \frac{1}{\delta \sigma_d} \right] \dots\dots\dots 9.3$$

$$= \frac{1}{2} \left[1 - \frac{\delta V}{V} \cdot \frac{1}{\delta \epsilon} \right] \dots\dots\dots 9.3$$

which means that, as V is a constant and $\delta \epsilon$ is the independent variable, the value of Poisson's Ratio obtained is dependent only on the measured value of δV (i.e. the change in volume of the test sample during test) and it cannot be affected by any peak-shaped variation in Young's Modulus (E) as would seem to be possible from equation 7.5.

Further, with regard to the initial decreasing portion of the $\mu_i:E$ curve, the same equation (9.3) shows that values of μ_i which are too large can be obtained if the value of δV used is too small, i.e., if the value of slug movement due to leakage only which was used for the determination of δV was larger than the actual value during test, since, the slug movement due to spindle entry only is a function only of the independent variable deflection (i.e. strain), and hence, cannot affect the value

of

In the case of partially saturated soils therefore, it may be necessary, depending on the nature of the purpose for which a value of Poisson's Ratio is required, to conduct a special test in order to determine the value applicable to the particular soil concerned, or it may suffice to use an approximate value based on the information given above. However, on occasion there may also be overriding considerations, such as when the condition of a soil mass as a whole is considered and it becomes necessary to adopt a particular value of Poisson's Ratio (such as in the case of the Westergaard equations), in order to obtain a result in close agreement with actual conditions.

Finally, it should again be stressed that in all cases the concept of Poisson's Ratio in soils only has a rational meaning when viewed in relation to soil conditions which can be considered to approximate the elastic state to which the theory of elasticity is applicable. Such soil conditions therefore constitute the only justifiable basis on which the significance of Poisson's Ratio in the determination of stress and settlement in soils can on any occasion be considered.

of δV . In effect, this means that if the assumed value of rate of leakage during test is too large, the resultant value of μ_i is too large and vice versa.

This was actually the case with the reduction of the test results, since as can be seen in Fig. (a), Section 8.1, the rate of leakage during the initial portion of a test was assumed to be a constant value equal to the rate of leakage measured immediately before the start of test, and, as was discussed in Section 8.2, this is a value which is most probably in excess of the actual value of rate of leakage occurring immediately after test commencement. Hence, the fact that values of μ_i which are too large were initially obtained. It also seems likely that while, soon after test commencement, the slug movement due to sample volume change only is still comparatively small in relation to the slug movement due to leakage only (see for example Test No. 1), an error in the assumed value of rate of leakage could cause a significant drop in the value of μ_i obtained. As the test progresses, and the slug movement due to sample volume change increases in relation to the slug movement due to leakage, an error in the rate of leakage has continually less significant effect on the values of δV and μ_i obtained. On the curve of μ_i vs ϵ this is manifested by steadily decreasing μ_i values until the $\mu_i(\text{const.})$ range is obtained. It is therefore considered that the values of $\mu_i(\text{const.})$ are the more reliable and will therefore be used.

With regard to the fact that μ_i again increases in value subsequent to the $\mu_i(\text{const.})$ range, it will be noted that this subsequent increase in value occurs simultaneously with the turning point in the Main Slug Movement: Deflection curve being approached, i.e. it occurs simultaneously with the commencement of the phenomenon of sample expansion on approaching failure conditions (see Section 7.7). This phenomenon results in decreasing values of δV (relative to the original sample volume V) and, as can be seen from equation 9.3, is the cause of the subsequent increasing values of μ_i .

However, the fact that the $\mu_i(\text{const.})$ range which precedes the range of increasing μ_i values, extends outside the limits of the linear range of the stress-strain curve, is considered to be due to inclusion of sample volume change due to consolidation effects in the measured value of δV . These consolidation effects occur as a result of the application of the deviator stress σ_d and possibly only become of significant effect near and beyond the end of the linear range and prior to the commencement of the phenomenon of sample expansion on approaching failure conditions. The curving over to the right of the stress-strain curve which commences from the end of the linear range, is considered (6) to be indicative of the inclusion of consolidation effects resulting from the application of the deviator stress. This can possibly be appreciated if it be considered that in some tests the linear range of the stress-strain curve lasted for about 15 minutes. As the test soil was partially saturated, in fact, nearly completely dry (generally less than 2%), and was also of a cohesionless nature, it is difficult to conceive especially as a result of the discussions in Sections 6.2 and 6.3, how some consolidation effects (possibly not in the form of expulsion of pore water from the test sample, but air), could have been avoided within the linear range of the stress-strain curve.

As these consolidation effects represent loss of mass during strain (see Chapter 2), they cannot be included in sample volume changes due to elasticity effects for the purposes of calculating Poisson's Ratio. The effect of their inclusion is to cause a larger value of δV than would otherwise have been the case, and which, according to equation 9.3, is therefore

the/

APPENDIX I

The possible Algebraic Signs of the Moduli of Elasticity E, G and K

(a) Young's Modulus (E):

By Hooke's Law (Chapter 2), $E = \frac{\sigma}{\epsilon}$ (a)

Since, if σ is +ve, ϵ is essentially +ve,
and if σ is -ve, ϵ is essentially -ve,

Therefore, E is always positive.

(b) Modulus of Rigidity (G):

From basic strength of Materials (Ref.2,p.55),

$$G = \frac{\tau}{\gamma} \text{ (b)}$$

Since, if τ is +ve, γ is essentially +ve,
and if τ is -ve, γ is essentially -ve,

Therefore G is always positive.

(c) Bulk Modulus (K):

From equation 3.2 : For fluid pressure conditions
when $\epsilon_1 = \epsilon_2 = \epsilon_3 = \epsilon$ say,

$$\Delta = 3\epsilon \text{ (c)}$$

and as discussed in (a) above:

if σ is +ve, ϵ is +ve, therefore in (c): Δ is +ve when σ is +ve,

and if σ is -ve, ϵ is -ve, therefore in (c): Δ is -ve when σ is -ve.

Hence, in equation 3.4: $K = \frac{\sigma}{\Delta}$

if Δ is +ve when σ is +ve, then $\frac{\sigma}{\Delta}$ is +ve,
and if Δ is -ve when σ is -ve, then $\frac{\sigma}{\Delta}$ is +ve.

Therefore K is always positive.

the cause of a smaller value of μ being obtained, and a delay in the start of the range of increasing μ values. Hence, the phenomenon that the μ (const.) range extends outside the limits of the linear range of the stress-strain curve.

Table XII on the next page shows the determination of the proportion of the constant μ range falling within the limit of the linear range of the stress-strain curve for each test. The table also compares in adjacent columns the values of μ_{sat} and μ (const.) obtained in each case. It appears that the values of both μ_{sat} and μ (const.) fell within the range 0.138-0.238, the values of μ (const.) being slightly larger than the corresponding values of μ_{sat} in each case.

These values show reasonable agreement with those obtained by Research workers of the D.S.I.R.'s Road Research Laboratory, Harmondsworth, Middlesex, England, (23), (24), (25) as a result of in-situ measurements made of the mechanical properties of soil by vibration methods. This research work is as yet unpublished. It was found that Poisson's Ratio for a silty clay with a liquid limit of 50% was approximately 0.45 at a moisture content quite near to its plastic limit of 30%. For the same silty clay, Poisson's Ratio was 0.25 at 5% moisture content, thus indicating a decrease in value with decreasing moisture content. For a heavy clay a value a little above 0.45 seemed to be indicated. No data are as yet available for sands, but the opinion was expressed (23) that the values will be below those for clays.

Information obtained from the Director, Waterways Experiment Station, U.S. Army Corps of Engineers, Vicksburg, Mississippi, (26), (27), (28), substantiates these findings of the D.S.I.R., England. Their work has been directed at comparing calculations by the theory of elasticity with the equivalent soil measurements. For a lean clay at a moisture content near the optimum, a Poisson's Ratio of 0.5 seemed to agree very well, while for a dry, fairly fine, uniform sand, a value of 0.3 was indicated, which thus verifies the opinion of the D.S.I.R., workers that the Poisson's Ratio values for sands are below those for clays.

Hence, if, according to the D.S.I.R. findings previously mentioned, the value of Poisson's Ratio for a silty clay drops from 0.45 to 0.25 for a drop in moisture content from near to 20% to 5% and if, in addition, the values of Poisson's Ratio for sands are below those for clays, then values between 0.138 and 0.238 for a silty sand at 1% - 2% moisture content would seem to be in reasonable agreement. It should especially be noted that all the values of Poisson's Ratio given above apply to partially saturated soil conditions.

In order to ascertain the possible effect of moisture content on the values of Poisson's Ratio determined from the test series, Table XIII was arranged in order of decreasing moisture content values, with the relevant values of Degree of Saturation

(Sr)/

APPENDIX II

Steps in the Final Reduction of the Mathematical Expressions in Flamant's paper (Ref.12)

It is useful to commence by considering in the first instance some basic relationships of the theory of elasticity which are involved in the work to follow in this Appendix. These relationships will only be quoted without their actual derivations being given. However, reference will be made to pages in Timoshenko's "Theory of Elasticity" (Ref.3) wherein the derivations are outlined in full. It is important to point out that Timoshenko uses the same notation as used by Love and other masters of the elastic theory, in that Poisson's Ratio is denoted by the Greek letter ν (Nu), whereas in this report Poisson's Ratio is in all cases denoted by μ . However, since Lamé's elastic constants which appear in Flamant's paper are denoted by λ and μ , Poisson's Ratio will in this Appendix only be denoted by ν , to avoid confusion in the work to follow. Furthermore, the unit volumetric strain or Dilation which throughout this report is denoted by Δ , is denoted by ϵ in Timoshenko's book as well as in Flamant's paper. Therefore the Dilation also will in this Appendix only be denoted by the symbol ϵ .

The first set of basic relationships which are involved in Flamant's work are those given by Timoshenko(3) in his equations (2), p.7, viz., that if with respect to a set of three mutually perpendicular axes OX, OY and OZ the small displacements of particles of a deformed body be resolved into components u , v , and w parallel to these respective coordinate axes, then:

(i) the linear strain components ϵ are expressible by:

$$\epsilon_x = \frac{\partial u}{\partial x} ; \epsilon_y = \frac{\partial v}{\partial y} ; \epsilon_z = \frac{\partial w}{\partial z} \dots\dots\dots (a)$$

and (ii) the shear strain components χ are expressible by:

$$\chi_{xy} = \frac{\partial u}{\partial y} + \frac{\partial v}{\partial x} ; \chi_{xz} = \frac{\partial u}{\partial z} + \frac{\partial w}{\partial x} ; \chi_{yz} = \frac{\partial v}{\partial z} + \frac{\partial w}{\partial y} \dots\dots\dots (b)$$

The second set of basic relationships which are involved are those given by Timoshenko(3) in his equations (11), p.11, relating the stresses and strains in a 3-dimensional system:

$$\begin{aligned} \sigma_x &= \lambda \epsilon + 2\mu \epsilon_x \\ \sigma_y &= \lambda \epsilon + 2\mu \epsilon_y \\ \sigma_z &= \lambda \epsilon + 2\mu \epsilon_z \end{aligned} \dots\dots\dots (c)$$

wherein:

(i) λ and μ are Lamé's elastic constants as given by:

$$\lambda = \frac{\nu E}{(1+\nu)(1-2\nu)} \dots\dots\dots (d)$$

$$\text{and } \mu = G = \frac{E}{2(1+\nu)} = \frac{\tau}{\chi} \dots\dots\dots (e)$$

where E = Young's Modulus
 ν = Poisson's Ratio
 G = Modulus of Rigidity

τ = shear stress
 χ = shear strain

(ii) ϵ is the unit volumetric strain as given by:

$$\epsilon = \epsilon_x + \epsilon_y + \epsilon_z \dots\dots\dots (f)$$

Equations (c) and (f) above are identical to equations 3.5 and 3.2 which appeared earlier in Chapter 3 of this report.

From equation (e) above, it should be noted that:

$$\tau = \mu \cdot \chi$$

whence

TEST No 4 : CALCULATION OF INSTANTANEOUS VALUES OF SAMPLE DILATION $(\frac{\Delta V}{V})$ (cont.)

OF ON ERED	TIME ELAPSED OVER RANGE CONSIDERED		RATE OF SLUG MOVEMENT DUE TO LEAKAGE ONLY		RATE OF SLUG MOVEMENT DUE TO SPINDLE ONLY		RATE OF SLUG MOVEMENT DUE TO SPINDLE ONLY		OBSERVED SLUG MOVEMENT OVER RANGE DUE TO THREE COMBINED EFFECTS.		HENCE SLUG MOVEMENT DUE TO SAMPLE COMPRESSION ONLY OVER RANGE CON- SIDERED		CROSS SECTION - AL AREA OF CAPILLARY TUBE	VOLUME CHANGE OF SAMPLE OVER RANGE OF STRAIN CONSIDERED	INITIAL SAMPLE VOLUME V	SAMPLE DILATION $\frac{\Delta V}{V}$
	min	sec	mm/min	mm/sec	mm/min	mm/sec	mm/min	mm/sec	mm/min	mm/sec	mm/min	mm/sec	sq mm	cc/cm	cc/cm	cc/cm
1.553	05	35	3.623	0.604	0.875	- 4.265	1.614	40.0	+ 64.660	+ 123.25	+ 182.025	+ 182.025	1.9935	384.86	85.0	5.79
1.417	05	50	5.833	0.972	0.875	- 5.104	1.614	42.5	+ 64.585	+ 139.00	+ 195.491	+ 195.491	1.9935	384.71	85.0	5.88
1.500	06	04	5.067	0.844	0.875	- 5.309	1.614	45.0	+ 78.630	+ 136.00	+ 205.391	+ 205.391	1.9935	404.31	85.0	5.92
1.238	06	14	6.317	0.875	0.875	- 6.427	1.614	47.5	+ 76.665	+ 142.75	+ 213.288	+ 213.288	1.9935	426.39	85.0	5.68
1.687	06	33	6.680	0.875	0.875	- 5.731	1.614	50.0	+ 80.700	+ 144.75	+ 219.719	+ 219.719	1.9935	432.01	85.0	5.18
1.438	06	56	6.953	0.888	0.888	- 5.880	1.614	55.0	+ 88.770	+ 144.00	+ 225.220	+ 225.220	1.9935	440.37	85.0	5.20
1.600	07	21	7.320	1.000	1.000	- 8.085	1.614	60.0	+ 96.840	+ 154.75	+ 223.505	+ 223.505	1.9935	445.56	85.0	5.24
1.417	07	45	7.750	1.212	1.212	- 9.393	1.614	65.0	+ 104.910	+ 111.00	+ 206.517	+ 206.517	1.9935	441.69	85.0	4.89
1.235	08	00	8.100	1.320	1.320	- 10.732	1.614	70.0	+ 112.980	+ 90.75	+ 192.998	+ 192.998	1.9935	384.74	85.0	4.53
1.600	08	27	8.430	1.438	1.438	- 12.151	1.614	75.0	+ 121.050	+ 69.25	+ 177.149	+ 177.149	1.9935	383.18	85.0	4.19
1.567	08	51	8.880	1.650	1.650	- 13.718	1.614	80.0	+ 129.130	+ 47.00	+ 162.402	+ 162.402	1.9935	383.75	85.0	3.91
1.800	09	13	9.217	1.662	1.662	- 15.319	1.614	85.0	+ 137.190	+ 23.80	+ 145.371	+ 145.371	1.9935	384.80	85.0	3.41
1.400	09	36	9.600	1.770	1.770	- 17.040	1.614	90.0	+ 145.260	+ 4.50	+ 132.720	+ 132.720	1.9935	364.50	85.0	3.11
1.467	09	47	9.983	1.808	1.808	- 18.948	1.614	95.0	+ 153.330	- 25.00	+ 109.482	+ 109.482	1.9935	318.52	85.0	2.97
1.433	10	24	10.400	2.000	2.000	- 20.800	1.614	100.0	+ 161.400	- 45.00	+ 95.600	+ 95.600	1.9935	190.68	85.0	2.04

TABLE XII: COMPARISON OF VALUES OF POISSONS' RATIO μ_{sec} AND μ_{int} -

TEST NUMBER	STRAIN AT END OF LINEAR RANGE OF STRESS STRAIN CURVE = a percent	STRAIN DUE TO BEDDING-IN EFFECTS = b percent	DIFFERENCE $a-b$ CORRECTED STRAIN AT END OF LINEAR RANGE OF STRESS STRAIN CURVE = c percent	CURVE OF $\mu_{L/VIS}$ CORRECTED STRAIN* VALUES (percent)		PROPORTION OF CONSTANT RANGE FALLING WITHIN THE LIMIT OF THE LINEAR RANGE OF THE STRESS STRAIN CURVE		POISSONS' RATIO μ_{sec}	POISSONS' RATIO μ_{int} (transient)	DIFFERENCE $\mu_{int} - \mu_{sec}$
				AT START OF CONSTANT μ_{L} RANGE = d	AT END OF CONSTANT μ_{L} RANGE = e	$\frac{c-d}{e-d}$	PERCENTAGE			
1	0.600	ZERO	0.600	0.500	1.000	$\frac{0.100}{0.500}$	20%	0.1387	0.1535	0.0148
2	0.833	0.150	0.683	—	—	—	—	0.1401	—	—
3	0.600	0.100	0.500	0.367	0.733	$\frac{0.133}{0.366}$	36%	0.1390	0.1793	0.0403
4	1.083	0.500	0.583	0.417	0.833	$\frac{0.167}{0.417}$	40%	0.2099	0.2372	0.0273
5	0.750	0.260	0.490	—	—	—	—	0.1425	—	—
6	0.750	0.150	0.600	0.230	0.483	$\frac{0.350}{0.253}$	100%	0.1429	0.1484	0.0055

* STRAIN DUE TO BEDDING-IN EFFECTS SUBTRACTED

TEST NO. 4 - CALCULATION OF INSTANTANEOUS VALUES OF POISSON'S RATIO (%)

RANGE OF STRAIN CONSIDERED	SAMPLE DILATION $\frac{\Delta V}{V}$	YOUNG'S MODULUS E	$\frac{\Delta V}{V} \times E$	CHANGE IN DEVIATION STRESS (MPa) = $\Delta(\sigma - \sigma_0)$ OVER RANGE CONSIDERED	$\frac{\Delta \sigma \times E}{V \times \Delta \sigma_0} \times 10^{-4}$	POISSON'S RATIO (%)
0.500 - 0.583	0.83	4470	2.1791	7.26	0.2771	0.7229
0.500 - 0.667	0.82	9916	5.1563	14.26	0.3114	0.6886
0.500 - 0.750	1.08	9648	10.4198	24.12	0.4320	0.5680
0.500 - 0.833	1.58	9330	14.7556	31.10	0.4744	0.5256
0.500 - 0.917	2.16	9538	20.5891	39.73	0.5180	0.4820
0.500 - 1.000	2.64	9174	4.2194	45.87	0.5280	0.4720
0.500 - 1.083	3.10	9154	28.3774	53.87	0.5317	0.4683
0.500 - 1.167	3.64	8823	31.0334	58.25	0.5307	0.4693
0.500 - 1.250	3.98	8628	34.3434	64.72	0.5306	0.4694
0.500 - 1.333	4.29	8290	36.5984	69.12	0.5150	0.4850
0.500 - 1.417	4.58	7958	36.4385	72.96	0.4994	0.5006
0.500 - 1.500	4.82	7520	36.6107	75.96	0.4920	0.5080
0.500 - 1.583	5.02	7291	36.6008	78.96	0.4835	0.5165
0.500 - 1.667	5.15	6984	35.6599	80.23	0.4413	0.5587
0.500 - 1.833	5.30	6241	33.0773	83.19	0.3976	0.6024

(S_r) alongside. From the data presented it is clear, however, that no conclusion can be drawn as to the effect of moisture content or Degree of Saturation on the value of Poisson's Ratio. Insufficient values are available and the range of moisture content is too small to show up any significant trend such as that found by the Road Research Laboratory of the D.S.I.R. For the same reasons no conclusion can be drawn about the effect of void ratio on the value of Poisson's Ratio (Table XIV).

However, Table XIV clearly indicates the important relationship between chamber pressure (P_3), void ratio (e) and sample dilation ($\delta V/V$) which has also been discussed by Taylor (17), viz., that for sandy soils, the nature and magnitude of the volumetric strains ($\delta V/V$) during test, depend on both the chamber pressure used and the void ratio of the sample. In the first instance, the volumetric strain ($\delta V/V$) for a reduction in volume, increases as the chamber pressure increases, and secondly, the lower the void ratio the greater the tendency for a volume increase after the initial volume decrease at the commencement of the test. Hence, for the two effects combined, the lower the void ratio and chamber pressure the less the initial volume decrease of the sample and, subsequently also, the more rapid the tendency to a volume increase. In the case of Tests No. 1 & 3, the effect of the higher chamber pressure in Test No. 1 apparently outweighed the effect of the lower void ratio and resulted in a larger volume decrease and a lesser tendency for a volume increase than in the case of Test No. 3. The effect of a lower void ratio at the same chamber pressure is clearly indicated in the case of Tests No. 3 & 4. In the case of Test No. 5 with both low void ratio and chamber pressure, the phenomenon of sample expansion subsequent to an initial compression to the extent of yielding a sample volume in excess of its original volume at the commencement of the test, was clearly realized, i.e., a change in sign of $\delta V/V$ from that corresponding to a decrease in volume to that corresponding to an increase in volume, was nearly effected.

The effect of variation in chamber pressure at a constant rate of strain, on the shear strength obtained, is firstly presented in Table XV. The Mohr circles for each of the three chamber pressures for the two respective rates of strain used, are shown in Fig. 10, and give the values of cohesion (c) and apparent angle of friction (ϕ_a) shown in Table (XV) in the column adjacent to the shear strength values. The values of c and ϕ_a are slightly different for the two rates of strain, the higher rate of strain yielding the higher value of apparent angle of friction and the lower value of cohesion. Individual Mohr circles for the case of the faster rate of strain, fit in better with the relevant Mohr rupture line, than in the case of the lower rate of strain. From the following discussion of the data presented in Table XVI, it will be seen that chamber pressure and rate of strain probably have no influence in causing this phenomenon.

The effect of both variation in chamber pressure at a constant rate of strain and variation in rate of strain at a constant chamber pressure (Tables XV and XVI), on the values of

Young's/

(a)

$(\sigma_1 - \sigma_3) \frac{118.59 \text{ in.}}{1}$

NOM Rate of Strain = 0.0125 in./min

$\sigma_3 = 2016 \text{ lb/sq in.}$

$\nu = 0.713$

$\omega = 0.66\%$

$\epsilon_r = 2.42\%$

end of linear range

STRAIN ϵ (percent)

$\frac{\Delta V}{V}$

(in percent)

Expansion

(b)

Compression

(c)

STRAINE (percent)

STRAIN ϵ (percent)

POISSON'S RATIO

TABLE XIII

TEST NUMBER	INITIAL MOISTURE CONTENT ω percent	INITIAL DEGREE OF SATURATION S_r percent	POISSONS RATIO μ_{set}	POISSONS RATIO $\mu_{d(ult+unp)}$
2	2.290	8.64	0.1401	—
3	1.820	6.24	0.1390	0.1793
5	1.750	6.42	0.1425	—
6	1.680	6.27	0.1429	0.1464
4	0.658	2.42	0.2099	0.2372
1	0.548	1.95	0.1387	0.535

TABLE XIV

TEST NUMBER	NOMINAL CHAMBER PRESSURE P_3 lb./sq. in.	INITIAL VOID RATIO e	POISSONS RATIO μ_{set}	POISSONS RATIO $\mu_{d(ult+unp)}$	DETAILS OF $\frac{\Delta V}{V} - E$ CURVE
1	30	0.737	0.1387	0.535	
3	20	0.764	0.1390	0.1793	
5	10	0.714	0.1425	—	—
4	20	0.713	0.2099	0.2372	
6	10	0.702	0.1429	0.1464	
2	30	0.625	0.1401	—	—

TEST No 6 : CALCULATION OF INSTANTANEOUS VALUES OF SAMPLE DILATION $(\frac{\Delta V}{V})$

TIME OF RANGE CONSIDERED	RATE OF HENCE SLUG MOVEMENT DUE TO LEAKAGE ONLY		RATE OF SLUG MOVE MENT DUE TO SPINDLE ENTRY ONLY	NUMBER OF DIVISIONS DEFLECT OVER RANGE CONSIDERED	HENCE OVER RANGE CONSIDERED DUE TO SPINDLE ENTRY ONLY	OBSERVED SLUG MOVEMENT OVER RANGE CONSIDERED DUE TO TAPER COMBINED EFFECTS	HENCE SLUG MOVEMENT DUE TO SAMPLE COMPRESSION ONLY OVER RANGE CON- SIDERED	CROSS SECTIONAL AREA OF CAPILLARY TUBE	PERCENTAGE CHANGE IN VOL. OF SAMPLE OVER RANGE OF STRAIN CONSIDERED	INITIAL SAMPLE VOLUME	SAMPLE DILATION $\frac{\Delta V}{V}$
	sec	min									
- 0.053	01 09	1.150	0.875 - 1.006	1	+ 1.614	+ 0.75	+ 1.368	1.9935	2.71	15.0	0.03
- 0.067	01 34	1.567	0.875 - 1.371	2	+ 3.228	+ 0.75	+ 2.607	1.9935	5.20	15.0	0.06
- 0.100	01 58	1.967	0.875 - 1.721	3	+ 4.842	+ 0.25	+ 3.391	1.9935	6.75	15.0	0.08
- 0.133	02 22	2.317	0.875 - 2.027	4	+ 6.456	+ 0.25	+ 4.679	1.9935	9.33	15.0	0.11
- 0.167	02 49	2.617	0.875 - 2.445	5	+ 8.070	+ 0.50	+ 6.120	1.9935	12.17	15.0	0.14
- 0.200	03 20	3.333	0.875 - 2.916	6	+ 9.684	+ 3.75	+ 10.618	1.9935	20.97	15.0	0.25
- 0.233	04 06	4.100	0.875 - 3.584	7	+ 11.298	+ 12.00	+ 19.710	1.9935	39.29	15.0	0.40
- 0.267	03 15	9.300	0.875 - 8.138	8	+ 12.912	+ 26.00	+ 30.774	1.9935	61.55	15.0	0.73
- 0.300	10 40	10.667	0.875 - 9.334	9	+ 14.526	+ 35.00	+ 40.212	1.9935	100.12	15.0	0.94
- 0.333	11 29	11.483	0.875 - 10.048	10	+ 16.140	+ 44.25	+ 50.342	1.9935	137.16	15.0	1.18
- 0.367	12 26	12.467	0.875 - 10.909	11	+ 17.754	+ 55.00	+ 61.545	1.9935	173.29	15.0	1.45
- 0.400	13 05	13.083	0.875 - 11.448	12	+ 19.368	+ 67.00	+ 74.820	1.9935	211.35	15.0	1.78
- 0.433	13 43	13.700	0.875 - 11.988	13	+ 20.982	+ 77.00	+ 85.894	1.9935	251.43	15.0	2.06
- 0.467	14 13	14.317	0.875 - 12.527	14	+ 22.596	+ 87.50	+ 97.569	1.9935	294.50	15.0	2.19
- 0.500	14 55	14.917	0.875 - 13.052	15	+ 24.210	+ 93.00	+ 104.158	1.9935	337.24	15.0	2.31

TABLE XV

TEST NUMBER	NOMINAL RATE OF STRAIN inches/min	NOMINAL CHAMBER PRESSURE σ_3 lb/sq in	SHEAR STRENGTH S lb/sq in	COHESION (C) AND FRICTION (ϕ) COMPONENTS OF SHEAR STRENGTH	YOUNGS' MODULUS E_{sof} lb/sq in	POISSONS' RATIO μ_{sof}	POISSONS' RATIO μ_{sof} (constant)
1	0.00256	30	89.6	C $= 9.3 \text{ lb/sq in}$	8163	0.1387	0.1535
3	0.00256	20	65.3	ϕ $= 30^\circ 08'$	7697	0.1390	0.1793
5	0.00256	10	60.6		8125	0.1429	0.1464
2	0.0125	30	102.0	C $= 9.3 \text{ lb/sq in}$	7750	0.1401	—
4	0.0125	20	83.9	ϕ $= 33^\circ 42'$	9557	0.2099	0.2372
5	0.0125	10	53.0		7212	0.1425	—

TABLE XVI

TEST NUMBER	NOMINAL CHAMBER PRESSURE σ_3 lb/sq in	NOMINAL RATE OF STRAIN inches/min	SHEAR STRENGTH S lb/sq in	YOUNGS' MODULUS E_{sof} lb/sq in	INITIAL MOISTURE CONTENT w percent	INITIAL VOID RATIO e
1	30	0.00256	89.6	8163	0.546	0.757
2	30	0.0125	102.0	7750	2.290	0.695
3	20	0.00256	65.3	7697	1.820	0.764
4	20	0.0125	83.9	9557	0.655	0.713
5	10	0.00256	60.6	8125	1.680	0.702
5	10	0.0125	53.0	7212	1.750	0.714

TEST NO 8 - CALCULATION OF INSTANTANEOUS VALUES OF SAMPLE DILATION $(\frac{\Delta V}{V})$ (Cont.)

RANGE OF STRAIN CONSIDERED	TIME ELAPSED OVER RANGE CONSIDERED		RATE OF HENCL SLUG MOVEMENT DUE TO LEAKAGE DURING RANGE ONLY	RATE OF SLUG MOVEMENT DUE TO SPINDLE ENTRY ONLY	NUMBER OF DIVISIONS OF REFLECTOR OVER RANGE TO SPINDLE ENTRY ONLY	HENCL SLUG MOVEMENT OVER RANGE CONSIDERED DUE TO SPINDLE ENTRY ONLY	DERIVED SLUG MOVEMENT OVER RANGE CONSIDERED DUE TO THREE CL. BINED EFFECTS	HENCL SLUG MOVEMENT DUE TO SAMPLE COMPRESSION ONLY OVER RANGE CONSIDERED	CROSS SECTIONAL AREA OF CAPILLARY TUBE	HENCL CHANGE IN VOL. (ΔV) OVER RANGE OF STRAIN CONSIDERED	INITIAL SAMPLE VOLUME	SAMPLE DILATION $\frac{\Delta V}{V}$
	min	sec	mm/min	mm/min	div	mm/min	mm/min	mm/min	sq. mm	cc/min	cc	units of 10^{-4}
0.000 - 0.003	15	34	0.875	1.614	16	+ 28.884	+ 103.50	+ 113.703	1.9935	230.68	85.0	2.71
0.003 - 0.007	16	12	0.875	1.614	17	+ 27.436	+ 112.75	+ 126.013	1.9935	251.21	85.0	2.96
0.007 - 0.010	16	45	0.875	1.614	18	+ 28.052	+ 114.00	+ 133.352	1.9935	266.84	85.0	3.13
0.010 - 0.013	17	29	0.875	1.614	19	+ 30.666	+ 126.00	+ 141.470	1.9935	282.08	85.0	3.32
0.013 - 0.017	17	52	0.875	1.614	20	+ 32.280	+ 131.00	+ 147.559	1.9935	294.16	85.0	3.46
0.017 - 0.020	18	34	0.875	1.614	21	+ 33.894	+ 135.50	+ 153.149	1.9935	309.30	85.0	3.59
0.020 - 0.023	18	59	0.875	1.614	22	+ 35.508	+ 140.50	+ 159.242	1.9935	317.47	85.0	3.73
0.023 - 0.027	19	47	0.875	1.614	23	+ 37.122	+ 144.75	+ 164.562	1.9935	329.08	85.0	3.86
0.027 - 0.030	20	21	0.875	1.614	24	+ 38.736	+ 148.00	+ 168.950	1.9935	339.76	85.0	3.98
0.030 - 0.033	20	51	0.875	1.614	25	+ 40.350	+ 150.00	+ 173.106	1.9935	345.02	85.0	4.04
0.033 - 0.037	21	26	0.875	1.614	26	+ 41.964	+ 151.50	+ 174.724	1.9935	349.32	85.0	4.10
0.037 - 0.040	21	56	0.875	1.614	27	+ 43.578	+ 152.00	+ 176.327	1.9935	351.86	85.0	4.14
0.040 - 0.043	22	23	0.875	1.614	28	+ 45.192	+ 152.12	+ 177.727	1.9935	354.30	85.0	4.17
0.043 - 0.047	22	52	0.875	1.614	29	+ 46.806	+ 152.12	+ 178.917	1.9935	356.67	85.0	4.20
0.047 - 0.050	23	21	0.875	1.614	30	+ 48.420	+ 152.00	+ 179.979	1.9935	359.39	85.0	4.22

Young's Modulus and Poisson's Ratio ν and, cannot readily be assessed from the data shown. In the case of Young's Modulus (E_{s1}), it seems probable, (also as a result of the discussion in the next paragraph on the data presented in Table XVI), that both the effects mentioned have little influence on the variation in value of Young's Modulus. As regards Poisson's Ratio, insufficient data is available to enable any definite conclusion to be drawn.

Table XVI shows values of Shear Strength (S) and Young's Modulus (E_{s1}) for tests conducted at the same chamber pressure (although not at the same rate of strain), with the corresponding values of initial moisture content (w) and initial void ratio (e) for each case. From the data shown, it can clearly be seen that the differences in Shear Strength and Young's Modulus values, can be accounted for very satisfactorily by the respective values of initial void ratio and initial moisture content. In the case of each of the test pairs: Nos. 1 & 2 ($\sigma_3 = 30 \text{ lb./sq. in.}$); Nos. 3 & 4 ($\sigma_3 = 50 \text{ lb./sq. in.}$); and Nos. 5 & 6 ($\sigma_3 = 10 \text{ lb./sq. in.}$), the higher Young's Modulus value occurs together with the lower moisture content value, while in the case of the Shear Strength values for the same test pairs, the higher Shear Strength value occurs together with the lower void ratio value. Where the higher value of moisture content and void ratio occur simultaneously in any one of a pair of tests, the reduction in both Shear Strength and Young's Modulus values is very marked (Tests No. 3 & 5), and conversely (Tests No. 4 & 6). It is thus clear that both the values of Shear Strength and Young's Modulus are affected by the initial moisture content and initial void ratio of the sample being tested, with void ratio having a particular effect on Shear Strength and moisture content a particular effect on Young's Modulus. Hence, also, in the case of the test pair Nos. 1 & 2, wherein the higher moisture content is accompanied by the lower void ratio in the case of Test No. 2 and conversely in the case of Test No. 1, the test with the lower void ratio has the higher Shear Strength, and the test with the lower moisture content has the higher value of Young's Modulus. It is thus not necessarily the higher rate of strain which leads to the higher Shear Strength, as would appear to be the case by comparing the Shear Strength values for the test pairs Nos. 1 & 2; and Nos. 3 & 4, especially as the test pair Nos. 5 & 6 shows the higher value of Shear Strength at the lower rate of strain.

As a result of this discussion it is also possible to explain the slight shift on the Mohr envelope (Fig. 13) in the case of the test group Nos. 1, 3 & 6 which was conducted at a constant rate of strain. The Mohr envelope is tangential to the Mohr circles for Test No. 1, with Tests Nos. 3 & 6 showing the wider fit. Test No. 3 has a higher void ratio (0.784), and Test No. 6 a lower void ratio (0.702) than Test No. 1 (0.737), and hence the relatively lower and higher strengths respectively obtained for these tests, leading to the Mohr circles passing below and above the Mohr envelope respectively. In the case of the test group Nos. 2, 4 & 5, the void ratios were in much closer agreement and hence gave a better fit on the Mohr envelope.

The average void ratio for the test group Nos. 1, 3 & 6 was 0.731 compared with an average of 0.707 for the test group Nos. 2, 4 & 5. Hence, the higher average strength in the case of the latter test group and thus the steeper angle of the Mohr envelope in this case, leading to the difference in apparent angle of friction (ϕ_a) between the two test groups.

AN

An effect which has not been discussed so far, is the restraint at the ends of a sample during test, as a result of the end plates used. These end plates tend to prevent the ends of the sample from expanding laterally while the compressive loading is being applied, so that the sample deforms as a cylinder in volume to be measured, then if the ends had been unrestrained. The phenomenon has also been discussed by Bishop and Senkel (22), who feel that at small strains, end restraint is of no importance. As the limit of the linear range in the case of every test in the figured that the effect of end restraint on the values of Poisson's Ratio determined would not have been serious.

Finally, with regard to the possible effect of test temperature (see Section 7.7) on the values of Poisson's Ratio determined, Table XVII below shows the tests arranged in order of decreasing average test temperature.

TABLE XVII

TEST NUMBER	AVERAGE TEST TEMPERATURE °C	POISSONS' RATIO μ_{sel}	POISSONS' RATIO $\mu_c(\text{const.})$
1	27.34	0.1387	0.1535
2	26.25	0.1471	-
4	22.75	0.2049	0.2372
5	24.0	0.1425	-
3	23.75	0.1470	0.1793
6	20.75	0.1429	0.1464

It is clear that no conclusion can be drawn as to the possible effect of the particular test temperature on the values of Poisson's Ratio determined.

whence equations (b) & (c) can also be written:

$$\tau_{xy} = \mu \gamma_{xy}; \quad \tau_{xz} = \mu \gamma_{xz}; \quad \tau_{yz} = \mu \gamma_{yz} \dots \dots \dots (g)$$

Turning now to Flamant's paper: The following is a closer investigation of the steps omitted in the paper in obtaining the expressions for the stresses N_x , N_z and T_y which in the notation used in Chapter 4 of this report, are the stresses σ_x , σ_y and τ_{yz} . On page 1467 Ref. 12, Flamant firstly obtains the expressions for the displacements u , v , w of any point (x, y, z) below the horizontal surface of the semi-infinite solid subjected to an infinitely extended line loading of P per unit length. These are given as:

$$u = \frac{P}{2\pi\mu} \left(\frac{xz}{x^2+z^2} - \frac{\mu}{\lambda+\mu} \arctan \frac{x}{z} \right)$$

$$v = 0$$

$$w = \frac{P}{2\pi\mu} \left(\frac{z^2}{x^2+z^2} + \frac{\lambda+2\mu}{\lambda+\mu} \lg \frac{2z}{\sqrt{x^2+z^2}} \right)$$

Hence, based on equations (v):

$$(i) \quad \epsilon_x = \frac{\partial u}{\partial x} = \frac{P}{2\pi\mu} \left[(x^2+z^2)^{-1} \cdot z + xz \left\{ -1(x^2+z^2)^{-2} \right\} 2x - \frac{\mu}{\lambda+\mu} \left(\frac{1}{z} \cdot \frac{1}{1+\frac{x^2}{z^2}} \right) \right]$$

$$= \frac{P}{2\pi\mu} \left[\frac{z}{x^2+z^2} - \frac{2x^2z}{(x^2+z^2)^2} - \frac{\mu}{\lambda+\mu} \left(\frac{1}{z} \cdot \frac{z^2}{x^2+z^2} \right) \right]$$

$$= \frac{P}{2\pi\mu} \left[\frac{(x^2+z^2)z - 2x^2z - \frac{\mu}{\lambda+\mu} \cdot z(x^2+z^2)}{(x^2+z^2)^2} \right]$$

$$= \frac{P}{2\pi\mu} \left[\frac{z(x^2+z^2)(1-\frac{\mu}{\lambda+\mu}) - 2x^2z}{(x^2+z^2)^2} \right]$$

$$= \frac{P}{2\pi\mu} \left[\frac{\frac{\lambda}{\lambda+\mu} \cdot \frac{z}{x^2+z^2} - \frac{2x^2z}{(x^2+z^2)^2}}{\dots} \right]$$

$$(ii) \quad \epsilon_y = \frac{\partial v}{\partial y} = 0$$

$$(iii) \quad \epsilon_z = \frac{\partial w}{\partial z} = \frac{P}{2\pi\mu} \left[(x^2+z^2)^{-1} \cdot 2z + z^2 \left\{ -1 \cdot (x^2+z^2)^{-2} \right\} 2z + \frac{\lambda+2\mu}{\lambda+\mu} \left\{ \frac{(x^2+z^2)^{-\frac{1}{2}}}{2z} \cdot 2 \right\} \right]$$

$$= \frac{P}{2\pi\mu} \left[\frac{2z}{x^2+z^2} - \frac{2z^3}{(x^2+z^2)^2} - \frac{\lambda+2\mu}{\lambda+\mu} \cdot \frac{1}{x^2+z^2} \right]$$

$$= \frac{P}{2\pi\mu} \left[\frac{(x^2+z^2) \cdot 2z - \frac{\lambda+2\mu}{\lambda+\mu} \cdot z(x^2+z^2) - 2z^3}{(x^2+z^2)^2} \right]$$

$$= \frac{P}{2\pi\mu} \left[\frac{z(x^2+z^2)(2-\frac{\lambda+2\mu}{\lambda+\mu}) - 2z^3}{(x^2+z^2)^2} \right]$$

$$\text{i.e. } \epsilon_z = \frac{\partial w}{\partial z} = \frac{P}{2\pi\mu} \left[\frac{\frac{\lambda}{\lambda+\mu} \cdot \frac{2z}{x^2+z^2} - \frac{2z^3}{(x^2+z^2)^2}}{\dots} \right]$$

Now by equation (f): $e = \frac{\delta V}{V} = \epsilon_x + \epsilon_y + \epsilon_z$

$$\therefore e = \frac{P}{2\pi\mu} \left[\frac{\lambda}{\lambda+\mu} \cdot \frac{2z}{x^2+z^2} - \frac{2x^2z}{(x^2+z^2)^2} - \frac{2z^3}{(x^2+z^2)^2} \right]$$

$$= \frac{P}{\pi\mu} \dots \dots \dots$$

$$\begin{aligned}
 &= \frac{P}{\pi \mu} \left[\frac{\lambda}{\lambda + \mu} \cdot \frac{z}{x^2 + z^2} - \frac{z(x^2 + z^2)}{(x^2 + z^2)^2} \right] \\
 &= \frac{P}{\pi \mu} \left(\frac{z}{x^2 + z^2} \right) \left(\frac{\lambda}{\lambda + \mu} - 1 \right) \\
 &= \frac{P}{\pi \mu} \left(\frac{z}{x^2 + z^2} \right) \left(-\frac{\mu}{\lambda + \mu} \right) \\
 &= -\frac{P}{\pi(\lambda + \mu)} \left(\frac{z}{x^2 + z^2} \right)
 \end{aligned}$$

Hence, by equations (c):

$$\begin{aligned}
 (1) \sigma_x &= \lambda e + 2\mu \epsilon_x \\
 &= \lambda \left[-\frac{P}{\pi(\lambda + \mu)} \cdot \frac{z}{x^2 + z^2} \right] + 2\mu \left[\frac{P}{2\pi\mu} \left\{ \frac{\lambda}{\lambda + \mu} \cdot \frac{z}{x^2 + z^2} - \frac{2xz}{(x^2 + z^2)^2} \right\} \right] \\
 &= -\frac{P}{\pi} \cdot \frac{\lambda}{\lambda + \mu} \cdot \frac{z}{x^2 + z^2} + \frac{P}{\pi} \cdot \frac{\lambda}{\lambda + \mu} \cdot \frac{z}{x^2 + z^2} - \frac{P}{\pi} \cdot \frac{2xz}{(x^2 + z^2)^2}
 \end{aligned}$$

$$\text{i.e. } \sigma_x = -\frac{2P}{\pi} \cdot \frac{x^2 z}{(x^2 + z^2)^2} \dots \dots \dots (1)$$

$$\begin{aligned}
 (11) \sigma_z &= \lambda e + 2\mu \epsilon_z \\
 &= \lambda \left[-\frac{P}{\pi(\lambda + \mu)} \cdot \frac{z}{x^2 + z^2} \right] + 2\mu \left[\frac{P}{2\pi\mu} \left\{ \frac{\lambda}{\lambda + \mu} \cdot \frac{z}{x^2 + z^2} - \frac{2z^3}{(x^2 + z^2)^2} \right\} \right] \\
 &= -\frac{P}{\pi} \cdot \frac{\lambda}{\lambda + \mu} \cdot \frac{z}{x^2 + z^2} + \frac{P}{\pi} \cdot \frac{\lambda}{\lambda + \mu} \cdot \frac{z}{x^2 + z^2} - \frac{P}{\pi} \cdot \frac{2z^3}{(x^2 + z^2)^2}
 \end{aligned}$$

$$\text{i.e. } \sigma_z = -\frac{2P}{\pi} \cdot \frac{z^3}{(x^2 + z^2)^2} \dots \dots \dots (2)$$

For the calculation of the Shear Stress τ_{xz} (i.e. τ_{zx}), the equation $\tau_{xz} = \frac{\partial u}{\partial z} + \frac{\partial v}{\partial x}$ is firstly used (equation (b))

$$\begin{aligned}
 u &= \frac{P}{2\pi\mu} \left\{ xz(x^2 + z^2)^{-1} - \frac{\mu}{\lambda + \mu} \arctan \frac{x}{z} \right\} \\
 \frac{\partial u}{\partial z} &= \frac{P}{2\pi\mu} \left[(x^2 + z^2)^{-1} \cdot x + xy(-1)(x^2 + z^2)^{-2} \cdot 2z - \frac{\mu}{\lambda + \mu} \cdot \left(-\frac{x}{z^2} \right) \left(\frac{1}{1 + \frac{x^2}{z^2}} \right) \right] \\
 &= \frac{P}{2\pi\mu} \left[\frac{x}{x^2 + z^2} - \frac{2xz^2}{(x^2 + z^2)^2} + \frac{\mu}{\lambda + \mu} \cdot \frac{x}{x^2 + z^2} \right] \\
 &= \frac{P}{2\pi\mu} \left[\frac{x}{x^2 + z^2} \left\{ 1 + \frac{\mu}{\lambda + \mu} \right\} - \frac{2xz^2}{(x^2 + z^2)^2} \right] \\
 &= \frac{P}{2\pi\mu} \left[\frac{\lambda + 2\mu}{\lambda + \mu} \cdot \frac{x}{x^2 + z^2} - \frac{2xz^2}{(x^2 + z^2)^2} \right]
 \end{aligned}$$

$$w = \frac{P}{2\pi\mu} \dots \dots \dots /$$

$$w = \frac{F}{2\pi\mu} \left[z^2 \cdot (x^2+z^2)^{-1} + \frac{\lambda+2\mu}{\lambda+\mu} \log \{ 2\ell (x^2+z^2)^{-\frac{1}{2}} \} \right]$$

$$\text{So } \frac{\partial w}{\partial x} = \frac{F}{2\pi\mu} \left[z^2 (-1) (x^2+z^2)^{-2} \cdot 2x + \frac{\lambda+2\mu}{\lambda+\mu} \left\{ \frac{(x^2+z^2)^{-\frac{1}{2}}}{2\ell} \cdot 2\ell \cdot (-\frac{1}{2}) (x^2+z^2)^{-\frac{3}{2}} \cdot 2x \right\} \right]$$

$$= \frac{F}{2\pi\mu} \left[-\frac{2xz^2}{(x^2+z^2)^2} - \frac{\lambda+2\mu}{\lambda+\mu} \left(\frac{x}{x^2+z^2} \right) \right]$$

Further, by equations (g):

$$\tau_{xz} = \mu \cdot \gamma_{xz} = \mu \left(\frac{\partial u}{\partial z} + \frac{\partial w}{\partial x} \right)$$

$$\text{So } \tau_{xz} = \mu \cdot \frac{F}{2\pi\mu} \left[\frac{\lambda+2\mu}{\lambda+\mu} \cdot \frac{x}{x^2+z^2} - \frac{2xz^2}{(x^2+z^2)^2} - \frac{\lambda+2\mu}{\lambda+\mu} \cdot \frac{x}{x^2+z^2} - \frac{2xz^2}{(x^2+z^2)^2} \right]$$

$$\text{ie. } \tau_{xz} = -\frac{2F}{\pi} \frac{xz^2}{(x^2+z^2)^2} \dots \dots \dots (3)$$

It should be noted that in each case, the stresses σ_x , σ_z and τ_{xz} finally do not contain terms of Lamé's constants, which in turn contain the moduli of elasticity including Poisson's Ratio.

The equations (1), (2) and (3) can be transformed into Polar coordinates, to bring them into the form given by Terzaghi Ref. 8 p.376, (also equations 4.1, 4.2 and 4.3 of this report) as follows:

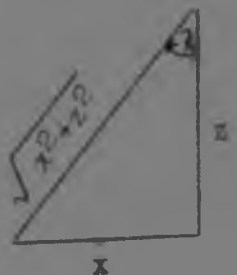
$$\cos \psi = \frac{z}{\sqrt{x^2+z^2}} ; \quad \sin \psi = \frac{x}{\sqrt{x^2+z^2}}$$

$$\therefore \cos^4 \psi = \frac{z^4}{(x^2+z^2)^2} ; \cos^2 \psi \sin^2 \psi = \frac{x^2 z^2}{(x^2+z^2)^2} ; \cos^3 \psi \sin \psi = \frac{z^3 x}{(x^2+z^2)^2}$$

$$\text{Hence in equation (1) : } \sigma_x = -\frac{2F}{\pi} \frac{x^2 z}{(x^2+z^2)^2}$$

$$= -\frac{2F}{\pi z} \frac{x^2 z^2}{(x^2+z^2)^2}$$

$$\therefore \sigma_x = -\frac{2F}{\pi z} \cos^2 \psi \cdot \sin^2 \psi$$



$$\text{in equation (b) : } \sigma_z = -\frac{2F}{\pi} \frac{z^3}{(x^2+z^2)^2}$$

$$= -\frac{2F}{\pi z} \frac{z^4}{(x^2+z^2)^2}$$

$$\text{ie. } \sigma_z = -\frac{2F}{\pi z} \cos^4 \psi$$

$$\text{in equation (c) : } \tau_{xz} = -\frac{2F}{\pi} \frac{xz^2}{(x^2+z^2)^2} = -\frac{2F}{\pi z} \frac{xz^3}{(x^2+z^2)^2}$$

$$\text{ie. } \tau_{xz} = -\frac{2F}{\pi z} \cos^3 \psi \sin \psi$$

It should be noted, however, that Terzaghi's sign convention is such that the expressions for the stresses are in each case taken to be positive.

APPENDIX III

(1) Comparison of values of S_{max} as determined from:

(1) $S_{max} = \sqrt{(\sigma_z - \sigma_r)^2 + 4\tau_{rz}^2}$ Eqn 5.3

(2) $S_{max} = \sqrt{(\sigma_z - \sigma_t)^2 + 4\tau_{tz}^2} = (\sigma_z - \sigma_t)$ Eqn 5.5 ($\tau_{tz} = 0$)

TABLE XVII

z	r	$\mu = 0$		$\mu = 0.125$	
		Eqn 5.3	Eqn 5.5	Eqn 5.3	Eqn 5.5
3	0	30.9468	30.9468	29.8415	29.8415
	5	3.1942	0.6027	3.2351	1.6915
	10	0.3495	0.3061	0.3610	0.2165
	20	0.0910	0.1390	0.0520	0.1038
	30	0.0536	0.0706	0.0336	0.0529
	45	0.0288	0.0340	0.0192	0.0255
	60	0.0175	0.0199	0.0128	0.0150
5	0	7.7365	7.7365	7.4604	7.4602
	5	3.2250	2.0427	3.1563	1.9761
	10	0.7983	0.1536	0.8089	0.1749
	20	0.0882	0.0763	0.0897	0.0540
	30	0.0316	0.0525	0.0212	0.0390
	45	0.0193	0.0294	0.0100	0.0221
	60	0.0132	0.0175	0.0087	0.0131
10	0	5.7052	2.7852	2.6857	2.6817
	5	1.9898	1.6011	1.8709	1.5426
	10	0.8751	0.4703	0.6614	0.4581
	20	0.1724	0.0040	0.1776	0.0137
	30	0.0447	0.0278	0.0471	0.0191
	45	0.0132	0.0222	0.0100	0.0165
	60	0.0080	0.0151	0	0.0113
15	0	1.2374	1.2374	1.1929	1.1932
	5	1.0414	0.9549	1.0072	0.9201
	10	0.6736	0.4933	0.6560	0.4758
	20	0.2201	0.0795	0.2196	0.0803
	30	0.0767	0.0024	0.0787	0.0066
	45	0.0200	0.0127	0.0212	0.0087
	60	0.0032	0.0111	0	0.0081
20	0	0.6263	0.6263	0.6717	0.6715
	5	0.6305	0.5984	0.6088	0.5770
	10	0.1829	0.3995	0.4684	0.3850
	20	0.2274	0.1183	0.2262	0.1148
	30	0.0938	0.0263	0.0943	0.0275
	45	0.0304	0.0032	0.0316	0.0008
	60	0.0100	0.0072	0.0112	0.0050
30	0	0.3095	0.3088	0.2984	0.2978
	5	0.2912	0.2897	0.2845	0.2791
	10	0.1600	0.2387	0.2513	0.2300
	20	0.1692	0.1234	0.1650	0.1190
	30	0.0975	0.0517	0.0960	0.0505
	45	0.0413	0.0119	0.0415	0.0125
	60	0.0200	0.0008	0.0206	0.0017
45	0	0.1374	0.1369	0.1328	0.1320
	5	0.1347	0.1337	0.1301	0.1289
	10	0.1271	0.1218	0.1226	0.1173
	20	0.1027	0.0876	0.0987	0.0843
	30	0.0750	0.0541	0.0728	0.0523
	45	0.0427	0.0231	0.0421	0.0225
	60	0.0245	0.0096	0.0244	0.0095
60	0	0.0772	0.0772	0.0740	0.0744
	5	0.0763	0.0756	0.0731	0.0730
	10	0.0744	0.0724	0.0712	0.0698
	20	0.0648	0.0597	0.0628	0.0575
	30	0.0543	0.0446	0.0526	0.0430
	45	0.0361	0.0247	0.0353	0.0239
	60	0.0255	0.0136	0.0250	0.0131

Z	T	$\mu = 0.25$		$\mu = 0.375$	
		Eqn. 5.3	Eqn. 5.5	Eqn. 5.3	Eqn. 5.5
3	0	26.7363	26.7363	27.6311	27.6311
	5	3.3214	0.7801	3.4562	0.8689
	10	0.4229	0.1270	0.5176	0.0375
	20	0.0284	0.0685	0.0483	0.0333
	30	0.0138	0.0351	0	0.0175
	45	0.0101	0.0170	0	0.0084
	60	0.0071	0.0100	0	0.0050
6	0	7.1839	7.1839	6.9073	6.9073
	5	3.0971	1.9094	3.0491	1.6428
	10	0.4307	0.1461	0.8827	0.2174
	20	0.1011	0.0315	0.1391	0.0098
	30	0.0229	0.0254	0.0350	0.0120
	45	0	0.0147	0.0043	0.0023
	60	0	0.0027	0	0.0014
10	0	2.4868	2.4868	2.4868	2.4868
	5	1.0141	1.4111	1.7612	1.8256
	10	0.4514	0.4460	0.8454	0.4339
	20	0.1843	0.0234	0.1390	0.0332
	30	0.0341	0.0103	0.0636	0.0016
	45	0.0121	0.0107	0.0173	0.0050
	60	0	0.0075	0.0056	0.0038
15	0	1.1491	1.1491	1.1053	1.1049
	5	0.8726	0.8852	0.9391	0.8504
	10	0.5336	0.4583	0.6243	0.4408
	20	0.2208	0.0811	0.2235	0.0820
	30	0.0819	0.0107	0.0882	0.0160
	45	0.0240	0.0048	0.0287	0.0008
	60	0.0055	0.0012	0.0095	0.0022
20	0	0.6477	0.6477	0.6215	0.6217
	5	0.4897	0.5556	0.5758	0.5340
	10	0.4551	0.3704	0.4402	0.3559
	20	0.3228	0.1118	0.3214	0.1089
	30	0.0960	0.0094	0.0991	0.0298
	45	0.0380	0.0015	0.0367	0.0010
	60	0.0122	0.0028	0.0150	0.0006
30	0	0.2873	0.2869	0.2761	0.2760
	5	0.2747	0.2685	0.2641	0.2580
	10	0.2437	0.2012	0.2346	0.2105
	20	0.1607	0.1146	0.1567	0.1102
	30	0.0847	0.0493	0.0941	0.0481
	45	0.0421	0.0131	0.0434	0.0137
	60	0.0218	0.0027	0.0230	0.0037
45	0	0.1272	0.1273	0.1225	0.1225
	5	0.1251	0.1241	0.1207	0.1194
	10	0.1182	0.1130	0.1139	0.1086
	20	0.0958	0.0812	0.0925	0.0780
	30	0.0712	0.0505	0.0694	0.0487
	45	0.0415	0.0219	0.0412	0.0213
	60	0.0214	0.0095	0.0250	0.0095
60	0	0.0716	0.0716	0.0692	0.0688
	5	0.0707	0.0704	0.0683	0.0678
	10	0.0691	0.0672	0.0667	0.0646
	20	0.0602	0.0553	0.0581	0.0531
	30	0.0512	0.0413	0.0497	0.0398
	45	0.0343	0.0231	0.0335	0.0223
	60	0.0245	0.0127	0.0245	0.0124

z	r	$\mu = 0.50$	
		Eqn 5.3	Eqn 5.5
3	0	26.5254	26.5254
	5	3.6166	0.9576
	10	0.629	0.0120
	20	0.0265	0.0018
	30	0.0260	0.0002
	45	0.0078	0.0001
	60	0	0
5	0	5.6312	5.6312
	5	3.0046	1.7761
	10	0.2034	0.2387
	20	0.1570	0.0127
	30	0.0502	0.0016
	45	0.0151	0
	60	0.0063	0
10	0	2.3873	2.3873
	5	1.7041	1.3671
	10	0.8434	0.4217
	20	0.2140	0.0430
	30	0.0751	0.0071
	45	0.0215	0.0008
	60	0.0103	0
15	0	1.0607	1.0607
	5	0.6048	0.3158
	10	0.6107	0.4233
	20	0.2848	0.0827
	30	0.0748	0.0191
	45	0.0335	0.0030
	60	0.0135	0.0008
20	0	0.5978	0.5978
	5	0.5446	0.5125
	10	0.4271	0.3444
	20	0.2252	0.1083
	30	0.1015	0.0310
	45	0.0403	0.0063
	60	0.0180	0.0016
30	0	0.2650	0.2650
	5	0.2343	0.2475
	10	0.2762	0.2037
	20	0.1535	0.1058
	30	0.0639	0.0470
	45	0.0215	0.0143
	60	0.0245	0.0047
45	0	0.1177	0.1177
	5	0.1161	0.1146
	10	0.1095	0.1042
	20	0.0898	0.0718
	30	0.0678	0.0470
	45	0.0412	0.0207
	60	0.0255	0.0095
60	0	0.0660	0.0660
	5	0.0652	0.0652
	10	0.0636	0.0620
	20	0.0561	0.0510
	30	0.0482	0.0382
	45	0.0331	0.0215
	60	0.0245	0.0120

2) Determination of the Points of Intersection of Stress Contour Lines with the Surface $z = 0$ of a Semi-Infinite Solid in the case of Stress Contour Diagrams for σ_r , σ_t and S_{max}

(i) The Horizontal Radial Stress σ_r is given by the expression:

$$\sigma_r = \frac{Q}{2H} \left[\frac{3r^2z}{(r^2+z^2)^{3/2}} - \frac{1-2\mu}{r^2+z^2+z\sqrt{r^2+z^2}} \right] \dots\dots\dots 4.8(a)$$

On the plane $z = 0$, this becomes:

$$\begin{aligned} \sigma_r &= \frac{Q}{2H} \left[-\frac{(1-2\mu)}{r^2} \right] \\ &= -\frac{Q}{2Hr^2} (1-2\mu) \end{aligned}$$

$$\text{i.e. } r^2 = -\frac{Q}{2H\sigma_r} (1-2\mu)$$

on the plane $z = 0$, σ_r is found by calculation to have negative values for all values of μ .

Hence:

$$r = \pm \sqrt{-\frac{Q}{2H\sigma_r} (1-2\mu)} \dots\dots\dots (a)$$

where $\sigma_r = -0.1, -0.2, -0.3$ etc. which therefore renders the term inside the square root a positive quantity.

(ii) The Horizontal Tangential stress σ_t is given by the expression:

$$\sigma_t = -\frac{Q}{2H} (1-2\mu) \left[\frac{z}{(r^2+z^2)^{3/2}} + \frac{1}{r^2+z^2+z\sqrt{r^2+z^2}} \right] \dots\dots\dots 4.9(c)$$

On the plane $z = 0$, this becomes:

$$\begin{aligned} \sigma_t &= -\frac{Q}{2H} (1-2\mu) \left(-\frac{1}{r^2} \right) \\ &= +\frac{Q}{2Hr^2} (1-2\mu) \end{aligned}$$

$$\text{i.e. } r^2 = +\frac{Q}{2H\sigma_t} (1-2\mu)$$

On the plane $z = 0$, σ_t is found by calculation to have positive values for all values of μ .

Hence:

$$r = \pm \sqrt{\frac{Q}{2H\sigma_t} (1-2\mu)} \dots\dots\dots (b)$$

(iii) The Maximum Shear Stress S_{max} is given by the expression:

$$S_{max} = \frac{1}{2} \sqrt{(\sigma_z - \sigma_r)^2 + 4\tau_{rz}^2} \dots\dots\dots 5.3$$

On/

On substituting the values of σ_z , σ_r and τ_{rz} as given by equations 4.7(e), 4.8(e) and 4.10(e) in the above equation 3.3, and in addition substituting $z = 0$, this gives the Maximum Shear Stress S_{max} on the plane $z = 0$ as:

$$\begin{aligned} S_{max} &= \left[\left\{ -\frac{Q}{2\pi} \left(-\frac{1-2\mu}{r^2} \right) \right\}^2 \right]^{\frac{1}{2}} \\ &= -\frac{Q}{2\pi} \left(-\frac{1-2\mu}{r^2} \right) \\ &= +\frac{Q}{2\pi r^2} (1-2\mu) \end{aligned}$$

$$\text{i.e. } r^2 = +\frac{Q}{2\pi S_{max}} (1-2\mu)$$

On the plane $z = 0$, S_{max} is found by calculation to be positive for all values of μ .

Hence:

$$r = \pm \sqrt{\frac{Q}{2\pi S_{max}} (1-2\mu)} \dots \dots \dots (c)$$

It will be seen that the equations (a), (b) and (c) reduce to the same equation if:

firstly ; $-\sigma_r = \sigma_z = S_{max} = K$ is substituted;

secondly; the same value of μ is used in each case.

Hence, for a particular numerical value of any contour, say the contour 1.0 units of $\sigma_{rr}/(\text{units of length})^2$, and the same value of μ , only one calculation is needed to find the value of r for the contour line $-\sigma_r = \sigma_z = S_{max} = 1.0$ units of $\sigma_{rr}/(\text{units of length})^2$.

The various calculations are shown in tabular form on the next page.

Equation

Equation: $r = \sqrt{\frac{S}{2\pi K} (1 - \mu)}$ where $-\sigma_r = \sigma_t = S_{max} = K$

TABLE KV-11

K	1-μ	$\frac{S}{2\pi K}$	$\frac{S}{2\pi K}$	$\frac{S}{2\pi K} (1-2\mu)$	$r = \sqrt{\frac{S}{2\pi K} (1-\mu)}$
Condition: μ = 0					
0.05	1	100.1040	3183.0989	3183.0989	56.4
0.1	1	"	1591.5494	1591.5494	39.9
0.2	1	"	795.7747	795.7747	28.2
0.5	1	"	318.3099	318.3099	17.8
1.0	1	"	159.1549	159.1549	12.6
2.0	1	"	79.5775	79.5775	8.9
5.0	1	"	31.8310	31.8310	5.6
10.0	1	"	15.9155	15.9155	4.0
Condition: μ = 0.25					
0.05	0.75	100.1040	3183.0989	3183.0989	56.4
0.1	"	"	1591.5494	1591.5494	39.9
0.2	"	"	795.7747	795.7747	28.2
0.5	"	"	318.3099	318.3099	17.8
1.0	"	"	159.1549	159.1549	12.6
2.0	"	"	79.5775	79.5775	8.9
5.0	"	"	31.8310	31.8310	5.6
10.0	"	"	15.9155	15.9155	4.0
Condition: μ = 0.75					
0.0125	0.25	100.1040	3183.0989	3183.0989	56.4
0.025	"	"	1591.5494	1591.5494	39.9
0.050	"	"	795.7747	795.7747	28.2
0.1	"	"	318.3099	318.3099	17.8
0.2	"	"	159.1549	159.1549	12.6
0.5	"	"	79.5775	79.5775	8.9
1.0	"	"	31.8310	31.8310	5.6
2.0	"	"	15.9155	15.9155	4.0
5.0	"	"	7.9577	7.9577	2.8
10.0	"	"	3.9789	3.9789	2.0

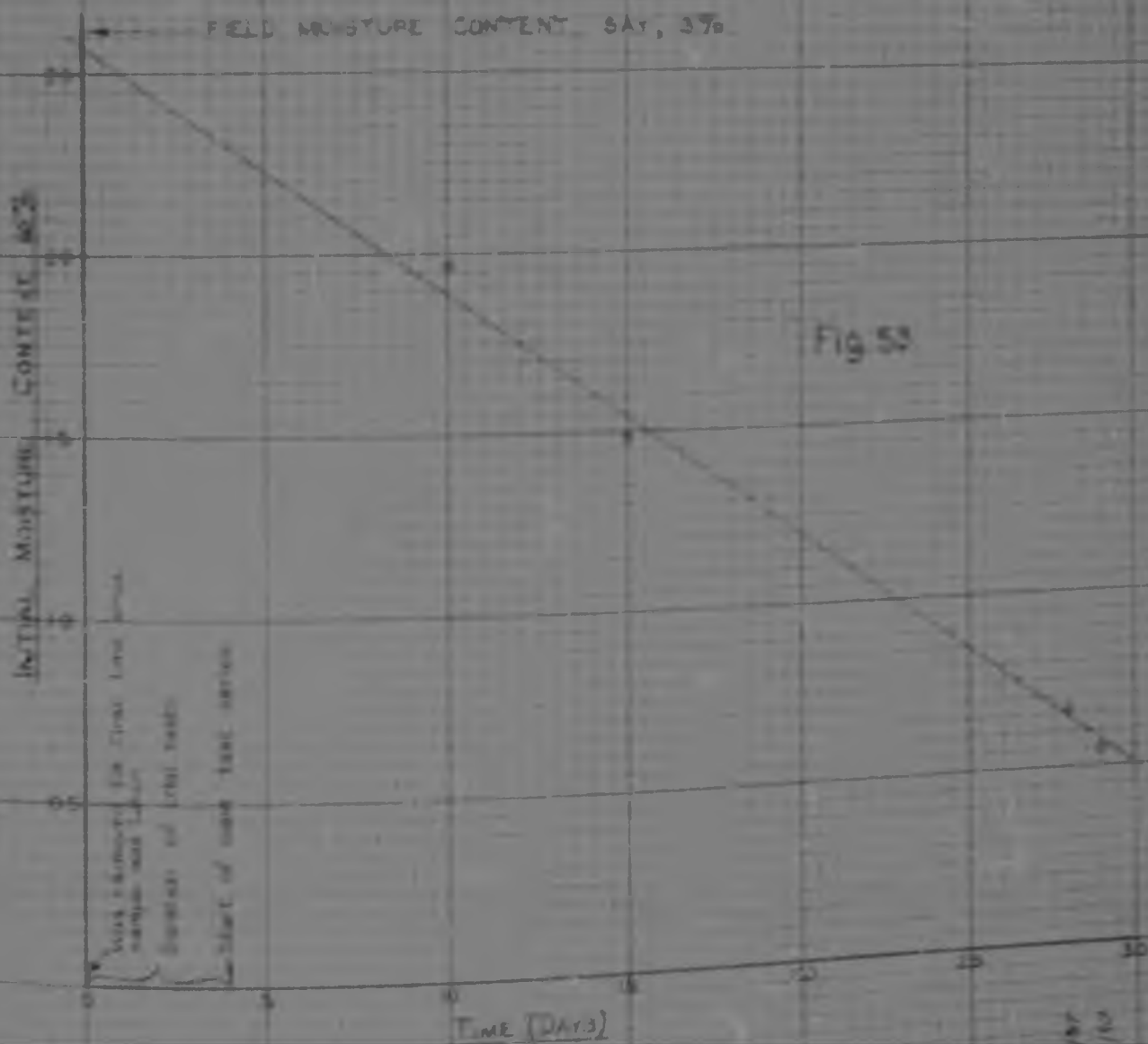
APPENDIX IV
MOISTURE CONTENT DETERMINATIONS

- 179 -

TABLE XX

DATE	TEST NO.	INITIAL MOISTURE CONTENT			MOISTURE CONTENT AFTER TEST		
		WT OF OVEN DRIED SOIL = W_d (gm)	WT. OF WATER = W_w (gm)	MOISTURE CONTENT (%)	WT OF OVEN DRIED SOIL = W_d (gm)	WT. OF WATER = W_w (gm)	MOISTURE CONTENT (%)
22 1 57	2	—	—	—	131.4	3.5	2.740
26 1 57	CONSOLIDOMETER	170.5	3.5	.881	—	—	—
29 1 57	3	—	—	—	126.2	3.0	2.377
30 1 57	5	—	—	—	124.5	2.7	2.079
31 1 57	6	—	—	—	130.9	2.3	1.910
22 2 57	* 6B	33.77	0.50	.481	126.1	2.1	1.665
15 2 57	4	48.61	0.32	0.156	130.0	4.8	3.538
16 2 57	1	23.74	0.13	0.348	128.2	4.2	3.276

* This test was not included in the test series reported on



2) DETERMINATION OF INITIAL VOID RATIO (e) AND DEGREE OF SATURATION (S_r)

OF EACH TEST SAMPLE

TABLE XXI

TEST NUMBER	WT OF OVEN DRIED SOIL = W _s gms.	SPECIFIC GRAVITY OF SOIL GRAINS = G _s	HENCE VOLUME OF SOIL SOLIDS = V _s = $\frac{W_s}{G_s}$ cc	OVERALL VOL OF SOIL SAMPLE = V cc	HENCE VOLUME OF VOIDS = V - V _s cc	HENCE INITIAL VOID RATIO = $e = \frac{V_v}{V_s}$	INITIAL MOISTURE CONTENT = w (From Fig 53) percent	HENCE INITIAL DEGREE OF SATURATION = $S_r = \frac{w G_s}{e}$ percent
1	128.2	2.62	48.74	85.00	36.26	0.737	0.548	1.948
2	131.4	2.62	50.16	85.00	34.84	0.695	2.230	6.636
3	126.2	2.62	48.17	85.00	36.83	0.764	1.820	6.237
4	130.0	2.62	49.62	85.00	35.38	0.713	0.658	2.417
5	129.9	2.62	49.60	85.00	35.40	0.714	1.750	6.422
6	130.9	2.62	49.95	85.00	35.05	0.702	1.660	6.272
CONSOLIDOMETER	179.5	2.62	68.13	115.85	47.72	0.700	1.951	7.331

APPENDIX V

1) Calibration of Capillary Tube

Measured length of capillary tube = $15\frac{9}{32}$ inches.
Weight of porcelain dish used = 20.17 gm.

Expt. No.	Wt. of Mercury to fill Capillary tube & Wt. of beaker.	Temperature
1	40.57 gm.	26.50C
2	40.64 gm.	
3	40.67 gm.	
4	40.67 gm.	
5	40.68 gm.	
Average:	40.66 gm.	26.50C

Wt. of Mercury to fill capillary tube = $(40.66 - 20.17)$ gm.
= 19.49 gm.

From Ref. 31, same vol. by interpolation:
Density of Mercury at 26.50C = 13.5351 gm/cc.

Hence, Volume of Mercury to fill capillary = $\frac{19.49}{13.5351} = 1.441$ cc.

From above, length of capillary = $15\frac{9}{32}$ inches = 2.04 cm.

Cross-sectional area of capillary = $A = \frac{1.441}{2.04} = 0.706$ sq. cm.
= 1.903×10^{-2} sq. cm.

Hence, Diameter of Capillary = $D = \sqrt{\frac{4A}{\pi}}$
= $\sqrt{\frac{4 \times 1.903 \times 10^{-2}}{\pi}}$
= 0.155 cm.
= 1.55 mm.

2) Calculation of Slug Movement due to pinhole entry hole.

Diameter of Loading Spindle = 0.5 inches.

Hence, Cross-sectional area of Spindle = $\frac{\pi \times (0.5)^2}{4}$ sq. in.

Fluid displaced per 1 division deflection (0.001 inch)

$$= \frac{\pi \times (0.5)^2}{4} \times 10^{-3} \text{ cu. in.}$$

$$= \frac{\pi \times (0.5)^2}{4} \times 10^{-3} \times 16.5 \text{ cu. cm.}$$

$$= \frac{\pi \times 16.5}{16} \times 10^{-3} \text{ cu. cm.}$$

$$= 0.21 \times 10^{-3} \text{ cc.}$$

From Item (1) of this appendix
Cross-sectional area of capillary tube = 1.903×10^{-2} sq. cm.

i.e. 1.903×10^{-2} sq. cm. of fluid displaced from the tank will cause a slug movement of 1 cm. in the capillary tube.

Hence, 3.2152×10^{-3} amp/cm. of fluid displaced from the capillary
 causes a plug movement of:

$$\frac{3.2152 \times 10^{-3}}{1.0055 \times 10^{-2}} \times 1.0 \text{ cm.}$$

$$= 1.2143 \times 10^{-1} \text{ cm.}$$

$$= \underline{1.214 \text{ cm.}}$$

Hence, per unit deflection (10^{-3} in.), the leading syringe plunger
 has a distance of 1.214×10^{-1} inches into the test cell, thereby causing
 a flow of fluid out of the test cell resulting in a plug
 movement of 1.214 cm. in the capillary tube, from left to right.

i.e. plug movement due to syringe entry only

$$= \underline{1.214 \text{ cm. per division deflection.}}$$

REFERENCES

1. TAYLOR, D.W. "Fundamentals of Soil Mechanics." Wiley (New York 1948). (1)p.209 (2)p.264 (3)p.251-252 (4)p.254 (5)p.240 (6)p.252-259 (7)p.543.
2. TIMOSHENKO, S. "Strength of Materials", Part I. Van Nostrand (New York 1940). (1)p.80-81 (2)p.2.
3. TIMOSHENKO, S. "Theory of Elasticity". McGraw-Hill (New York 1934). (1)p.1 (2)p.5 (3)p.7 (4)p.12-13 (5)p.117 (6)p.2 (7)p.327-339.
4. OCKLETON, A.J. Discussion during post-graduate Advanced Theory of Structures lecture. Witwatersrand University (1966).
5. TIMOSHENKO, S. "History of Strength of Materials". McGraw-Hill (New York 1953). (1)p.20.
6. REINER, W. "Building Materials, their Elasticity and Inelasticity." North-Holland (Amsterdam 1964). (1)p.315 (2)p.146.
7. KRYNINE, D.P. and JUDD, W.R. "Principles of Engineering Geology and Geotechnics." McGraw-Hill (New York 1957). p.65.
8. TERZAGHI, L. "Theoretical Soil Mechanics". Wiley (New York 1943). (1)p.369 (2)p.23-247 (3)p.372 (4)p.376 (5)p.374 (6)p.375 (7)p.377 (8)p.378 (9)p.382 (10)p.386 (11)p.388.
9. SEARLE, G.F. "Experimental Elasticity". University Press (Cambridge 1905). p.20.
10. KAYE, G.W. and Laby, T. "Tables of Physical and Chemical Constants". Longmans (London 1952). 7.35.
11. MICHELL, J.H. "The Direct Determination of Stress in an Elastic Solid, with application to the Theory of Plates." Proc. London Math. Soc., Vol.31 (1899), p.100 et seq.
12. FLAMANT, A. Comptes rendus des sciences de l'Académie des Sciences. Vol.11- (1892). p.1467-1469.
13. MICHELL, J.H. Solution in Proc. London Math. Soc., Vol.32, 1900.
14. CAROTHERS, S. "Direct Determination of Stresses". Proc. Royal Soc. of London. Series A, Vol.XCVII.
15. JOHNSON, L. "The Application of Theories of Elasticity and Plasticity to Foundation Problems". J. Boston Soc. Civ. Engrs. Vol.21, No.3 (July 1944). p.208-211.
16. POISSON, S.D. "Application des Potentiels à l'étude de l'équilibre et du mouvement des Solides élastiques." Gauthier-Villars (Paris 1885).
17. LOVE, A.E.H. "The Stress Produced in a Semi-infinite solid by Pressure on Part of the Boundary". Phil. Trans. Roy. Soc. Series A, Vol. 228 (1929). p.377-420.
18. NEWMARK, N.M. "Simplified Computation of Vertical Pressures in Elastic Foundations". Univ. Illinois Engrg. Experimental Station. Circular 24 (1935).
19. SCHLEICHER, F. "Zur Theorie des Baugrundes". Der Bauingenieur. Vol. 7 (1906). p.931-935, 949-952.

20. KANTEY, B. and HARR, H. "The Distribution of Stresses in Soil under Load." *M.E.S.I. Bull.* No. 4 (May 1930). p. 3.
21. SKEPTON, A.W., PECK, R.B. and MACDONALD, D.B. "Settlement Analysis of Six Structures in Chicago and London". *Proc. Inst. Civ. Engrs.* Vol. 5, No. 1 (July 1955). p. 525-528.
22. SKEPTON, A.W. and BJERRUP, L. "A Contribution to the Settlement Analysis of Foundations on Clay." *Geotechnique*. Vol. 7, No. 4 (December 1957). p. 16.
23. WHIPPEN, A.O. Letter to Prof. J.E. Jennings of Witwatersrand University. D.S.I.R. Road Res. Lab. (July 1957).
24. JONES, R. "In-situ measurement of the Mechanical Properties of Soil by Vibration Methods I. The Propagation of Surface Vibrations". D.S.I.R. Road Res. Lab. Note No. RN/3015/RH. (April 1957). Unpublished.
25. JONES, R. "In-situ Measurement of the Mechanical Properties of Soil by Vibration Methods II. Measurement of Local Shear Modulus by a Resonance Method". D.S.I.R. Road Res. Lab. Note No. RN/3010/RJ. (April 1957). Unpublished.
26. TURNBULL, W.J. Letter to Prof. J.E. Jennings of Witwatersrand University. U.S. Army Corps of Engrs., Waterways Experiment Station. (Vicksburg, Missis. August 1956).
27. "Investigations of Pressures and Deflections for Flexible Pavements", Report No. 1. "Homogeneous Clayey-silt Test Section". U.S. Army Corps of Engrs., Waterways Experiment Station. (Vicksburg, Missis. March 1951). TM-3-323.
28. "Investigations of Pressures and Deflections for Flexible Pavements", Report No. 2. "Homogeneous Sand Test Section". U.S. Army Corps of Engrs., Waterways Experiment Station. (Vicksburg, Missis. December 1951). TM-3-323. p. 37-47.
29. HISHOP, A., and REMNIE, D.J. "The Measurement of Soil Properties in the Triaxial Test". Edward Arnold (London 1957). p. 29-30.
30. MACLEOD, D.J. "The Application of Soil Mechanics to Roads and Engineering Foundations". *J. Instn. Mun. Engrs.* (January 1955) p. 323.
31. "Handbook of Chemistry and Physics". Chemical Rubber Publishing Co. (Cleveland, Ohio. 38th Ed. 1956-1957). p. 1991.

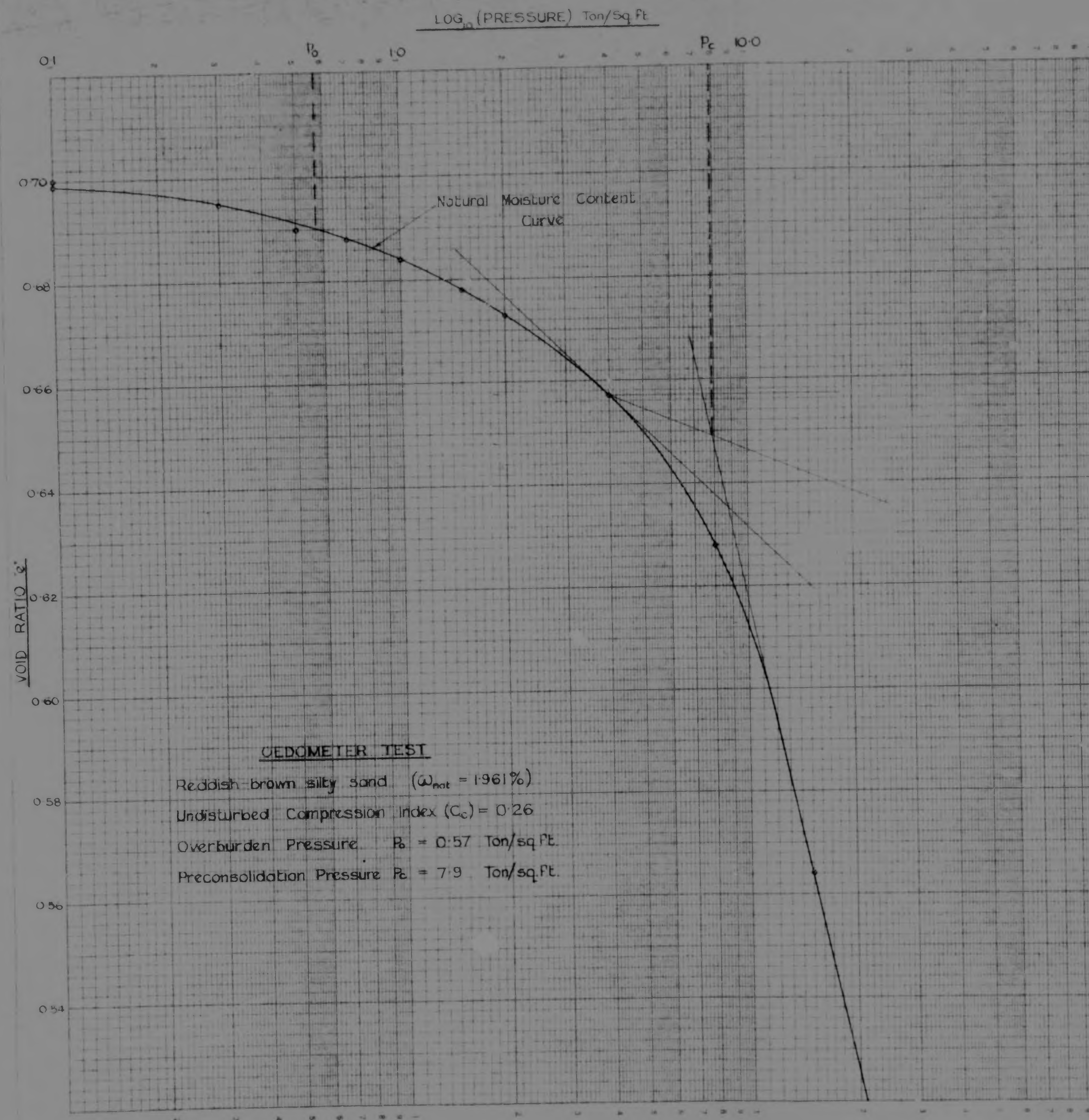


Fig. 18 — Pressure : Void Ratio Curve for the Test Soil
(Normal 1-Dimensional Consolidation Test)

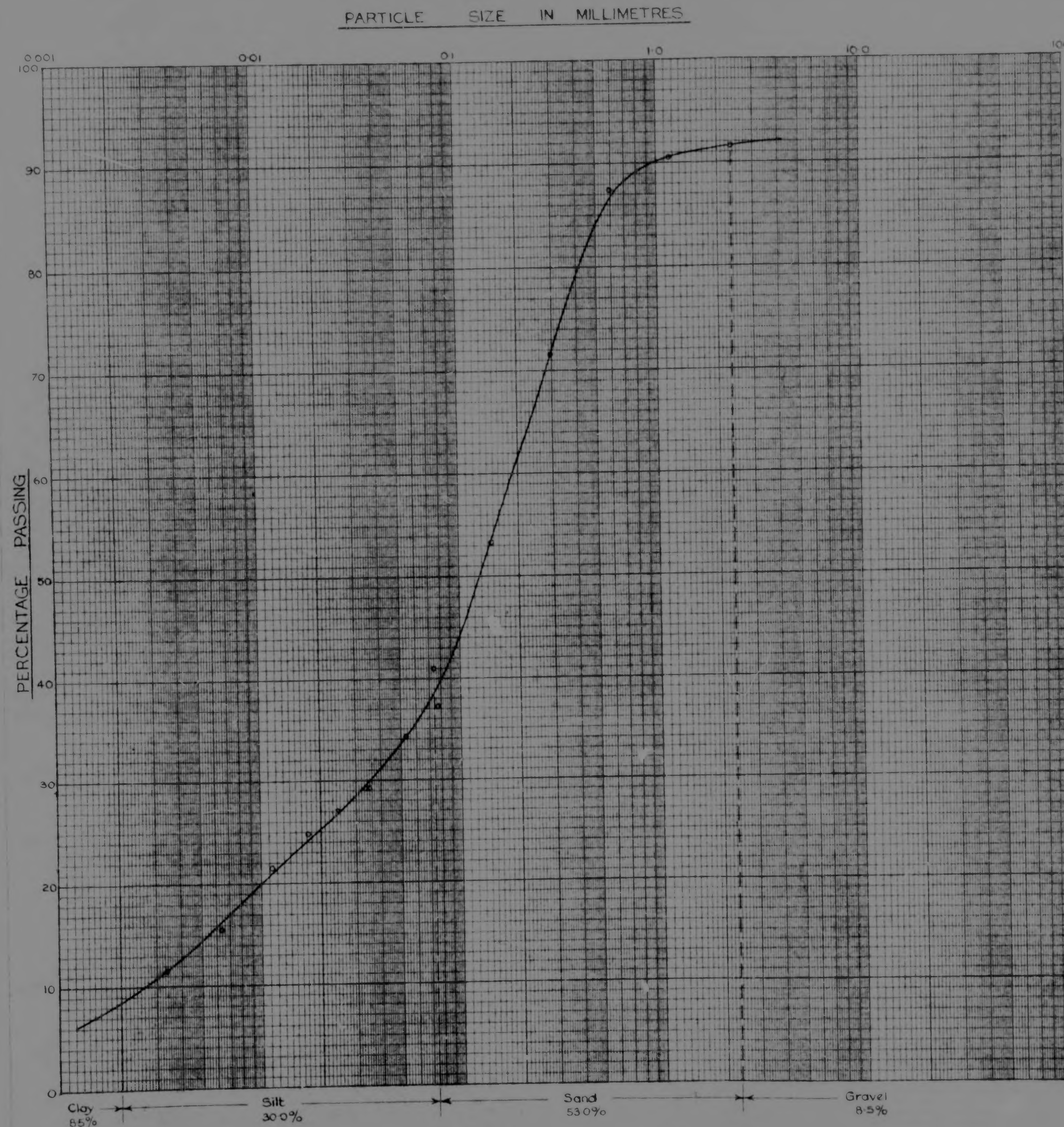


Fig. 17 Grading Curve for the Test Soil

THE SIGNIFICANCE
OF
POISSON'S RATIO IN THE DETERMINATION
OF
STRESS AND SETTLEMENT IN SOILS

H.P. RAUCH
B.Sc.(Eng.)(Rend), A.M.(S.A.)I.C.E.

A thesis presented to the University of the
Witwatersrand, for the degree Master of Science
in Civil Engineering.

1758

Author Rauch H P

Name of thesis The significance of Poisson's Ratio in the determination of stress and settlement in soils 1958

PUBLISHER:

University of the Witwatersrand, Johannesburg

©2013

LEGAL NOTICES:

Copyright Notice: All materials on the University of the Witwatersrand, Johannesburg Library website are protected by South African copyright law and may not be distributed, transmitted, displayed, or otherwise published in any format, without the prior written permission of the copyright owner.

Disclaimer and Terms of Use: Provided that you maintain all copyright and other notices contained therein, you may download material (one machine readable copy and one print copy per page) for your personal and/or educational non-commercial use only.

The University of the Witwatersrand, Johannesburg, is not responsible for any errors or omissions and excludes any and all liability for any errors in or omissions from the information on the Library website.